FINAL REPORT

STATISTICAL APPROACH TO PHYSICALLY BASED LOAD MODELING

By
C. Y. Chong
R. P. Malhami

Prepared for
U. S. DEPARTMENT OF ENERGY
ELECTRIC ENERGY SYSTEMS DIVISION

Under
Contract No. DE–AS01–77ET29116

April 1983

GEORGIA INSTITUTE OF TECHNOLOGY
A UNIT OF THE UNIVERSITY SYSTEM OF GEORGIA
SCHOOL OF ELECTRICAL ENGINEERING
ATLANTA, GEORGIA 30332

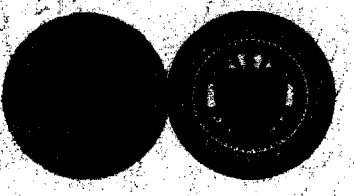

STATISTICAL APPROACH TO PHYSICALLY BASED LOAD MODELING

C. Y. Chong and R. P. Malhami

Final Report Prepared For

U.S. Department of Energy
Office of Energy Systems Research
Electric Energy Systems Division

Under Contract No. DE-AS01-77ET29116 on "Development of an Electrical Load Demand and Response Model Based on a Rational Synthesis From Elementary Devices."

April 1983

NOTICE

ABSTRACT

A methodology for synthesizing the electric load for a system starting from the elementary device models is proposed. Since the methodology is physically based and captures the stochastic nature of the decision processes which generate the load, it is more suitable than identification based approaches in applications such as load management. It generates a hierarchy of models from the customer or building level to the bulk power level. At each level, the methodology consists of four steps, the representation of primitive components, the classification of components, aggregation and model validation. This research focuses on modeling the load demand of a large number of similar devices at the lowest level.

Each elementary device in the system is represented by two models: the functional model which gives the "on" or "off" status of the device and the electric device model which summarizes the effects of voltage and frequency. Only loads with similar functional and electric characteristics can be replaced by an equivalent model. For such a homogenous group, statistical aggregation yields a model consisting of coupled ordinary and partial differential equations. The methodology is used to model the space heating of a large number of houses. Simulation of cold load pickup is used to illustrate the main features of the final model. Data requirements for such models are discussed and found to be modest.

TABLE OF CONTENTS

LIST OF FIGURES

1. INTRODUCTION AND SUMMARY

1.1 Project Goal

The objective of this project is to develop a methodology which can be used to synthesize models of power system load at various points in the system. The methodology is physically based, i.e., the models are synthesized from physical models for the elementary devices (loads) in the system and their composition. The models are potentially useful for many areas of power system operation and planning such as automatic generation control, security assessment, emergency state control, restorative control, load management, operations scheduling, generation and transmission expansion planning, etc.

The emphasis of the project has been in developing the overall methodology for synthesizing load demand models in particular. This is an area where traditional approaches have been inadequate in certain application areas such as load management and restorative state control. Demand models for a particular class of devices (loads) are developed in detail to illustrate the feasibility of the approach.

1.2 Background and Motivation of Research

The modeling of power system loads is a very important problem since loads are ultimately the driving force behind the entire system. Power system load models can be divided into two types according to the kinds of questions which they address. The first type consists of load response models. These relate the real and reactive power injected at some point in the system to the voltage and frequency. The second type consists of load demand models. They provide the power demand at a given point in the system at some (present or future) time.

Load response models are useful for on-line operations such as automatic generation control, detection of emergencies, transient stability analysis and so on. Traditionally, they have been motivated by the need for simplicity [1-3], with loads frequently in the form of a constant resistance, inductance, capacitance, or a combination thereof. These models are usually inaccurate when the system undergoes large excursions outside its normal steady state. More elaborate models based on finding the equivalent of a group of loads are also available [4-7].

Load demand models can either be long term (years) or short term (days to minutes). Long term load demand models are used primarily for planning and depend on economic factors which generate changes in the capital stocks of loads. Short term load demand models, which are the emphasis of this research, are needed in the operation of the system. For example, total system load is needed for operations scheduling; bus load forecasts are useful for security assessment as well as online control. Furthermore, effective load management requires the use of load demand models.

Short term load demand modeling and forecasting has been studied extensively. Traditional approaches [8-18] are mostly based on model identification. Empirical load data at the bulk (system or subsystem) level are used to find the parameters in a postulated model structure. These approaches can be roughly divided into two kinds: those utilizing the stochastic state space model [19] and those utilizing time series or ARIMA (autoregressive integrated moving average) models [20]. Since excellent surveys [21,22] and bibliographies [23,24] are available, we shall not go into the details here. A comparison of these models can also be found in the thesis [25].

The identification based approach models the total load as seen by the utility by a black box, with little reference to the internal processes which

generate the demand and the load composition. Historical data is then used to generate the parameters values for the black box. This approach may have been satisfactory in the past when things are quite static. With the introduction of new practices in operating electric power systems, the limitations in these approaches have begun to surface. One such practice which calls for the use of better models is load management.

Load management can be defined as "the deliberate control or influencing of the customer load in order to shift the time and amount of use of electric power and energy" [26]. The use of load management thus requires a better understanding of the physical composition of the load and the customer behavior than is possible from an identification based model. For example, after a service interruption to a group of customers, the behavior of the load depends very much on the composition of the load and its physical characteristics. Historical data can be useful in arriving at a load model, but only after a model structure appropriate for the group has been found.

This need has motivated the research in so called physically based load modeling [27-39]. This approach explicitly recognizes the fact that the load at any point in the system is determined by a large number of devices with different characteristics and belonging to different consumers. A "bottom up" synthesis should then be used to generate the load at any point starting from the elementary component loads. The synthesis process can be either simulation based, as in [27,28] or analytic as in [29,30,37-39]. Simulation based approaches have the potential of being more realistic since more complicated models can be used. They are not, however, suitable for analytical studies.

Much of the work in physically based load modeling assumed that the component demands are more or less deterministic. Exceptions are the work reported in [38-40]. However, the fundamental decision processes which gener-

ate these demands are stochastic in nature. Emphasis on the stochastic aspects of the problem has been a feature of our research.

1.3 Overview of Results

We have developed a methodology for synthesizing the electric load at a point in the system starting from a description of the elementary devices. The fundamental decision processes which generate the load for each device are modeled by means of stochastic processes. These models are physically based and reflect the basic energy conversion function of the devices responding to the needs of the customers.

The overall synthesis methodology is hierarchical in nature, moving in stages from the distribution level to the bulk power level. At each level, aggregation techniques are used to generate an aggregate model for a group of loads below that level. Four steps are needed at each level: modeling of the primitive loads, classification of loads, aggregation and model validation. These steps have been investigated for the lowest level.

A canonical model for an elementary device is shown to consist of two parts: a functional model which accounts for the dynamics of energy storage in the load and an electric device model which describes the effects of a change in the voltage and frequency. These two models correspond to the load demand and response models at the elementary component or device level.

Since aggregation of load response models is a better known topic, our emphasis in aggregation has been on load demand models. The functional models can be aggregated statistically to obtain the load demand models. The feasibility of the aggregation technique has been illustrated on a class of functional models which represent space heating or air conditioning. The result consists of coupled partial differential equations which can be used to describe the fraction of "on" loads in a class at any particular time. This

model can be used to study effects of load management schemes as well as the payback phenomenon in cold load pickup. For this class of loads, the parameters needed for the model can be obtained readily by collecting data on the individual loads. Simulations have been conducted to highlight the use of the aggregate model using cold load pickup as the scenario.

1.4 Report Organization

This report is organized as follows. Section 2 describes the overall modeling methodology. A canonical model for the elementary component load is presented in Section 3. In Section 4, the classification of the elementary components loads into classes which can be aggregated is discussed. Section 5 presents the aggregation of functional models to obtain an aggregate load demand model. The technique is applied to a class of loads corresponding to space heating. Some analytic results pertaining to this model are also given. Numerical simulation results for the cold load pickup problem are given in Section 6. Section 7 discusses the data requirements for this model as well as its validation. Some concluding remarks and suggestions for future research are given in Section 8. Several appendices contain the miscellaneous proofs and derivations.

Some additional results related to this research can also be found in [25].

2. OVERALL METHODOLOGY

2.1 Model Hierarchy

The overall load modeling methodology is bottom-up, i.e., the load model at any point in the system is to be synthesized using the elementary component loads as the starting point. Because of the structure of the system, it is natural to synthesize the system load in a hierarchical manner. Figure 2.1 illustrates the natural hierarchy associated with the load models. At the lowest level in the hierarchy, we have the individual electrical devices (components). The next level consists of individual buildings. In many cases these correspond to individual customers or billing units. The individual customers are connected to the substations which constitute the next level. The substations are then connected to the overall system. Frequently the customers are partitioned into groups for load management. Some elementary loads corresponding to large machines may be directly connected to the substation or bulk power level.

The overall load model can then be synthesized in a hierarchical manner. A load model at the building level can be found for the group of electrical loads in the building. The various building load models can then be used to synthesize the load model at the substation level. The substation level loads are then aggregated or combined to obtain the load model at the bulk power level. Frequently, however, it may be desirable to find models at the substation level from the elementary devices since there may be little similarity among the loads at the building level to warrant any meaningful aggregation.

The different levels may exhibit different characteristics. For example, individual buildings are connected to a substation by the distribution network

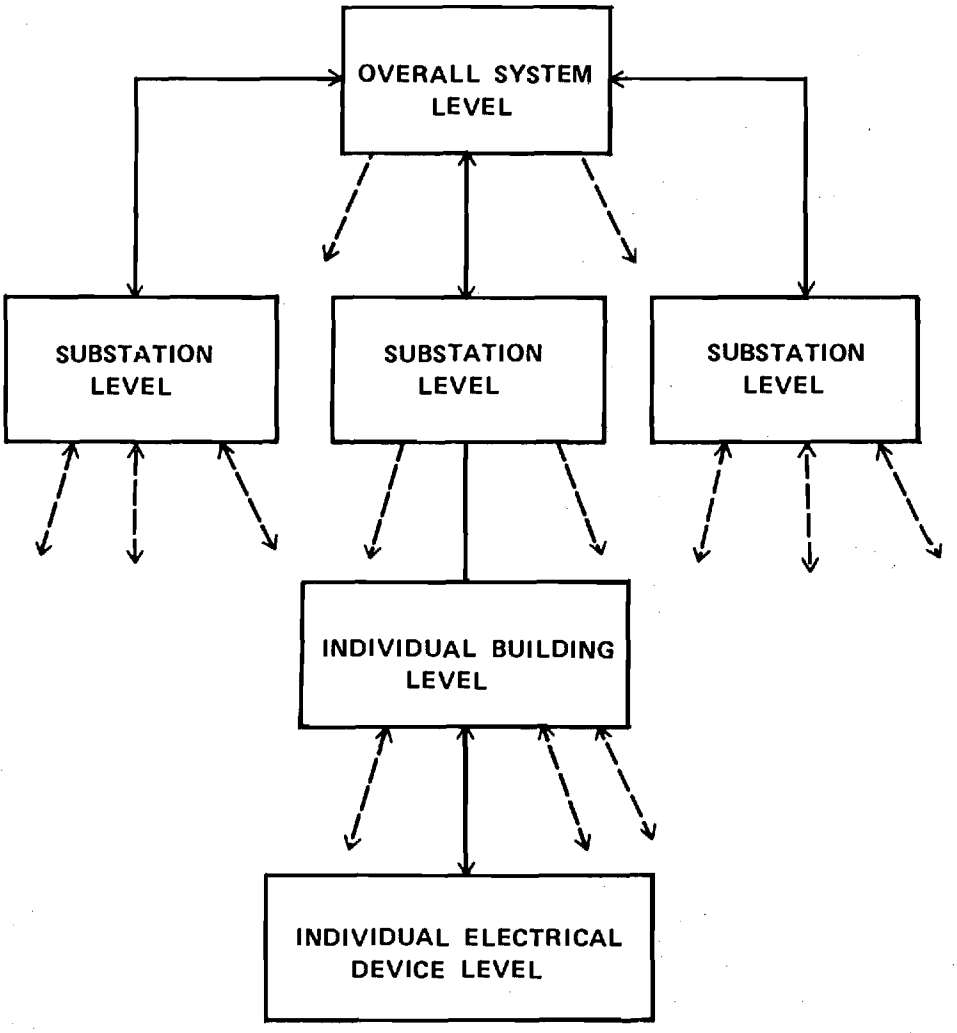

Figure 2-1. Hierarchies Associated with Load Model

which is usually radial. On the other hand, substations are usually connected by a network which is not radial. These differences in the network configuration as well as in the types of loads will result in different load models at each level. However, certain basic steps will be used to generate the load model at one level using the load models at the lower level. These steps will be discussed in the next subsection.

2.2 Procedure at Each Level

At each level in the modeing hierarchy, four basic steps are needed to generate the load model at the next level. They are:

(a) Modeling of the Primitive Components

A model is postulated for each component at that level to reflect the key features affecting the load. If the level is the lowest one, then this step models the elementary component loads in the system. At any other level, the primitive component should already have a model which is the result of modeling efforts at a lower level. On the other hand, sometimes further manipulation may be needed to bring out the relevant features at a given level.

(b) Classification of Loads

One would expect that only component loads which are similar can be aggregated or combined into equivalent loads at the next level. It is thus necessary to classify the loads into equivalent classes for which simplified models can be obtained. Similarity is a function of the representation of the load chosen for the level. At the lowest level, similarity can be defined in terms of demand and electrical characteristics.

(c) Aggregation of Primitive Components

The loads which are similar in characteristics are then aggregated to obtain an equivalewnt model for the group. In general, both load response and load demand models will be generated. The exact aggregation procedure depends

on the models to be aggregated. For example, load response models represented by dynamic system equations can be aggregated using techniques from system theory. Statistical techniques may be needed for aggregating load models represented by stochastic processes.

(d) Model Validation

The resulting models can be validated by comparing the predictions of the model with real data or a detailed simulation.

As a result of these four steps, we gradually move up the model hierarchy to arrive at a model with the desired level of detail. We should note that for this procedure to be meaningful, the primitive components should have parameters which are either known or can be estimated from measurements. Furthermore, the complexity of the model is not specified a priori, but depends on the natural complexity in the system reflected in the number of dissimilar groups and other factors.

These four steps will be elaborated in the rest of the report by focussing on the modeling of load demand at a substation starting at the lowest level. The application of the methodology at other levels will be similar although the detailed aggregation technique depends on the particular level and can be quite complicated if networks are involved.

3. REPRESENTATION OF ELEMENTARY COMPONENT LOAD

3.1 Introduction

Since the load modeling methodology is physically based, we need to develop models for the individual components or devices which constitute the elementary (primitive) loads in the system. These include individual lights, air conditioners, space heaters, water heaters, refrigerators, washers and dryers, etc., in the residential sector, and various industrial loads such as synchronous and induction motors, or arc furnaces in the industrial sector. A similar list can be given for the commercial sector. The power demand of each of these components is affected by a variety of inputs such as human use patterns, the weather, the system voltage and frequency. The exact relationship depends on the particular component in question but may be dynamic in nature since the present load may depend on the past history of the influence factors. Furthermore, the relationship is usually nonlinear. Thus the model of an elementary component load is in general a nonlinear dynamic system. Such nonlinear dynamic systems are difficult to analyze and even more difficult to aggregate. To facilitate our analysis we hypothesize a canonical structure for each device based on an examination of the process by which the influence factors affects the load. This canonical model, used to represent each elementary load, consists of the interconnection of two dynamic systems: a functional model which relates the demand for the service of the component to the functional state of the device and an electrical model which summarizes the effect on the load demand due to changes in the voltage or the frequency.

In the following subsections, we shall elaborate on the decomposition of the load model. This decomposition allows us to establish the connection

between load demand and load response at the component level. Once aggregation has been carried out, the same questions can then be answered at the system level. This canonical model has been reported previously in [31] and [41].

3.2 Structure of Individual Component Load Models

For any individual component, the load (real and reactive power) depends on the time (hour of the day, day of the week, etc.), the weather, human use patterns, the voltage and the frequency of the electric supply. The dependence is generally dynamic in nature so that a component load model is a dynamic system with the following inputs and outputs:

Inputs - weather
human use patterns
voltage
frequency

Outputs - real power
reactive power

Note that the human use patterns may be a function of the weather which is usually dependent on time. The inputs can be divided into two types:

a. Energy demand-generating inputs: These are inputs which generate a demand for the energy provided by the component. They depend on the time of the day, the weather and the human use pattern. The energy demand is the net input into the component load model and is independent of the voltage and frequency. It may be modified by actions such as time-of-the-day pricing and other incentives.

b. System inputs: Inputs such as voltage and frequency originate from the supply end of the power system. They are independent of the individual service demands, but are determined at the system level by the total load con-

nected, the configuration of the network and the state of the generating system.

These two types of inputs interact to determine the output (load) of the component in the following manner. The main function of each component is energy conversion, transforming electrical energy into other types of energy on demand. This demand is the energy demand and depends on certain inputs as described above. The energy needed is provided by the energy converter and its supply depends on the system inputs, namely, the voltage and frequency. In many components, the physical construction allows for some storage of the energy demanded. In this case, a demand for the energy of the component may not result immediately in a demand for electricity. Rather, a control mechanism determines the operating state of the energy converter, whether it should be on or off, or somewhere in between, based on the energy storage and the energy demand. Table 3.1 lists several residential component loads, the types of energy demanded and whether storage is possible.

The partition of the inputs into two types affecting different parts of the component with distinct functions suggests the decomposition of the load model into a functional model and an electric device model. The functional model has as its external inputs all factors which affect the energy demand of the component and generates the operating state of the energy converter as its output. Physically, it corresponds to the energy storage portion of the component (plus the part of the environment that affects the energy storage) and the control mechanism. The electrical device model has as its external inputs the voltage and frequency of the power supply and generates the electrical loads as the output. Physically it corresponds to the energy conversion portion of the component.

Table 3-1. Residential Components as Energy Converters

Component	Type of energy demanded	Possibility of energy storage
Incandescent lights	Thermal radiation in the visible range	No
Hi-Fi equipment	Mechanical energy in the audio range	No
Electric oven	Thermal energy	Yes
Electric water heater	Thermal energy	Yes
Electric space heater	Thermal energy	Yes
Washer	Mechanical energy	No

There is interaction between the two subsystems in the load model. The functional (operating) state of the functional model evolves according to the power supplied by the energy converter as well as the energy withdrawal due to the external inputs. The operation of the electric device model, of course, depends on the functional state. The interconnection of the two models are given in Figure 3.1.

Mathematically we have the following. Let:

$u(t)$ be the vector of system inputs, i.e., voltage and frequency at time t,

$v(t)$ be the demand due to human use pattern

$w(t)$ be the weather input

$y(t)$ be the power demand at time t.

Then the component load model is

$$y(t) = F(t,u(\tau),v(\tau),w(\tau),\ \tau \leq t) \tag{3.1}$$

where F depends on the component under consideration. Note that in general $y(t)$ depends on the past histories of the inputs. The decomposition of the load model implies that (3.1) is now replaced by the following three equations

$$y(t) = F_e(t,u(\tau),m(\tau),\ \tau \leq t)\ , \tag{3.2}$$

$$p(t) = G(y(t))\ , \tag{3.3}$$

and

$$m(t) = F_f(t,v(\tau),w(\tau),p(\tau)\ \ \tau \leq t) \tag{3.4}$$

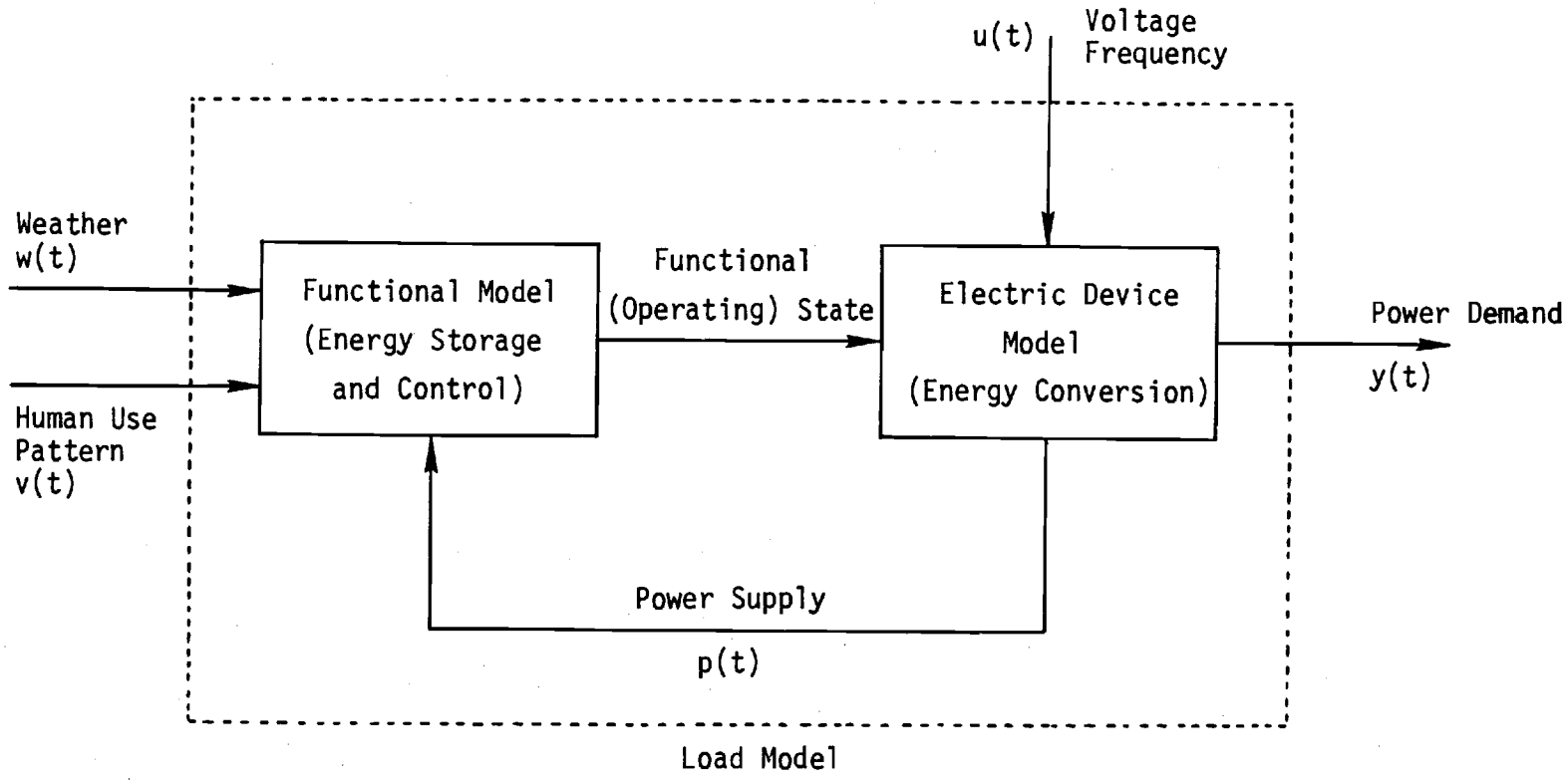

Figure 3-1. Decomposition of Component Load Model

where m(t) is the functional state of the load and p(t) is the power supplied. F_e describes the electric device model and F_f the functional model. Note that as far as F_e is concerned, m(t) is an external input. Similarly, p(t) is the external input to the functional model. p(t) represents the feedback from the electric device model to the functional model and summarizes the effect of the system input u(t) on the functional state. In a water heater, for instance, a drop in the thermal power supplied by the energy converter due to a drop in the voltage will result in longer time for the water to heat up to the temperature of the thermostat setting. The functional state will then evolve at a different rate.

3.3 Functional Model

The functional model is a very important part of the overall component model. It is highly dependent on the intended use of the device and its interaction with the environment. Two devices which have the same electrical construction may have radically different functional models if they serve different purposes. One example is two identical heaters installed in two houses with different thermal characteristics. The functional model characterizes the evolution of the load due to environmental and human use factors. In the absence of voltage and frequency changes, the functional model determines the dynamic behavior of the load demand. It is essential for components with energy storage and causes the component service demand and the electrical power demand to be in general different. As a result, a good understanding of the functional model is essential if one wants to understand, predict and manage the electrical power load.

Given the power p(t) supplied by the electric device model, the functional model relates m(t), the operating state of the electric device model to v(t) and w(t) which generate the energy demand for the component. One cannot

over-emphasize the point that the operating state of the component may not be the same as the energy demand. Take two water heaters with the same construction as an example. Identical demands for hot water may cause one water heater to turn on but not the other, depending on the initial temperature of the water. This is true whenever energy storage is possible in the component. Thus, m(t) should not be assumed a prior but should be computed given v(t), w(t), and p(t).

the external inputs into the functional model are v(t) and w(t). Since the use patterns for individual users are not known exactly, v(t) is a stochastic process. It is also reasonable to assume that conditional on w(t), the demand v(t) for different users will be independent. This will be used in the aggregation procedure later. The weather w(t) is actually a stochastic process, but can be assumed to be known if we want to characterize the behavior of a large number of component loads given the weather. m(t) may take on continuous values, as in the case of an incandescent light with a dimmer, or only discrete values as in a water heater. For discrete m(t), there may be two (Boolean or on-off) states as in the single element water heater or multiple states as in the dual element water heater. We shall be mostly concerned with the Boolean case.

Before a general functional model is introduced, we shall consider three typical classes of functional models. These three classes are not exhaustive but represent the bulk of component loads in the residential sector.

3.3.1 Memoryless Functional Model

In many devices, such as incandescent and fluorescent lights, television sets, etc., there is no energy storage in the component. The functional model becomes a memoryless or static system and m(t), the functional state of the component depends on the instantaneous value of v(t), the demand for service of the device.

$$m(t) = F_f(t,v(t)) \tag{3.5}$$

Statistically, if v(t) has only two states such as in a fluorescent light and on and off being the two states, it can be represented by means of an alternating renewal process [42]. The durations over which the demand is on is modeled as a sequence of independent random variables t_1, t_2, ... Similarly the durations over which the device is off is modeled as another sequence of independent random variables τ_1, τ_2, ... An interval t_i is followed by an interval τ_i, then by t_{i+1} and so on. This is illustrated in Figure 3.2. m(t) will exhibit the same type of on-off behavior. The probability distributions of the random variables t_i and τ_i may depend on time as well as another process such as the weather. If the probability densities of t_i and τ_i are exponential, then v(t) is a Markov jump process with two states.

In a general case, the magnitude of the demand v(t) may also be random but constant over each on period. We then have a general jump process. The functional state will also be a general jump process. This is the situation where the load is variable, as in an incandescent light with a dimmer.

3.3.2 Weakly Driven Functional Model

In some devices, the electrical energy is converted into other forms of energy which can be stored. Furthermore, the external factors which influence the energy storage behave like random noises with fairly flat spectral densities. An example may be found in the cooling or heating system of a building. In a residential building, heating and/or air conditioning account for a major part of the electrical load. The load model of such systems has been considered in [32]. The electrical part of the device turns on or off when the temperature reaches certain fixed values. To be specific, we shall

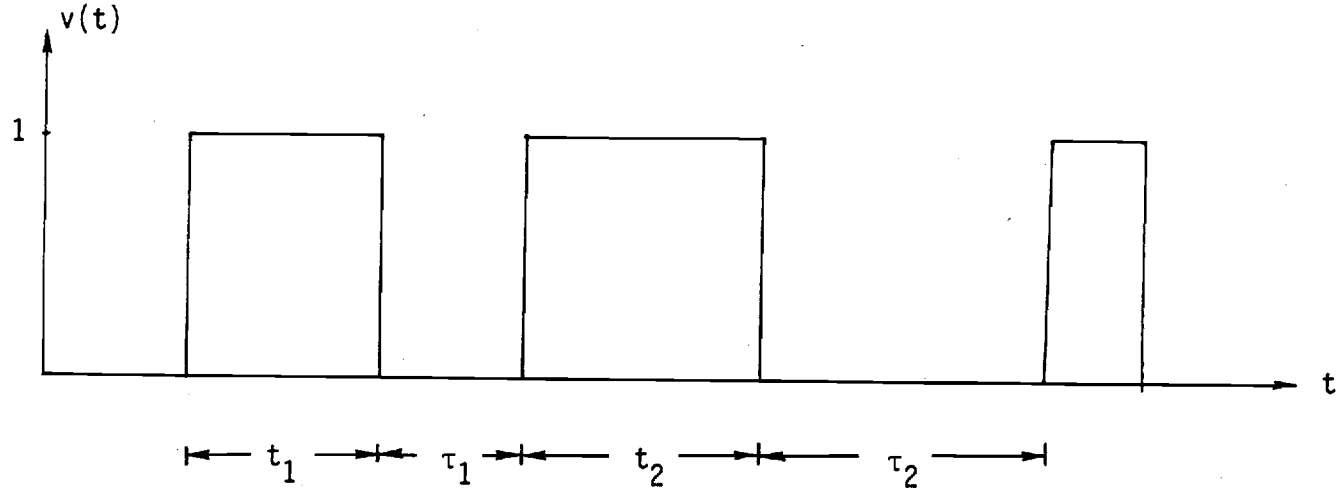

Figure 3-2. Service Demand Process v(t)

consider an electric heating system with a resistive heater activated by a thermostat. Heat is lost from the building through the walls, the floor and the roof. In addition, heat is also lost when somebody enters and leaves the building and gained from human activity. This type of effect can be modeled as noise. Functional models for a building can be very complicated. As a start we shall consider a highly simplified linear model given by the following stochastic differential equation

$$Cdx(t) = -\alpha(x(t) - x_a(t))dt + dv'(t) + p(t)m(t)b(t)dt \qquad (3.6)$$

where

- C is the average thermal capacity of the building
- α is the average loss rate through floors, walls and ceilings, etc.
- $v'(t)$ is a Wiener process of zero mean and variance parameter ν
- $x(t)$ is the temperature inside the building
- $x_a(t)$ is the ambient temperature
- $p(t)$ is the rate of heat supply from the resistive element
- $m(t)$ is the binary functional state: 1 (on) or 0 (off)
- $b(t)$ is the binary variable representing the load management control by the utility (1 if the device is connected, 0 otherwise).

Division of (3.6) by C yields

$$dx(t) = -a(x(t) - x_a(t))dt + dv(t) + Rm(t)b(t)dt \qquad (3.7)$$

where the definition of a and R is obvious. $v(t)$ is a Wiener process with variance parameter $\sigma = \nu C^{-1/2}$.

The switching of m(t) depends on the thermostat settings. Let x_+ and x_- be the temperature at which the heater is turned off and on. Then for arbitrarily small time increment Δt;

$$m(t + \Delta t) = m(t) + \pi(x(t), m(t); x_+, x_-) \tag{3.8}$$

where π is defined as:

$$\pi(x, m; x_+, x_-) = \begin{cases} 0 & x_- < x < x_+ \\ -m & x_+ \leq x \\ +m & x \leq x_- \end{cases} \tag{3.9}$$

Thus the functional model is composed of two interconnected subsystems (as shown in Figure 3.3): a linear system with a continuous state x(t) whose evolution depends on m(t) and a nonlinear system with discrete state m(t) whose transition is triggered by x(t). The continuous state system is the energy storage component while the discrete state system corresponds to the control mechanism. Notice that if the noise v(t) is absent, then the switching of m(t) between 0 and 1 is periodic. When noise is present, the cycling of m(t) is no longer deterministic. This type of cycling is observed in electric heaters and several other devices.

3.3.3 Strongly Driven Functional Model

The strongly driven functional model has the same structure as the weakly driven functional model of the previous section. v(t), the service demand, however, is now not a noise process. Rather, it is conscious demand by the consumer and can be modeled as a jump process, i.e., a random driving input which is piecewise constant. An example of this type of functional model can

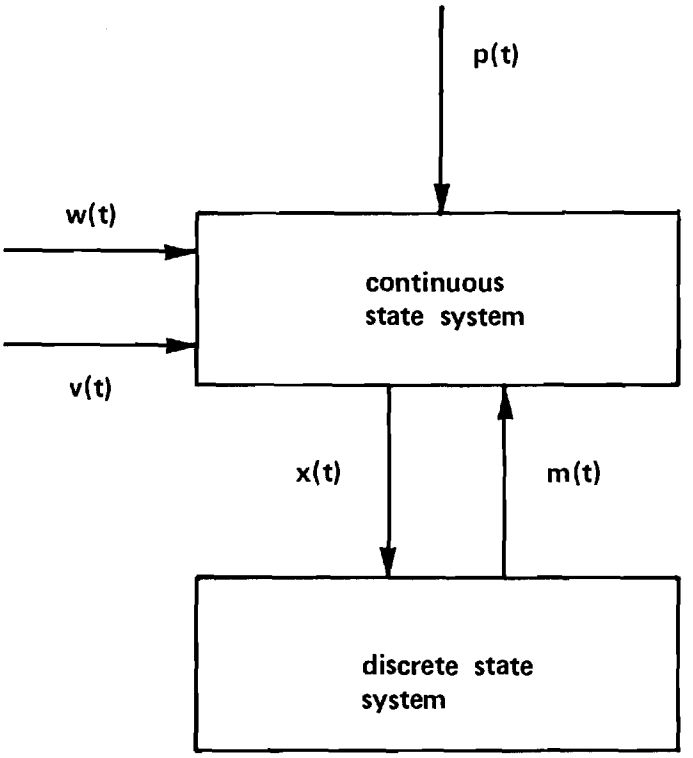

Figure 3-3. Interconnection of Continuous and Discrete States Subsystems.

be found in the electric water heater. A simple model of this, derived in Appendix A is given by

$$C\dot{x}(t) = -\alpha(x(t) - x_a(t)) - v(t)(x_d - x_i(t)) + p(t)m(t)b(t) \qquad (3.10)$$

where the symbols are as defined in Appendix A. For $x_i(t)$ constant the equation is similar to equation (3.6) except that v(t) is now piecewise constant with random switching times and random amplitudes. The discrete state m(t) switches between 0 and 1 according to equation (3.8).

Note that in this strongly driven model, m(t) is no longer a cycling process but depends on the arrival of the service demands. Furthermore, its switching time may also depend on the magnitude of v(t).

3.3.4 Stochastic Hybrid State Model

We now consider a general stochastic hybrid state model which includes all the special cases discussed earlier.

Given p(t), the feedback from the electric device model, each functional model is a dynamical system driven by v(t), the service demand which is a stochastic process. The output process m(t) is the electric device operating state. While it is possible for m(t) to take on continuous values, the more interesting case is when m(t) is a jump process with a finite set of possible values. If one seeks a state variable description, then two kinds of states will be present, a continuous state x(t) and a discrete state m(t) which also happens to the output. This type of model is a stochastic hybrid state system, which can be formalized as follows.

Let x(t) be a n-dimensional vector. Let the service demand v(t) be of the form

$$v(t) = \begin{vmatrix} v_1(t) \\ v_2(t) \end{vmatrix} \tag{3.11}$$

where $v_1(t)$ is a Wiener process and $v_2(t)$ a jump process. Both $v_1(t)$ and $v_2(t)$ may be vector-valued.

The continuous state $x(t)$ evolves according to the following stochastic differential equation

$$dx(t) = f(x(t),m(t),v_2(t),t)dt + g(x(t),m(t),v_2(t),t)dv_1(t) \tag{3.12}$$

where f and g are known functions. Note that the dependence on $p(t)$ has been suppressed for the time being. The evolution of $x(t)$ thus depends on the driving processes $v_1(t)$ and $v_2(t)$ as well as on the discrete state $m(t)$ and the supplied power $p(t)$ which is included in the functions f and g.

The discrete state $m(t)$ takes values in a set

$$M = \{m_1, m_2, \ldots\} \tag{3.13}$$

which may be assumed to be finite. For the special cases considered before in the previous sections

$$M = \{0, 1\} . \tag{3.14}$$

The switching of $m(t)$ depends on the continuous state $x(t)$. In the most general form, the probability of transition of $m(t)$ from m_j to m_i at time t depends on the past histories of both x and m. This can be expressed as

$$Pr\{m(t+dt) = m_i | x^t, m^t, m(t) = m_j\} = \lambda_{ij}(x^t, m^t, t)dt \tag{3.15}$$

where

$$x^t = \{x(s),\ s \leq t\}$$
$$m^t = \{m(s),\ s \leq t\} \tag{3.16}$$

and λ_{ij} is the instantaneous rate of transition m_j to m_i given x^t and m^t.

In Figure 3.3, the two subsystems can thus be described by equations (3.12) and (3.15) respectively. It is obvious that both the weakly driven and strongly driven functional models are special cases of this general model. Since little is known about the aggregation of this general model, we will not pursue this formalism in this report. Further discussion can be found in references [31] and [41].

3.4 Electric Device Models

The electric device model relates the electric power demand of the device to the supply voltage and frequency given the operating state of the electrical portion.

$$y(t) = F_e(t, u(\tau), m(\tau),\ \tau \leq t) \tag{3.17}$$

m(t), the operating state or functional state, may be Boolean, indicating whether the electrical device or energy converter is on or off. Or it may take on a continuous range of values as in the mechanical load a motor is called on to deliver. u(t), the system voltage and frequency, is an external input. y(t) is the electrical power demand on the supply system. p(t), the power supplied by the energy converter depends on the inputs m(t) and u(t) and affects the functional model.

Two components having identical functional models may have different electric models if the constructions of the energy converters are different. Under these circumstances, the responses of the two components to the same change in voltage or frequency will be different. For example, incandescent and fluorescent lights behave differently when there is a dip in the line voltage. When there is a feedback from the electric model to the functional model, the functional states will then also behave differently.

Strictly speaking, the initial states of the electric device models are also quite important. In many components, however, the dynamics of the electric models is much faster than that of the functional model so that for all practical purposes, one may deal with a steady state electric device model.

Since the modeling of electrical devices has been extensively studied (see references [4,5]), the rest of this report will focus on functional models and their aggregation.

4. CLASSIFICATION OF LOADS

4.1 The Classification Problem

Our goal is to represent the behavior of a group of loads by an equivalent model. Obviously components which have widely different characteristics cannot be grouped together. Thus the next step in the load modeling methodology is to identify the component loads which can be considered together as a group for which an aggregate load model can be obtained. The groups should be disjoint but collectively they should span the entire set of loads. With this decomposition, the overall load can then be represented in terms of all the equivalent group loads.

4.2 Homogeneous Groups

In this section we provide a scheme for partitioning the elementary component loads into groups with similar characteristics. As we have seen in Section 3, each elementary device can be characterized by a functional model which reflects its energy supply and demand dynamics and an electric device model which is related to its electrical characteristics. Furthermore, a device in general belongs to only one customer indexed by k. This suggests the following natural partitioning of the elementary loads. Consider a partitioning of all functional models into similar classes indexed by i and a similar partitioning of all electrical device models into similar classes indexed by j. All functional models in the same class would have similar energy storage characteristics. Likewise, all electric device models in the same class would react to a change in voltage and frequency in the same way.

An elementary device is thus indexed by the triple (i,j,k) where

i: functional class to which the device belongs;

j: electrical class to which the device belongs;

k: kth customer.

At the minimum the loads in each homogeneous group should have similar functional and electrical characteristics. Thus only devices or components with the same indices i and j can belong to the same homogeneous group. This condition is, however, not enough to guarantee similarity in the load behavior since different customers with the same components may generate different load profile if their use patterns are different. Thus we would further partition the set of customers into classes with similar use patterns such as education level, income, family size and so on. The effect of weather can also be incorporated if a class extends only over a limited geographical region. In some applications such as load management, it may also be desirable to have these classes coincide with the customers which are to be controlled together in load management.

As a result, we now have the following partitioning of the elementary component loads. Two loads indexed by (i,j,k) and (i',j',k') are similar if i=i', j=j' and k and k' belong to the same customer class. A set of similar loads then form a homogeneous group. A homogeneous group thus consists of devices which are similar in functional characteristics, electrical characteristics and use patterns.

5. AGGREGATION OF FUNCTIONAL MODELS

5.1 Problem Formulation

Given a classification of the loads with homogeneous groups, the aggregation process attempts to find an equivalent model for each group of loads. This represents the most difficult part in the load modeling methodology and the bulk of the research has been devoted to this topic.

Suppose the homogeneous group consists of the collection of devices represented by $\{i\}_1^n$. Let $P_i(t)$ be the power demand of the i^{th} device at time t. If the time constants are such that the electric and electromechanical transients can be nelgected, one has

$$P_i(t) = P_i(V,f)m_i(t) \tag{5.1}$$

where $P_i(V,f)$ as function of voltage and frequency is given by the steady state electric device model, and $m_i(t)$ is the functional state.

At the substation level, the total power demand for the group is given by

$$P(V,f,t) = \sum_{i=1}^{n} P_i(V,f)m_i(t) \tag{5.2}$$

where we have assumed that the loss in the network is negligible. If the group is assumed to be homogeneous, the electric device models for the loads should be similar, i.e., for all i

$$P_i(V,f) \approx P_{eq}(V,f) \tag{5.3}$$

where $P_{eq}(V,f)$ can be obtained as

$$P_{eq}(V,f) = \frac{1}{n} \sum_{i=1}^{n} P_i(V,f) \tag{5.4}$$

If we define

$$\bar{m}(t) = \frac{1}{n} \sum_{i=1}^{n} m_i(t) \tag{5.5}$$

to be the fraction of loads which are "on" at any time, then (5.2) can be approximately written as

$$P(V,f,t) \approx n\, P_{eq}(V,f)\bar{m}(t) \tag{5.6}$$

The following can be noted:

- Equation (5.6) is an approximation which improves as the similarity of the individual models increases.
- If it is desired to account for one type of dynamics (e.g. electromechanical transients associated with induction motors running compressors for cooling), $P_{eq}(v,f)$ can be replaced by $P_{eq}(v,f,t)$ in (5.6) where $P_{eq}(v,f,t)$ represents the dynamics of an "equivalent" machine.
- Although (5.6) can be modified to account for electrical transients, the calculation of $\bar{m}(t)$ need not be affected since any response model dynamics (electrical or electromechanical) are usually much faster than functional model dynamics (thermal). Thus the functional model "sees" only the steady-state of the response model.

Equation (5.6) elucidates the advantages of the decomposition introduced in Section 3. This decompositon allows the separation of the aggregation problem into two decoupled tasks: electric device model aggregation (equation (5.4))

to obtain the load response model and the functional model aggregation (equation (5.5)) to obtain the load demand model. The former is a deterministic aggregation problem and has been treated elsewhere [4-6]. Functional model aggregation, schematically represented in Figure 5-1, is a new stochastic aggregation problem and is our principal interest. The objective is to determine the dynamics of $\bar{m}(t)$ which will be called the aggregate functional state. Physically, $\bar{m}(t)$ represents the fraction of devices in the "on" state at time t.

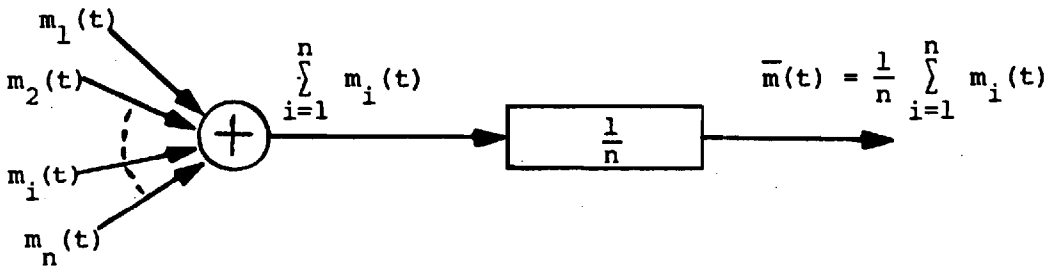

Fig. 5-1. Schematic Representation of Functional Model Aggregation.

The solution of the aggregation problem is considered only in the weakly-driven case (air conditioning and electric space heating). Important difficulties occur at two levels with the strongly-driven case: the precise modeling of service demand and the mathematics associated with a jump process.

In the following section, the aggregation problem is solved for the case of a homogeneous group of weakly-driven devices. This group consists of nearly identical devices with nearly identical functional models. A reasonable example of this can be found in a large apartment complex.

5.2 Aggregation of a Homogeneous Group

consider the case of a large homogeneous group of n weakly-driven devices. Also, for ease of discussion, suppose the devices are electric space heaters. We would like to compute $\bar{m}(t)$ for the group. The aggregation is based on the following assumptions.

Assumptions

a. Common external inputs: The loads are geographically close together so that any variations in the common inputs such as weather can be ignored.

b. Elemental Independence: Conditional on the weather and all other common inputs, the devices behave independently. In more rigorous terms, conditional on the common input proces such as the ambient temperature $x_a(t)$, all the random processes $m_i(t)$ are independent random processes.

Based on these assumptions and using Kolmogorov's law of large numbers [43], for n "large enough," $\bar{m}(t)$ can be approximated by

$$\bar{m}(t) = E_w(m_i(t)) \quad \forall\ i = 1,\ldots,n \tag{5.7}$$

where $E_w(\cdot)$ is the expected value operator conditional on weather treated as a known time varying input.

Equation (5.7) is fundamental to our research. First, it is a process of going from a discrete random variable ($\bar{m}(t)$) to a continuous one ($E_w(m_i(t))$). As such, it can be considered as a diffusion approximation (by analogy to the process of going from a discrete random walk to a continuous Brownian motion). Secondly, in the context of stochastic processes, we can view the homogeneous group as an approximate but finite ensemble realization

of the stochastic process described by equation (3.7). The evolution of the states from t=0 to t=∞ for any individual electric space heater would represent a particular sample path of the process. In this light, equation (5.7) can be interpreted as the process of estimating a statistical property of an ensemble ($E_w(m_i(t))$ via a finite sample average $\bar{m}(t)$.

5.2.1 Aggregate Functional Model

In this section, we present the results of the aggregation procedure which will be derived in Appendix B.

Theorem 1

$\bar{m}(t)$ evolves to the following system of coupled ordinary and partial differential equations,

$$\frac{d\bar{m}}{dt} = \frac{\sigma^2}{2} \frac{\partial}{\partial\lambda} f_{1b}(x_+,t) + \frac{\sigma^2}{2} \frac{\partial}{\partial\lambda} f_{ob}(x_-,t) \tag{5.8}$$

where $f_{1a}(\lambda,t)$ and $f_{ob}(\lambda,t)$ are the solutions of the following Coupled Fokker-Planck Equations (CFPE):

$$\frac{\partial f_1}{\partial t}(\lambda,t) = \frac{\partial}{\partial\lambda}[(a(\lambda - x_a(t)) - b(t)R) f_1(\lambda,t)]$$

$$+ \frac{\sigma^2}{2} \frac{\partial^2}{\partial\lambda^2} f_1(\lambda,t) \tag{5.9}$$

in regions a, b of Fig 5-2 and:

$$\frac{\partial f_o}{\partial t}(\lambda,t) = \frac{\partial}{\partial\lambda}[(a(\lambda - x_a(t)) f_o(\lambda,t)] + \frac{\sigma^2}{2} \frac{\partial^2}{\partial\lambda^2} f_o(\lambda,t) \tag{5.10}$$

in regions b, c of Fig 5-2, subject to the following boundary conditions.

Absorbing Boundaries:

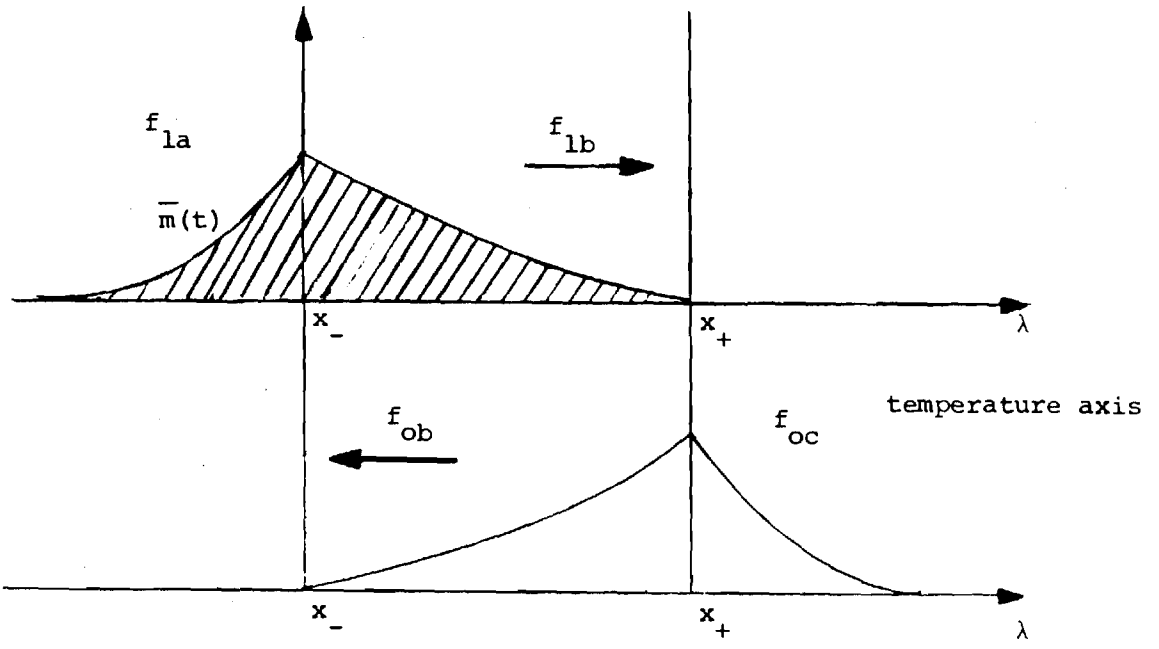

Figure 5-2. Illustration of Dynamical System. x_- and x_+ are the lower and upper edges of thermostat dead band respectively. $\bar{m}(t)$ is the total area under the "on" density at any time. The arrows represent the direction of temperature drift (in the case of electric space heating).

$$f_{1b}(x_+,t) = f_{ob}(x_-,t) = 0 \qquad t > 0 \tag{5.11}$$

Conditions at Infinity:

$$f_{1a}(-\infty,t) = f_{oc}(+\infty,t) = 0 \qquad t > 0 \tag{5.12}$$

Continuity Conditions:

$$f_{1a}(x_-,t) = f_{1b}(x_-,t) \qquad t > 0 \tag{5.13}$$

$$f_{ob}(x_+,t) = f_{oc}(x_+,t) \qquad t > 0 \tag{5.14}$$

Probability Conservation:

$$-\frac{\partial}{\partial\lambda} f_{1a}(x_-,t) + \frac{\partial}{\partial\lambda} f_{1b}(x_-,t) + \frac{\partial}{\partial\lambda} f_{ob}(x_-,t) = 0 , \qquad t > 0 \tag{5.15}$$

$$\frac{\partial}{\partial\lambda} f_{oc}(x_+,t) - \frac{\partial}{\partial\lambda} f_{ob}(x_+,t) - \frac{\partial}{\partial\lambda} f_{1b}(x_+,t) = 0 \qquad t > 0 \tag{5.16}$$

The above results can be interpreted in the following way. $f_1(\lambda,t)$ and $f_o(\lambda,t)$ are actually probability densities for the "hybrid states" $\{x(t),m(t)\}$ of the functional model. To be more precise

$$f_1(\lambda,t)d\lambda = \Pr[(\lambda < x(t) \leq \lambda + d\lambda) \cap (m(t) = 1)] \tag{5.17}$$

$$f_o(\lambda,t)d\lambda = \Pr[(\lambda < x(t) \leq \lambda + d\lambda) \cap (m(t) = 0)] \tag{5.18}$$

Equations (5.9) and (5.10) describe how the probability densities of the temperature x(t) evolve given that it is in a given functional state m(t). The evolution depends on the heat (temperature) gain and loss rate as well as the noise variance parameter. Equation (5.8) and $\bar{m}(t)$ can be written as

$$\frac{d\bar{m}}{dt} = g_o(t) - g_1(t) \tag{5.19}$$

where

$$g_o(t) = \frac{\sigma^2}{2} \frac{\partial f_{ob}}{\partial \lambda} (x_-,t) \tag{5.20}$$

and

$$g_1(t) = -\frac{\sigma^2}{2} \frac{\partial f_{1b}}{\partial \lambda} (x_+,t) \tag{5.21}$$

$g_1(t)$ and $g_o(t)$ are the rates of probability absorption from "on" to "off" through boundary x_+, and from "off" to "on" through boundary x_- respectively, at time t. Thus $d\bar{m}(t)/dt$ is the rate of loads being turned on minus the rate of loads being turned off.

The boundary conditions fall into four classes. (5.15) and (5.16) are the conservation equations. They couple the partial differential equations (5.9) and (5.10) together and state that the probability lost by the on state has to move into the off state and vice versa.

5.2.2 Approximate Analysis of the CFPE Model

In this section we consider a simplified version of the equations (5.9) and (5.10) which are more amenable to analysis. It is assumed that most of the densities $f_1(\lambda,t)$ and $f_o(\lambda,t)$ are confined within the dead band. This should generally be true in practical situations. The dead band itself is a very narrow range of temperature (typically 1.1°C). This means in equation (3.7), the charging rate $(Rb(t) - a(\lambda - x_a(t)))$ and the discharge rate $(a(\lambda - x_a(t))$ are practically constant (for constant weather conditions,

and for the duration of the control b(t)). Designate these values by r and c respectively. Under the assumption (5.9)-(5.10) reduce to:

$$\frac{\partial f_1}{\partial t}(\lambda,t) = -r\frac{\partial}{\partial \lambda} f_1(\lambda,t) + \frac{\sigma^2}{2}\frac{\partial^2}{\partial \lambda^2} f_1(\lambda,t) \tag{5.22}$$

$$\frac{\partial f_o}{\partial t}(\lambda,t) = c\frac{\partial}{\partial \lambda} f_o(\lambda,t) + \frac{\sigma^2}{2}\frac{\partial^2}{\partial \lambda^2} f_o(\lambda,t) \tag{5.23}$$

This approximation of the CFPE model becomes a system of space-homogeneous, linear time-invariant Fokker-Planck equations coupled through boundary conditions (5.15)-(5.16). In the following, we develop results pertaining to (5.22)-(5.23) in the transform domain.

For a given function f(t) denote by f*(s) the unilateral Laplace transform of f(t) when it exists. Laplace transformation of (5.22)-(5.23) and (5.11)-(5.16) yields the following two groups of equations:

$$\mathbf{P_1} - \qquad sf_1^*(\lambda,s) - f_1^o(\lambda) = -r\frac{\partial}{\partial \lambda} f_1^*(\lambda,s) + \frac{\sigma^2}{2}\frac{\partial^2}{\partial \lambda^2} f_1^*(\lambda,s) \tag{5.24}$$

in regions a, b and c of Fig. 5-2 and:

$$f_1^*(x_+,s) = 0 \tag{5.25}$$

$$\lim_{\lambda \to -\infty} f_1^*(\lambda,s) = 0 \tag{5.26}$$

$$-\frac{\partial}{\partial \lambda} f_{1a}^*(x_-,s) + \frac{\partial}{\partial \lambda} f_{1b}^*(x_-,s) = -\frac{2}{\sigma^2} g_o^*(s) \tag{5.27}$$

$$\mathbf{P_2} - \qquad sf_o^*(\lambda,s) - f_o^o(\lambda) = c\frac{\partial}{\partial \lambda} f_o^*(\lambda,s) + \frac{\sigma^2}{2}\frac{\partial^2}{\partial \lambda^2} f_o^*(\lambda,s) \tag{5.28}$$

in regions b and c of Fig 5-2 and:

$$f_o^*(x_-,s) = 0 \tag{5.29}$$

$$\lim_{\lambda\to+\infty} f_o^*(\lambda,s) = 0 \tag{5.30}$$

$$\frac{\partial}{\partial\lambda} f_{oc}^*(x_+,s) - \frac{\partial}{\partial\lambda} f_{ob}^*(x_+,s) = -\frac{2}{\sigma^2} g_1^*(s) \tag{5.31}$$

where g_o and g_1 are defined in (5.20) and (5.21)

$f_1^*(\lambda,s)$ and $f_o^*(\lambda,s)$ are completely decoupled except through boundary conditions (5.27) and (5.31). Therefore, if $g_1^*(s)$ and $g_o^*(s)$ are considered to be known functions of s, systems P_1 and P_2 can be solved separately.

System P_1 is now considered. The second order linear differential equation (5.24) in λ, with constant coefficients can be written in state form as:

$$\frac{\partial}{\partial\lambda}\begin{vmatrix} f_1^*(\lambda,s) \\ \frac{\partial}{\partial\lambda} f_1^*(\lambda,s) \end{vmatrix} = \begin{vmatrix} 0 & 1 \\ \frac{2s}{\sigma^2} & \frac{2r}{\sigma^2} \end{vmatrix} \begin{vmatrix} f_1^*(\lambda,s) \\ \frac{\partial}{\partial\lambda} f_1^*(\lambda,s) \end{vmatrix} - \frac{2}{\sigma^2}\begin{vmatrix} 0 \\ 1 \end{vmatrix} f_1^o(\lambda) \tag{5.32}$$

Using the state transition matrix [19] for the above system, it is possible to write the solutions in regions a and b of Fig. 5-2 in terms of the value of the state at $\lambda = x_-$, i.e. in terms of $f_1^*(x_-,s)$ and $\frac{\partial}{\partial\lambda} f_{1a}^*(x_-,s)$ or $f_1^*(x_-,s)$ and $\frac{\partial}{\partial\lambda} f_{1b}^*(x_-,s)$ respectively:

$$f_1^*(\lambda,s) = \phi_{11}(\lambda-x_-,s) f_1^*(x_-,s) + \phi_{12}(\lambda-x_-,s) \frac{\partial f_1^*}{\partial\lambda}(x_-,s)$$

$$- \frac{2}{\sigma^2}\int_{x_-}^{\lambda} \phi_{12}(\lambda-x,s) f_1^o(x)\,dx \tag{5.33}$$

$$\frac{\partial f_1^*}{\partial \lambda}(\lambda,s) = \phi_{21}(\lambda-x_-,s) f_1^*(x_-,s) + \phi_{22}(\lambda-x_-,s) \frac{\partial f_1^*}{\partial \lambda}(x_-,s)$$

$$- \frac{2}{\sigma^2} \int_{x_-}^{\lambda} \phi_{22}(\lambda-x,s) f_1^o(x)\,dx \tag{5.34}$$

where it can be shown (Appendix C) that:

$$\underline{\phi}(\lambda,s) = [\phi_{ij}(\lambda,s)] = \exp\begin{vmatrix} 0 & 1 \\ \frac{2s}{\sigma^2} & \frac{2r}{\sigma^2} \end{vmatrix} \lambda \tag{5.35}$$

and

$$\phi_{11}(\lambda,s) = \theta^{-1}(s)\left[\theta_1(s) e^{\theta_2(s)\lambda} - \theta_2(s) e^{\theta_1(s)\lambda}\right], \tag{5.36}$$

$$\phi_{12}(\lambda,s) = \theta^{-1}(s)\left[e^{\theta_1(s)\lambda} - e^{\theta_2(s)\lambda}\right], \tag{5.37}$$

$$\phi_{21}(\lambda,s) = \frac{2s}{\sigma^2}\theta^{-1}(s)\left[e^{\theta_1(s)\lambda} - e^{\theta_2(s)\lambda}\right], \tag{5.38}$$

$$\phi_{22}(\lambda,s) = \theta^{-1}(s)\left[\theta_1(s) e^{\theta_1(s)\lambda} - \theta_2(s) e^{\theta_2(s)\lambda}\right]. \tag{5.39}$$

With

$$\theta(s) = \frac{2}{\sigma^2}(r^2 + 2s\sigma^2)^{1/2},$$

$$\theta_1(s) = \frac{r}{\sigma^2} + \frac{\theta(s)}{2}, \tag{5.40}$$

$$\theta_2(s) = \frac{r}{\sigma^2} - \frac{\theta(s)}{2}. \tag{5.41}$$

Now consider boundary condition (5.26). It requires that as $\lambda \to -\infty$, $f_1^*(\lambda,s)$ remains bounded. However, the expression (5.33) for $f_1^*(\lambda,s)$ contains an unstable exponential since for Re[s] > 0 as $\lambda \to -\infty$, $e^{\theta_2(s)\lambda} \to +\infty$. The unstable component of $f_1^*(\lambda,s)$ can be written:

$$I(\lambda) = \Big[e^{-\theta_2(s)x_-}\theta_1(s)\theta^{-1}(s)f_1^*(x_-,s) - \theta^{-1}(s)e^{-\theta_2(s)x_-}\frac{\partial}{\partial\lambda}f_{1a}^*(x_-,s)$$

$$+\frac{2}{\sigma^2}\int_{x_-}^{\lambda}\theta^{-1}(s)e^{-\theta_2(s)x}f_1^o(x)dx\Big]e^{\theta_2(s)\lambda} \qquad (5.42)$$

In order that $f_1^*(\lambda,s)$ remain bounded, it is necessary that:

$$(\theta_1(s)e^{-\theta_2(s)x_-})f_1^*(x_-,s) - e^{-\theta_2(s)x_-}\frac{\partial f_{1a}^*}{\partial\lambda}(x_-,s)$$

$$+\frac{2}{\sigma^2}\int_{x_-}^{-\infty}e^{-\theta_2(s)x}f_1^o(x)dx = 0 \qquad (5.43)$$

Boundary condition (5.25) yields:

$$f_1^*(x_+,s) = 0 = f_1^*(x_-,s)\big[\theta_1(s)e^{\theta_2(s)\Delta} - \theta_2(s)e^{\theta_1(s)\Delta}\big]\theta^{-1}(s)$$

$$+\theta^{-1}(s)\big[e^{\theta_1(s)\Delta} - e^{\theta_2(s)\Delta}\big]\frac{\partial f_{1b}^*}{\partial\lambda}(x_-,s)$$

$$-\frac{2}{\sigma^2}\int_{x_-}^{x_+}\theta^{-1}(s)\big[e^{\theta_1(s)(x_+-x)} - e^{\theta_2(s)(x_+-x)}\big]f_1^o(x)dx \qquad (5.44)$$

where $\Delta = x_+ - x_-$ (width of the dead band).

Recalling (5.27) and using (5.43)-(5.44) we obtain:

$$f_1^*(x_-,s) = 2\big(\sigma^2\theta(s)\big)^{-1}\Big[(g_o^*(s) - \int_{x_-}^{-\infty}e^{\theta_2(s)(x_--x)}f_1^o(x)dx)(1-e^{-\theta(s)\Delta})$$

$$+ e^{-\theta_1(s)\Delta} \int_{x_-}^{x_+} \left(e^{\theta_1(s)(x_+-x)} - e^{\theta_2(s)(x_+-x)}\right) f_1^o(x)\,dx\Big] , \tag{5.45}$$

$$\frac{\partial f_{1a}^*}{\partial \lambda}(x_-,s) = 2(\sigma^2\theta(s))^{-1}\Big[\theta_1(s) g_o^*(s)(1 - e^{-\theta(s)\Delta})$$

$$+ \int_{-\infty}^{x_-} e^{-\theta_2(s)(x-x_-)} f_1^o(x)\,dx\ (\theta_2(s) - \theta_1(s) e^{-\theta(s)\Delta})$$

$$+ \theta_1(s) e^{-\theta_1(s)\Delta} \int_{x_-}^{x_+} \left(e^{\theta_1(s)(x_+-x)} - e^{\theta_2(s)(x_+-x)}\right) f_1^o(x)\,dx\Big] , \tag{5.46}$$

$$\frac{\partial f_{1b}^*}{\partial \lambda}(x_-,s) = 2(\sigma^2\theta(s))^{-1}\Big[\Big(g_o^*(s) + \int_{-\infty}^{x_-} e^{-\theta_2(s)(x-x_-)} f_1^o(x)\,dx\Big)$$

$$(\theta_2(s) - \theta_1(s) e^{-\theta(s)\Delta})$$

$$+ \theta_1(s) e^{-\theta_1(s)\Delta} \int_{x_-}^{x_+} \left(e^{\theta_1(s)(x_+-x)} - e^{\theta_2(s)(x_+-x)}\right) f_1^o(x)\,dx\Big] . \tag{5.47}$$

From knowledge of boundary conditions $f_1^*(x_-,s)$, $\frac{\partial f_{1a}^*}{\partial \lambda}(x_-,s)$, $\frac{\partial f_{1b}^*}{\partial \lambda}(x_-,s)$ and equation (5.33) it is possible to write an expression for $f_1^*(\lambda,s)$ everywhere.

In region a of Fig. 5-2, using (5.33), (5.45), (5.46), we have:

$$f_1^*(\lambda,s) = 2(\sigma^2\theta(s))^{-1}\Big[\int_{-\infty}^{\lambda} e^{\theta_2(s)(\lambda-x)} f_1^o(x)\,dx\left(1 - e^{\theta(s)(\lambda-x_+)}\right)$$

$$+ g_o^*(s) e^{\theta_1(s)(\lambda-x_-)} (1 - e^{-\theta(s)\Delta})$$

$$+ \int_{\lambda}^{x_+} e^{\theta_1(s)(\lambda-x)} \left(1 - e^{\theta(s)(x-x_+)}\right) f_1^o(x)\,dx\Big] \tag{5.48}$$

Similarly, in region b of Fig. 5-2, using (5.33), (5.45), (5.47) we have:

$$f_1^*(\lambda,s) = 2(\sigma^2\theta(s))^{-1}\Big[\big(1 - e^{\theta(s)(\lambda-x_+)}\big)\big(g_o^*(s)e^{\theta_2(s)(\lambda-x_-)} + \int_{-\infty}^{\lambda} e^{\theta_2(s)(\lambda-x)} f_1^o(x)\,dx\big) + \int_{\lambda}^{x_+} e^{\theta_1(s)(\lambda-x)} f_1^o(x)\big(1-e^{\theta(s)(x-x_+)}\big)dx\Big] \tag{5.49}$$

Recalling (5.21) we have:

$$g_1^*(s) = -\frac{\sigma^2}{2}\frac{\partial f_{1b}^*}{\partial\lambda}(x_+,s) \tag{5.50}$$

Differentiation of (5.49) with respect to λ yields:

$$\begin{aligned}\frac{\partial f_1^*}{\partial\lambda}(\lambda,s) = {} & 2(\sigma^2\theta(s))^{-1}\big(1 - e^{\theta(s)(\lambda-x_+)}\big)\frac{\partial}{\partial\lambda}\Big[g_o^*(s)e^{\theta_2(s)(\lambda-x_-)} + \int_{-\infty}^{\lambda} e^{\theta_2(s)(\lambda-x)} f_1^o(x)\,dx\Big] \\ & - \frac{2}{\sigma^2} e^{\theta(s)(\lambda-x_+)}\Big[g_o^*(s)e^{\theta_2(s)(\lambda-x_-)} + \int_{-\infty}^{\lambda} e^{\theta_2(s)(\lambda-x)} f_1^o(x)\,dx\Big] \\ & - 2(\sigma^2\theta(s))^{-1}\big[1 - e^{\theta(s)(\lambda-x_+)}\big]f_1^o(\lambda) \\ & + \int_{\lambda}^{x_+} \theta_1(s)e^{\theta_1(s)(\lambda-x)} 2(\sigma^2\theta(s))^{-1}\big(1 - e^{\theta(s)(x-x_+)}\big)f_1^o(x)\,dx\end{aligned} \tag{5.51}$$

At $\lambda = x_+$, (5.51), (5.50) and (5.25) yield:

$$g_1^*(s) = g_o^*(s)e^{\theta_2(s)\Delta} + \int_{-\infty}^{x_+} e^{\theta_2(s)(x_+-x)} f_1^o(x)\,dx \tag{5.52}$$

Assuming $g_o^*(s)$ is known, equations (5.48)-(5.49) and (5.52) represent the solution of P_1 in the transform domain.

We now turn to the problem of deriving corresponding results for system P_2, i.e. for the "off" density. Lengthy computations can be avoided if it is recognized that by using a change of variable:

$$y = x_+ + x_- - \lambda$$

and replacing r by c and $g_o^*(s)$ by $g_1^*(s)$ in equations (5.24)-(5.27), system P_1 can be transformed into a system formally identical to P_2.

To verify this, note that:

$$f_1^*(\lambda,s) = f_1^*(-y + x_+ + x_-, s) = f_1^{*'}(y,s) \tag{5.53}$$

$$\frac{\partial}{\partial\lambda} f_1^*(\lambda,s) = -\frac{\partial f_1^*}{\partial y}(-y + x_+ + x_-, s) = -\frac{\partial f_1^{*'}}{\partial y}(y,s) \tag{5.54}$$

$$\frac{\partial^2}{\partial\lambda^2} f_1^*(\lambda,s) = \frac{\partial^2 f_1^*}{\partial y^2}(x_+ + x_- - y, s) = \frac{\partial^2 f_1^{*'}}{\partial y^2}(y,s) \tag{5.55}$$

Substituting (5.53)-(5.55) into (5.24), and replacing r by c yields:

$$sf_1^{*'}(y,s) - f_1^{0'}(y) = c\frac{\partial f_1^{*'}}{\partial y}(y,s) + \frac{\sigma^2}{2}\frac{\partial^2}{\partial y^2} f_1^{*'}(y,s) \tag{5.56}$$

Futhermore (5.25)-(5.26) yield:

$$f_1^{*'}(x_-,s) = 0 \tag{5.27}$$

$$\lim_{y\to+\infty} f_2^{*'}(y,s) = 0 \tag{5.58}$$

Finally, using (5.54) and replacing $g_o^*(s)$ by $g_1^*(s)$ in (5.27) yields:

$$\frac{\partial}{\partial y} f_{1c}^{*'}(x_+,s) - \frac{\partial}{\partial y} f_{1b}^{*'}(x_+,s) = \frac{-2}{\sigma^2} g_1^*(s) \tag{5.59}$$

Clearly (5.56)-(5.59) is a system of equations formally identical to (5.28)-(5.31). This means that in general:

$$f_o^*(\lambda,s) = f_1^{*'}(\lambda,s) = f_1^*(x_+ + x_- - \lambda,s) \tag{5.60}$$

i.e., the solution of system $\mathbf{P_2}$ can be derived from the solution of system $\mathbf{P_1}$ by replacing λ by $(x_+ + x_- - \lambda)$, r by c and $g_o^*(s)$ by $g_1^*(s)$.

Using the above remark, the following results are obtained: In region b of Fig 5-2,

$$f_o^*(\lambda,s) = 2(\sigma^2\gamma(s))^{-1}\Big[\Big(g_1^*(s)e^{\gamma_2(s)(x_+-\lambda)} + \int_\lambda^{+\infty} e^{\gamma_2(s)(x-\lambda)} f_o^o(x)\,dx\Big)$$

$$\Big(1 - e^{\gamma(s)(x_--\lambda)}\Big)$$

$$+ \int_\lambda^{x_-} e^{\gamma_1(s)(x-\lambda)}\Big(1 - e^{\gamma(s)(x_--x)}\Big) f_o^o(x)\,dx\Big] \tag{5.61}$$

In region c of Fig. 5-2,

$$f_o^*(\lambda,s) = 2(\sigma^2\gamma(s))^{-1}\Big[\int_\lambda^{+\infty} e^{\gamma_2(s)(x-\lambda)} f_o^o(x)\,dx\Big(1 - e^{\gamma(s)(x_--\lambda)}\Big)$$

$$+ g_1^*(s)e^{\gamma_1(s)(x_+-\lambda)}\Big(1 - e^{-\gamma(s)\Delta}\Big)$$

$$+ \int_{x_-}^{\lambda} e^{\gamma_1(s)(x-x_-)} \left(1 - e^{-\gamma(s)(x_--x)}\right) f_o^o(x)\,dx \tag{5.62}$$

Finally:

$$g_o^*(s) = g_1^*(s) e^{\gamma_2(s)\Delta} + \int_{x_-}^{+\infty} e^{\gamma_2(s)(x-x_-)} f_o^o(x)\,dx \tag{5.63}$$

where in (5.61)-(5.63):

$$\gamma(s) = \frac{2}{\sigma^2}\left(c^2 + 2s\sigma^2\right)^{1/2},$$

$$\gamma_1(s) = \frac{c}{\sigma^2} + \frac{\gamma(s)}{2}, \tag{5.64}$$

$$\gamma_2(s) = \frac{c}{\sigma^2} - \frac{\gamma(s)}{2}. \tag{5.65}$$

Equation (5.52) and (5.63) yield:

$$g_1^*(s) = \int_{x_-}^{+\infty} \frac{e^{\theta_2(s)\Delta}\, e^{\gamma_2(s)(x-x_-)}}{F(s)} f_o^o(x)\,dx$$

$$+ \int_{-\infty}^{x_+} \frac{e^{\theta_2(s)(x_+-x)}}{F(s)} f_1^o(x)\,dx, \tag{5.66}$$

$$g_o^*(s) = \int_{-\infty}^{x_+} \frac{e^{\gamma_2(s)\Delta}\, e^{\theta_2(s)(x_+-x)}}{F(s)} f_1^o(x)\,dx$$

$$+ \int_{x_-}^{+\infty} \frac{e^{\gamma_2(s)(x-x_-)}}{F(s)} f_o^o(x)\,dx \tag{5.67}$$

where in (5.66)-(5.67)

$$F(s) = 1 - e^{(\theta_2(s) + \gamma_2(s))\Delta}$$

Recalling equations (5.19)-(5.21) we have:

$$\frac{\overline{dm}^*}{dt}(s) = g_o^*(s) - g_1^*(s) \tag{5.68}$$

(5.66)-(5.68) yield:

$$\frac{\overline{dm}^*}{dt}(s) = \int_{x_-}^{+\infty} \frac{\left(1 - e^{\theta_2(s)\Delta}\right)}{F(s)} e^{\gamma_2(s)(x-x_-)} f_o^o(x)\,dx$$

$$- \int_{-\infty}^{x_+} \frac{\left(1 - e^{\gamma_2(s)\Delta}\right)}{F(s)} e^{\theta_2(s)(x_+-x)} f_1^o(x)\,dx \tag{5.69}$$

Equation (5.69) gives an expression for the Laplace transform of $\frac{\overline{dm}}{dt}(t)$, i.e. the rate of change of the aggregate functional state $\overline{m}(t)$ for the homogeneous control group. Equations (5.48)-(5.49), (5.61)-(5.62), (5.66)-(5.67), (5.69) together represent the complete solution of the CFPE model in the transform domain. The inversion problem of the Laplace transform in equation (5.69) is, however, nontrivial.

5.2.3 Steady State Densities

In this section, the steady state solution (if it exists) for the system (5.22)-(5.23) is determined by applying the final value theorem [44] to the Laplace transforms in equations (5.48), (5.49), (5.66) and (5.67). The following results are obtained.

$$f_{1a}^{ss}(\lambda) = \lim_{s\to 0} s\, f_{1a}^{*}(\lambda,s)$$

$$= \frac{1}{r}\left(\lim_{s\to 0} s\, g_o^{*}(s)\right) e^{-\frac{2r}{\sigma^2}(x_- - \lambda)}\left[1 - e^{-\frac{2r\Delta}{\sigma^2}}\right], \qquad (5.70)$$

$$f_{1b}^{ss}(\lambda) = \lim_{s\to 0} s\, f_{1b}^{*}(\lambda,s)$$

$$= \frac{1}{r}\left(\lim_{s\to 0} s\, g_o^{*}(s)\right)\left(1 - e^{-\frac{2r}{\sigma^2}(x_+ - \lambda)}\right), \qquad (5.71)$$

$$f_{ob}^{ss}(\lambda) = \lim_{s\to 0} s\, f_{ob}^{*}(\lambda,s)$$

$$= \frac{1}{c}\left(\lim_{s\to 0} s\, g_1^{*}(s)\right)\left[1 - e^{-\frac{2c}{\sigma^2}(\lambda - x_-)}\right], \qquad (5.72)$$

$$f_{oc}^{ss}(\lambda) = \frac{1}{c}\left(\lim_{s\to 0} s\, g_1^{*}(s)\right) e^{-\frac{2c}{\sigma^2}(\lambda - x_+)}\left(1 - e^{-\frac{2\Delta c}{\sigma^2}}\right). \qquad (5.73)$$

where in (5.70)-(5.73), a superscript ss stands for steady-state, and:

$$\lim_{s\to 0} s\, g_1^{*}(s) = \lim_{s\to 0} \frac{s}{1 - e^{-(\theta_2(s) + \gamma_2(s))\Delta}}\left[\int_{x_-}^{\infty} f_o^{o}(x)\,dx + \int_{-\infty}^{x_+} f_1^{o}(x)\,dx\right] \qquad (5.74)$$

However:

$$\int_{x_-}^{\infty} f_o^{o}(x)\,dx + \int_{-\infty}^{x_+} f_1^{o}(x)\,dx = 1 \qquad (5.75)$$

and using L'Hôpital's rule:

$$\lim_{s\to 0} \frac{s}{1 - e^{-(\theta_2(s) + \gamma_2(s))\Delta}}$$

$$= \lim_{s\to 0} \frac{1}{\Delta e^{-(\theta_2(s) + \gamma_2(s))\Delta} \frac{d}{ds}(\theta_2(s) + \gamma_2(s))} \tag{5.76}$$

But, recalling (5.40) and (5.66), we have:

$$\frac{d}{ds}(\theta_2(s) + \gamma_2(s)) = \frac{1}{\sigma^2}\left[\frac{2\sigma^2}{\sqrt{r^2 + 2s\sigma^2}} + \frac{2\sigma^2}{\sqrt{c^2 + 2s\sigma^2}}\right] \tag{5.77}$$

(5.74), (5.76) and (5.77) yield:

$$\lim_{s\to 0} s\, g_1^*(s) = \frac{1}{\frac{\Delta}{r} + \frac{\Delta}{c}} \tag{5.78}$$

One can similarly show that:

$$\lim_{s\to 0} s\, g_o^*(s) = \frac{1}{\frac{\Delta}{r} + \frac{\Delta}{c}} \tag{5.79}$$

Substituting (5.78)-(5.79) back into (5.70)-(5.73) yields:

$$f_{1a}^{ss}(\lambda) = \frac{c}{\Delta(r+c)}\left[e^{-\frac{2rx_-}{\sigma^2}} - e^{-\frac{2rx_+}{\sigma^2}}\right] e^{\frac{2r\lambda}{\sigma^2}} \tag{5.80}$$

$$f_{1b}^{ss}(\lambda) = \frac{c}{\Delta(r+c)}\left[1 - e^{-\frac{2r}{\sigma^2}(x_+ - \lambda)}\right] \tag{5.81}$$

$$f_{ob}^{ss}(\lambda) = \frac{r}{\Delta(r+c)}\left[1 - e^{-\frac{2c}{\sigma^2}(\lambda - x_-)}\right] \tag{5.82}$$

$$f_{oc}^{ss}(\lambda) = \frac{r}{\Delta(r+c)} \left[e^{\frac{2cx_+}{\sigma^2}} - e^{\frac{2cx_-}{\sigma^2}} \right] e^{-\frac{2c\lambda}{\sigma^2}} \tag{5.83}$$

Finally, $\bar{m}_{ss}$, the steady-state of $\bar{m}(t)$ is given by:

$$\bar{m}_{ss} = \int_{-\infty}^{x_-} f_{1a}^{ss}(\lambda)\,d\lambda + \int_{x_-}^{x_+} f_{1b}^{ss}(\lambda)\,d\lambda \tag{5.84}$$

Substituting (5.80)-(5.81) into (5.84) we obtain after simple computations:

$$\bar{m}_{ss} = \frac{c}{r+c} \tag{5.85}$$

Remark 1: The steady-state densities (5.80)-(5.83) are very important because they represent the natural state of the uncontrolled system.

Remark 2: At this point, it is possible to verify whether, at least in a steady-state, the constant rates approximation of section 5.2.2 is valid or not. One should remember that the approximation rests on the assumption that under normal conditions most of the temperature probability densities lie within the dead band. A quantitative measure of the validity of this assumption is the fraction of the probability density outside the dead band.

For the on density, the fraction is:

$$\frac{\int_{-\infty}^{x_-} f_{1a}^{ss}(\lambda)\,d\lambda}{\int_{-\infty}^{x_+} f_{1}^{ss}(\lambda)\,d\lambda} = \frac{\frac{\sigma^2 c}{2r(r+c)} \cdot \left[1 - e^{-\frac{2r\Delta}{\sigma^2}}\right]}{\frac{c}{r+c}} = \frac{\bar{\sigma}^2\bar{\tau}}{2} \left[1 - e^{-\frac{2}{\bar{\tau}\bar{\sigma}^2}}\right] \tag{5.86}$$

where $\bar{\sigma} = \frac{\sigma}{\Delta}$, and $\bar{\tau} = \frac{\Delta}{r}$ (average duration of "on" state). For the "off" density the corresponding measure is:

$$\frac{\int_{x_+}^{+\infty} f_{oc}^{ss}(\lambda)d\lambda}{\int_{x_-}^{+\infty} f_{o}^{ss}(\lambda)d\lambda} = \frac{\bar{\sigma}^2\bar{\tau}'}{2}\left[1 - e^{-\frac{2}{\bar{\sigma}^2\bar{\tau}'}}\right] \tag{5.87}$$

where $\bar{\tau}' = \frac{\Delta}{c}$ (average duration of "off" state). (5.86)-(5.87) will be used in section 6 where results of a numerical simulation of the CFPE model are reported. In both equations, it appears that "diffusion lengths" $\bar{\sigma}\sqrt{\bar{\tau}}$ and $\bar{\sigma}\sqrt{\bar{\tau}'}$ are the important quantities.

Remark 3: Note the surprising result in (5.85) which indicates that the steady state fraction of devices in the "on" state is independent of the noise variance. On the other hand, the result is intuitive because:

$$\bar{m}_{ss} = \frac{c}{r + c} = \frac{\Delta/\bar{\tau}'}{\Delta/\bar{\tau} + \Delta/\bar{\tau}'} = \frac{\bar{\tau}}{\bar{\tau}' + \bar{\tau}} \tag{5.88}$$

(5.88) essentially states that at steady-state, the fraction of devices in the "on" state is the ratio of average "on" time divided by average cycle duration.

5.2.4 Relationship to Previous Work

In [29], Ihara and Schweppe have developed on somewhat more heuristic grounds a very simple model which closely resembles the approximate CFPE model in equations (5.22)-(5.23). The model is a traveling wave-type with a forward and backward wave traveling at different speeds (see Fig. 5-3). Although developed independently, the Ihara-Schweppe model can be shown to be related to our model. This is because it is a limiting case of the CFPE model under conditions that are now described. Consider equation (5.69) where the transform of $\frac{d\bar{m}}{dt}$ is expressed in terms of $\theta_2(s)$, $\lambda_2(s)$, i.e. r, c and σ. Under the

conditions:

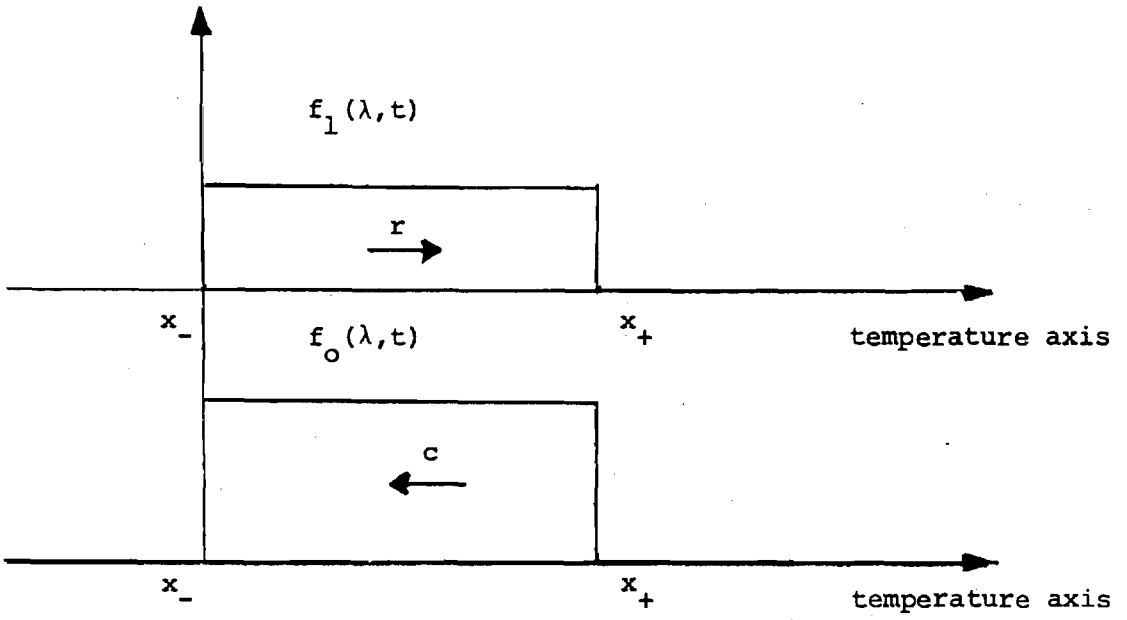

Figure 5-3. Graphical Representation of the Ihara-Schweppe Model. Arrows indicate the direction of temperature drift.

$$\sigma << r \ , \tag{5.89}$$

and:

$$\sigma << c \ , \tag{5.90}$$

i.e. when the effect of the noise in (3.7) is practically negligible. We have approximately:

$$\theta_2(s) = \frac{r}{\sigma^2}\left(1 - (1 + \frac{2s\sigma^2}{r^2})^{1/2}\right)$$

$$\approx \frac{r}{\sigma^2}\left(1 - (1 + \frac{1}{2} \cdot 2s\,\frac{\sigma^2}{r^2})\right)$$

$$\approx -\frac{s}{r} \ . \tag{5.91}$$

Similarly, using (5.90) it can be shown that:

$$\gamma_2(s) \approx -\frac{s}{c} \tag{5.92}$$

Equations (5.69), (5.91)-(5.92) yield approximately:

$$\frac{\overline{dm}^*}{dt}(s) = \int_{x_-}^{+\infty} \frac{1 - e^{-s\bar{\tau}}}{1 - e^{-s(\bar{\tau}+\bar{\tau}')}} \cdot e^{-\frac{s}{c}(x-x_-)} f_o^o(x)\,dx$$

$$- \int_{-\infty}^{x_+} \frac{1 - e^{-s\bar{\tau}'}}{1 - e^{-s(\bar{\tau}+\bar{\tau}')}} e^{-\frac{s}{r}(x_+-x)} f_1^o(x)\,dx \tag{5.93}$$

Now define:

$$T_o^*(x,s) = e^{-\frac{s}{c}(x-x_-)} - e^{-s\left(\frac{x-x_-}{c} + \bar{\tau}\right)}, \tag{5.94}$$

$$T_1^*(x,s) = e^{-\frac{s}{r}(x_+-x)} - e^{-s\left(\frac{x_+-x}{r} + \bar{\tau}'\right)}, \tag{5.95}$$

Then:

$$T_o(x,t) = \delta\left(t - \frac{(x-x_-)}{c}\right) - \delta\left(t - \bar{\tau} - \left(\frac{x-x_-}{c}\right)\right), \tag{5.96}$$

$$T_1(x,t) = \delta\left(t - \frac{(x_+-x)}{r}\right) - \delta\left(t - \bar{\tau}' - \frac{(x_+-x)}{r}\right), \tag{5.97}$$

where in (5.96)-(5.97) $\delta(\cdot)$ represents the Dirac delta function. It is possible to show that:

$$M_o(x,t) = L^{-1}\left[\frac{T_o^*(x,s)}{1 - e^{-s(\bar{\tau} + \bar{\tau}')}}\right] = \sum_{i=0}^{\infty} T_o[x,t-i(\bar{\tau} + \bar{\tau}')] \tag{5.98}$$

and

$$M_1(x,t) = L^{-1}\left[\frac{T_1^*(x,s)}{1 - e^{-s(\bar{\tau} + \bar{\tau}')}}\right] = \sum_{i=0}^{\infty} T_1[x,t-i(\bar{\tau} + \bar{\tau}')] \tag{5.99}$$

Substituting (5.98)-(5.99) back into (5.93) yields:

$$\frac{dm^*}{dt}(s) = \int_{x_+}^{+\infty} M_o(x,t) f_o^o(x)\,dx - \int_{-\infty}^{x_+} M_1(x,t) f_1^o(x)\,dx \tag{5.100}$$

This is essentially the result in [29].

5.3 Aggregation of a Non-Homogeneous Group

The aggregation problem has been considered only for the case of a class of devices described by equation (3.9) and where all the parameters involved

were essentially identical. Such a class was called a homogeneous group. In reality however, some spread in the parameters is to be expected. One way is to treat the parameters as random variables themselves. We would like to assess the effects of varying the parameters.

Here, the analysis of section 5.2 is generalized to a group of devices exhibiting a measure of parameter spread. Such an aggregate of devices will be called a non-homogeneous control group. A perturbation approach is utilized. Let the variable parameters be compiled into a vector $\underline{\xi} = (\xi_1, \xi_2, \ldots \xi_p)^T$. $\underline{\xi}$ could contain parameters such as thermostat set points, building insulation parameters, noise variance, weather (as a function of geographical location, not time). In this more general framework, a more accurate statement of (5.7) is:

$$\bar{m}(t) \simeq E\left[E[m_i(t)|\underline{\xi}]\right] \tag{5.101}$$

If we denote:

$$\bar{m}(t,\underline{\xi}) = E[m_i(t)|\underline{\xi}] \tag{5.102}$$

Then the system of equations (5.8)-(5.16), i.e. the CFPE model can be interpreted as giving $\bar{m}(t,\underline{\xi})$ for a particular choice of $\underline{\xi}$.

Now, assuming that $\bar{m}(t,\underline{\xi})$ is a smooth function of the parameters around their mean value vector $\underline{\xi}_o$, and for parameters narrowly distributed around $\underline{\xi}_o$, a second order truncated Taylor series can be written:

$$\bar{m}(t,\underline{\xi}) \simeq \bar{m}(t,\underline{\xi}_o) + \sum_{i=1}^{p} \frac{\partial \bar{m}}{\partial t}(t,\underline{\xi})\Big|_{\underline{\xi}=\underline{\xi}_o} (\xi_i - \xi_{io})$$

$$+ \left[\sum_{i=1}^{p} \sum_{j=1}^{p} \frac{1}{2} \frac{\partial^2 \overline{m}}{\partial \xi_i \partial \xi_j} (t, \underline{\xi}) \Big|_{\underline{\xi}=\underline{\xi}_o} (\xi_i - \xi_{io})(\xi_j - \xi_{jo}) \right] \tag{5.103}$$

Furthermore, let:

$$E[(\underline{\xi} - \underline{\xi}_o)(\underline{\xi} - \underline{\xi}_o)^T] = [\sigma_{ij}^2]_{\substack{i=1,\ldots,p \\ j=1,\ldots,p}} \tag{5.104}$$

(5.104) yields after taking expected values on both sides:

$$\overline{m}(t) \simeq \overline{m}(t, \underline{\xi}_o) + \sum_{i=1}^{p} \sum_{j=1}^{p} \frac{1}{2} \frac{\partial^2 \overline{m}}{\partial \xi_i \partial \xi_j} (t, \underline{\xi}) \Big|_{\underline{\xi}=\underline{\xi}_o} \sigma_{ij}^2 \tag{5.105}$$

The following remarks can be made:

- If covariance terms σ_{ij}^2 (or the associated second partial derivatives in (5.103)) are sufficiently small, then it is reasonable to use the CFPE model (equations (5.8)-(5.16)) with parameter vector $\underline{\xi}_o$ to compute $\overline{m}(t)$.
- In case a first order approximation proves insufficient, then (5.105) is a second order approximation which requires the estimation of covariances σ_{ij}^2 as well as the associated partial derivatives. If analytic estimation of these "sensitivity" coefficients is not possible, a numerical estimation has to be used.
- As the parameter spread increases, higher order terms have to be introduced in (5.105). This means in effect the double penalty of having to estimate higher order moments of the joint parameters distribution, and higher order partial derivatives. At this point, it

becomes more advantageous to split the large nonhomogeneous group into several smaller groups with less parameter spread, and carry out the computations for each group separately.

6. SIMULATION RESULTS

6.1 Introduction

In Section 5 we develop the coupled Fokker-Planck equations (CFPE) model to describe the aggregate behavior of a large number of loads. This model is novel in the literature, especially in the power system area, although equations of a similar type have been obtained in studying nerve systems [45-49]. We have also analyzed an approximate version of this model and gained much insight about the steady state behavior. Unfortunately, our analysis does not apply to the more general time-varying case, or for large excursions of the system outside its normal steady state as in the case for a power outage of long duration. Therefore, in general one has to resort to numerical simulations.

In this section, results of a numerical study of the CFPE model are given. The dynamics of homogeneous, nonhomogeneous and completely general groups of devices are investigated. This particular scenario chosen is cold load pickup [50]. The expected dynamics of the fractional (or per unit) demand in a group of devices following a temporary interruption of power supply is considered. All simulations are based on a "completely implicit difference scheme" developed in [25]. In selecting the data for the runs, effort was made to retain possible "on"/"off" switching time constants ($\overline{\tau}$ and $\overline{\tau}'$). However, the data is entirely fictitious and was mainly designed for the purpose of illustrating the dynamics of the CFPE model. Three groups of figures can be distinguished corresponding to properties of homogeneous, nonhomogeneous and general groups respectively. Data for each of the runs are given below.

6.2 Simulation of Homogeneous Groups

The sensitivity of the post outage dynamics of an homogeneous group to changes in noise variance, average heating rate, and outage duration was studied by starting from base case values and observing the effect of a change in one parameter at a time.

In the notation of equation (3.7), base case data was as follows:

$$\Delta = 1.1 \text{ deg C} ,$$

$$\frac{x_a(t)}{\Delta} = 15 ,$$

$$\frac{x_-}{\Delta} = 35$$

$$\frac{a}{\Delta} = .01774 \text{ (deg C mn)}^{-1} ,$$

$$\overline{R} = \frac{R}{\Delta} = .4 \text{ (mn)}^{-1} ,$$

$$\overline{\sigma} = \frac{\sigma}{\Delta} = .3 \text{ (mn)}^{-1/2} . \qquad (6.1)$$

The data in (6.1) yields approximately:

$$\overline{\tau} \approx \overline{\tau}' \approx 5 \text{ mn} , \qquad (6.2)$$

i.e. the average duration of the "on" time is approximately equal to that of the "off" time and they are both in the neighborhood of five minutes.

Figures 6-1 and 6-2 demonstrate the effect of a change in noise variance for four different values of outage duration. Figures 6-3 and 6-4 demonstrate

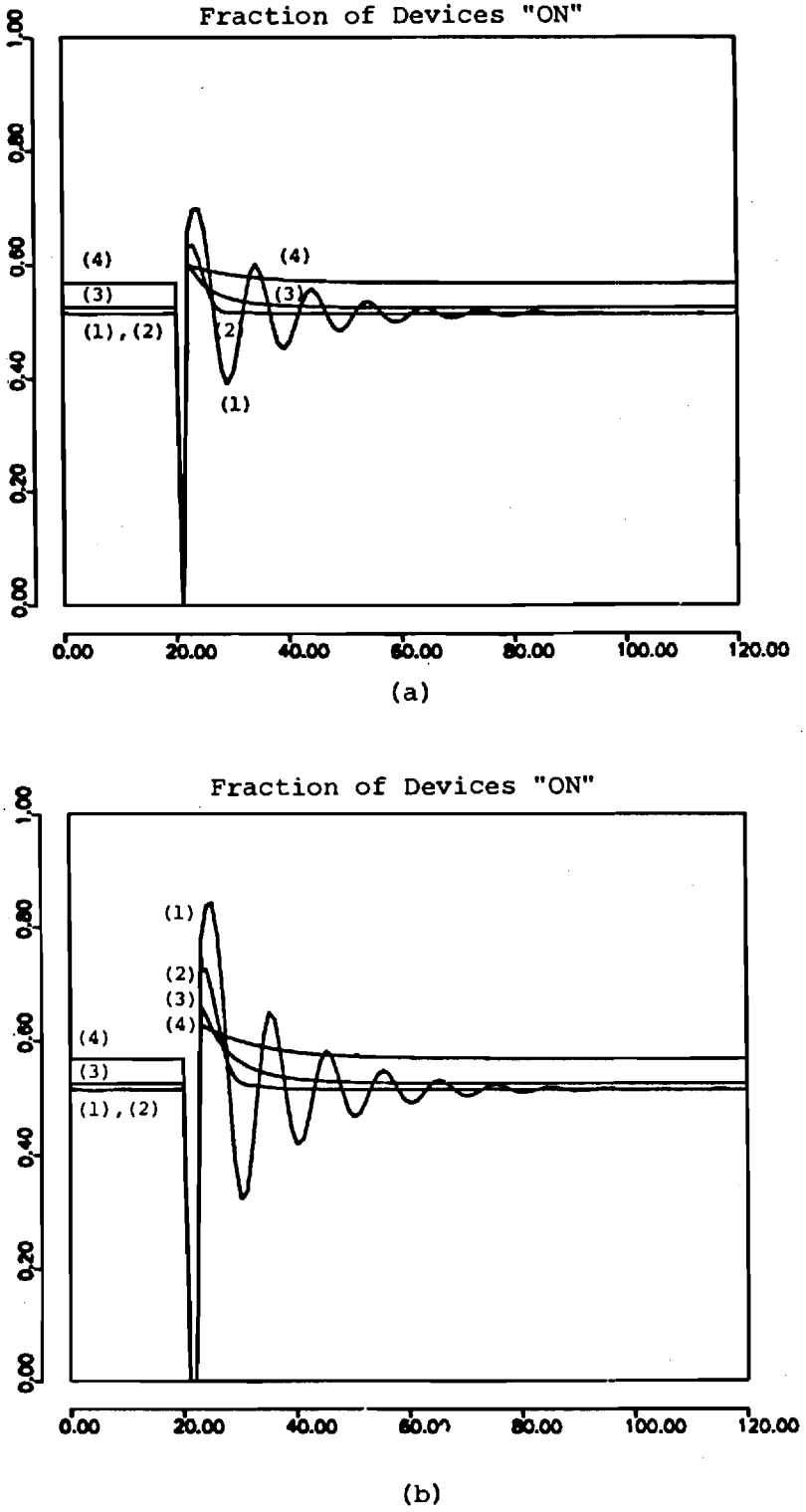

Fig. 6-1. Dependence of Cold Load Pickup Dynamics on Normalized Noise Variance Parameters $\bar{\sigma}$. Outage Durations: (a) 1 mn, (b) 2mns. Values of $\bar{\sigma}$ in $(mn)^{-1/2}$ are: (1) $\bar{\sigma}$ = .1, (2) $\bar{\sigma}$ = .3, (3) $\bar{\sigma}$ = .5, (4) $\bar{\sigma}$ = 1.0. All other parameters are as in base case. The horizontal axis corresponds to time in minutes.

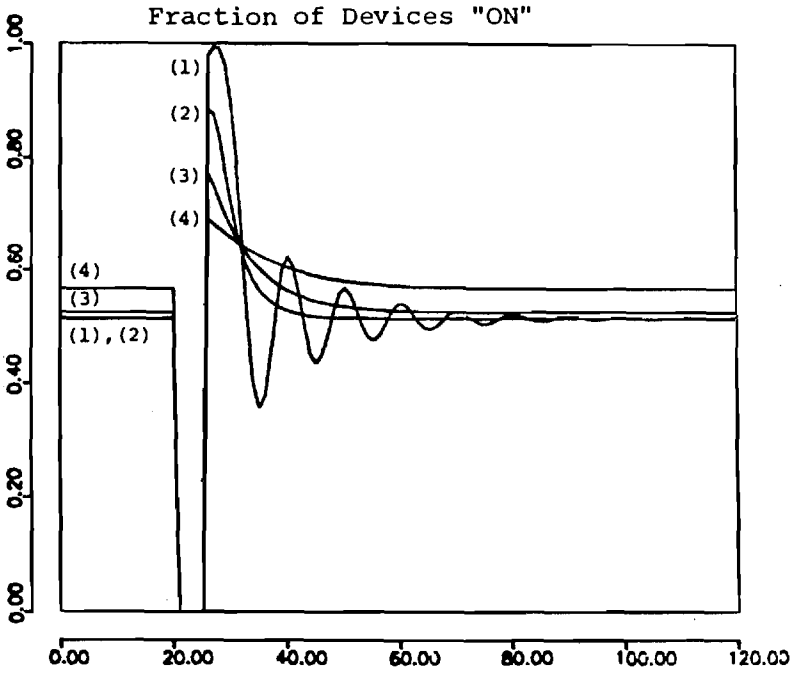

(a)

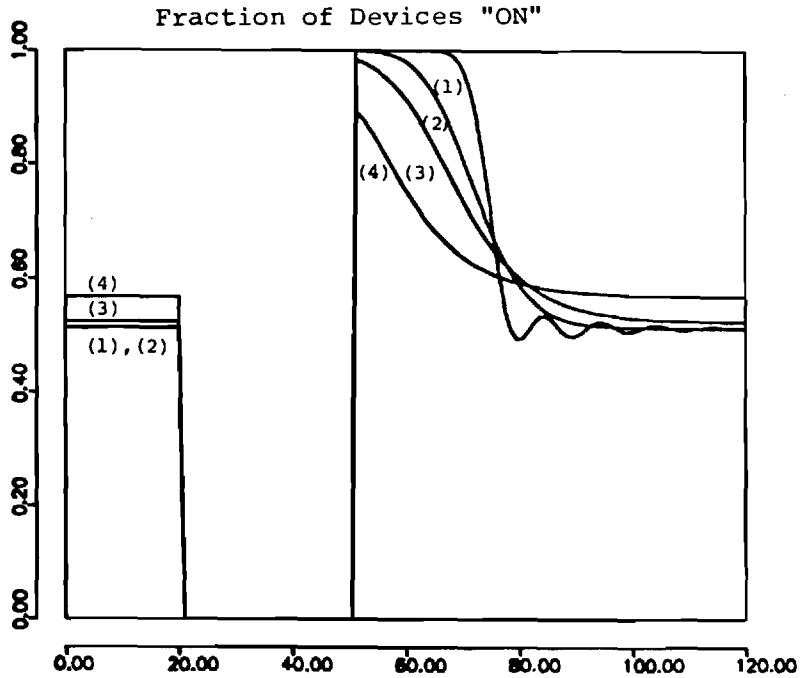

(b)

Fig. 6-2. Dependence of Cold Load Pickup Dynamics on Normalized Noise Variance Parameter $\bar{\sigma}$. Outage Durations are: (a) 5mns, (b) 30 mns. Values of $\bar{\sigma}$ in $(mn)^{-1/2}$ are: (1) $\bar{\sigma}$ = .1, (2) $\bar{\sigma}$ = .3, (3) $\bar{\sigma}$ = .5, (4) $\bar{\sigma}$ = 1.0. All other parameters are as in base case. The horizontal axis corresponds to time in minutes.

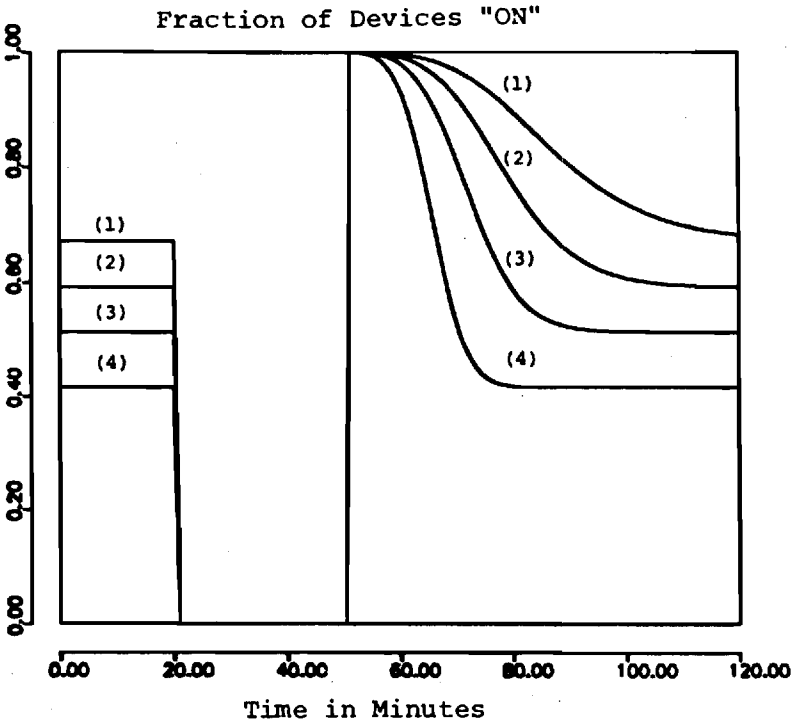

Fig. 6-3. Dependence of Cold Load Pickup Dynamics on the Heating Rate Parameter R for an Outage Duration of 30 mn. Values $R\Delta^{-1}$ in $(mn)^{-1}$ are .3, .344, .4 and .5 for responses (1), (2), (3), and (4) respectively. All other parameters are as in base case.

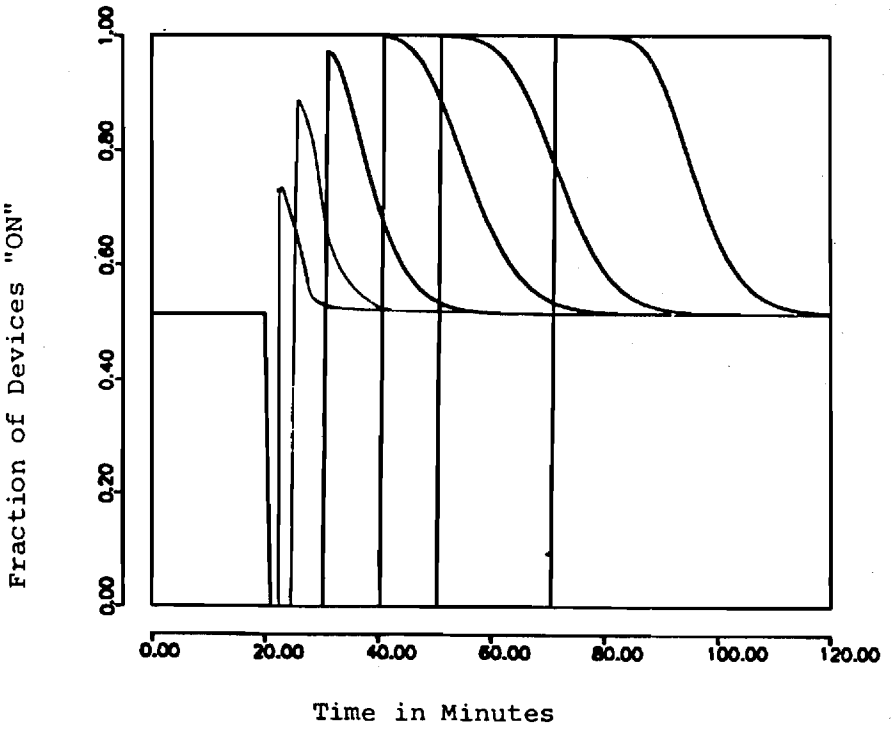

Fig. 6-4. Dependence of Cold Load Pickup Dynamics on Outage Duration. Outage durations are 2, 5, 10, 20, 30 and 50 mns respectively. All other parameters are as in base case.

the effect of changes in the average heating rate and outage duration respectively.

6.3 Simulation of Nonhomogeneous Groups

Here, the effect of some parameter variance within the group was assessed by simulating with the mean data as well as two "neighboring" sets of data, and using this information to evaluate the sensitivity coefficients in (5.105) numerically. Subsequently (5.105) was used to generate post-outage dynamics in the nonhomogenenous group for various levels of parameter variance. Only the effect of one parameter, namely thermostat set point x_-, was considered. The average data was identical to (6.1) except for $\bar{\sigma} = .2\ (\text{mn})^{-1/2}$. The results are summarized in Figure 6-5.

6.4 Simulation of General Groups

In this set of runs, the dynamics of a general group were simulated by assuming that, at the outset, it has been broken up into its constitutive homogeneous groups and, subsequently obtaining aggregate dynamics by superposition of the individual dynamics for each homogeneous subgroup.

The general group that was studied was assumed to be made up of sixteen homogeneous groups. Data for the homogeneous groups was as follows:

$$\Delta = 1.1 \text{ deg C} ,$$

$$\frac{x_a(t)}{\Delta} = 15 , \quad \frac{x_-}{\Delta} = 35 ,$$

$$\frac{a}{\Delta} = .01774\ (\text{deg C mn})^{-1} ,$$

$$\bar{R} = r_i\ (\text{mn})^{-1} ,$$

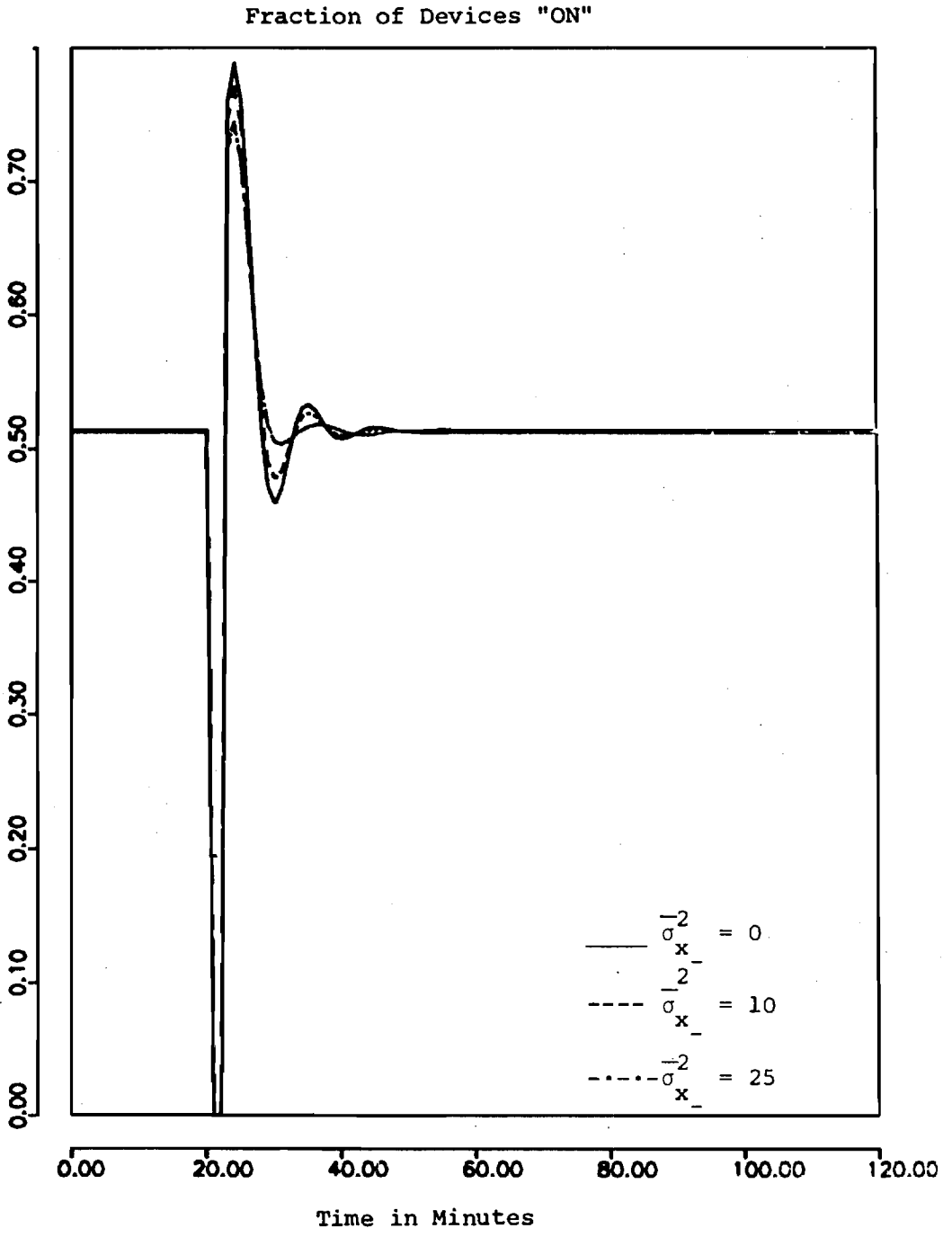

Figure 6-5. Effect of Spread in Thermostat Set Points on Cold Load Pickup Dynamics for a Nonhomogeneous Control Group. Mean values are as in section 6.3. $\overline{\sigma^2_{x_-}}$ represents the normalized set point variance. The duration of the outage is 2 mn.

$$\bar{\sigma} = \sigma_j \, (mn)^{-1/2} \, . \tag{6.3}$$

for i = 1,...,4, and j = 1,...,4, where in (6.3):

$$\underline{R} \equiv [r_i] = \begin{vmatrix} .35 \\ .4 \\ .5 \\ .6 \end{vmatrix} \, , \quad \text{and} \quad \underline{V} \equiv [\sigma_j] = \begin{vmatrix} .1 \\ .3 \\ .5 \\ .8 \end{vmatrix} \tag{6.4}$$

The nominal size of the heating element was assumed to be identical for all devices. Several parameter distributions were studied. Each parameter distribution was characterized by a set of weights, w_{ij}, such that:

$$\Pr\left[\left(\frac{R}{\Delta} = r_i\right) \cap (\bar{\sigma} = \sigma_j)\right] = w_{ij} \tag{6.5}$$

for i = 1,...,4, and j = 1,...,4, where in (6.5):

$\underline{W} = [w_{ij}]$ is a given 4 x 4 matrix of weights.

The following values of $\underline{W}$ were used:

$$\underline{W}_1 = \frac{1}{16} \begin{vmatrix} 1 & 1 & 1 & 1 \\ 1 & 1 & 1 & 1 \\ 1 & 1 & 1 & 1 \\ 1 & 1 & 1 & 1 \end{vmatrix} \tag{6.6}$$

$$\underline{W}_2 = \frac{1}{64} \begin{vmatrix} 1 & 3 & 3 & 1 \\ 3 & 9 & 9 & 3 \\ 3 & 9 & 9 & 3 \\ 1 & 3 & 3 & 1 \end{vmatrix} \tag{6.7}$$

$$\underline{W}_3 = \frac{1}{64}\begin{vmatrix} 9 & 3 & 3 & 1 \\ 9 & 3 & 3 & 1 \\ 9 & 3 & 3 & 1 \\ 9 & 3 & 3 & 1 \end{vmatrix} \tag{6.8}$$

Finally, global dynamics were obtained using:

$$\bar{m}(t) = \sum_{i=1}^{4} \sum_{j=1}^{4} w_{ij}\, \bar{m}_{ij}(t) \tag{6.9}$$

where in (6.9) $\bar{m}_{ij}(t)$ denotes the aggregate functional state with parameters r_i and σ_j. The results are summarized in Figure 6-6.

6.5 Interpretations of the Results

The following groups of remarks can be made:

(a) From Figures 6-1 and 6-2 it appears that:

- The noise variance parameter $\bar{\sigma}$ is crucial in shaping the dynamical response of homogeneous groups. Therefore, ignoring this parameter completely, as is the case for the Ihara/Schweppe model, can result in serious error.
- As the noise variance parameter increases there is a simultaneous decrease in post-outage dynamical fluctuations. The system reaches its steady-state faster. $\bar{\sigma}$ acts like a damping factor. This is to be expected since an increase in system noise promotes an increase in the diversity of the system. This increase in diversity in turn tends to oppose the decrease in diversity caused by the power outage, thus yielding a more stable system.
- Unlike its approximate version (5.22)-(5.23) which predicts that the steady-state connected fraction of devices is independent of $\bar{\sigma}$, the CFPE model simulator indicates a dependence of the steady-state on noise variance. However, the dependence is

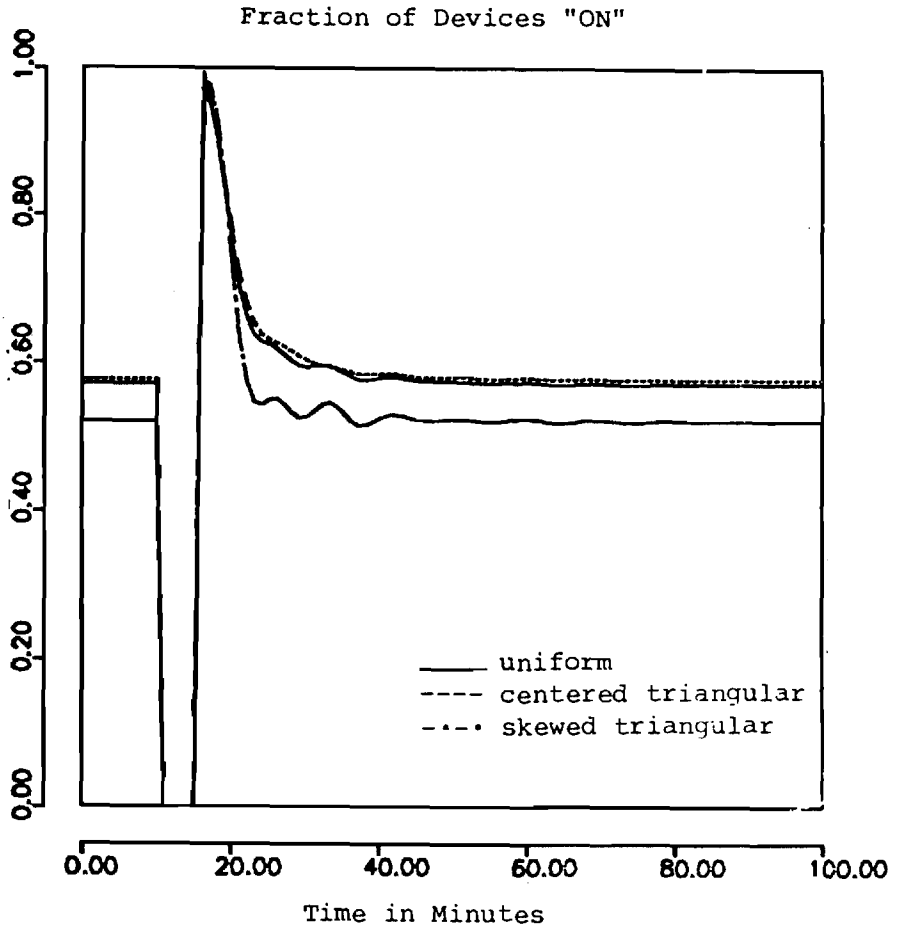

Figure 6-6. Effect of Parameter Distribution on Cold Load Pickup Dynamics for a General Control Group. All values are as in section 6.4. The duration of the outage is 5 mn.

apparent only for large values of $\bar{\sigma}$. This is consistent with the constant rate approximation validity criterion developed in equations (5.86)-(5.87) as we now show. In the simulations of figures 6-1 and 6-2, $\bar{\tau}$ = 5 mn. Hence for $\bar{\sigma}$ = 1.0, the performance criterion in (5.86) yields .82. This means that for $\bar{\sigma}$ = 1.0, 82% of the steady state "on" density lies outside the thermostat dead band, thus invalidating the constant rates approximation.

(b) From figures 6-3 through 6-4, we have respectively the predictable results that as the average heating rate increases, the steady state fraction of devices in the "on" state decreases (mainly because a device spends on the average less time in the "on" state) and as the outage duration increases the fraction of devices in the "on" state after the recovery increases, as well as the duration of the restoration period.

(c) From Fig. 6-5, it appears that post-outage dynamic fluctuations for a nonhomogeneous group decrease as the parameter variance within the group increases. As argued in (a), this effect can be understood by remarking that an increase in parameter variance results in an increase in the diversity of the system.

(d) From Fig. 6-6, it appears that the parameter distribution within a general group can alter significantly the restoration dynamics following a power outage. Uniform and centered triangular parameter distributions yield smooth dynamics for our example.

7. DATA REQUIREMENTS AND MODEL VALIDATION

7.1 Data Requirements and Parameter Estimation

The load modeling methodology developed would be useless if the parameters needed for the model cannot be estimated. The data requirements for a physically based load modeling methodlogy are higher than those for an identification based modeling methodology. In the following we discuss ways of estimating the necessary parameters with respect to the space heating example.

As a first step, we need to classify the loads into groups with similar characteristics. For this, the composition of the loads in the service area of interest is needed. Many utilities have conducted load research for their systems. As this data base becomes more established, the classification problem is likely to become more feasible.

Once we have the devices in a homogeneous group, we can then estimate the parameters needed in the aggregate model. Consider first the constant heat rate approximation for space heating.

The significant parameters in the approximate model are normalized heat gain rate $\bar{r}$, heat loss $\bar{c}$, and noise variance $\bar{\sigma}$ for an individual dwelling. The gathering of such data for a significant sample of houses eventually allows the division of the sector into homogeneous groups as defined in Section 4. It is only then that the methods of Section 5 can be applied. Here, we recall the definition of the parameters of interest:

$$\bar{r} = \frac{1}{\Delta} \cdot [\text{average value of } r_1(\lambda,t)] \tag{7.1}$$

$$\bar{c} = \frac{1}{\Delta} \cdot [\text{average value of } r_o(\lambda,t)] \tag{7.2}$$

$$\bar{\sigma} = \frac{\sigma}{\Delta} \tag{7.3}$$

where in (7.1)-(7.2):

$$r_1(\lambda,t) = R\text{-}a(\lambda - x_a(t)) \tag{7.4}$$

$$r_o(\lambda,t) = a(\lambda - x_a(t)) \tag{7.5}$$

Recall that Δ is the width of the thermostat dead band.

$$\bar{r}\Delta = \frac{\int_{-\infty}^{x_+} f_1(\lambda,t)\, r_1(\lambda,t)\, d\lambda}{\int_{-\infty}^{x_+} f_1(\lambda,t)\, d\lambda} = R\text{-}a(E(\lambda,t) - x(t)) \tag{7.6}$$

$$\bar{c}\Delta = \frac{\int_{x_-}^{+\infty} f_o(\lambda,t)\, r_o(\lambda,t)\, d\lambda}{\int_{x_-}^{\infty} f_o(\lambda,t)\, r_o(\lambda,t)\, d\lambda} = a(E(\lambda,t) - x(t)) \tag{7.7}$$

where $E_1(\lambda,t)$ and $E_o(\lambda,t)$ are expected mean temperatures in the "on" and "off" states respectively at time t. Let $T = [t_1,t_2]$ be the time interval over which the load model is to be used. Throughout Sections 5.2.2-5.2.3, the quantities in (7.6)-(7.7) have been considered constant. This means in effect the following:

(i) The noise variance σ and the ambient temperature $x_a(t)$ cannot vary significantly over T.

(ii) The expectations in (7.6)-(7.7) can be considered constant over T.

In order to make (ii) possible, it will be assumed that the system starts in its steady-state and is not significantly removed from it during T. These

assumptions are made in addition to the dead band confinement asssumption discussed in Section 5.2.3. Clearly, the totality of the assumptions limits the applicability of the linearized model. However, if (i) and (ii) are verified, an algebraic estimation of $\bar{\sigma}$, $\bar{r}$, $\bar{c}$ is possible from a record of the "on"/"off" cycling of the thermostat during the time interval of interest. To show this, first define the following:

$\underline{\tau}$: sample mean of "on" durations

$\underline{\tau}'$: sample mean of "off" durations

$\underline{\sigma}_{\tau}^2$: sample variance of "on" durations

$\underline{\sigma}_{\tau'}^2$: sample variance of "off" durations.

The probability densities of the "on" and "off" durations can be shown to be first passage time densities for (3.7) to go from x_- to x_+ and from x_+ to x_-.

The theoretical means of these passage times are given by $\bar{r}^{-1}$ and $\bar{c}^{-1}$ respectively. The theoretical variances are given by $\frac{\bar{\sigma}^2}{\bar{r}^3}$ and $\frac{\bar{\sigma}^2}{\bar{c}^3}$ respectively.

Therefore, we have the estimates:

$$\bar{r} = \frac{1}{\underline{\tau}} \tag{7.8}$$

$$\bar{c} = \frac{1}{\underline{\tau}'} \tag{7.9}$$

$$\bar{\sigma}^2 = \frac{1}{2}\left(\underline{\tau}^3\underline{\sigma}_{\tau}^2 + \underline{\tau}'^3\underline{\sigma}_{\tau}^2\right) \tag{7.10}$$

Clearly, the answers obtained will be a function of weather and time of the day. Thus a table of coefficients as a function of weather and time would have to be set up for use under any conditions. Finally, it is believed that this same method can be extended for the estimation of the parameters in the more general (and in fact more widely applicable) temperature inhomogeneous model of equation (3.7).

7.2 Model Validation

The emphasis of our research has been in the development of the load modeling methodology. Therefore, we have not conducted data collections to estimate the parameters or field tests to validate the models. We have discussed how parameters can be estimated from data in Section 7.1. In the following we briefly describe ways of validating the model and fine tuning its parameters.

One way is to conduct a detailed simulation model of all the loads under consideration. Simulation results using this model can then be used to compare with the results predicted by the aggregate model. The advantage of this approach is that all kinds of tests can be carried out to evaluate the model in different regimes of operation. Another possibility is to conduct actual field tests. If a homogeneous group can be isolated for testing, the validation method is quite straightforward. If one has to test the model at a higher level where networks of many groups are involved, more sophisticated techniques would have to be developed to include the effects of the network, etc. In particular, the loss in the network may have to be considered.

8. CONCLUSIONS AND SUGGESTIONS FOR FUTURE RESEARCH

We have developed a methodology for synthesizing the electric power system load starting from the elementary device models. The methodlogy goes through a hierarchy of models and terminates when the desired level is reached. At each level the four steps used are: modeling of primitive components, classification of components, aggregation and model validation. The emphasis of our research has been the modeling of the elementary component loads and the aggregation of the functional models to obtain the load demand models.

Compared to other work in physically based load modeling, our approach has the following characteristics: precise modeling of the decision processes which generate the elementary component demands and statistical aggregation of these demand processes. The former is accomplished through decomposition of the elementary model into a functional model and an electrical device model. The functional model is modeled by means of a stochastic hybrid state system to represent the actual process which generates the "on" or "off" status of the device. The continuous state corresponds to the state of the energy storage such as temperature and the discrete state corresponds to the actual functional state. Noise is assumed to be present. We believe that this model is a better representation of what actually goes on at the component level.

Statistical aggregation of these elementary functional models is accomplished by using some results in the theory of stochastic processes. For the class of loads studied the resulting load model is given by a system of coupled ordinary and partial differential equations. These equations have very nice interpretations. The partial differential equations describe the dynamics of the population of loads which may be on or off. The ordinary differential equation gives the total fraction of loads which are on.

The model is applied to the cold load pickup problem where the effect of a service interruption on the demand dynamics is investigated. A simplification model for the space heating of a house, similar to those used in [29] and [37] are assumed. The simulation results illustrated the computational feasibility of the model and how it can be used for operational and planning studies.

In our view this work contains some basic results needed for statistical physically based load modeling. Some additional areas which ought to be investigated to make the methodology practical are:

1. Test and evalution of the aggregate model on real data.

We have concentrated on the theoretical development of the aggregation techniques in our research and thus the resulting model has not been tested on real data. Field tests are absolutely necessary to validate the assumptions made in the canonical model as well as the aggregation scheme. Furthermore, we can also gain more insight on the actual data requirements as well as the sensitivity to parameter variations.

2. Development of aggregate models for other types of loads.

In our research we have developed an aggregate model for weakly driven functional models to demonstrate the feasibility of the approach. A highly simplified model for space heating has been chosen. One can consider more complicated models with higher dimensions to model the house. We believe the aggregate model will be structurally similar except for more complicated boundary conditions. Strongly driven functional models used to model the demand of water heaters can also be considered. The resulting aggregate models will probably be similar, although some further research on the theory of stochastic processes is needed.

3. Development of load management strategies.

The models developed are particulary suitable for evaluating various load management strategies, either for actual implementation or for planning purposes. This is particularly the case if some optimization schemes are to be used. An analytic model of the type developed may provide more guidance in this case than a purely simulation based model.

BIBLIOGRAPHY

1. "System Load Dynamics - Simulation Effects and Determination of Load Characteristics," IEEE Trans. on Power Apparatus and Systems, vol. PAS-92, pp. 600-609, March-April 1973.

2. H. Kent, W. R. Schmus, F. A. McCrackin and L. M. Wheeler, "Dynamic Modeling of Loads in Stability Studies," IEEE Trans. on Power Apparatus and Systems, vol. PAS-88, pp. 138-146, May 1969.

3. F. P. DeMello, "Power System Dynamics Overview," Symposium on Adequacy and Philosophy of Modeling: Dynamic System Performance, IEEE pamphlet 75 CH0970-4-PWR, pp. 5-15.

4. M. M. Abdel-Hakim and Y. G. Berg, "Dynamic Single-Unit Representation of Induction Motor Groups," IEEE Trans. on Power Apparatus and Systems, vol. PAS-95, pp. 155-165, January/February 1976.

5. F. Illiceto and A. Capasso, "Dynamic Equivalents of Asynchronous Motor Loads in System Stability Studies," IEEE Trans. on Power Apparatus and Systems, vol. PAS-93, pp. 1650-1659, 1974.

6. S. Ihara, "An Algebraic Aggregation of Interconnected Power System Loads," CDC Proceedings, pp. 270-272, 1979.

7. S. Ihara and R. Baheti, "A Dynamic Model of Aggregate Induction Motor Load for Large Voltage Dips," Proceedings Joint Automatic Control Conference, San Francisco, CA, 1980.

8. G. T. Heinemann, D. A. Nordman, and E. C. Plant, "The Relationship between Summer Weather and Summer Loads - Regression Analysis," IEEE Trans. on Power Apparatus and Systems, vol. PAS-85, pp. 1144-1154, Nov. 1966.

9. P. C. Gupta and K. Yamada, "Adaptive Short Term Forecasting of Hourly Loads Using Weather Information," IEEE Trans. on Power Apparatus and Systems, vol. PAS-91, no. 5, pp. 2085-2094, Sept./Oct. 1972.

10. J. Toyoda et. al., "An Application of State Estimation to Short Term Load Forecasting," IEEE Trans. on Power Apparatus and Systems, vol. PAS-89, pp. 1678-1682, Oct. 1970.

11. G. Singh et. al., "Load Modeling for Real Time Monitoring of Power Systems," IEEE Trans. on Power Apparatus and Systems, vol. PAS-96, pp. 1908-1914, Nov. 1977.

12. G. Singh et. al., "Power System Load Forecasting Using Smoothing Techniques," Int. J. Systems Science, vol. 9, no. 4, pp. 363-368, 1978.

13. J. F. De Queiroz, "A Load Demand Prediction Algorithm for Electric Power System Monitoring," 1979 Control of Power Systems Conference and Exposition Conference Record, College Station, pp. 161-166.

14. A. Keyhani and A. M. El-Abiad, "One-Step-Ahead Load Forecasting for On-Line Applications," paper C75 027-8, IEEE Winter Power Meeting, 1975.

15. F. D. Galiana et. al., "Identification of Stochastic Electric Load Models from Physical Data," IEEE Trans. on Automat. Control, vol. AC-19, pp. 887-893, Dec. 1974.

16. S. Vemuri et. al., "Load Forecasting Using Stochastic Models," in Proc. of 1973 PICA Conference.

17. A. R. Mahalanabis et. al., "Load Modeling of an Interconnected Power System for Short Term Prediction," Int. J. Systems Science, vol. 11, no. 4, pp. 445-453, 1980.

18. M. Hagan and R. Klein, "On-Line Maximum Likelihood Estimation for Load Forecasting," IEEE Trans. on Syst., Man and Cyber, vol. SMC-8, Sept. 1978.

19. A. Gelb ed., Applied Optimal Estimation, M.I.T. Press, Cambridge, MA, 1974.

20. G. E. P. Box and G. M. Jenkins, Time Series Analysis - Forecasting and Control, Holden-Day, San Francisco, 1970.

21. M. A. Abu-El-Magd and N. K. Sinha, "Short-Term Load Demand Modeling and Forecasting: A Review," IEEE Trans. Systems, Man and Cybernetics, vol. SMC-12, no. 3, pp. 370-382, May/June 1982.

22. F. C. Galiana, "Short Term Load Forecasting," Proc. Engineering Foundation Conference, Systems Engineering for Power: Status and Prospects, pp. 105-115. August, 1975.

23. IEEE Comittee Report, "Load Forecast Bibliography, Phase 1," IEEE Trans. on Power Apparatus and Systems, vol. PAS-99, no. 1, pp. 53-58, 1980.

24. M. S. Sachdev, R. Billinton and C. A. Peterson, "Representation Bibliography on Load Forecasting," IEEE Trans. on Power Apparatus and Systems, vol. PAS-96, no. 6, pp. 697-700, 1977.

25. M. P. Malhami, "A Statistical Approach for Modeling a Class of Power System Loads," Ph.D. Thesis, Georgia Institute of Technology, March 1982.

26. IEEE Committee Report, "Bibliography on Load Management," IEEE Trans. on Power Apparatus and Systems, vol. PAS-100, no. 5, May 1981.

27. M. L. Chan, E. N. Marsh, J. Y. Yoon, G. B. Ackerman, and N. Stoughton, "Simulation-Based Load Synthesis Methodology for Evaluating Load Management Programs," IEEE Trans. for Power Apparatus and Systems, Vol. PAS-100, pp. 1771-1778, April 1981.

28. "Pacific Gas and Electric Residential Air Conditioning Load Control Simulation Study," prepared by Honeywell Technology Strategy Center, 2600 Ridgeway Parkway, Minneapolis, MN, October 1980.

29. S. Ihara and F. C. Schweppe, "Physically Based Modeling of Cold Load Pickup," IEEE Trans. on Power Apparatus and Systems, vo. PAS-100, pp. 4142-4150, Sept. 1981.

30. W. W. Lang, M. D. Anderson, and D. R. Fannin, "An Analytical Method for Quantifying the Electrical Space Heating Component of a Cold Load Pickup," IEEE Trans. on Power Apparatus and Systems, vol. PAS-101, pp. 924-932, April 1982.

31. C. Y. Chong and A. S. Debs, "Statistical Synthesis of Power System Functional Load Models," CDC Proceedings, pp. 264-269, 1979.

32. J. B. Woodard, Jr., "Electric Load Modeling," Ph.D. Thesis, Department of Electrical Engineering, M.I.T., September 1976, EPSEL Report No. 50.

33. M. F. Ruane, Y. Manichaikul, F. C. Schweppe, and J. B. Woodard, "Physically Based Load Modeling," IEEE Summer Power Meeting, 1979.

34. M. F. Ruane, F. C. Schweppe, and S. Ihara, "Physically Based Modeling of Aggregate Loads," IEEE Winter Power Meeting, 1981.

35. Y. Manichaikul, "Industrial Electric Load Modeling," Ph.D. Thesis, Department of Electrical Engineering, M.I.T., September 1974, EPSEL Report No. 54.

36. Y. Manichaikul and F. C. Schweppe, "Physically Based Industrial Electric Load," IEEE Trans. on Power Apparatus and Systems, vol. PAS-98, pp. 1439-1445, July 1979.

37. T. M. Calloway and C. W. Brice, III, "Physically-based Model of Demand with Applications to Load Management Assessment and Load Forecasting," IEEE Trans. on Power Apparatus and Systems, vol. PAS-101, pp. 4625-4631, Dec. 1982.

38. H. T. T. Nquyen and J. D. Birdwell, "A Physically-based Low-Order Model for Aggregate Air Conditioner Loads," Proceedings 1982 American Control Conference, Arlington, Virginia.

39. D. Nelson et. al., "Aggregation Oriented Load Models," Engineering Foundation Conference, Henniker, NH, Aug. 1979.

40. P. A. Frick, "On the Load Modeling Problem - A Parametric Stochastic Approach," Proceedings 1980 Joint Automatic Control Conference, San Francisco, CA.

41. Georgia Institute of Technology, "Development of an Electrical Load Demand and Response Model Based on a Rational Synthesis from Elementary Devices," Report to U.S. Department of Energy, No. DOE/ET-5109-1, 1979.

42. D. R. Cox and H. D. Miller, The Theory of Stochastic Processes, Wiley, New York, 1965.

43. K. L. Chung, A Course in Probability Theory, Academic Press, New York, 1968.

44. G. Doetsch, Guide to the Applications of the Laplace and z Transforms, Van Nostrand Reinhold, London, 1971.

45. A. Holden, Models of the Stochastic Activity of Neurons, Springer Verlag, Berlin, 1976.

46. M. Fen Hoppen, "Probabilistic Firing of Neurons Considered as a First Passage Problem," Biophysical Journal, vol. 6, pp. 435-451, 1966.

47. H. Sugiyama, G. P. Moore, and D. H. Perkel, "Solutions for a Stochastic Model of Neuronal Spike Production," Mathematical Biosciences, vol. 8, pp. 323-341, 1970.

48. G. Gerstein and B. Mandelbrot, "Random Walk Models for the Spike Activity of a Single Neuron," Biophysical J., vol. 4, pp. 41-68, 1964.

49. P. I. M. Johanesma, "Diffusion Models for the Stochastic Activity of Neurons," in Neural Networks - Proceedings of the School on Neural Networks, June 1967 at Ravello. (Ed. E. R. Caianiello) Springer-Verlag, New York, 1968.

50. J. E. McDonald, A. M. Bruning, and W. R. Mahica, "Cold Load Pickup," IEEE Trans. on Power Apparatus and Systems, vol. PAS-98, pp. 1386-1387, July/August 1979.

51. J. L. Doob, Stochastic Processes, Wiley, New York, 1953.

52. A. N. Kolmogorov, "Uber Die Analytischen Methoden in Der Wahrscheinlichkeitsrechnung," Math. Ann., no. 104, pp. 415-458, 1931.

53. A. T. Bharucha-Reid, Elements of the Theory of Markov Processes and Their Applications, McGraw Hill, New York, 1960.

54. R. B. Bartle, The Elements of Integration, Wiley, New York, 1966.

55. D. A. Darling and A. J. Siegert, "The First Passage Time Problem for a Continuous Markov Process," Annals of Mathematical Statistics, vol. 24, pp. 624-639, 1953.

APPENDIX A.

FUNCTIONAL MODEL FOR ELECTRIC WATER HEATER

In this appendix, we consider a simplified model of a single element electric water heater. A complete model will involve more differential equations but our model is sufficient for the intended use in this study.

Let the following quantities be defined:

$v(t)$: hot water demand at time t (vol./sec.)

$x_i(t)$: inlet water temperature

C: tank thermal capacity

$x(t)$: tank water temperature at time t

x_d: desired water outlet temperature

$v_h(t)$: hot water removed at temperature $x(t)$ (vol./sec.)

$v_c(t)$: cold water mixed with $v_d(t)$ (vol./sec.)

α: heat loss constant

$x_a(t)$: ambient temperature

$p(t)$: power supplied by the heater element

$m(t)$: functional state of the heater

$b(t)$: load management variable (1 when on, 0 when off)

From volume balance, we have

$$v(t) = v_h(t) + v_c(t) \tag{A.1}$$

From heat balance, for small Δt, we have

$$Cx(t+\Delta t) = Cx(t) - \alpha(x(t) - x_a(t))\Delta t - v_h(t)(x(t) - x_i(t))\Delta t$$

$$+ p(t)m(t)\Delta t \qquad (A.2)$$

$$C(x(t+\Delta t) - x(t)) = -\alpha(x(t) - x_a(t))\Delta t - v_h(t)(x(t) - x_i(t))\Delta t$$

$$+ y(t)m(t)\Delta t \qquad (A.2)$$

Dividing by Δt and letting Δt approach 0, we obtain

$$C\frac{dx(t)}{dt} = -\alpha(x(t) - x_a(t)) - v_h(t)(x(t) - x_i(t))$$

$$+ y(t)m(t) \qquad (A.3)$$

But

$$v_h(t)x(t) + v_c(t)x_i(t) = v(t)x_d \qquad (A.4)$$

and

$$v_h(t)x_i(t) + v_c(t)x_i(t) = v(t)x_i(t) \qquad (A.5)$$

Thus

$$v_h(t)(x(t) - x_i(t)) = v(t)(x_d - x_i(t)) \qquad (A.6)$$

Substituting into equation (A.3), the equation becomes

$$C\frac{dx(t)}{dt} = -\alpha(x(t) - x_a(t)) - v(t)(x_d - x_i(t)) + p(t)m(t) \qquad (A.7)$$

APPENDIX B

THE AGGREGATION PROBLEM: FORMULATION AND SOLUTION

We provide two separate proofs: a heuristic derivation of equation (5.8) and a more formal proof for the coupled partial differential equations and the boundary conditions.

B.1 Deviation of Equation (5.8)

The following "hybrid" probability densities will be needed in the subsequent developments:

$$f_1^c(\lambda,t)d\lambda = Pr\left[(\lambda < x(t) \leq \lambda + d\lambda) | m(t) = 1\right] \tag{B.1}$$

$$f_o^c(\lambda,t)d\lambda = Pr\left[(\lambda < x(t) \leq \lambda + d\lambda) | m(t) = 0\right] \tag{B.2}$$

$$f_1(\lambda,t)d\lambda = Pr\left[(\lambda < x(t) \leq \lambda + d\lambda) \cap (m(t) = 1)\right] \tag{B.3}$$

$$f_o(\lambda,t)d\lambda = Pr\left[(\lambda < x(t) \leq \lambda + d\lambda) \cap (m(t) = 0)\right] \tag{B.4}$$

We need to study the following problem:

Given $\bar{m}(t)$, $f_1(\lambda,t)$, $f_o(\lambda,t)$ at time t, express if possible $\bar{m}(t + \delta t)$ in terms of the above mentioned quantities when δt is a small time increment.

Let $n_1(t)$ be the total number of electric space heaters in the "on" state at time t. Also, for the "on" population of space heaters, let:

$$S_1(t,\delta t) = \sum_{i=1}^{n_1(t)} m_i(t + \delta t) \tag{B.5}$$

Finally let:

$p_1(t,\delta t)$ = probability that an individual space heater remains in the "on" state at time $t + \delta t$, given that it was in the "on" state at time t.

$q_1(t,\delta t) = 1 - p_1(t,\delta t)$.

$S_1(t,\delta t)$ corresponds to the summation of $n_1(t)$ identically distributed independent Bernoulli random variables with $p_1(t,\delta t)$ as probability of success and $q_1(t,\delta t)$ as probability of failure. For $n_1(t)$ "large enough," the central limit theorem [43] yields:

$$S_1(t,\delta t) \sim n_1(t)p_1(t,\delta t) + G(0,n_1(t)p_1(t,\delta t)q_1(t,\delta t)) \tag{B.6}$$

where in (B.6) $\sim$ indicates convergence in distribution and $G(\alpha,\beta)$ denotes a Gaussian random variable with mean α and variance β. Similarly define:

$$S_o(t,\delta t) = \sum_{i=1}^{n_o(t)} m_i(t + \delta t) \tag{B.7}$$

where $n_o(t)$ is the number of space haters in the "off" state at time t. Also, let:

$p_o(t,\delta t)$ = probability that an individual space heater remains in the "off" state at time $t + \delta t$, given that it was in the "off" state at time t.

$q_o(t,\delta t) = 1 - p_o(t,\delta t)$.

It can be shown that for $n_o(t)$ "large enough":

$$S_o(t,\delta t) \sim n_o(t)q_o(t,\delta t) + G(0,n_o(t)p_o(t,\delta t)q_o(t,\delta t)) \tag{B.8}$$

(B.6) and (B.8) yield using the independence assumption:

$$n_1(t + \delta t) - n_1(t) \sim -n_1(t)q_1(t,\delta t) + n_o(t)q_o(t,\delta t)$$

$$+ G[0,n_1(t)p_1(t,\delta t)q_1(t,\delta t)$$

$$+ n_o(t)p_o(t,\delta t)q_o(t,\delta t)] \qquad \text{(B.9)}$$

Dividing equation (B.9) by n yields for n "large enough":

$$\bar{m}(t + \delta t) - \bar{m}(t) \simeq -\bar{m}(t)q_1(t,\delta t) + (1 - \bar{m}(t))q_o(t,\delta t) \qquad \text{(B.10)}$$

Furthermore, dividing equation (B.10) by δt and considering limits as δt goes to zero yields:

$$\frac{d\bar{m}}{dt} \simeq -\bar{m}(t) \lim_{\delta t \to 0} \frac{1}{\delta t} q_1(t,\delta t) + (1 - \bar{m}(t)) \lim_{\delta t \to 0} \frac{1}{\delta t} q_o(t,\delta t) \qquad \text{(B.11)}$$

The limits in (B.11) can be evaluated as follows:

$$\lim_{\delta t \to 0} \frac{q_1(t,\delta t)}{\delta t} = \lim_{\delta t \to 0} \frac{1}{\delta t} \Pr[x(t') > x_+$$

$$\text{for } t' \varepsilon [t,t + \delta t] \mid m(t) = 1]$$

$$= \lim_{\delta t \to 0} \frac{1}{\delta t} \Pr[x(t) - a(x(t') - x_a(t'))(t'-t)$$

$$+ v(t') - v(t) > x_+ \text{ for } t' \varepsilon [t,t+\delta t] \mid m(t) = 1] \qquad \text{(B.12)}$$

where equation (3.7) has been used. However as $\delta t \to 0$, $\delta v(t)$ is of the order of $\sigma\sqrt{\delta t}$. Therefore, in the difference $\delta v(t)$ and $a(x(t) - x_a(t))\delta t$, the latter term can be neglected, in which case (B.12) reads:

$$\lim_{\delta t\to 0} \frac{1}{\delta t} q_1(t,\delta t) = \lim_{\delta t\to 0} \frac{1}{\delta t} \Pr\big[x(t) + v(t') - v(t) \geq x_+$$

$$\text{for } t' \varepsilon [t, t+\delta t] \,|\, m(t) = 1\big]$$

$$= 2 \lim_{\delta t\to 0} \frac{1}{\delta t} \big[\Pr[x(t) + \delta v(t) \geq x_+] \,|\, m(t) = 1\big] \tag{B.13}$$

where in (B.13) Désiré André's reflection principle [51] has been used. (B.9) and the law of total probability yield:

$$\lim_{\delta t\to 0} \frac{1}{\delta t} q_1(t,\delta t) = 2 \lim_{\delta t\to 0} \frac{1}{\delta t} \int_0^\infty \big[F_1^c(x_+,t) - F_1^c(x_+-u,t)\big] f_{\delta v}(u)\,du \tag{B.14}$$

where $F_1^c(\lambda,t)$ is the distribution function associated with $f_1^c(\lambda,t)$ and $f_{\delta v}(u)$ is the probability density of $\delta v(t)$, i.e.:

$$f_{\delta v}(u) = \frac{1}{\sqrt{2\pi\delta t}\,\sigma} e^{-\frac{u^2}{2\sigma^2\delta t}} \tag{B.15}$$

Assuming $f_1^c(\lambda,t)$ is twice differentiable, a Taylor series expansion of $F_1^c(x_+-u,t)$ in the neighborhood (left) of x_+ yields:

$$\lim_{\delta t\to 0} \frac{1}{\delta t} q_1(t,\delta t) = 2 \lim_{\delta t\to 0} \frac{1}{\delta t} \int_0^\infty \Big[f_1^c(x_+,t)u - \frac{1}{2} \frac{\partial f_1^c}{\partial x}(x_+,t)u^2$$

$$+ \frac{1}{6} \frac{\partial^2 f_1^c}{\partial x^2}(\eta(u),t)u^3\Big] f_{\delta v}(u)\,du \tag{B.16}$$

where $x_+ - u \leq \eta(u) \leq x_+$. Using (B.15) it is possible to show that:

$$\lim_{\delta t \to 0} \frac{1}{\delta t} \int_0^\infty f_1^c(x_+,t)\, u\, f_{\delta v}(u)\, du = O(\delta t)^{-1/2} \to \infty \qquad \text{(B.17)}$$

The limit in (B.16) represents the rate of decrease of $F_1^c(x_+,t)$ at time t. Now, the limit in (B.17) is infinite. This means that if $f_1^c(x_+,t)$ is nonzero for a finite time δt, $F_1^c(x_+,t)$ would decrease by an infinite amount which is impossible ($F_1^c(x_+,t)$ is a probability). This means:

$$f_1^c(x_+,t) = 0 \quad \forall\ t \qquad \text{(B.18)}$$

(B.15), (B.16) and (B.18) yield:

$$\lim_{\delta t \to 0} \frac{q_1(t,\delta t)}{\delta t} = -\frac{1}{2}\sigma^2 \frac{\partial f_1^c}{\partial x}(x_+,t) \qquad \text{(B.19)}$$

Similar arguments yield the following equations:

$$f_o^c(x_-,t) = 0 \quad \forall\ t \qquad \text{(B.20)}$$

$$\lim_{\delta t \to 0} \frac{q_o(t,\delta t)}{\delta t} = \frac{1}{2}\sigma^2 \frac{\partial f_o^c}{\partial x}(x_-,t) \qquad \text{(B.21)}$$

(B.11), (B.19) and (B.21) yield:

$$\frac{d\bar{m}}{dt} = \bar{m}(t)\left(\frac{\sigma^2}{2} \frac{\partial f_1^c}{\partial x}(x_+,t)\right) + (1-\bar{m}(t))\left(\frac{\sigma^2}{2} \frac{\partial f_o^c}{\partial x}(x_-,t)\right) \qquad \text{(B.22)}$$

Finally, if we note that:

$$f_1(x,t) = f_1^c(x,t)\bar{m}(t) \tag{B.23}$$

$$f_o(x,t) = f_o^c(x,t)(1 - \bar{m}(t)) \tag{B.24}$$

Then (B.22) yields:

$$\frac{d\bar{m}}{dt} = \frac{\sigma^2}{2} \frac{\partial f_1}{\partial x}(x_+,t) + \frac{\sigma^2}{2} \frac{\partial f_o}{\partial x}(x_-,t) \tag{B.25}$$

Equation (B.25) clearly indicates that by solving for the dynamics of the time functions $\frac{\partial f_1}{\partial x}(x_+,t)$ and $\frac{\partial f_o}{\partial x}(x_-,t)$ the evolution of the aggregate functional state $\bar{m}(t)$ can be determined. This will be the object of Appendix B.2.

Finally, in light of equations (B.11), (B.19) and (B.21), the terms in the right-hand side of (B.25) can be interpreted as being the average fraction of devices that switch from "off" to "on" $\left(\frac{\sigma^2}{2} \frac{\partial f_o}{\partial x}(x_-,t)\right)$ minus the average fraction of devices that switch from "on" to "off" $\left(-\frac{\sigma^2}{2} \frac{\partial f_o}{\partial x}(x_+,t)\right)$ per unit time at time t.

B.2 Ensemble Analysis: The Coupled Fokker-Planck Equations (CFPE) Model

Here, a formal analysis of the dynamics of $E_w(m_i(t))$ is undertaken. Equation (5.7) is repeated below for convenience:

$$\bar{m}(t) = E_w(m_i(t)) \tag{B.26}$$

We have:

$$E_w(m_i(t)) = 1.\Pr(m_i(t) = 1) + 0.\Pr(m_i(t) = 0) \tag{B.27}$$

but

$$\Pr(m_i(t) = 1) = \int_{-\infty}^{x_+} f_1(\lambda,t)d\lambda \tag{B.28}$$

(B.26)-(B.28) yield:

$$\bar{m}(t) = \int_{-\infty}^{x_+} f_1(\lambda,t)d\lambda = F_1(x_+,t) \tag{B.29}$$

where $F_1(\lambda,t)$ represents the distribution function associated with $f_1(\lambda,t)$. Equations (B.25) and (B.29) represent two alternative ways of computing $\bar{m}(t)$. At the end of this appendix their mutual consistency will be established.

As in the original derivation of the Fokker-Planck or forward Kolmogorov equation for Markov diffusion processes by Kolmogorov [52] and reported in [53], our proof starts from the Chapman-Kolmogorov equations [53]. For this particular hybrid state system, the Chapman-Kolmogorov equations can be modified as follows:

$$f_{ij}(\lambda',t',\lambda,t) = \sum_{k=0}^{1} \int_{-\infty}^{+\infty} f_{ik}(\lambda',t',z,\tau) f_{kj}(z,\tau,\lambda,t)dz$$

$$\text{for } i=0,1\ , \quad j=0,1 \quad \text{and any } \tau \in (t',t) \tag{B.30}$$

and where transition probability density functions:

$$f_{ij}(\lambda',t',\lambda,t)d\lambda = \Pr[(\lambda < x(t) \leq \lambda + d\lambda) \cap (m(t) = j) \mid$$

$$x(t') = \lambda', m(t') = i] \tag{B.31}$$

for $i=0,1$, $j = 0,1$ have been introduced. Also, defining:

$$f_1^o(\lambda) = f_1(\lambda,0) \tag{B.32}$$

$$f_o^o(\lambda) = f_o(\lambda,0) \tag{B.33}$$

We can write:

$$f_i(\lambda,t) = \sum_{k=0}^{1} \int_{-\infty}^{+\infty} f_{ki}(\lambda',0,\lambda,t) f_k^o(\lambda') d\lambda' \tag{B.34}$$

for i=0,1.

The derivations to follow are divided in two parts, A and B. In part A, we derive equation (5.9) only for $f_1(\lambda,t)$ and on the interval $(x_-,x_+]$, i.e. in region b of Fig. 5-2. The partial differential equations satisfied by $f_1(\lambda,t)$ in region a, and by $f_o(\lambda,t)$ (equation 5.10) in regions b and c of Fig 5-2 can be obtained using an exactly analogous procedure. In part B, we show that the boundary conditions (5.11)-(5.16) hold.

A. Derivation of Equation (5.9) on the Interval $(x_-,x_+]$:

Let ε be an arbitrarily small positive number. Also, let $R(\lambda)$ be an arbitrarily non-negative continuous function such that: $R(\lambda) = 0$ for $\lambda < x_- + \varepsilon$ and $\lambda > x_+$, and the function is three times differentiable and vanishes together with its first three derivatives at $x_- + \varepsilon$ and x_+. In the following, it is assumed that all the needed partial derivatives exist and are continuous in the interval of interest. It is also assumed that sufficient conditions (such as those dictated by Lebesgue's dominated convergence theorem [54]) are satisfied to allow interchange of orders of integration and differentiation whenever applicable. For $h > 0$:

$$\lim_{h\to 0} \int_{x_-+\varepsilon}^{x_+} \frac{f_{11}(\lambda',t',\lambda,t+h) - f_{11}(\lambda',t',\lambda,t)}{h} R(\lambda)d\lambda$$

$$= \int_{x_-+\varepsilon}^{x_+} \frac{\partial}{\partial t} f_{11}(\lambda',t',\lambda,t+h)R(\lambda)d\lambda \qquad \text{(B.35)}$$

Using (B.30), and setting i=j=1, we have:

$$f_{11}(\lambda',t',\lambda,t+h) = \int_{-\infty}^{+\infty} f_{11}(\lambda',t',z,t)f_{11}(z,t,\lambda,t+h)dz$$

$$+ \int_{-\infty}^{+\infty} f_{10}(\lambda',t',z,t)f_{01}(z,t,\lambda,t+h)dz \qquad \text{(B.36)}$$

Correspondingly,

$$\int_{x_-+\varepsilon}^{x_+} \frac{\partial}{\partial t} f_{11}(\lambda',t',\lambda,t)R(\lambda)d\lambda$$

$$= \lim_{h\to 0} \frac{1}{h} \left[\int_{x_-+\varepsilon}^{x_+} \int_{-\infty}^{+\infty} f_{11}(\lambda',t',z,t)f_{11}(z,t,\lambda,t+h)R(\lambda)dzd\lambda\right.$$

$$\left. - \int_{x_-+\varepsilon}^{x_+} f_{11}(\lambda',t',\lambda,t)R(\lambda)d\lambda\right]$$

$$+ \lim_{h\to 0} \frac{1}{h} \int_{x_-+\varepsilon}^{x_+} \int_{-\infty}^{+\infty} f_{10}(\lambda',t',z,t)f_{01}(z,t,\lambda,t+h)R(\lambda)dzd\lambda \qquad \text{(B.37)}$$

Now, define:

$$\tau_{11t}^{\lambda,\lambda'} = \inf\{(t'-t):x(t') = \lambda', m(t')=1 | x(t) = \lambda, m(t) = 1\} \qquad (B.38)$$

for any λ,λ', i.e. $\tau_{11t}^{\lambda,\lambda'}$ is the first passage time random variable [55] from hybrid state $\binom{1}{\lambda}$ at time t to hybrid state $\binom{1}{\lambda'}$.

Then clearly for h infinitesimal:

$$\int_{x_-+\varepsilon}^{x_+} \int_{-\infty}^{+\infty} f_{10}(\lambda',t',z,t) f_{01}(z,t,\lambda,t+h)\,dz\,d\lambda \leq \Pr\left[\tau_{11t}^{x_-,x_-+\varepsilon} \leq h\right]$$

$$\leq \Pr\left[\sup x(t') > x_- + \varepsilon\ ,\ m(t') = 1\right.$$

$$\text{for } t' \in [t,t+h] \,|\, (m(t) = 1) \cap (x(t) = x_-)]$$

$$\leq \Pr\left[(R - a(x_- - x_a(t))(t'-t)\right.$$

$$\left. + v(t') - v(t) > \varepsilon, \quad \text{for } t' \in (t,t+h)\right] \qquad (B.39)$$

where equation (3.7) has been used. However, as argued in Appendix B.1, as $h \to 0$, $\delta v(t)$ is of the order of $\sigma\sqrt{h}$. Therefore, in the difference of $\delta v(t)$ and $(R - a(x_- - x_a(t)))h$, the latter term can be neglected. (B.39) yields:

$$\int_{x_-+\varepsilon}^{x_+} \int_{-\infty}^{+\infty} f_{10}(\lambda',t',z,t) f_{01}(z,t,\lambda,t+h)\,dz\,d\lambda \leq \Pr\left[v(t') - v(t)\right.$$

$$\left. > \varepsilon \text{ for } t' \in [t,t+h]\right] \leq 2 \Pr\left[\delta v(t) > \varepsilon\right] \qquad (B.40)$$

where in the above, Desire Andre's reflection principle has been used. Consequently:

$$0 \leq \lim_{h\to 0} \frac{1}{h} \int_{x_-+\varepsilon}^{x_+} \int_{-\infty}^{+\infty} f_{10}(\lambda',t',z,t) f_{01}(z,t,\lambda,t+h)\,dz\; R(\lambda)\,d\lambda$$

$$\leq \lim_{h\to 0} \frac{2}{h} \Pr[\delta v(t) > \varepsilon] R_{max} \qquad \text{(B.41)}$$

where R_{max} is the minimum of $R(\lambda)$ over the interval. Due to the almost sure continuity of sample paths of Brownian motion, [51], the limit in (B.41) must be zero. Now:

$$\lim_{h\to 0} \frac{1}{h} \int_{x_-+\varepsilon}^{x_+} \int_{-\infty}^{+\infty} f_{11}(\lambda',t',z,t) f_{11}(z,t,\lambda,t+h) R(\lambda)\,dz\,d\lambda$$

$$= \lim_{h\to 0} \frac{1}{h} \int_{-\infty}^{+\infty} \int_{x_-+\varepsilon}^{x_+} f_{11}(\lambda',t',z,t) f_{11}(z,t,\lambda,t+h) R(\lambda)\,d\lambda\,dz$$

$$= \lim_{h\to 0} \frac{1}{h} \int_{-\infty}^{+\infty} \int_{x_-+\varepsilon}^{x_+} f_{11}(\lambda',t',\lambda,t) f_{11}(\lambda,t,z,t+h) R(z)\,dz\,d\lambda$$

$$= \lim_{h\to 0} \frac{1}{h} \int_{-\infty}^{+\infty} f_{11}(\lambda',t',\lambda,t) \int_{-\infty}^{+\infty} f_{11}(\lambda,t,z,t+h) R(z)\,dz\,d\lambda \qquad \text{(B.42)}$$

And:

$$\lim_{h\to 0} \frac{1}{h} \left[\int_{x_-+\varepsilon}^{x_+} \int_{-\infty}^{+\infty} f_{11}(\lambda',t',z,t) f_{11}(z,t,\lambda,t+h) R(\lambda)\,dz\,d\lambda \right.$$

$$- \int_{x_-+\varepsilon}^{x_+} f_{11}(\lambda',t',\lambda,t)R(\lambda)d\lambda\Big]$$

$$= \lim_{h\to 0} \frac{1}{h}\Big[\int_{-\infty}^{+\infty} f_{11}(\lambda',t',\lambda,t)\Big[\int_{-\infty}^{+\infty} f_{11}(\lambda,t,z,t+h)R(z)dz - R(\lambda)\Big]d\lambda\Big] \qquad (B.43)$$

Using a Taylor series expansion for R(z), we have:

$$R(z) = R(\lambda) + (z-\lambda)R'(\lambda) + \frac{1}{2}(z-\lambda)^2 R''(\lambda)$$

$$+ \frac{1}{6}(z-\lambda)^3 R'''\big(\eta(\lambda,z)\big) \qquad (B.44)$$

where $\lambda \leq \eta(y,z) \leq z$. Substituting (B.44) in (B.43), (B.37) and recalling (B.41), we obtain:

$$\int_{x_-+\varepsilon}^{x_+} \frac{\partial}{\partial t} f_{11}(\lambda',t',\lambda,t)R(\lambda)d\lambda$$

$$= \lim_{h\to 0} \int_{-\infty}^{+\infty} f_{11}(\lambda',t',\lambda,t)\Big[\frac{1}{h}\int_{-\infty}^{+\infty} f_{11}(\lambda,t,z,t+h)(z-\lambda)dz\ R'(\lambda)$$

$$+ \frac{1}{h}\int_{-\infty}^{+\infty} f_{11}(\lambda,t,z,t+h)\ \frac{1}{2}(z-\lambda)^2 dz\ R''(\lambda)$$

$$+ \frac{1}{h}\int_{-\infty}^{+\infty} f_{11}(\lambda,t,z,t+h)\ \frac{1}{6}(z-\lambda)^3 dz\ R'''(\eta(\lambda,z))\Big]d\lambda \qquad (B.45)$$

From equation (3.7):

$$\lim_{h\to 0} \frac{1}{h} \int_{-\infty}^{+\infty} f_{11}(\lambda,t,z,t+h)(z-\lambda)dz = [-a(\lambda-x_a(t)) + Rb(t)] \qquad (B.46)$$

and

$$\lim_{h\to 0} \frac{1}{h} \int_{-\infty}^{+\infty} f_{11}(\lambda,t,z,t+h)(z-\lambda)^2 dz = \sigma^2 \qquad (B.47)$$

Also:

$$\lim_{h\to 0} \frac{1}{h} \int_{-\infty}^{+\infty} f_{11}(\lambda,t,z,t+h)(z-\lambda)^3 dz = 0 \qquad (B.48)$$

In (B.45), it can be shown that the integrand satisfies conditions that permit the application of Lebesgue's dominated convergence theorem [54]. In this case, the limit operation in (B.45) can be moved past the integral sign. Using (B.46)-(B.48) one obtains:

$$\int_{x_-+\varepsilon}^{x_+} \frac{\partial}{\partial t} f_{11}(\lambda',t',\lambda,t)R(\lambda)d\lambda = \int_{-\infty}^{+\infty} f_{11}(\lambda',t',\lambda,t)$$

$$\left[(-a(\lambda - x_a(t)) + Rb(t))\ R'(\lambda) + R''(\lambda)\ \frac{\sigma^2}{2}\ \right]d\lambda \qquad (B.49)$$

Integration by parts (twice) of the right-hand side of (B.49) and recalling properties of $R(\lambda)$ yields:

$$\int_{x_-+\varepsilon}^{x_+} \left[\frac{\partial}{\partial t} f_{11}(\lambda',t',\lambda,t)\right.$$

$$\left. + \frac{\partial}{\partial \lambda} [-a(\lambda-x_a(t)) + Rb(t)] f_{11}(\lambda',t',\lambda,t)\right.$$

$$- \frac{\sigma^2}{2} \frac{\partial^2}{\partial \lambda^2} f_{11}(\lambda',t',\lambda,t)]R(\lambda)d\lambda = 0 \qquad (B.50)$$

Since (B.50) is satisfied for any positive $R(\lambda)$ (subject to the constraints mentioned earlier) and for an arbitarily small ε, we conclude that for almost any λ on $(x_-,x_+]$:

$$\frac{\partial}{\partial t} f_{11}(\lambda',t',\lambda,t)$$

$$+ \frac{\partial}{\partial \lambda} [-a(\lambda - x_a(t)) + Rb(t)] f_{11}(\lambda',t',\lambda,t)$$

$$- \frac{\sigma^2}{2} \frac{\partial^2}{\partial \lambda^2} f_{11}(\lambda',t',\lambda,t) = 0 \qquad (B.51)$$

Furthermore, starting from the Chapman-Kolmogorov equation for $f_{01}(\lambda',t',\lambda,t)$ (equation (B.30)) and using a similar approach one can show that $f_{01}(\lambda',t',\lambda,t)$ satisfies:

$$\frac{\partial}{\partial t} f_{01}(\lambda',t',\lambda,t)$$

$$+ \frac{\partial}{\partial \lambda} [-a(\lambda - x_a(t)) + Rb(t)] f_{01}(\lambda',t'\lambda,t)$$

$$- \frac{\sigma^2}{2} \frac{\partial^2}{\partial \lambda^2} f_{01}(\lambda',t',\lambda,t) = 0 \qquad (B.52)$$

Setting $t' = 0$ in (B.51)-(B.52) and multiplying both equations by $f_1^o(\lambda')$ and $f_o^o(\lambda')$ respectively, we obtain after addition:

$$\sum_{k=0}^{2} [\frac{\partial}{\partial t} f_{k1}(\lambda',0,\lambda,t)$$

$$+ \frac{\partial}{\partial\lambda} [-a(\lambda - x_a(t)) + Rb(t)] f_{k1}(\lambda', 0, \lambda, t)$$

$$- \frac{\sigma^2}{2} \frac{\partial^2}{\partial\lambda^2} f_{k1}(\lambda', 0, \lambda, t)] f_k^o(\lambda') = 0 \qquad \text{(B.53)}$$

Integrating (B.53) from $-\infty$ to $+\infty$, and using (B.33) we have after interchanging orders of integration and partial differentiation:

$$\frac{\partial f_1}{\partial t}(\lambda, t) + \frac{\partial}{\partial\lambda} [-a(\lambda - x_a(t)) + Rb(t)] f_1(\lambda, t)$$

$$- \frac{\sigma^2}{2} \frac{\partial^2}{\partial\lambda^2} f_1(\lambda, t) = 0 \qquad \text{(B.54)}$$

This completes the derivation of equation (5.9).

B. Boundary Conditions

We discuss only equations (5.11), (5.12), (5.13), and (5.15). The remaining boundary conditions follow by analogy. Equation (5.11) has already been established in B.1 (equations (B.18) and (B.20)). Equation (5.12) follows from the continuity of $f_1(\lambda, t)$ on $(-\infty, x_+]$ and the fact that it must be integrable on that interval (the integral is a probability and is accordingly finite). Equation (5.13) expresses the continuity of $f_1(\lambda, t)$ across boundary x_-. Assumptions of continuity can always be made as long as they do not generate contradictions. We now proceed to establish equation (5.15). It is clear that equations (5.9) and (5.10) are mathematically reminiscent of a diffusion process (in the presence of a gravitational field). In what follows, the analogy is used freely. In Fig. B-1, an infinitesimal strip of width ε on either side of x_- is considered. Let $L_1(t, \varepsilon)$, $L_2(t, \varepsilon)$, $L_3(t)$, $L_4(t)$ represent respectively:

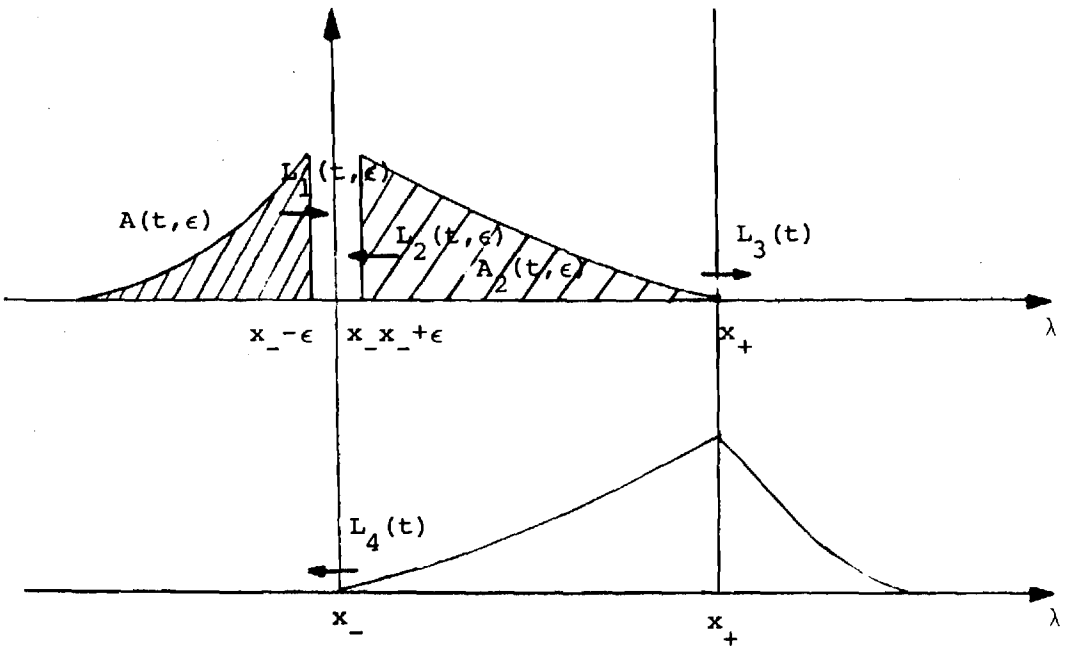

Figure B-1. Graphical Representation of the Flow of Probability within a Rectangular Strip of Width 2ε around x_-.

- The rate at which probability diffuses from left to right past the edge at $x_- - \varepsilon$.
- The rate at which probability diffuses from right to left past the edge at $x_- + \varepsilon$.
- The rate at which probability diffuses from $f_1(\lambda,t)$ to $f_o(\lambda,t)$ past the edge x_+.
- The rate at which probability diffuses from $f_o(\lambda,t)$ to $f_1(\lambda,t)$ past the edge x_-.

Finally $A_1(t,\varepsilon)$ and $A_2(t,\varepsilon)$ are the hatched areas represented in Fig. B-1. Using equations (B.55), we have:

$$L_1(t,\varepsilon) = -\frac{\partial}{\partial t} A_1(t,\varepsilon) = -\frac{\partial F_1}{\partial t}(x_- - \varepsilon,t)$$

$$= [-a(x_- - \varepsilon - x_a(t)) + Rb(t)] f_{1a}(x_- - \varepsilon,t)$$

$$-\frac{\sigma^2}{2}\frac{\partial}{\partial \lambda} f_{1a}(x_- - \varepsilon,t) \qquad (B.55)$$

where use has been made of:

$$\lim_{\lambda \to -\infty} f_{1a}(\lambda,t) = \lim_{\lambda \to -\infty} \frac{\partial f_{1a}}{\partial \lambda}(\lambda,t) = 0$$

Furthermore:

$$\frac{\partial A_2}{\partial t}(t,\varepsilon) = \frac{\partial}{\partial t}[F_1(x_+,t) - F_1(x_- + \varepsilon,t)]$$

$$= -[-a(x_+ - x_a(t)) + Rb(t)] f_{1b}(x_+,t) + \frac{\sigma^2}{2}\frac{\partial}{\partial \lambda} f_{1b}(x_+,t)$$

$$+ [-a(x_+ + \varepsilon - x_a(t)) + Rb(t)] f_{1b}(x_+ + \varepsilon, t) - \frac{\sigma^2}{2} \frac{\partial}{\partial \lambda} f_{1b}(x_- + \varepsilon, t) \quad (B.56)$$

Using (5.11) the first term on the right hand side of (B.55) can be dropped from the expression. Furthermore, from (B.19) we recognize that:

$$L_3(t) = - \frac{\sigma^2}{2} \frac{\partial}{\partial \lambda} f_{1b}(x_+, t) \quad (B.57)$$

Also:

$$\frac{\partial A_2}{\partial t} (t, \varepsilon) = -L_2(t, \varepsilon) - L_3(t) \quad (B.58)$$

(B.56)-(B.58) yield:

$$L_2(t, \varepsilon) = \frac{\sigma^2}{2} \frac{\partial}{\partial \lambda} f_{1b}(x_- + \varepsilon, t) - [-a(x_- + \varepsilon - x_a(t)) + Rb(t)] f_{1b}(x_+ + \varepsilon, t) \quad (B.59)$$

Let $I(t, \varepsilon)$ be the rate of probability increase within the rectangular strip in Fig. B-1, then from probability conservation:

$$I(t, \varepsilon) = L_1(t, \varepsilon) + L_2(t, \varepsilon) + L_4(t) \quad (B.60)$$

Also, recalling (B.21):

$$L_4(t) = \frac{\sigma^2}{2} \frac{\partial}{\partial \lambda} f_{ob}(x_-, t) \quad (B.61)$$

In (B.62), letting ε go to zero and using the continuity of $f_1(\lambda, t)$ at x_-, (B.55) and (B.59), we obtain:

$$\lim_{\varepsilon \to 0} I(t,\varepsilon) = 0 = -\frac{\sigma^2}{2} \frac{\partial}{\partial \lambda} f_{1a}(x_-,t) + \frac{\sigma^2}{2} \frac{\partial}{\partial \lambda} f_{1b}(x_-,t)$$

$$+ \frac{\sigma^2}{2} \frac{\partial}{\partial \lambda} f_{ob}(x_-,t) \tag{B.62}$$

and hence (5.15). This completes the proof of the theorem. •

Remark 1: The fact that the limit in (B.41) is zero has an important significance. It means that for h infinitesimal, the Chapman-Kolmogorov equation in (B.36) (written from t to t+h) reduces to the ordinary Chapman-Kolmogorov equation for a one dimensional Markov process. This in turn, means that the various transition probability densities defined in (B.31) behave "locally" like transition densities of some one dimensional Markov process. Therefore, it is no surprise that each of them satisfies individually some Fokker-Planck equation. In this light, boundary conditions (5.11) can be viewed as standard for Markov diffusion processes encountering an absorbing boundary.

Remark 2: It is possible to show that (B.29) is consistent with (B.25). We have:

$$\bar{m}(t) = \int_{-\infty}^{x_-} f_1(\lambda,t)d\lambda + \int_{x_-}^{x_+} f_1(\lambda,t)d\lambda$$

i.e.

$$\frac{d\bar{m}}{dt} = \int_{-\infty}^{x_-} \frac{\partial f_1}{\partial t}(\lambda,t)d\lambda + \int_{x_-}^{x_+} \frac{\partial f_1}{\partial t}(\lambda,t)d\lambda \tag{B.63}$$

Recalling (5.9), (5.11) and (5.13) one obtains:

$$\frac{d\bar{m}}{dt} = \frac{\sigma^2}{2} \frac{\partial}{\partial \lambda} f_{1a}(x_-,t) - \frac{\sigma^2}{2} \frac{\partial}{\partial \lambda} f_{1b}(x_-,t) + \frac{\sigma^2}{2} \frac{\partial}{\partial \lambda} f_{1b}(x_+,t) \tag{B.64}$$

Using (5.15), (B.64) yields:

$$\frac{d\bar{m}}{dt} = \frac{\sigma^2}{2} \frac{\partial}{\partial \lambda} f_{1b}(x_+, t) + \frac{\sigma^2}{2} \frac{\partial}{\partial \lambda} f_{ob}(x_-, t) \qquad \text{(B.65)}$$

APPENDIX C

COMPUTATION OF TRANSITION MATRIX IN (5.35)

We use a transform technique to compute the state transition matrix in (5.35). If γ represents the complex variable in the transformation, we have:

$$\underline{\phi}(\lambda,s) = L^{-1}\left|\begin{matrix}\gamma & -1\\ -\frac{2s}{\sigma^2} & \gamma-\frac{2r}{\sigma^2}\end{matrix}\right|^{-1} \tag{C.1}$$

where in (C.1), $L^{-1}\{\cdot\}$ represents the inverse Laplace transform operator. From (C.1):

$$\underline{\phi}(\lambda,s) = L^{-1}\left\{\frac{\sigma^2}{\gamma^2\sigma^2 - 2\gamma r - 2s}\left|\begin{matrix}\gamma-\frac{2r}{\sigma^2} & 1\\ \frac{2s}{\sigma^2} & \gamma\end{matrix}\right|\right\} \tag{C.2}$$

which yields:

$$\phi_{11}(\lambda,s) = L^{-1}\left[\frac{\gamma\sigma^2 - 2r}{\sigma^2(\gamma-\theta_1(s))(\gamma-\theta_2(s))}\right]$$

$$= \theta^{-1}(s)\left[\theta_1(s)e^{\theta_2(s)\lambda} - \theta_2(s)e^{\theta_1(s)\lambda}\right] \tag{C.3}$$

where in (C.3), $\theta(s)$, $\theta_1(s)$, $\theta_2(s)$ have already been defined in (5.40)-(5.41)

$$\phi_{12}(\lambda,s) = L^{-1}\left[\frac{\sigma^2}{\sigma^2(\gamma-\theta_1(s))(\gamma-\theta_2(s))}\right]$$

$$= \theta^{-1}(s)\left[e^{\theta_1(s)\lambda} - e^{\theta_2(s)\lambda}\right] \tag{C.4}$$

$$\phi_{21}(\lambda,s) = L^{-1}\left[\frac{2s}{\sigma^2(\gamma - \theta_1(s))(\gamma - \theta_2(s))}\right]$$

$$= \frac{2s}{\sigma^2}\left[e^{\theta_1(s)\lambda} - e^{\theta_2(s)\lambda}\right]\theta^{-1}(s) \qquad \text{(C.5)}$$

$$\phi_{22}(\lambda,s) = L^{-1}\left[\frac{\gamma\sigma^2}{\sigma^2(\gamma - \theta_1(s))(\gamma - \theta_2(s))}\right]$$

$$= \theta^{-1}(s)\left[\theta_1(s)e^{\theta_1(s)\lambda} - \theta_2(s)e^{\theta_2(s)\lambda}\right] \qquad \text{(C.6)}$$

Georgia Institute of Technology

School of Electrical Engineering

FINAL REPORT

A STATISTICAL APPROACH FOR MODELING A CLASS OF POWER SYSTEM LOADS

Project E21-618

Project Director

Dr. Atif S. Debs

STAFF

Dr. C. Y. Chong

Dr. R. Malhami

Preface

This report constitutes the final document for project E21-618 entitled originally as "Development of an Electrical Load Demand and Response Models Based on a Rational Synthesis from Elementary Devices," which was conducted under contract EC-77-5-01-5109 with the US Department of Energy. The report is a replica of the Ph.D. dissertation of Dr. Malhami.

ACKNOWLEDGEMENT

The author is grateful to his first dissertation advisor, Dr. Atif Debs, for providing a challenging thesis topic. He is also deeply indebted to Dr. Chee Yee Chong for countless stimulating conversations and insightful suggestions both when Dr. Chong was a faculty member at Georgia Tech and later after he joined "Advanced Information and Decision Systems" in Mountainview, CA. But foremost is his debt to Dr. Frank Lewis, his second dissertation advisor, who throughout the process of this author's graduate studies, has been a constant source of inspiration, guidance, support, and an admirable model of intellectual discipline.

Other persons to be thanked are the members of the dissertation reading committee, Drs. A. P. Meliopoulos and E. I. Verriest, for their careful review of the thesis manuscript, and valuable suggestions. The author is also grateful to Dr. Verriest for sharing with him as an interim advisor after Dr. Debs' departure, inspiring conversations and relevant suggestions.

The author would also like to thank Professors D. C. Ray, T. K. White, and R. P. Webb for their friendship. Dr. Meliopoulos is warmly thanked for his constant support.

Finally, acknowledgements are due to Mrs. Pamela Majors for her great patience and an excellent job of typing a complex manuscript within a record time.

This research was supported in part by the U.S. Department of Energy, Division of Electric Energy Systems under Contract No. EX-78-C-01-5109.

TABLE OF CONTENTS

LIST OF ILLUSTRATIONS

SUMMARY

A new model based on the Fokker-Planck equation is proposed to describe the electric behavior of large aggregates of electric space heaters or air conditioners. An understanding of the dynamics of such loads is essential for the construction of effective load management policies when load management by direct device control is considered.

The synthesis of the model follows the general philosophy of physically-based load modeling approaches, where the demand of individual components at the user level is modeled first. Subsequently, these component demands are aggregated to obtain the load at a point in the system.

The point of departure for the construction of the model is a recently proposed stochastic hybrid-state model for the demand of individual devices. The originality of the proposed approach lies in the method of aggregation which, like the methods of statistical mechanics from which it is inspired, yields an aggregate model which is exact in a limiting statistical sense.

The model is a system of coupled ordinary and partial differential equations (Fokker-Planck). A number of approximate analytical properties of this system are derived. Thus a better understanding of its dynamics is achieved. Subsequently, a more accurate numerical simulation algorithm is proposed and implemented. With this simulation tool at hand, cold load pickup dynamics are obtained for various outage durations and various load mixes.

From a practical standpoint, the results of this research appear to be promising. At a more theoretical level, the thesis presents a method (and no such method appears to exist in the literature) of writing Fokker-Planck equations for a particular hybrid-state (discrete/continuous) Markovian process. This leads one to speculate about the possibility of generalizing the results to a larger class of hybrid-state Markov processes.

CHAPTER I

A REVIEW OF CLASSICAL LOAD MODELING METHODS

1.1 Introduction

Power system load modeling can be said to encompass any activity aimed at modeling the dynamic behavior of electric loads (viewed as active and reactive power demands) either as a function of time (demand models), or of power system voltage and frequency (response models).

The vast majority of the work in the electric load modeling literature for both response and demand modeling is devoted to model identification based approaches [14]. These approaches are based on fitting parameters in a predetermined model structure to empirical load data at the bulk (system or subsystem) level. Until recently, no effort was aimed at relating explicitly model structures to the physical composition of the load. Hence the selected structures always appeared to be ad hoc.

Traditional load response models [1-3] have been motivated by the need for simplicity. Thus some of the selected models have taken the form of a constant resistance, inductance, capacitance, or a combination of these [1,2]. The resulting models do not work well when the power system undergoes large excursions outside its normal steady state.

A highly successful area of model building has been the construction of load demand models for prediction purposes both in the

short and the long term. Although the models suffer from the same weakness as the response models (ad hoc nature), their greater success is in part owed to the fact that they are selected from a class of models such as stochastic state-space or ARIMA (Autoregressive Integrated Moving Average) models known to be sufficiently rich to fit a large number of physical processes. In section 1.2 we describe the above model structures in some detail, and briefly survey the results in the literature.

1.2 Traditional Load Demand Models

If we ignore the refinements due to the introduction of weather-dependent modeling [4,5], the traditional load demand modeling approaches in the literature [5-9,13-18] can be roughly divided into two kinds: those utilizing a stochastic state space model to represent the evolution of the load, and those utilizing time-series or ARIMA models [11]. Usually, the choice of representation dictates the techniques subsequently involved in the identification of the models and the on-line updating of their parameters, as well as the form of the load predictor. In what follows, we describe the models, and discuss the identification and estimation techniques encountered in the load modeling literature.

Stochastic State-Space Models

If we ignore the possibility of introducing exogenous inputs (weather variables or others), the model is of the form:

$$\underline{x}_{k+1} = \underline{A}_k \underline{x}_k + \underline{W}_k \qquad (1.1)$$

$$\underline{y}_k = \underline{H}\,\underline{x}_k + \underline{v}_k \tag{1.2}$$

where $\underline{x}_k$ is the state vector $\varepsilon\ R^n$. $\underline{y}_k$ is the output vector $\varepsilon\ R^r$ (representing measurements at various stations), $\underline{A}_k$ is in general a time-varying [nxn] matrix of parameters, and $\underline{H}$ is an [rxn] constant output matrix. $\underline{w}_k$ and $\underline{v}_k$ are independent Gaussian vector processes, also independent of $\underline{x}_k$, and such that:

$$E[\underline{w}_k] = E[\underline{v}_k] = 0$$

$$E[\underline{w}_k \underline{w}_j^T] = \underline{Q}_k \delta_{kj}$$

$$E[\underline{v}_k \underline{v}_j^T] = \underline{R}_k \delta_{kj} \tag{1.3}$$

where $\underline{Q}_k$ and $\underline{R}_k$ are respectively [nxn] and [rxr] positive definite matrices, and δ_{kj} is the Kronecker delta.

It is also assumed that the initial state vector is a Gaussian random vector independent of $\underline{w}_k$, $\underline{v}_k$, such that $E[\underline{x}(0)] = \underline{x}_o$ and $E[(\underline{x}(0) - \underline{x}_o)(\underline{x}(0) - \underline{x}_o)^T] = \underline{P}_o$. The modeling approaches either assume that all parameters (1.1)-(1.2) are entirely known from physical considerations [6], or that some or all of them are to be estimated [5,7,9]. They either assume that the output measurement is scalar [5,6], or a vector [7,9] (thus allowing for a more realistic modeling of the actual load measurement procedure). The model parameters can be held constant [6], or allowed to drift slowly as in [5,7,9]. Finally in [9], the parameters in the covariance matrices in (1.3) are viewed as stochastic processes.

The chief advantage of representation (1.1)-(1.2) is that, once the required parameters are identified, it allows the recursive processing of the incoming measurements for state estimation and or prediction. The method used is the Kalman filter [10]. Under the assumptions discussed upon introduction of the model, the output of the filter is optimal in the sense of being a minimum variance unbiased estimate of the state.

If the parameters of the model do not vary, they can be identified off-line. However, it is desirable to allow the model to be adaptive, i.e. to change its own parameters as the measurements on which it was based become outdated. For this purpose, equation (1.1) can be rewritten as:

$$\underline{x}_{k+1} = f(\underline{P}_k, \underline{x}_k) + \underline{W}_k \tag{1.5}$$

where $\underline{P}_k$ represents the vector of parameters in $\underline{A}_k$. Now these parameters can be viewed as a stochastic process [5,8] such that:

$$\underline{P}_{k+1} = \underline{P}_k + \underline{\eta}_k \tag{1.6}$$

where $\underline{\eta}_k$ is a zero mean white Gaussian process with covariance matrix $\underline{Q}^P(k)$. Equation (1.2) can then be rewritten as:

$$\underline{y}_k = [\underline{H} \mid \underline{0}] \left| \begin{matrix} \underline{x}_k \\ \hline \underline{P}_k \end{matrix} \right| \tag{1.7}$$

(1.5)-(1.7) constitute an augmented state dynamic system that could estimate the parameters and states of (1.1)-(1.2) simultaneously. However, because of the cross terms between states, it is no longer linear, and the extended Kalman filter [10] must be used. Because of its poor convergence properties when the number of parameters is larger then the number of states, and also because the dimension of the filtering problem could go up to n(n+1) in the worst case, a two stage (parameter/state) prediction algorithm is suggested in [7]. This same procedure is applied in [9], except that an additional two stage estimator is incorporated to estimate the parameters of the input noise covariance matrices ($\underline{Q}_k$, $\underline{Q}_k^P$), which themselves are now viewed as stochastic processes.

Input noise covariance matrices $\underline{Q}_k$ in [6], and $\underline{Q}_k$, $\underline{Q}_k^P$ in [7] are viewed as constants. The important problem of estimating these matrices on line is considered in [6,7].

ARMA Models

ARMA models were first introduced by Box and Jenkins in [11] where they were studied in depth as a means of fitting a model to past history time series data.

The models of Box and Jenkins were subsequently generalized by Kashyap and Rao [12] to the case of vector time series data, i.e. multiple output systems, and the attending identification problems were discussed. Generally speaking, in the load modeling literature, state space approaches [5-9] are prevalent. However, some authors have preferred time series load models [13-17]. Although most use scalar time series [8,13-15,17], Mahalanabis [16] introduced load

models using vector time series. We discuss only scalar time series models.

The basic model introduced by Box and Jenkins is of the form:

$$x_k = \sum_{i=1}^{n} \phi_i x_{k-i} + \sum_{j=0}^{m} \theta_i u_{k-j} \tag{1.8}$$

where $\{x_k\}$ is the scalar time series of interest, and $\{u_k\}$ is a sequence of white Gaussian random variables, with zero mean and variance σ_u^2, representing an unmeasurable input. $\{\phi_i\}$ and $\{\theta_i\}$ are constant parameters.

If no $\{\phi_i\}$ are present in (1.8), the model is called a pure moving average (MA) model. If the $\{\theta_j\}$ $(j \neq 0)$ are absent, the model is called a pure autoregressive (AR) model. As clearly seen, (1.8) is simply a scalar stochastic difference equation.

If the backward shift operator is introduced $(Bu_k = u_{k-1})$, (1.8) can be rewritten as:

$$\phi(B)x_k = \theta(B)u_k \tag{1.9}$$

where $\phi(B)$ and $\theta(B)$ are appropriate polynomials in B. Note that one can easily go from (1.9) to an equivalent state-space formulation (1.1), where prediction via Kalman filtering can be used.

Model (1.8) can be refined in two ways [11] when the original time series is a nonstationary process:

(a) Nonperiodic, nonstationarities can sometimes be eliminated if a high enough degree of differencing is applied to

the original time series. This is the detrending procedure and should generally eliminate polynomial trends. For that purpose, define the one step difference operator ∇_1 such that:

$$\nabla_1 x_k = x_k - x_{k-1} \tag{1.10}$$

If d is the degree of differencing, (1.9) can now be rewritten:

$$\phi(B)\nabla_1^d x_k = \theta(B)u_k \tag{1.11}$$

(1.11) is called an autoregressive integrated moving average (ARIMA) model.

(b) After the elimination of nonperiodic nonstationarities, the time series could still contain periodic nonstationarities. This is particularly true for load demand time series which clearly exhibit daily and weekly periodic nonstationarities. The periodic trends could be eliminated using a high enough degree of m^{th} step differencing, where m is the periodicity of interest. For that purpose, define the m^{th} step difference operator ∇_m such that:

$$\nabla_m x_k = x_k - x_{k-m} \tag{1.12}$$

If e is the degree of m^{th} step differencing, then (1.11) becomes

$$\phi(B)\nabla_1^d\nabla_m^e x_k = \theta(B)u_k \ . \qquad (1.13)$$

However, at this stage, it could be found that the noise process u_k still has periodic correlations. If we now view u_k as the output of a linear filter such that:

$$\psi(B_m)u_k = \Theta(B_m)v_k \qquad (1.14)$$

where v_k is a white Gaussian noise sequence, $\psi(B_m)$ and $\Theta(B_m)$ are polynomials in $B_m(=B^m)$, then (1.13)-(1.14) yield:

$$\phi(B)\psi(B_m)\nabla_1^d\nabla_1^e x_k = \theta(B)\Theta(B^m)v_k \ . \qquad (1.15)$$

Multiple periodicities can be modeled likewise.

When the general form (1.15) is used, the models are called ARIMA multiplicative seasonal models [10]. Galiana et. al. [14], Keyhani and El-Abiad [13] have used ARMA models. The model parameters are estimated using maximum likelihood techniques [14], or via an estimate of the autocorrelation function of the process [13]. Keyhani et al. [13], further introduced an algorithm for the determination of the structure (orders) of their model. Singh et. al. [8], used an AR model, and introduced smoothing techniques (in the sense

of estimation theory) in constructing the load predictor. Mahalanabis et. al. [16], dealt with a vector AR model, and generalized the structure determination algorithm in Keyhani et. al., to a vector time series.

In [14], the parameters are constant and estimated off line. In constrast [8,13,16] consider adaptive models. In [8] a two stage (state/parameter) estimation procedure analogous to the one developed in [7] is proposed. A simple Kalman filter is utilized in [13,16] for on-line parameter estimation.

Finally, Vemuri et. al. [15] and Hagan and Klein [17] introduce seasonal ARMA scalar models (1.15). Vemuri's model is not adaptive. At this point it is of interest to note that prediction or parameter updating (when present) in all of the above methods, except [15], [17], [13], is accomplished via state-space techniques due to their attractive recursive character. However, Hagan and Klein work entirely in the framework of ARMA models. The parameters are first identified off-line via maximum likelihood techniques. They are then updated on-line using a result in on-line maximum likelihood estimation developed by Gertler et. al. [18]. Finally, prediction is accomplished via the techniques developed by Box and Jenkins [11].

In summary, ARIMA models are attractive because of their ability to model accurately a range of time-series originating in a wide variety of physical phenomena. In particular, multiple periodicities can be easily incorporated via multiplicative seasonal models, in contrast to the situation with stochastic state-space models. However, at this stage, the predictive and adaptive methods developed

for state space models appear to be much more attractive. Many authors [8,13-16] have tried to take advantage of both approaches by formulating their original model in ARMA form, identifying the parameters and subsequently converting the model to its equivalent state space representation for load prediction [8,13-15], and parameter updating [8,13,16].

1.3 Towards Physically-Based Load Modeling

The literature study in section 1.2, although brief, is indicative of the high degree to which identification based approaches to electric load modeling, at least in the area of demand modeling, have been refined. With the gradual introduction of new concepts in electric utilities practice however, questions have arisen that highlighted the limitations of such approaches. This point is now illustrated in the case of load management.

Load Management can be defined as "the deliberate control or influencing of the customer load in order to shift the time and amount of use of electric power and energy" [19]. The effort is directed toward producing a constant demand profile. This is because the existence of peaks and valleys in the load demand curve results in increased generation costs and diminished system reliability.

Three methods of load management may be defined: (1) direct control of specific customer appliances; (2) voluntary load control by the customer (i.e. the use of economic incentives and disincentives offered through the electric rate structure to encourage voluntary changes in customer consumption patterns and appliance mix); and (3) the use of thermal energy storage on the customer side of the meter under either utility or customer control.

Clearly, these three forms of load management require detailed understanding of the physical composition of the load and of customer behavior. Neither load physical composition nor customer behavior are significantly reflected in the load models discussed in section 1.2. This deficiency has prompted research in the synthesis of so called "physically-based" load models [20,23-25,29-34].

In the present research, we address the problem of synthesizing physically-based load models in the evaluation of load management policies of the first kind (direct control of user appliances).

In load management via direct device control (method 1), the utility modifies the load shape by acting directly on the power system. Accordingly, with the prior agreement of the users participating in the load management program, and at appropriate hours of the day (period of peak demand), service is interrupted intermittently for a selected class of customer appliances. Favored types of appliances for this method of load management have traditionally been electric water heaters, electric space heaters and air conditioners, because all of these are associated with some form of energy storage. The existence of stored energy makes a temporary interruption of power to the device hardly noticeable by the user. In an uncontrolled power system however, there exists a natural diversity (i.e. only a fraction of the total number of connected devices is in the "on" state at any particular time). The application of direct controls tends to disrupt this natural diversity. Thus, excessive load management can create undesirable electric demand peaks upon

restoration of service. Models are needed (and are presented here) to evaluate this type of effect.

The rest of the thesis is organized as follows: in chapter II, necessary background in the area of physically-based load modeling is presented. In chapter III, we draw on previous work in this area [29] and the theory of Markovian processes [38,39] to obtain models of the electric load component of large groups of controlled electric space heaters or air conditioners as a function of the control strategy. In chapter IV, some approximate analytical properties of the models are developed. Finally, in chapters V and VI, the dynamic behavior of the models is investigated via numerical techniques. Simulation results are presented.

CHAPTER II

BACKGROUND IN PHYSICALLY-BASED LOAD MODELING

2.1 Physically-Based Load Modeling

This research fits within the general area of physically-based electric load modeling. Grouped under this name are all research efforts utilizing a constructive approach (starting from load demand at the individual user level) for the synthesis of particular components of electric loads. Broadly speaking, the literature on physically-based load models deals either with general methodologies or with particular load models.

General Methodologies [20,29-34]: Here, a general theoretical framework for model synthesis is articulated with little focus on the actual application. We have developed the following general load model synthesis procedure which serves as a framework unifying the various model synthesis methodologies in the literature:

(a) First, a selection criterion is formulated which allows the identification of components of electric load exhibiting similar characteristics.

The similarity could for example, be in the electrical characteristics of the loads (e.g. air conditioners, water heaters), or in terms of the particular group of customers utilizing the devices (e.g. residential, commercial, etc.), or any combination of properties. Components which satisfy the same selection criterion will be called a group.

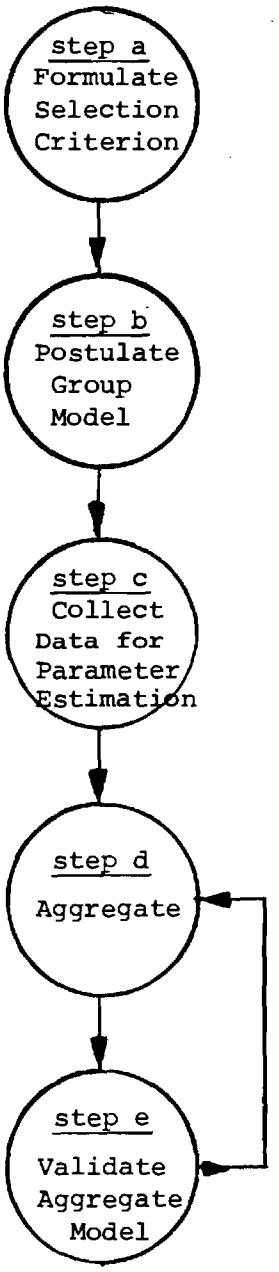

Fig. 2-1. Schematic Representation of General Load Model Synthesis Procedure

(b) A general model structure is determined for the electric demand of any device within a group.

(c) Based on step (b), data is collected for the identification of models for elemental load demands within groups.

(d) The elemental models are aggregated to obtain the overall electric behavior first of a group, then if necessary of an ensemble of groups.

(e) The model is validated by demonstrating its accuracy either by means of simulation-based method (i.e. compare the output of the model to a detailed simulation of the actual load), or by comparison with results from an actual field experiment.

This general load model synthesis procedure is schematically represented in Fig. 2-1. The various approaches in the literature to date differ in the following respects:

- The selection criterion in (a) is more or less discriminatory.
- The models in (b) are simple [29], or highly detailed [20,30-33] deterministic [20] or probabilistic [29-33].
- The aggregation method is either simulation-based [20], or capitalizes on the statistical properties of the aggregated models [29-33].

Among general synthesis methodologies, the work of Chong and Debs [29] is particularly relevant to this research and will be discussed in detail in section 2.2.

Particular Load Models [20,23-25,33-35]: Here, either an existing load synthesis methodology is applied to solve a particular load modeling problem, or a load synthesis methodology is created for a particular problem with no reference to previous work. The nature of the models depends strongly on the intended application. Important application areas are planning [33-34], load management using an inverted rate structure [35], and load management using directive device control [20,23]. An important area of research where modeling needs are closely related to load management method 1 is the cold load pickup problem [26]. This is the problem of predicting load behavior following a power outage. Devices associated with energy storage play an important role in the load dynamics in this problem.

In the literature, electric load models for groups of devices under load management range from the purely simulation-based [20,23] to completely analytic models [24,25]. Simulation-based approaches have the disadvantage of being costly, and do not lend themselves easily to analysis. On the other hand, the models are more realistic than purely analytic models because a greater modeling complexity is allowed.

References [24,25] both present analytic models of aggregate loads of electric space heaters. They have the common shortcoming of ignoring noise processes due to customer behavior, a weakness which is corrected in the modeling procedure of this dissertation. Furthermore, it will be shown in Chapter IV that our results incorporate [24] as a particular case.

2.4 The Classification of Chong and Debs

This research builds upon a device model classification proposed by Chong and Debs in [29]. In their work, two models are associated with every electrical device: an electrical response model and a functional model.

1. The Electrical Response Model: This corresponds to the portion of the device associated with energy conservation. For example, the resistance associated with an electric water heater. Among the inputs to this model are voltage and frequency.
2. The Functional Model: This is mainly useful in conjunction with devices that normally have a discrete number of modes in which to operate. For example, thermostat controlled electric space heaters oscillate between "on" and "off" modes. Among inputs to this model are weather w(t) and service demand v(t) (which summarizes the role of the customers).

Functional and response models are interrelated as shown in Figure 2-2. As we proceed to analyze functional models further, it will become apparent that this response/functional device model decomposition is tantamount to a model component decomposition into a deterministic subsystem with fast dynamics and a probabilistic subsystem with slow dynamics. The functional models of devices associated with energy storage are dynamic. This means that their operating state m(t) is not a memoryless function of service demand. For example, there is no fixed relationship at each instant of time between the

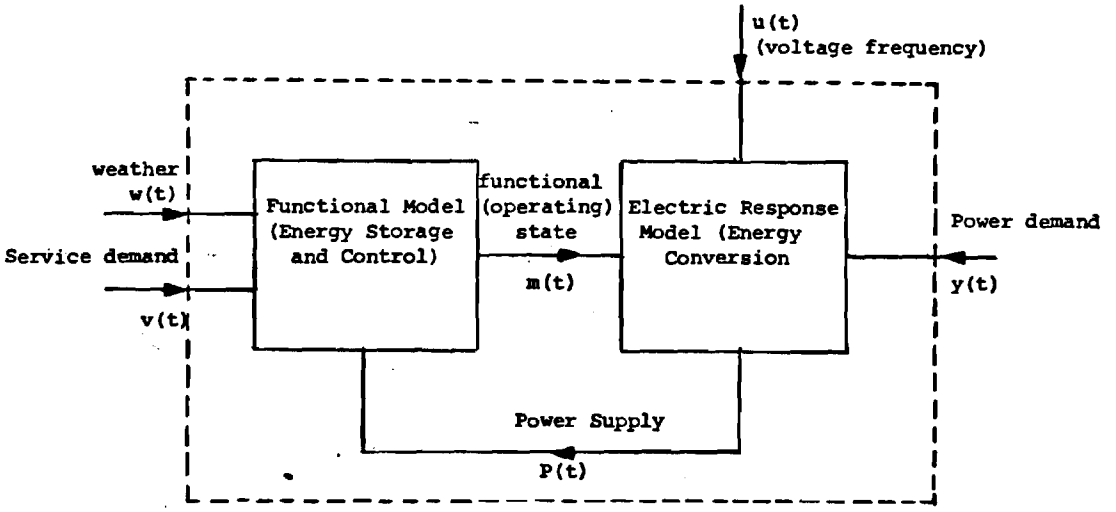

Fig. 2-2. Decomposition of Component Load Model.

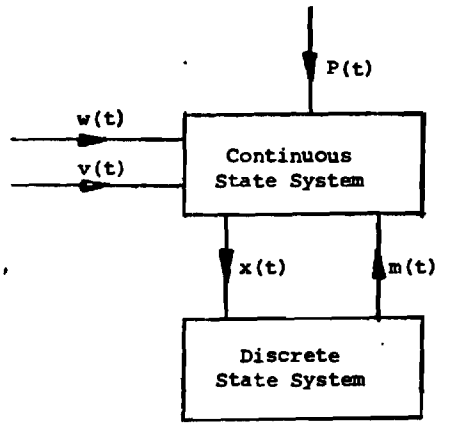

Fig. 2-3. The Chong and Debs Hybrid State Model.

demand for hot water and the functional state ("on"/"off") of a thermostat-controlled water heater.

Among dynamic functional models, Chong and Debs distinguish two types, weakly-driven and strongly-driven, depending on the nature of service demand v(t). A stochastic hybrid-state model (continuous/discrete) is associated with either case (see Fig. 2-3). The continuous state represents the energy storage component of the model. The discrete state m(t) corresponds to the switching mechanism. The two types of dynamic functional models are now discussed.

Weakly-Driven Functional Model. Here, the role of the customer (i.e. service demand) is indirect in the form of a noise process. An example may be found in the cooling or heating system of a building. To be specific, consider an electric space heating system with a thermostat-controlled resistive heater. Heat is lost from the building through the walls, floor, and roof. In addition, heat is lost when somebody enters and leaves the building and is gained from human activity. This type of effect can be modeled as noise. A simplified hybrid-state model is proposed by Chong and Debs for the group of devices which are weakly driven.

The continuous state x(t) (temperature) is governed by the first order differential equation:

$$C\,dx(t) = -\alpha\big(x(t) - x_a(t)\big)dt + dv(t) + P(t)m(t)b(t)dt \qquad (2.1)$$

where

C: is the average thermal capacity of the building

α: is the average loss rate through floors, walls and ceilings

$v(t)$: is a Weiner process of zero mean and variance parameter ν

$x(t)$: is the temperature inside the building

$x_a(t)$: is the ambient temperature

$P(t)$: is the rate of heat supply from the resistive element

$m(t)$: is the functional state (1 or 0)

$b(t)$: is a binary variable representing the control applied by the utility. It is 1 if the device is connected, 0 otherwise.

Division of (2.1) by C yields:

$$dx(t) = -a\big(x(t) - x_a(t)\big)dt + dv'(t) + Rm(t)b(t)dt \qquad (2.2)$$

where the definition of a and R is obvious. $v'(t)$ is a Wiener process with variance parameter $\sigma = \nu C^{-1/2}$.

The discrete state $m(t)$ is governed by a thermostat with temperature setting x_+ and x_-. Mathematically, for arbitrary small time increment Δt:

$$m(t + \Delta t) = m(t) + \pi\big(x(t), m(t); x_+, x_-\big)$$

with π defined as

$$\pi(x,m;x_+,x_-) = \begin{cases} 0 & x_- < x < x_+ \\ -m & x > x_+ \\ 1-m & x < x_- \end{cases} \qquad (2.3)$$

Thus (as shown in Fig. 2-3), the functional model is composed of two interconnected subsystems: a linear part with a continuous state x(t) whose evolution depends on m(t), and a nonlinear part with discrete state m(t) whose transition depends on x(t). Notice that if the noise v(t) is absent, then the switching of m(t) between 0 and 1 is periodic. When noise is present, the cycling of m(t) is no longer deterministic. This type of cycling is observed in electric heaters and several other devices.

Strongly-Driven Functional Models. The model structure here is essentially the same as for the weakly-driven case. However, service demand is no longer a noise process. Rather, it is a conscious demand by the consumer and can be modeled as a jump process, i.e. a random driving input which is piecewise constant. An example of this type of functional model can be found in the electric water heater. The general model for the devices which are strongly driven is given by:

$$C\dot{x}(t) = -\alpha(x(t) - x_a(t)) - v(t)(x_d - x_i(t)) + P(t)m(t)b(t) \qquad (2.4)$$

where the above variables are the water heater analogs of equation (2.2), and x(t) is again the continuous state (temperature).

In equation (2.4):

v(t): is the hot water demand at time t (vol/sec)

$x_i(t)$: is the inlet water temperature

x_d: is the desired water outlet temperature.

For $x_i(t)$ constant, (2.4) is similar to (2.1), except that v(t) is now piecewise constant with random switching times and random amplitudes. The discrete state m(t) will switch between 1 and 0 according to equation (2.3). Thermostat-controlled electric space heaters or air conditioners have dynamic functional models of the weakly-driven type (equations (2.2)-(2.3)).

In summary, Chong and Debs have developed the device response/functional model decomposition and a general (hybrid-state) representation for dynamic functional models. Within the framework of the general load synthesis methodology (Fig. 2-1), this represents the completion of steps (a) and (b).

The hybrid state model of Chong and Debs for weakly-driven devices (Equations (2.2)-(2.3)) constitutes the starting point of our model building endeavor. We use this model as a general representation for functional models of electric space heaters or air conditioners, and proceed to implement the remaining steps of the load synthesis methodology in Fig. 2-1. In the next chapter the aggregation problem for this particular class of devices is formulated and solved. Before undertaking the analysis of the parameter estimation problem (step (c) of the methodology) some theoretical results need to be developed. As a result, questions of parameter estimation are postponed until chapter IV.

CHAPTER III

THE AGGREGATION PROBLEM: FORMULATION AND SOLUTION

3.1 Exact Formulation of the Aggregation Problem

Step d of the general load synthesis methodology (Fig. 2-1) is aggregation. It represents the most difficult step associated with the methodology and the major part of our work will be concerned with its solution. In the following, the aggregation problem for a group of devices is defined.

Given a collection of devices represented by indices $\{i\}_1^n$, the associated aggregation problem is that of determining the dynamics of total power demand for that group as a function of time, system voltage and system frequency. Let $P_i(v,f)$ represent a steady state response model for the i^{th} device. If as a first approximation electrical and electromechanical transients for the devices are neglected, one has:

$$P(v,f,t) = \sum_{i=1}^{n} P_i(v,f)m_i(t) \tag{3.1}$$

where $P(v,f,t)$ represents the total real power demand for the aggregate. Furthermore, if we define:

$$P_{eq}(v,f) = \frac{1}{n} \sum_{i=1}^{n} P_i(v,f) \tag{3.2}$$

$$\bar{m}(t) = \frac{1}{n} \sum_{i=1}^{n} m_i(t) \tag{3.3}$$

Then (3.1) can be approximately written:

$$P(v,f,t) \simeq n\, P_{eq}(v,f)\bar{m}(t) \qquad (3.4)$$

The following can be noted:

- Equation (3.4) is an approximation which improves as the similarity of the aggregated response models increases.
- If it is desired to account for one type of dynamics (e.g. electromechanical transients associated with induction motors running compressors for cooling), $P_{eq}(v,f)$ can be replaced by $P_{eq}(v,f,t)$ in (3.4) where $P_{eq}(v,f,t)$ represents dynamics of an "equivalent" machine.
- Although (3.4) can be modified to account for transients, the calculation of $\bar{m}(t)$ need not be affected since any response model dynamics (electrical or electromechanical) are usually much faster than functional model dynamics (thermal). Thus the functional model "sees" only the steady-state of the response model.

Equation (3.4) elucidates the advantages of the Chong-Debs functional/respone model decomposition [29]. This decomposition allows the separation of the aggregation problem into two decoupled tasks: response model aggregation (equation 3.2) and functional model aggregation (equation 3.3). The former is a deterministic aggregation problem and has been treated elsewhere [26-28]. Functional model aggregation, schematically represented in Fig. 3-1, is a new stochas-

tic aggregation problem and is our principal interest. The objective is to determine the dynamics of $\bar{m}(t)$ which will be called the aggregate functional state. Physically, $\bar{m}(t)$ represents the function of devices in the "on" state at time t.

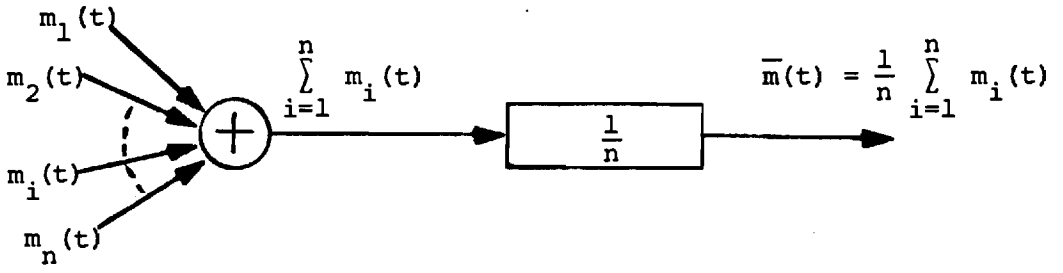

Fig. 3-1. Schematic Representation of Functional Model Aggregation.

The solution of the aggregation problem is considered only in the weakly-driven case (air conditioning and electric space heating). Important difficulties occur at two levels with the strongly-driven case: the precise modeling of service demand and the mathematics associated with a jump process.

In the following section, the aggregation problem is solved for the case of a homogeneous control group of weakly-driven devices. A homogeneous control group is defined as a group of nearly identical devices with nearly identical functional models and subject to the same control within a load management program. A reasonable example of this can be found in a large apartment complex.

3.2 The Case of a Homogeneous Control Group

Consider the case of a large homogeneous control group of n weakly-driven devices. Also, for the purpose of this analysis, suppose the devices are electric space heaters. The following "elemental independence assumption" (Chong and Debs [29]) is made throughout this work: conditional on weather information, load demands of individual devices correspond to independent stochastic processes. Based on this assumption and using Kolmogorov's strong law of large numbers [37], it is possible to conclude that for n "large enough:"

$$\bar{m}(t) = E_w(m_i(t)) \quad V_i = 1,\ldots,n \tag{3.6}$$

where $E_w(\cdot)$ is the expectation operator conditional on weather information (weather is treated as a known time varying input).

Equation (3.6) is fundamental to this work. First, it is a process of going from a discrete random variable ($\bar{m}(t)$) to a continuous one ($E_w(m_i(t))$). As such, it can be considered as a diffusion approximation (by analogy to the process of going from a discrete random walk to a continuous Brownian motion). Secondly, in the stochastic processes context, we could view the homogeneous control group as an approximate, because finite, ensemble realization of the stochastic process described by equation (2.1). The evolution of the states from t=0 to t=∞ for any individual electric space heater would represent a particular sample path of the process. In this light, equation (3.6) can be interpreted as the process of estimating a statistical property of an ensemble ($E_w(m_i(t))$ via a finite sample

average ($\bar{m}(t)$). In section 3.2.1, this "physical" interpretation of equation (3.6) is utilized to generate some preliminary results and gain an intuitive understanding of the dynamics of $E_w(m_i(t))$ by examining instead the dynamics of the aggregate functional state $\bar{m}(t)$. Guided by these results, we consider in section 3.2.2 a formal derivation of the dynamics of $E_w(m_i(t))$. A system of coupled partial differential equations of parabolic type (Fokker-Planck equations [38,39]) is obtained. This system of equations together with equation (3.6) constitute the solution of the aggregation problem in the homogeneous control group case.

3.2.1 Some Preliminary Results

The following "hybrid" probability densities will be needed in the subsequent developments:

$$f_1^c(\lambda,t)d\lambda = Pr\left[(\lambda < x(t) \leq \lambda + d\lambda) | m(t) = 1\right] \tag{3.7}$$

$$f_o^c(\lambda,t)d\lambda = Pr\left[(\lambda < x(t) \leq \lambda + d\lambda) | m(t) = 0\right] \tag{3.8}$$

$$f_1(\lambda,t)d\lambda = Pr\left[(\lambda < x(t) \leq \lambda + d\lambda) \cap (m(t) = 1)\right] \tag{3.9}$$

$$f_o(\lambda,t)d\lambda = Pr\left[(\lambda < x(t) \leq \lambda + d\lambda) \cap (m(t) = 0)\right] \tag{3.10}$$

We propose to study the following problem.

Given $\bar{m}(t)$, $f_1(\lambda,t)$, $f_o(\lambda,t)$ at time t, express if possible $\bar{m}(t + \delta t)$ in terms of the above mentioned quantities when δt is a small time increment.

Let $n_1(t)$ be the total number of electric space heaters in the "on" state at time t. Also, for the "on" population of space heaters, let:

$$S_1(t,\delta t) = \sum_{i=1}^{n_1(t)} m_i(t + \delta t) \tag{3.11}$$

Finally let:

$p_1(t,\delta t)$ = probability that an individual space heater remains in the "on" state at time $t + \delta t$, given that it was in the "on" state at time t.

$q_1(t,\delta t) = 1 - p_1(t,\delta t)$.

$S_1(t,\delta t)$ corresponds to the summation of $n_1(t)$ identically distributed independent Bernoulli random variables with $p_1(t,\delta t)$ probability of success and $q_1(t,\delta t)$ probability of failure. For $n_1(t)$ "large enough," the central limit theorem [37] yields:

$$S_1(t,\delta t) \sim n_1(t)p_1(t,\delta t) + G(o,n_1(t)p_1(t,\delta t)q_1(t,\delta t)) \tag{3.12}$$

where in (3.12) $\sim$ indicates convergence in distribution and $G(\alpha,\beta)$ denotes a Gaussian random variable with mean α and variance β. Similarly define:

$$S_o(t,\delta t) = \sum_{i=1}^{n_o(t)} (m_i(t + \delta t) \tag{3.13}$$

where $n_o(t)$ is the number of space haters in the "off" state at time t. Also, let:

$P_o(t,\delta t)$ = probability that an individual space heater remains in the "off" state at time $t + \delta t$, given that it was in the "off" state at time t.

$q_o(t,\delta t) = 1 - p_o(t,\delta t)$.

It can be shown that for $n_o(t)$ "large enough n":

$$S_o(t,\delta t) \sim n_o(t)p_o(t,\delta t) + G(0,n_o(t)p_o(t,\delta t)q_o(t,\delta t)) \quad (3.14)$$

(3.12) and (3.14) yield using the independence assumption:

$$n_1(t + \delta t) - n_1(t) \sim -n_1(t)q_1(t,\delta t) + n_o(t)q_o(t,\delta t)$$

$$+ G[0,n_1(t)p_1(t,\delta t)q_1(t,\delta t)$$

$$+ n_o(t)p_o(t,\delta t)q_o(t,\delta t)] \quad (3.15)$$

Dividing equation (3.15) by n yields for n "large enough":

$$\bar{m}(t + \delta t) - \bar{m}(t) \simeq -\bar{m}(t)q_1(t,\delta t) + (1 - \bar{m}(t))q_o(t,\delta t) \quad (3.16)$$

Furthermore, dividing equation (3.16) by δt and considering limits as δt goes to zero yields:

$$\frac{d\bar{m}}{dt} \simeq -\bar{m}(t) \lim_{\delta t \to 0} \frac{1}{\delta t} q_1(t,\delta t) + (1 - \bar{m}(t)) \lim_{\delta t \to 0} \frac{1}{\delta t} q_o(t,\delta t) \quad (3.17)$$

The limits in (3.17) can be evaluated as follows:

$$\lim_{\delta t \to 0} \frac{q_1(t,\delta t)}{\delta t} = \lim_{\delta t \to 0} \frac{1}{\delta t} \Pr\big[\sup x(t') > x_+$$

$$\text{for } t' \in [t, t+\delta t] \,|\, m(t) = 1\big]$$

$$= \lim_{\delta t \to 0} \frac{1}{\delta t} \Pr\big[\sup\big[x(t') - a(x(t') - x_a(t'))(t'-t)$$

$$+ v(t') - v(t)\big] > x_+ \text{ for } t' \in [t, t+\delta t] \,|\, m(t) = 1\big] \qquad (3.18)$$

where equation (2.1) has been used. However as $\delta t \to 0$, $\delta v(t)$ is of the order of $\sigma\sqrt{\delta t}$. Therefore, in the difference $\delta v(t)$ and $a(x(t) - x_a(t))\delta t$, the latter term can be neglected, in which case (3.18) reads:

$$\lim_{\delta t \to 0} \frac{1}{\delta t} q_1(t,\delta t) = \lim_{\delta t \to 0} \frac{1}{\delta t} \Pr\big[\sup(x(t) + v(t') - v(t)) > x_+$$

$$\text{for } t' \in [t, t+\delta t] \,|\, m(t) = 1\big]$$

$$= 2 \lim_{\delta t \to 0} \frac{1}{\delta t} \big[\Pr[x(t) + \delta v(t) > x_+] \,|\, m(t) = 1\big] \qquad (3.19)$$

where in (3.19) Desire Andre's reflection principle [47] has been used. (3.15) and the law of total probability yield:

$$\lim_{\delta t \to 0} \frac{1}{\delta t} q_1(t,\delta t) = 2 \lim_{\delta t \to 0} \frac{1}{\delta t} \int_0^\infty \big[F_1^c(x_+,t) - F_1^c(x_+-u,t)\big] f_{\delta v}(u)\,du \qquad (3.20)$$

where $F_1^c(\lambda,t)$ is the distribution function associated with $f_1^c(\lambda,t)$ and $f_{\delta v}(u)$ is the probability density of $\delta v(t)$, i.e.:

$$f_{\delta v}(u) = \frac{1}{\sqrt{2\pi\delta t}\,\sigma} e^{-\frac{u^2}{2\sigma^2\delta t}} \tag{3.21}$$

Assuming $f_1^c(\lambda,t)$ is twice differentiable, a Taylor expansion of $F_1^c(x_+-u,t)$ in the neighborhood (left) of x_+ yields:

$$\lim_{\delta t\to 0}\frac{1}{\delta t} q_1(t,\delta t) = 2\lim_{\delta t\to 0}\frac{1}{\delta t}\int_0^\infty \left[f_1^c(x_+,t)u - \frac{1}{2}\frac{\partial f_1^c}{\partial x}(x_+,t)u^2 + \frac{1}{6}\frac{\partial^2 f_1^c}{\partial x^2}(\eta(u),t)u^3\right] f_{\delta v}(u)\,du \tag{3.22}$$

where $x_+-u \le \eta(u) \le x_+$. Using (3.17) it is possible to show that:

$$\lim_{\delta t\to 0}\frac{1}{\delta t}\int_0^\infty f_1^c(x_+,t)u\, f_{\delta v}(u)\,du = O(\delta t)^{-1/2} \to \infty \tag{3.23}$$

The limit in (3.22) represents the rate of decrese of $F_1^c(x_+,t)$ at time t. Now, the limit in (3.23) is infinite. This means that if $f_1^c(x_+,t)$ is nonzero for a finite time δt, $F_1^c(x_+,t)$ would decrease by an infinite amount which is impossible ($F_1^c(x_+,t)$ is a probability). This means:

$$f_1^c(x_+,t) = 0 \quad \forall t \tag{3.24}$$

(3.21), (3.22) and (3.24) yield:

$$\lim_{\delta t \to 0} \frac{q_1(t,\delta t)}{\delta t} = -\frac{1}{2}\sigma^2 \frac{\partial f_1^c}{\partial x}(x_+,t) \qquad (3.25)$$

Similar arguments yield the following equations:

$$f_o^c(x_-,t) = 0 \quad \forall t \qquad (3.26)$$

$$\lim_{\delta t \to 0} \frac{q_o(t,\delta t)}{\delta t} = \frac{1}{2}\sigma^2 \frac{\partial f_o^c}{\partial x}(x_-,t) \qquad (3.27)$$

(3.16), (3.25) and (3.27) yield:

$$\frac{d\bar{m}}{dt} = \bar{m}(t)\left(\frac{\sigma^2}{2} \frac{\partial f_1^c}{\partial x}(x_+,t)\right) + (1-\bar{m}(t))\left(\frac{\sigma^2}{2} \frac{\partial f_o^c}{\partial x}(x_-,t)\right) \qquad (3.28)$$

Finally, if we note that:

$$f_1(x,t) = f_1^c(x,t)\bar{m}(t) \qquad (3.29)$$

$$f_o(x,t) = f_o^c(x,t)(1 - \bar{m}(t)) \qquad (3.30)$$

Then (3.28) yields:

$$\frac{d\bar{m}}{dt} = \frac{\sigma^2}{2} \frac{\partial f_1}{\partial x}(x_+,t) + \frac{\sigma^2}{2} \frac{\partial f_o}{\partial x}(x_-,t) \qquad (3.31)$$

Equation (3.31) clearly indicates that by solving for the dynamics of the time functions $\frac{\partial f_1}{\partial x}(x_+,t)$ and $\frac{\partial f_o}{\partial x}(x_-,t)$ the evolution of the aggregate functional state $\bar{m}(t)$ can be determined. This will be the object of section 3.2.2.

Finally, in light of equations (3.17), (3.25) and (3.27), the terms in the right-hand side of (3.31) can be interpreted as being the average fraction of devices that switch from "off" to "on" $\left(\frac{\sigma^2}{2} \frac{\partial f_o}{\partial x} (x_-,t)\right)$ minus the average fraction of devices that switch from "on" to "off" $\left(-\frac{\sigma^2}{2} \frac{\partial f_o}{\partial x} (x_+,t)\right)$ per unit time at time t.

3.2.2 Ensemble Analysis: The Coupled Fokker-Planck Equations (CFPE) Model

Here, a formal analysis of the dynamics of $E_w(m_i(t))$ is undertaken. Equation (3.6) is repeated below for convenience:

$$\bar{m}(t) = E_w(m_i(t)) \tag{3.32}$$

We have:

$$E_w(m_i(t)) = 1.\Pr(m_i(t) = 1) + 0.\Pr(m_i(t) = 0) \tag{3.33}$$

but

$$\Pr(m_i(t) = 1) = \int_{-\infty}^{x_+} f_1(\lambda,t)\,d\lambda \tag{3.34}$$

(3.32)-(3.34) yield:

$$\bar{m}(t) = \int_{-\infty}^{x_+} f_1(\lambda,t)\,d\lambda = F_1(x_+,t) \tag{3.35}$$

where $F_1(\lambda,t)$ represents the distribution function associated with $f_1(\lambda,t)$. Equations (3.31) and (3.35) represent two alternative ways of computing $\bar{m}(t)$. At the end of this section their mutual

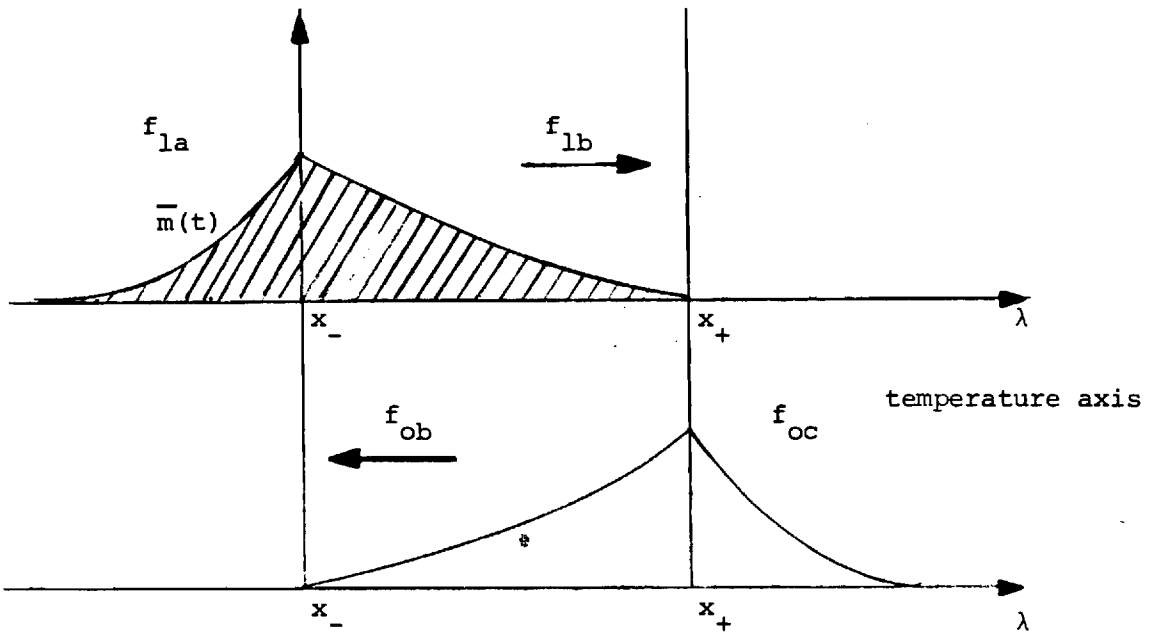

Fig. 3-2. Illustration of Dynamical System. x_- and x_+ are the lower and upper edges of thermostat at dead band respectively. $\bar{m}(t)$ is the total area under the "on" density at any time. The arrows represent the direction of temperature drift (in the case of electric space heating).

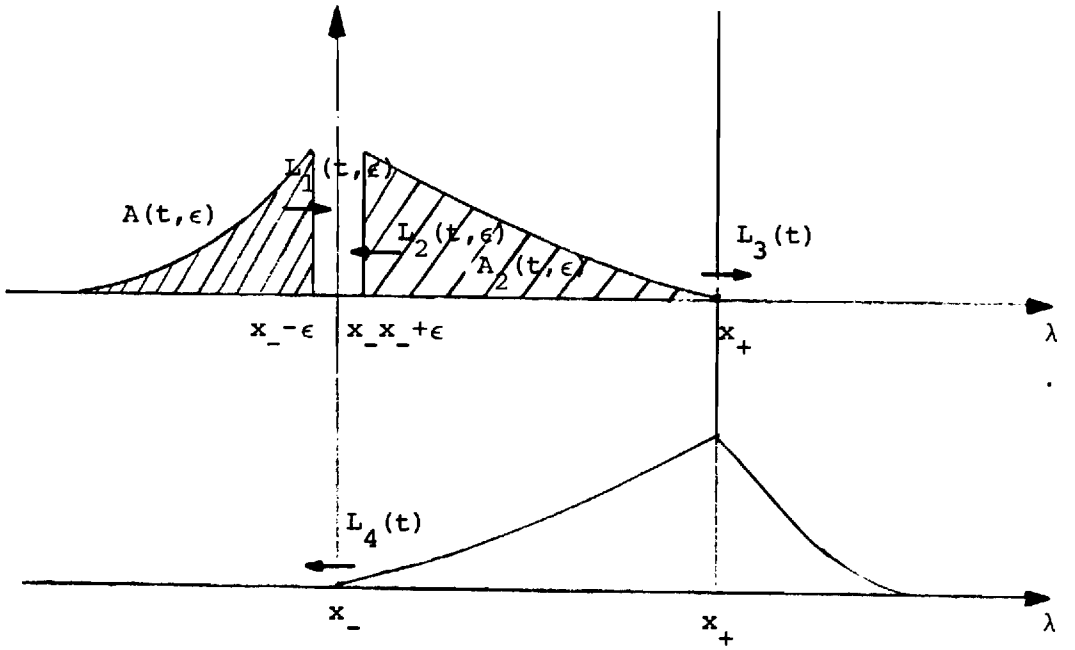

Fig. 3-3. Graphical Representation of the Flow of Probability within a Rectangular Strip of Width 2ϵ around x_-.

consistency will be established. The vector stochastic process $s(t) \triangleq \begin{pmatrix} x(t) \\ m(t) \end{pmatrix}$ can be regarded as a hybrid-state (discrete/continuous) Markov process. Two hybrid state probability densities $f_1(\lambda,t)$ and $f_o(\lambda,t)$ as defined in section 3.2.1 can be associated with it. We now establish the following result.

THEOREM 1:

The hybrid state probability densities $f_1(\lambda,t)$, $f_o(\lambda,t)$ satisfy the following system of coupled Fokker-Planck equations:

$$\frac{\partial f_1}{\partial x}(\lambda,t) = \frac{\partial}{\partial \lambda}\left[(a(\lambda - x_a(t)) - b(t)R) f_1(\lambda,t)\right] + \frac{\sigma^2}{2}\frac{\partial^2}{\partial \lambda^2} f_1(\lambda,t) \qquad (3.36)$$

in regions a, b of Fig 3-2 and:

$$\frac{\partial f_o}{\partial t}(\lambda,t) = \frac{\partial}{\partial x}\left[(a(\lambda - x_a(t)) f_o(\lambda,t)\right] + \frac{\sigma^2}{2}\frac{\partial^2}{\partial \lambda^2} f_o(\lambda,t) \qquad (3.37)$$

in regions b, c of Fig 3-2, subject to the following boundary conditions.

Absorbing Boundaries:

$$f_{1b}(x_+,t) = f_{ob}(x_-,t) = 0 \quad \forall t > 0 \qquad (3.38)$$

Conditions at Infinity:

$$f_{1a}(-\infty,t) = f_{oc}(+\infty,t) = 0 \quad \forall t > 0 \qquad (3.39)$$

Continuity Conditions:

$$f_{1a}(x_-,t) = f_{1b}(x_-,t) \quad \forall t > 0 \tag{3.40}$$

$$f_{ob}(x_+,t) = f_{oc}(x_+,t) \quad \forall t > 0 \tag{3.41}$$

Probability Conservation:

$$-\frac{\partial}{\partial\lambda} f_{1a}(x_-,t) + \frac{\partial}{\partial\lambda} f_{1b}(x_-,t) + \frac{\partial}{\partial\lambda} f_{ob}(x_-,t) \quad \forall t > 0 \tag{3.42}$$

$$\frac{\partial}{\partial\lambda} f_{oc}(x_+,t) - \frac{\partial}{\partial\lambda} f_{ob}(x_+,t) - \frac{\partial}{\partial\lambda} f_{1b}(x_+,t) = 0 \quad \forall t > 0 \tag{3.43}$$

Proof:

As in the original derivation of the Fokker-Planck or forward Kolmogorov equation for Markov diffusion processes by Kolmogorov [48] and reported in [38], our proof starts from the Chapman-Kolmogorov equations [38]. For this particular hybrid state system, the Chapman-Kolmogorov equations can be modified as follows:

$$f_{ij}(\lambda',t',\lambda,t) = \sum_{k=0}^{1} \int_{-\infty}^{+\infty} f_{ik}(\lambda',t',z,\tau) f_{kj}(z,\tau,\lambda,t)\,dz$$

$$\text{for } i=0,1\ , \quad j=0,1 \quad \text{and any } \tau \in (t',t) \tag{3.44}$$

and where transition probability density functions:

$$f_{ij}(\lambda',t',\lambda,t)d\lambda = Pr[(\lambda < x(t) \leq \lambda + d\lambda) \cap (m(t) = j) |$$

$$x(t') = \lambda', m(t') = i] \tag{3.45}$$

for i=0,1 , j = 0,1 have been introduced. Also, defining:

$$f_1^o(\lambda) = f_1(\lambda,0) \tag{3.46}$$

$$f_o^o(\lambda) = f_o(\lambda,0) \tag{3.47}$$

We can write:

$$f_i(\lambda,t) = \sum_{k=0}^{1} \int_{-\infty}^{+\infty} f_{ki}(\lambda',0,\lambda,t) f_k^o(\lambda') d\lambda' \tag{3.48}$$

for i=0,1.

The derivations to follow are divided in two parts, A and B. In part A, we derive equation (3.36) only for $f_1(\lambda,t)$ and on the interval $(x_-,x_+]$, i.e. in region b of Fig. 3-2. The partial differential equations satisfied by $f_1(\lambda,t)$ in region a, and by $f_o(\lambda,t)$ (equation 3.37) in regions b and c of Fig 3-2 can be obtained using an exactly analogous procedure. In part B, we show that the boundary conditions (3.38-3.43) hold.

A. Derivation of Equation (3.36) on the Interval $(x_-,x_+]$:

Let ϵ be an arbitrarily small positive number. Also, let $R(\lambda)$ be an arbitrarily non-negative continuous function such that: $R(\lambda) = 0$ for $\lambda < x_- + \epsilon$ and $\lambda > x_+$, and the function is three times differ-

entiable and vanishes together with its first three derivatives at $x_- + \varepsilon$ and x_+. In the following, it is assumed that all the needed partial derivatives exist and are continuous in the interval of interest. It is also assumed that sufficient conditions (such as those dictated by Lebesgue's dominated convergence theorem [49]) are satisfied to allow interchange of orders of integration and differentiation whenever applicable. For $h > 0$:

$$\lim_{h\to 0} \int_{x_-+\varepsilon}^{x_+} \frac{f_{11}(\lambda',t',\lambda,t+h) - f_{11}(\lambda',t',\lambda,t)}{h} R(\lambda)d\lambda$$

$$= \int_{x_-+\varepsilon}^{x_+} \frac{\partial}{\partial t} f_{11}(\lambda',t',\lambda,t+h)R(\lambda)d\lambda \qquad (3.49)$$

Using (3.43), and setting i=j=1, we have:

$$f_{11}(\lambda',t',\lambda,t+h) = \int_{-\infty}^{+\infty} f_{11}(\lambda',t',z,t)f_{11}(z,t,\lambda,t+h)dz$$

$$+ \int_{-\infty}^{+\infty} f_{10}(\lambda',t',z,t)f_{01}(z,t,\lambda,t+h)dz \qquad (3.50)$$

Correspondingly,

$$\int_{x_-+}^{x_+} \frac{\partial}{\partial t} f_{11}(\lambda',t',\lambda,t)R(\lambda)d\lambda$$

$$= \lim_{h\to 0} \frac{1}{h} \left[\int_{x_-+}^{x_+} \int_{-\infty}^{+\infty} f_{11}(\lambda',t',z,t)f_{11}(z,t,\lambda,t+h)R(\lambda)dzd\lambda\right.$$

$$- \int_{x_-+\varepsilon}^{x_+} f_{11}(\lambda',t',\lambda,t)R(\lambda)d\lambda\Big]$$

$$+ \lim_{h\to 0} \frac{1}{h} \int_{x_-+\varepsilon}^{x_+} f_{10}(\lambda',t',z,t)f_{01}(z,t,\lambda,t+h)R(\lambda)dzd\lambda \qquad (3.51)$$

Now, define:

$$\tau_{11t}^{\lambda,\lambda'} = \inf\{(t'-t):x(t') = \lambda', m(t')=1 | x(t) = \lambda, m(t) = 1\} \qquad (3.52)$$

for any λ,λ', i.e. $\tau_{11t}^{\lambda,\lambda'}$ is the first passage random variable [40] from hybrid state $\binom{1}{\lambda}$ to hybrid state $\binom{1}{\lambda'}$ at time t'.

Then clearly for h infinitesimal:

$$\int_{x_-+\varepsilon}^{x_+} \int_{-\infty}^{+\infty} f_{10}(\lambda',t',z,t)f_{01}(z,t,\lambda,t+h)dzd\lambda \leq \Pr\Big[\tau_{11t}^{x_-,x_-+\varepsilon} \leq h\Big]$$

$$\leq \Pr\Big[(\sup x(t') > x_- + \varepsilon$$

$$\text{for } t' \in [t,t+h] \,|\, (m(t) = 1) \cap (x(t) = x_-)\Big]$$

$$\leq \Pr\Big[\sup(R-a(x_- - x_a(t))(t'-t)$$

$$+ v(t') - v(t)) > \varepsilon, \quad \text{for } t' \in (t,t+h)\Big]\Big] \qquad (3.53)$$

where equation (2.1) has been used. However, and as argued in section 3.2.1, ash $h \to 0$, $\delta v(t)$ is of the order of $\sigma\sqrt{h}$. Therefore, in the difference of $\delta v(t)$ and $(R - a(x_- - x_a(t)))h$, the latter term can be neglected. (3.53) yields:

$$\int_{x_-+\varepsilon}^{x_+} \int_{-\infty}^{+\infty} f_{10}(\lambda',t',z,t) f_{01}(z,t,\lambda,t+h)\,dz\,d\lambda \leq \Pr\left[\sup(v(t') - v(t)) \right.$$

$$\left. > t \text{ for } t' \in (t,t+h)\right] \leq 2 \Pr\left[\delta v(t) > \varepsilon\right] \qquad (3.54)$$

where in the above, Désiré André's reflection principle has been used. Consequently:

$$0 \leq \lim_{h\to 0} \frac{1}{h} \int_{x_-+\varepsilon}^{x_+} \int_{-\infty}^{+\infty} f_{10}(\lambda',t',z,\tau) f_{01}(z,\tau,\lambda,t+h)\,dz\; R(\lambda)\,d\lambda$$

$$\leq \lim_{h\to 0} \frac{2}{h} \Pr[\delta v(t) > \varepsilon] K \qquad (3.55)$$

K is an upper bound for $R(\lambda)$ on $[x_-+\varepsilon, x_+]$. Due to the almost sure continuity of sample paths of Brownian motion, [47], the limit in (3.55) must be zero. Now:

$$\lim_{h\to 0} \frac{1}{h} \int_{x_-+\varepsilon}^{x_+} \int_{-\infty}^{+\infty} f_{11}(\lambda',t',z,t) f_{11}(z,t,\lambda,t+h) R(\lambda)\,dz\,d\lambda$$

$$= \lim_{h\to 0} \frac{1}{h} \int_{-\infty}^{+\infty} \int_{x_-+\varepsilon}^{x_+} f_{11}(\lambda',t',z,t) f_{11}(z,t,\lambda,t+h) R(\lambda)\,d\lambda\,dz$$

$$= \lim_{h\to 0} \frac{1}{h} \int_{-\infty}^{+\infty} \int_{x_- -\varepsilon}^{x_+} f_{11}(\lambda',t',\lambda,t) f_{11}(\lambda,t,z,t+h) R(z)\, dz d\lambda$$

$$= \lim_{h\to 0} \frac{1}{h} \int_{-\infty}^{+\infty} f_{11}(\lambda',t',\lambda,t) \int_{-\infty}^{+\infty} f_{11}(\lambda,t,z,t+h) R(z)\, dz d\lambda \qquad (3.56)$$

And:

$$\lim_{h\to 0} \frac{1}{h} \Big[\int_{x_- +\varepsilon}^{x_+} \int_{-\infty}^{+\infty} f_{11}(\lambda',t',z,t) f_{11}(z,t,\lambda,t+h) R(\lambda)\, dz d\lambda$$

$$- \int_{x_- +\varepsilon}^{x_+} f_{11}(\lambda',t',z,t) R(z)\, dz \Big]$$

$$= \lim_{h\to 0} \frac{1}{h} \Big[\int_{-\infty}^{+\infty} f_{11}(\lambda',t',\lambda,t) \Big[\int_{-\infty}^{+\infty} f_{11}(\lambda,t,z,t+h) R(z)\, dz - R(\lambda) \Big] d\lambda \Big] \qquad (3.57)$$

Using a Taylor expansion for R(z), we have:

$$R(z) = R(\lambda) + (z-\lambda) R'(\lambda) + \frac{1}{2} (z-\lambda)^2 R''(\lambda)$$

$$+ \frac{1}{6} (z-\lambda)^3 R'''(\eta(\lambda,z)) \qquad (3.58)$$

where $\lambda \leq \eta(y,z) \leq z$. Substituting (3.58) in (3.57), (3.51) and recalling (3.50), we obtain:

$$\int_{x_- +\varepsilon}^{x_+} \frac{\partial}{\partial t} f_{11}(\lambda',t',\lambda,t) R(\lambda)\, d\lambda$$

$$= \lim_{h\to 0} \int_{-\infty}^{+\infty} f_{11}(\lambda',t',\lambda,t) \left[\frac{1}{h} \int_{-\infty}^{+\infty} f_{11}(\lambda,t,z,t+h)(z-\lambda)dz\ \eta'(\lambda)\right.$$

$$+ \frac{1}{h} \int_{-\infty}^{+\infty} f_{11}(\lambda,t,z,t+h)\ \frac{1}{2}(z-\lambda)^2 dz\ R''(\lambda)$$

$$\left. + \frac{1}{h} \int_{-\infty}^{+\infty} f_{11}(\lambda,t,z,t+h)\ \frac{1}{6}(z-\lambda)^3 dz\ R'''(\eta(\lambda,z))\right] d\lambda \qquad (3.59)$$

From equation (2.1):

$$\lim_{h\to 0} \frac{1}{h} \int_{-\infty}^{+\infty} f_{11}(\lambda,t,z,t+h)(z-\lambda)dz = [-a(\lambda-x_a(t)) + Rb(t)] \qquad (3.60)$$

and

$$\lim_{h\to 0} \frac{1}{h} \int_{-\infty}^{+\infty} f_{11}(\lambda,t,z,t+h)(z-\lambda)^2 dz = \sigma^2 \qquad (3.61)$$

Also:

$$\lim_{h\to 0} \frac{1}{h} \int_{-\infty}^{+\infty} f_{11}(\lambda,t,z,t+h)(z-\lambda)^3 dz = 0 \qquad (3.62)$$

In (3.59), it can be shown (proof 1, appendix B) that the integrand satisfies conditions that permit the application of Lebesgue's dominated convergence theorem [49]. In this case, the limit operation in (3.59) can be moved past the integral sign. Using (3.60-3.62) one obtains:

$$\int_{x_-+\varepsilon}^{x_+} \frac{\partial}{\partial t} f_{11}(\lambda',t',\lambda,t)R(\lambda)d\lambda = \int_{-\infty}^{+\infty} \left[f_{11}(\lambda',t',\lambda,t)\right.$$

$$\left.(-a(\lambda - x_a(t)) + Rb(t)\right] R'(\lambda) + R''(\lambda) \frac{\sigma^2}{2} \Big]d\lambda \qquad (3.63)$$

Integration by parts (twice) of the right-hand side of (3.63) and recalling properties of $R(\lambda)$ yields:

$$\int_{x_-+\varepsilon}^{x_+} \Big[\frac{\partial}{\partial t} f_{11}(\lambda',t',\lambda,t)$$

$$+ \frac{\partial}{\partial \lambda} [-a(\lambda - x_a(t)) + Rb(t)] f_{11}(\lambda',t',\lambda,t)$$

$$- \frac{\sigma^2}{2} \frac{\partial^2}{\partial \lambda^2} f_{11}(\lambda',t',\lambda,t)\Big]R(\lambda)d\lambda = 0 \qquad (3.64)$$

Since (3.64) is satisfied for any positive $R(\lambda)$ (subject to the constraints mentioned earlier) and for an arbitarily small ε, we conclude that for almost any λ on $(x_-,x_+]$:

$$\frac{\partial}{\partial t} f_{11}(\lambda',t',\lambda,t)$$

$$+ \frac{\partial}{\partial \lambda} [-a(\lambda - x_a(t)) + Rb(t)] f_{11}(\lambda',t',\lambda,t)$$

$$- \frac{\sigma^2}{2} \frac{\partial^2}{\partial \lambda^2} f_{11}(\lambda',t',\lambda,t) = 0 \qquad (3.65)$$

Furthermore, starting from the Chapman-Kolmogorov equation for $f_{01}(\lambda',t',\lambda,t)$ (equation (3.44)) and using a similar approach one can show that $f_{01}(\lambda',t',\lambda,t)$ satisfies:

$$\frac{\partial}{\partial t} f_{01}(\lambda',t',\lambda,t)$$

$$+ \frac{\partial}{\partial \lambda} [-a(\lambda - x_a(t)) + Rb(t)] f_{01}(\lambda',t'\lambda,t)$$

$$- \frac{\sigma^2}{2} \frac{\partial^2}{\partial \lambda^2} f_{01}(\lambda',t',\lambda,t) = 0 \qquad (3.66)$$

Setting $t' = 0$ in (3.65)-(3.66) and multiplying both equations by $f_1^o(\lambda')$ and $f_o^o(\lambda')$ respectively, we obtain after addition:

$$\sum_{k=0}^{2} [\frac{\partial}{\partial t} f_{k1}(\lambda',0,\lambda,t)$$

$$+ \frac{\partial}{\partial \lambda} [-a(\lambda - x_a(t)) + Rb(t)] f_{k1}(\lambda',0,\lambda,t)$$

$$- \frac{\sigma^2}{2} \frac{\partial^2}{\partial \lambda^2} f_{k1}(\lambda',0,\lambda,t)] f_k^o(\lambda') = 0 \qquad (3.67)$$

Integrating (3.67) from $-\infty$ to $+\infty$, and using (3.47) we have after interchanging orders of integration and partial differentiation:

$$\frac{\partial f_1}{\partial t}(\lambda,t) + \frac{\partial}{\partial \lambda} [-a(\lambda - x_a(t)) + Rb(t)] f_1(\lambda,t)$$

$$- \frac{\sigma^2}{2} \frac{\partial^2}{\partial \lambda^2} f_1(\lambda,t) = 0 \qquad (3.68)$$

This completes the derivation of equation (3.36).

B. Boundary Conditions

We discuss only equations (3.38), (3.39), (3.40), and (3.42). The remaining boundary conditions follow by analogy. Equation (3.38) has already been established in 3.2.1 (equations (3.24) and (3.26)). Equation (3.39) follows from the continuity of $f_1(\lambda,t)$ on $(-\infty,x_+]$ and the fact that it must be integrable on that interval (the integral is a probability and is accordingly finite). Equation (3.40) expresses the continuity of $f_1(\lambda,t)$ across boundary x_-. Assumptions of continuity can always be made as long as they do not generate contradictions. We now proceed to establish equation (3.42). It is clear that equations (3.36) and (3.37) are mathematically reminiscent of a diffusion process (in the presence of a gravitational field). In what follows, the analogy is used freely. In Fig 3-2, an infinitesimal strip of width ε on either side of x_- is considered. Let $L_1(t,\varepsilon)$, $L_2(t,\varepsilon)$, $L_3(t)$, $L_4(t)$ represent respectively:

- The rate at which probability diffuses from left to right past the edge at $x_- - \varepsilon$.
- The rate at which probability diffuses from right to left past the edge at $x_- + \varepsilon$.
- The rate at which probability diffuses from $f_1(\lambda,t)$ to $f_o(\lambda,t)$ past the edge x_+.
- The rate at which probability diffuses from $f_o(\lambda,t)$ to $f_1(\lambda,t)$ past the edge x_-.

Finally $A_1(t,\varepsilon)$ and $A_2(t,\varepsilon)$ are the hatched areas represented in Fig. 3-2. Using equations (3.68), we have:

$$L_1(t,\varepsilon) = -\frac{\partial}{\partial t} A_1(t,\varepsilon) = \frac{\partial F_1}{\partial t}(x_- - \varepsilon,t)$$

$$= [-a(x_- - \varepsilon - x_a(t)) + Rb(t)]f_{1a}(x_- - \varepsilon,t)$$

$$- \frac{\sigma^2}{2} \frac{\partial}{\partial \lambda} f_{1a}(x_- - \varepsilon,t) \qquad (3.69)$$

where use has been made of:

$$\lim_{\lambda \to \infty} f_{1a}(\lambda,t) = \lim_{\lambda \to \infty} \frac{\partial f_{1a}}{\partial \lambda}(\lambda,t) = 0$$

Furthermore:

$$\frac{\partial A_2}{\partial t}(t,\varepsilon) = \frac{\partial}{\partial t}[F_1(x_+,t) - F_1(x_+ + \varepsilon,t)]$$

$$= -[-a(x_+ - x_a(t)) + Rb(t)]f_{1b}(x_+,t) + \frac{\sigma^2}{2} \frac{\partial}{\partial \lambda} f_{1b}(x_+,t)$$

$$+ [-a(x_+ + \varepsilon - x_a(t)) + Rb(t)]f_{1b}(x_+ + \varepsilon,t) - \frac{\sigma^2}{2} \frac{\partial}{\partial \lambda} f_{1b}(x_- + \varepsilon,t) \qquad (3.70)$$

Using (3.38) the first term on the right hand side of (3.69) can be dropped from the expression. Furthermore, from (3.25) we recognize that:

$$L_3(t) = -\frac{\sigma^2}{2} \frac{\partial}{\partial \lambda} f_{1b}(x_+,t) \qquad (3.71)$$

Also:

$$\frac{\partial A_2}{\partial t}(t,\varepsilon) = -L_2(t,\varepsilon) - L_3(t) \tag{3.72}$$

(3.70)-(3.72) yield:

$$L_2(t,\varepsilon) = \frac{\sigma^2}{2}\frac{\partial}{\partial\lambda} f_{1b}(x_-+\varepsilon,t) - [-a(x_-+\varepsilon-x_a(t))+Rb(t)]f_{1b}(x_+ +\varepsilon,t) \tag{3.73}$$

Let $I(t,\varepsilon)$ be the rate of probability increase within the rectangular strip in Fig. 3-2, then from probability conservation:

$$I(t,\varepsilon) = L_1(t,\varepsilon) + L_2(t,\varepsilon) + L_4(t) \tag{3.74}$$

Also, recalling (3.27):

$$L_4(t) = \frac{\sigma^2}{2}\frac{\partial}{\partial\lambda} f_{ob}(x_-,t) \tag{3.75}$$

In (3.76), letting ε go to zero and using the continuity of $f_1(\lambda,t)$ at x_-, (3.69) and (3.73), we obtain:

$$\lim_{\varepsilon\to 0} I(t,\varepsilon) = 0 = -\frac{\sigma^2}{2}\frac{\partial}{\partial\lambda} f_{1a}(x_-,t) + \frac{\sigma^2}{2}\frac{\partial}{\partial\lambda} f_{1b}(x_-,t)$$

$$+ \frac{\sigma^2}{2}\frac{\partial}{\partial\lambda} f_{ob}(x_-,t) \tag{3.76}$$

Hence (3.42). This completes the proof of the theorem. •

Remark 1: The fact that the limit in (3.55) is zero has an important significance. It means that for h infinitesimal, the Chapman-Kolmogorov equation in (3.50) (written from t to t+h) reduces to the ordinary Chapman-Kolmogorov equation for a one dimensional Markov process. This in turn, means that the various transition probability densities defined in (3.45) behave "locally" like transition densities of some one dimensional Markov process. Therefore, it is no surprise that they each satisfy individually some Fokker-Planck equation. In this light, boundary conditions (3.38) can be viewed as standard for Markov diffusion processes encountering an absorbing boundary.

Remark 2: It is possible to show that (3.35) is consistent with (3.31). We have:

$$\bar{m}(t) = \int_{-\infty}^{x_-} f_1(\lambda,t)d\lambda + \int_{x_-}^{x_+} f_1(\lambda,t)d\lambda$$

i.e.

$$\frac{d\bar{m}}{dt} = \int_{-\infty}^{x_-} \frac{\partial f_1}{\partial t}(\lambda,t)d\lambda + \int_{x_-}^{x_+} \frac{\partial f_1}{\partial t}(\lambda,t)d\lambda \qquad (3.77)$$

Recalling (3.36), (3.38) and (3.40) one obtains:

$$\frac{d\bar{m}}{dt} = \frac{\sigma^2}{2}\frac{\partial}{\partial\lambda} f_{1a}(x_-,t) - \frac{\sigma^2}{2}\frac{\partial}{\partial\lambda} f_{1b}(x_-,t) + \frac{\sigma^2}{2}\frac{\partial}{\partial\lambda} f_{1b}(x_+,t) \qquad (3.78)$$

Using (3.42), (3.78) yields:

$$\frac{d\bar{m}}{dt} = \frac{\sigma^2}{2} \frac{\partial}{\partial \lambda} f_{1b}(x_+,t) + \frac{\sigma^2}{2} \frac{\partial}{\partial \lambda} f_{ob}(x_-,t) \qquad (3.79)$$

which is precisely equation (3.35).

3.3 The Case of a Non-Homogeneous Control Group

The aggregation problem has been considered only for the case of a class of devices described by equation (2.1) and where all the parameters involved were essentially identical. Such a class was called a homogeneous control group. In reality however, some spread in the parameters is to be expected. In fact they can best be thought of as random variables themselves. How can the effect of this parametric variability be assessed?

Here, the analysis of section 3.2 is generalized to a group of devices exhibiting a measure of parameter spread. It is nevertheless assumed that the devices are still subjected to the same control within a load management program. Such an aggregate of devices will be called a homogeneous control group. A perturbation approach is utilized. Let the potentially important highly variable parameters be compiled into a vector $\underline{\xi} = (\xi_1, \xi_2, \ldots \xi_p)^T$. $\underline{\xi}$ could contain parameters such as thermostat set points, building insulation parameters, noise variance, weather (as a function of geographical location, not time). In this more general framework, a more accurate statement of (3.6) is:

$$\bar{m}(t) \simeq E\left[E[m_i(t) | \underline{\xi}] \right] \qquad (3.80)$$

If we denote:

$$\bar{m}(t,\underline{\xi}) = E[m_i(t) \mid \underline{\xi}] \tag{3.81}$$

Then the system of equations (3.35)-(3.42), i.e. the CFPE model can be interpreted as giving $\bar{m}(t,\underline{\xi})$ for a particular choice of $\underline{\xi}$.

Now, assuming that $\bar{m}(t,\underline{\xi})$ is a smooth function of the parameters around their mean value vector $\underline{\xi}_o$, and for parameters narrowly distributed around $\underline{\xi}_o$, a second order truncated Taylor series can be written:

$$\bar{m}(t,\underline{\xi}) \simeq \bar{m}(t,\underline{\xi}_o) + \sum_{i=1}^{p} \frac{\partial \bar{m}}{\partial t}(t,\underline{\xi})\Big|_{\underline{\xi}=\underline{\xi}_o} (\xi_i - \xi_{io})$$

$$+ \Big[\sum_{i=1}^{p} \sum_{j=1}^{p} \frac{1}{2} \frac{\partial^2 \bar{m}}{\partial \xi_i \partial \xi_j}(t,\underline{\xi})\Big|_{\underline{\xi}=\underline{\xi}_o} (\xi_i - \xi_{io})(\xi_j - \xi_{jo}) \Big] \tag{3.82}$$

Furthermore, let:

$$E[(\underline{\xi} - \underline{\xi}_o)(\underline{\xi} - \underline{\xi}_o)^T] = [\sigma_{ij}^2]_{\substack{i=1,\ldots,p \\ j=1,\ldots,p}} \tag{3.83}$$

(3.83) yields after taking expected values on both sides:

$$\bar{m}(t) \simeq \bar{m}(t,\underline{\xi}_o) + \sum_{i=1}^{p} \sum_{j=1}^{p} \frac{1}{2} \frac{\partial^2 \bar{m}}{\partial \xi_i \partial \xi_j}(t,\underline{\xi})\Big|_{\underline{\xi}=\underline{\xi}_o} \sigma_{ij}^2 \tag{3.84}$$

The following remarks can be made:

- If covariance terms σ^2_{ij} (or the associated second partial derivatives in (3.82)) are sufficiently small, then it is reasonable to use the CFPE model (equations 3.35-3.42) with parameter vector $\underline{\xi}_o$ to compute $\overline{\underline{m}}(t)$.
- In case a first order approximation proves insufficient, then (3.84) is a second order approximation which requires the estimation of covariances σ^2_{ij} as well as the associated partial derivatives. In Chapter IV, some ideas for the analytic estimation of these "sensitivity" coefficients will be discussed. However, a numerical estimation is always possible.
- As the parameter spread increases, higher order terms have to be introduced in (3.84). This means in effect the double penalty of having to estimate higher order moments of the parameters joint distribution, and higher order partial derivatives. At this point, it becomes more advantageous to split the large homogeneous group into several smaller groups with less parameter spread, and carry the computations for each group separately.

This completes the discussion on the aggregation problem.

CHAPTER IV

ANALYSIS OF THE CFPE MODEL

4.1 Introduction

The CFPE model is a system of two Fokker-Planck equations (3.63) and (3.37) coupled through boundary conditions (3.42-3.43). In the following, the origins and importance of the Fokker-Planck equation in the literature on stochastic processes are briefly discussed.

The Fokker-Planck or forward Kolmogorov equation is a partial differential equation of a type called parabolic. It evolved from a study of a mathematical model of Brownian motion proposed by Einstein in 1905. Statistical physicists were interested in determining the average characteristics of the behavior of a high order system (note the similarity to the aggregation problem) without actually solving the equations which determine the system.

In the years that followed Einstein's formulation of his model, a series of works by Smoluchowski, Fokker, Planck, Ornstein, were devoted to the study of his model and the derivation of the Fokker-Planck equations.

The developments in statistical physics stimulated work by mathematicians in the general area of stochastic processes. The connection between the Fokker-Planck equation and the general Markov diffusion processes (loosely speaking Markov processes with continuous sample paths), was being gradually elucidated. In 1931,

Kolmogorov [48] presented his forward (Fokker-Planck) and backward equations for Markov diffusion processes, of which Brownian motion was an important but nevertheless particular example.

The Fokker-Planck equation represented an indirect way of studying the evolution of a class of stochastic processes without a close analysis of the properties of their sample paths (or trajectories). However, it created a first connection between the study of stochastic processes and the general theory of differential equations. It was Wiener [50] who initiated the study of sample paths for the particular case of Brownian motion. His work was extended by Lévy [51]. Further developments in this field ultimately led to a complete theory of stochastic differential equations (Îto and McKean [52], Dynkin [53]), essentially a device to reconstruct trajectories of a stochastic process.

An important advance in the study of Kolmogorov's equations was made in the years 1952-53 when Feller [54] applied the theory of semi-groups to the investigation of the general boundary conditions for these equations. Feller's results are reported by Bharucha-Reid [38].

Due to the frequent occurence of Markov diffusion processes as models of physical processes, the Fokker-Planck equation appears in numerous applications (engineering, biology, ecology, physics, etc.). An important engineering application is the analysis of phase-lock loops [44] in electrical communication systems. Unfortunately, the types of Fokker-Planck equations that appear there (periodic coefficients) bear little relationship to the CFPE model.

The Fokker-Planck equation also plays a role in the solution of an important problem in the literature on stochastic processes: the first-passage time problem, i.e. the determination of the probability density for a random variable of the type defined earlier in equation (3.52). In section 4.2.1, it is established that success in determining the dynamics of the CFPE model analytically rests on the ability to solve two first passage time problems.

First passage time problems occur in a variety of areas (storage theory and the theory of dams [57], level crossing problems in communications theory [44]). We are particularly concerned with their occurence in the analysis of mathematical models of nervous system activity, because as will be shown in section 4.2.2, some passage time problems are encountered which are formally identical to what is needed for a solution of the CFPE model dynamics.

Inspired by the results in nervous system modeling research, we formulate and analyze in section 4.3 a mathematically more tractable approximation of the CFPE model.

4.2 Some Relevant Results in Nervous System Modeling

4.2.1 Two First Passage Time Densities and Their Importance in the Dynamics of the CFPE Model

We propose to study the following problem. Assuming that in equation (2.1), the ambient temperature process is a constant, solve for $E_w(m_i(t))$ in a homogeneous control group if it is given that:

$$f_1^o(\lambda) = \delta(\lambda - x_-) \tag{4.1}$$

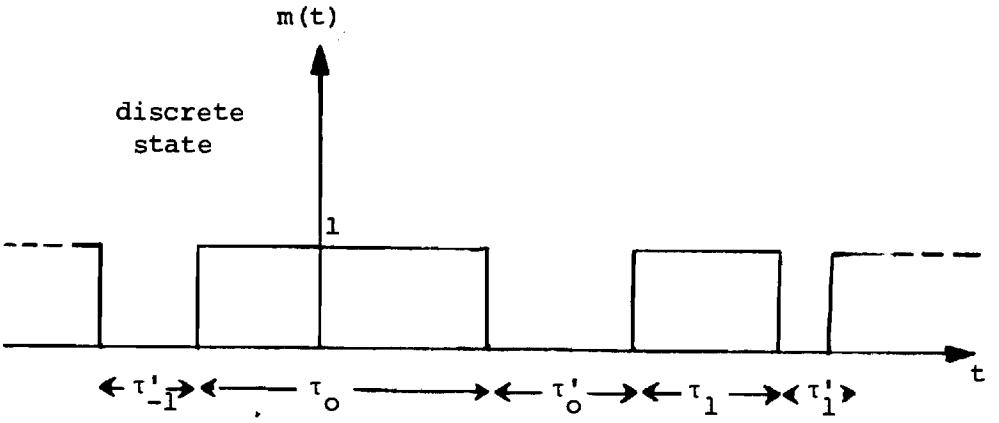

Fig. 4-1. A Typical Trajectory of Discrete State $m_i(t)$.

$$f_o^o(\lambda) = 0 \tag{4.2}$$

In (4.1) $\delta(\cdot)$ is the Dirac delta function.

The problem is approached from the standpoint of renewal processes. Fig. 4-1 represents a typical trajectory of $m_i(t)$. From (4.1), it is known that the device is "on" a time zero and the temperature state is x_-. Let τ_i, τ_i' be respectively the durations of "on" time and "off" time for the i^{th} cycle. In view of the switching mechanisms described in equation (2.3), τ_i and τ_i' can be considered as first-passage time random variables from x_- to x_+ for a device initially "on" and vice versa for a device initially "off", respectively.

For a constant ambient temperature process $x_a(t)$ and considering the properties of white noise, it is clear that the sequence $\{\tau_i\}_{i=-\infty}^{+\infty}$ is a sequence of identically distributed independent random variables. The same holds for $\{\tau_i'\}_{i=-\infty}^{+\infty}$. The following functions are now defined:

$f_\tau(u)$: probability density function of τ_i, $i=0,\pm1,\pm2,\ldots$ (4.3)

$f_{\tau'}(u)$: probability density function of τ_i', $i=0,\pm1,\pm2,\ldots$ (4.4)

$$f_T(u) = f_\tau * f_{\tau'}(u) \tag{4.5}$$

$$f_T^{(i)}(u) = \underbrace{f_T * \text{---} * f_T}_{i \text{ times}}(u) \tag{4.6}$$

In the above * indicates the convolution operation. Also, define the sequence of events:

$$A_1 = [\tau_1 > t]$$

$$A_2 = [((\tau_1 + \tau_1' < t) \cap ((\tau_1 + \tau_1' + \tau_2) > t)]$$

$$\vdots$$

$$A_i = \left[\left(\sum_{j=1}^{i-1} (\tau_j + \tau_j') < t\right) \cap \left(\tau_i + \sum_{j=1}^{i-1} (\tau_j + \tau_j' > t)\right]\right.$$

$$\vdots \qquad (4.7)$$

Recalling (4.1)-(4.2) we have

$$E_w(m_i(t)) = Pr[m_i(t) = 1]$$

$$= Pr\left[\bigcup_{i=1}^{\infty} A_i\right] . \qquad (4.8)$$

However $\{A_i\}_{i=1}^{\infty}$ is a disjoint sequence of events. Consequently:

$$E_w(m_i(t)) = \sum_{i=1}^{\infty} Pr(A_i) \qquad (4.9)$$

Using the densities in (4.3)-(4.5) and independence, we have:

$$Pr(A_1) = \int_t^{\infty} f_\tau(u)du ,$$

$$Pr(A_2) = \int_0^t \int_{t-v}^{\infty} f_\tau(u) f_T(v)du\, dv$$

$$\Pr(A_i) = \int_0^t \int_{t-v}^{\infty} f_\tau(u) f_T^{(i)}(v)\,du\,dv \ ,$$
$$\vdots \qquad\qquad (4.10)$$

(4.9)-(4.10) yield:

$$E_w(m_i(t)) = \int_t^{\infty} f_\tau(v)\,dv + \sum_{i=1}^{\infty} \left[\int_0^t \int_{t-v}^{\infty} f_\tau(u) f_T^{(i)}(v)\,du\,dv\right] \qquad (4.11)$$

Equation (4.11) clearly indicates the dependence of $E_w(m_i(t))$ on two density functions $f_\tau(u)$ and $f_T(u)$, or recalling (4.5), $f_\tau(u)$ and $f_{\tau'}(u)$. This means that success in determining analytically the dynamics of $E_w(m_i(t))$ depends on our ability to solve two first-passage time problems: switching time from "on" to "off" given that the device is initially "on" and at temperature x_-, and switching time from "off" to "on" given that the device is initially "off" and at temperature x_+.

4.2.2 First-Passage Time Problems in the Modeling of Neuronal Activity

As elaborated in section 4.2.1, success in analyzing the dynamics of the CFPE model rests on the ability to determine two first-passage time densities $f_\tau(u)$ and $f_{\tau'}(u)$ ((4.3)-(4.4)). The literature on nervous system modeling [41] presents numerous examples of such problems. In the following, some of the stochastic models encountered and the associated first-passage time problems are discussed. Relevant results are underlined. The focus is on the modeling of neuronal electric activity.

Neurons have an "all or none" behavior which depends on their electric potential hitting a critical value known as the action potential, upon which a neuronal discharge occurs. What is important here is the distribution of interarrival times of the spikes. Each neuron receives signals from many other neurons through terminal contacts referred to as synapses. If the number of synaptic inputs to a neuron is large, if the inputs are relatively independent, and if the electrochemical effect of each input is small relative to the neuron's threshold, the electric potential process (similar to our temperature process $x(t)$) can be viewed as being analogous to the position of a particle undergoing a random walk, with the action potential being analogous to the position of an absorbing barrier for the particle. Gerstein and Mandelbrot [55] first suggested such a random walk model, thus stimulating research into stochastic models for neuronal activity. The early random walk models had discrete inputs and were cumbersome to analyze. Subsequently, approximations were made that allowed the input to be a white noise process, thus yielding diffusion models [56]. Among the diffusion models, two are particularly relevant to this research.

The Perfect Integrator Model with Constant Threshold: Here, the input is a Gaussian white noise process with mean m and variance σ. The dynamics of the neuron potential $v(t)$ are given by:

$$dv(t) = m\,dt + \sigma\,dw(t) \qquad (4.12)$$

w(t) is a zero mean, unit variance, white noise process. If the threshold (or action potential) is a constant k, and if the rest level is x_o, the probability density of spikes interarrival times is a first passage time density across a constant level and has been obtained in closed form [41]:

$$P(t) = \frac{k - x_o}{\sigma(2\pi t^3)^{1/2}} \exp\left[\frac{-(k - x_o - mt)^2}{2\sigma^2 t}\right] \qquad (4.13)$$

The Leaky Integrator Model with Constant Threshold: This model is exactly analogous to the previous one, except that, in the absence of input, v(t) decays exponentially to some rest value x_r. The dynamics of v(t) obey:

$$dv(t) = -\frac{1}{\tau}(v(t) - x_r)dt + mdt + \sigma\, dw(t) \qquad (4.14)$$

Again here, for a threshold k and a reset potential x_o, the probability density of spikes interarrival times is a first-passage time density across a constant barrier. Note that before hitting k, v(t) evolves like an Ornstein-Uhlenbeck process [39]. Although the leaky integrator model has been extensively investigated [42,43], the problem of determining analytically the first passage time density in this case was never solved. A perfect similarity can be noted between the dynamics of v(t) the electric potential, and x(t) the temperature process in the "on" state (equation 2.1, m(t) = 1), and in the "off" state (equation 2.1, m(t) = 0). Edges x_+ and x_- are analogous to the action potential k and the reset potential x_o.

Finally, for constant ambient temperature, x_r is analogous to $x_a(t)$. Thus, the solution of $f_\tau(u)$ and $f_{\tau'}(u)$ ((4.3)-(4.4)) is formally equivalent to the determination of spikes interarrival densities in the case of the leaky integrator model. In view of the known analytic intractability of the latter model, it can be concluded that the CFPE model will also be intractable. Approximations must be made.

In the following section, a simplified version of the CFPE model is formulated and analyzed.

4.3 Approximate Analysis of the CFPE Model - The Contant Rates Approximation

Using the nomenclature developed in the preceding section, the constant rates approximation is tantamount to going from a leaky integrator model to a perfect integrator model. It is assumed that most of the densities $f_1(\lambda,t)$ and $f_o(\lambda,t)$ are confined within the dead band. This should generally be true in practical situations. The dead band itself is a very narrow range of temperature (typically $|\cdot|^\circ C$). This means in equation (2.1), the charging rate ($Rb(t) - a(\lambda - x_a(t))$) and the discharge rate ($a(\lambda - x_a(t))$ are practically constant (for constant weather conditions, and for the duration of the control b(t)). Designate these values by r and c respectively. Under the assumption (3.36)-(3.37) reduce to:

$$\frac{\partial f_1}{\partial t}(\lambda,t) = -r\frac{\partial}{\partial \lambda} f_1(\lambda,t) + \frac{\sigma^2}{2}\frac{\partial^2}{\partial \lambda^2} f_1(\lambda,t) \qquad (4.15)$$

$$\frac{\partial f_o}{\partial t}(\lambda,t) = c\frac{\partial}{\partial \lambda} f_o(\lambda,t) + \frac{\sigma^2}{2}\frac{\partial^2}{\partial \lambda 2} f_o(\lambda,t) \qquad (4.16)$$

This approximation of the CFPE model becomes a system of space-homogeneous, linear time-invariant Fokker-Planck equations coupled through boundary conditions (3.42)-(3.43). In the next two sections 4.3.1 and 4.3.2, we develop results pertaining to (4.15)-(4.16).

4.3.1 Results in the Transform Domain

A Direct Approach. Let us define the following functions:

$$g_1(t) = -\frac{\sigma^2}{2}\frac{\partial f_1}{\partial \lambda}(x_+,t) \tag{4.17}$$

$$g_o(t) = \frac{\sigma^2}{2}\frac{\partial f_o}{\partial \lambda}(x_-,t) \tag{4.18}$$

Recalling (3.25, 3.27), $g_1(t)$ and $g_o(t)$ can be be interpreted as rates of probability absorption from "on" to "off" through boundary x_+, and from "off" to "on" through boundary x_- respectively, at time t.

Also, for a given function f(t) denote by f*(s) the unilateral Laplace transform of f(t) when it exists. Laplace transformation of (4.15)-(4.16) and (3.38)-(3.43) yields the following two groups of equations:

$$P_1 - \quad sf_1^*(\lambda,s) - f_1^o(\lambda) = -r\frac{\partial}{\partial \lambda} f_1^*(\lambda,s) + \frac{\sigma^2}{2}\frac{\partial^2}{\partial \lambda^2} f_1^*(\lambda,s) \tag{4.19}$$

in regions a, b and c of Fig. 3-1 and:

$$f_1^*(x_+,s) = 0 \tag{4.20}$$

$$\lim_{\lambda \to -\infty} f_1^*(\lambda,s) = 0 \tag{4.21}$$

$$-\frac{\partial}{\partial\lambda} f_{1a}^*(x_-,s) + \frac{\partial}{\partial\lambda} f_{1b}^*(x_-,s) = -\frac{2}{\sigma^2} g_o^*(s) \tag{4.22}$$

$$P_2 - \qquad sf_o^*(\lambda,s) - f_o^o(\lambda) = c\frac{\partial}{\partial\lambda} f_o^*(\lambda,s) + \frac{\sigma^2}{2}\frac{\partial^2}{\partial\lambda^2} f_o^*(\lambda,s) \tag{4.23}$$

in regions b and c of Fig 3-1 and:

$$f_o^*(x_-,s) = 0 \tag{4.24}$$

$$\lim_{\lambda \to +\infty} f_o^*(\lambda,s) = 0 \tag{4.25}$$

$$\frac{\partial}{\partial\lambda} f_{oc}^*(x_+,s) - \frac{\partial}{\partial\lambda} f_{ob}^*(x_+,s) = -\frac{2}{\sigma^2} g_1^*(s) \tag{4.26}$$

$f_1^*(\lambda,s)$ and $f_o^*(\lambda,s)$ are completely decoupled except through boundary conditions (4.22) and (4.26). Therefore, if $g_1^*(s)$ and $g_o^*(s)$ are considered to be known functions of s, systems P_1 and P_2 can be solved separately.

System P_1 is now considered. The second order linear differential equation in λ (4.19), with constant coefficients can be written in state form as:

$$\frac{\partial}{\partial\lambda}\begin{vmatrix} f_1^*(\lambda,s) \\ \frac{\partial}{\partial\lambda} f_1^*(\lambda,s) \end{vmatrix} = \begin{vmatrix} 0 & 1 \\ \frac{2s}{\sigma^2} & \frac{2r}{\sigma^2} \end{vmatrix} \begin{vmatrix} f_1^*(\lambda,s) \\ \frac{\partial}{\partial\lambda} f_1^*(\lambda,s) \end{vmatrix} - \frac{2}{\sigma^2}\begin{bmatrix} 0 \\ 1 \end{bmatrix} f_1^o(\lambda) \tag{4.27}$$

Using the state transition matrix [10] for the above system, it is possible to write the solutions in regions a and b of Fig. 3-1 in terms of the value of the state at $\lambda = x_-$, i.e. in terms of $f_1^*(x_-,s)$ and $\frac{\partial}{\partial\lambda} f_{1a}^*(x_-,s)$ or $f_1^*(x_-,s)$ and $\frac{\partial}{\partial\lambda} f_{1b}^*(x_-,s)$ respectively:

$$f_1^*(\lambda,s) = \phi_{11}(\lambda-x_-,s) f_1^*(x_-,s) + \phi_{12}(\lambda-x_-,s) \frac{\partial f_1^*}{\partial\lambda}(x_-,s) - \frac{2}{\sigma^2}\int_{x_-}^{\lambda} \phi_{12}(\lambda-x,s) f_1^o(x)\,dx \tag{4.28}$$

$$\frac{\partial f_1^*}{\partial\lambda}(\lambda,s) = \phi_{21}(\lambda-x_-,s) f_1^*(x_-,s) + \phi_{22}(\lambda-x_-,s) \frac{\partial f_o^*}{\partial\lambda}(x_-,s) - \frac{2}{\sigma^2}\int_{x_-}^{\lambda} \phi_{22}(\lambda-x,s) f_1^o(x)\,dx \tag{4.29}$$

Where it can be shown (proof 2, Appendix B) that:

$$\underline{\phi}(\lambda,s) = [\phi_{ij}(\lambda,s)] = \exp\begin{vmatrix} 0 & 1 \\ \frac{2s}{\sigma^2} & \frac{2r}{\sigma^2} \end{vmatrix} \lambda \tag{4.30}$$

and

$$\phi_{11}(\lambda,s) = \theta^{-1}(s)\left[\theta_1(s)e^{\theta_2(s)\lambda} - \theta_2(s)e^{\theta_1(s)\lambda}\right], \tag{4.31}$$

$$\phi_{12}(\lambda,s) = \theta^{-1}(s)\left[e^{\theta_1(s)\lambda} - e^{\theta_2(s)\lambda}\right], \tag{4.32}$$

$$\phi_{21}(\lambda,s) = \frac{2s}{\sigma^2}\left[e^{\theta_1(s)\lambda} - e^{\theta_2(s)\lambda}\right], \tag{4.33}$$

$$\phi_{22}(\lambda,s) = \theta^{-1}(s)\left[\theta_1(s)e^{\theta_1(s)\lambda} - \theta_2(s)e^{\theta_2(s)\lambda}\right] . \qquad (4.34)$$

With

$$\theta(s) = \frac{2}{\sigma^2}(r^2 + 2s\sigma^2)^{1/2} ,$$

$$\theta_1(s) = \frac{r}{\sigma^2} + \frac{\theta(s)}{2} , \qquad (4.35)$$

$$\theta_2(s) = \frac{r}{\sigma^2} - \frac{\theta(s)}{2} . \qquad (4.36)$$

Now consider boundary condition (4.21). It requires that as $\lambda \to -\infty$ $f_1^*(\lambda,s)$ remain bounded. However, the expression (4.28) for $f_1^*(\lambda,s)$ contains an unstable exponential since for Re[s] > 0 as $\lambda \to -\infty$, $e^{\theta_2(s)\lambda} \to +\infty$. The unstable content of $f_1^*(\lambda,s)$ can be written:

$$I(\lambda) = \left[e^{-\theta_2(s)x_-}\theta_1(s)\theta^{-1}(s)f_1^*(x_-,s) - \theta^{-1}(s)e^{-\theta_2(s)x_-}\frac{\partial}{\partial\lambda}f_{1a}^*(x_-,s)\right.$$

$$\left. + \frac{2}{\sigma^2}\int_{x_-}^{\lambda}\theta^{-1}(s)e^{-\theta_2(s)x_-}f_1^o(x)dx\right]e^{\theta_2(s)\lambda} \qquad (4.37)$$

In order that $f_1^*(\lambda,s)$ remain bounded, it is necessary that:

$$(\theta_1(s)e^{-\theta_2(s)x_-})f_1^*(x_-,s) - e^{-\theta_2(s)x_-}\frac{\partial f_{1a}^*}{\partial\lambda}(x_-,s)$$

$$+ \frac{2}{\sigma^2}\int_{x_-}^{-\infty} e^{-\theta_2(s)x}f_1^o(x)dx = 0 \qquad (4.38)$$

Boundary condition (4.20) yields:

$$f_1^*(x_+,s) = 0 = f_1^*(x_-,s)\left[\theta_1(s)e^{\theta_2(s)\Delta} - \theta_2(s)e^{\theta_1(s)\Delta}\right]\theta(s)$$

$$+ \theta^{-1}(s)\left[e^{\theta_1(s)\Delta} - e^{\theta_2(s)\Delta}\right]\frac{\partial f_{1b}^*}{\partial\lambda}(x_+,s)$$

$$- \frac{2}{\sigma^2}\int_{x_-}^{x_+}\theta^{-1}(s)\left[e^{\theta_1(s)(x_+-x)} - e^{\theta_2(s)(x_+-x)}\right]f_1^o(x)dx \quad (4.39)$$

Where $\Delta = x_+ - x_-$ (width of the dead band).

Recalling (4.22) and using (4.38)-(4.39) we obtain:

$$f_1^*(x_-,s) = 2\sigma^2\theta^{-1}(s)\left[(g_o^*(s) - \int_{x_-}^{+\infty} e^{\theta_2(s)(x_--x)}f_1^o(x)dx)(1-e^{-\theta(s)\Delta}) - e^{-\theta_1(s)\Delta}\int_{x_-}^{x_+}(e^{\theta_1(s)(x_+-x)} - e^{\theta_2(s)(x_+-x)})f_1^o(x)dx\right], \quad (4.40)$$

$$\frac{\partial f_{1a}^*}{\partial\lambda}(x_-,s) = 2(\sigma^2\theta(s))^{-1}\left[\theta_1(s)g_o^*(s)(1 - e^{-\theta(s)\Delta}) + \int_{-\infty}^{x_-} e^{-\theta_2(s)(x-x_-)}f_1^o(x)dx\,(\theta_2(s) - \theta_1(s)e^{-\theta(s)\Delta}) - \theta_1(s)e^{-\theta_1(s)\Delta}\int_{x_-}^{x_+}(e^{\theta_1(s)(x_+-x)} - e^{\theta_2(s)(x_+-x)})f_1^o(x)dx\right], \quad (4.41)$$

$$\frac{\partial f_{1b}^*}{\partial\lambda}(x_-,s) = 2(\sigma^2\theta(s))^{-1}\left[(g_o^*(s) + \int_{-\infty}^{x_+} e^{-\theta_2(s)(x-x_-)}f_1^o(x)dx\right)$$

$$(\theta_2(s) - \theta_1(s)e^{-\theta(s)\Delta})$$

$$- \theta_1(s) e^{-\theta_1(s)\Delta} \int_{x_-}^{x_+} \left(e^{\theta_1(s)(x_+ - x)} - e^{\theta_2(s)(x_+ - x)} \right) f_1^o(x)\,dx \Big] \,. \tag{4.42}$$

From knowledge of boundary conditions $f_1^*(x_-,s)$, $\frac{\partial f_{1a}^*}{\partial \lambda}(x_-,s)$, $\frac{\partial f_{1b}^*}{\partial \lambda}(x_-,s)$ and equation (4.28) it is possible to write an expression for $f_1^*(\lambda,s)$ everywhere.

In region a of Fig. 3-2, using (4.28,4.40-4.41), we have:

$$f_1^*(\lambda,s) = 2(\sigma^2\theta(s))^{-1} \Big[\int_{-\infty}^{\lambda} e^{\theta_2(s)(\lambda - x)} f_1^o(x)\,dx \left(1 - e^{\theta(s)(\lambda - x_+)}\right)$$

$$+ g_o^*(s) e^{\theta_1(s)(\lambda - x_-)} \left(1 - e^{\theta(s)\Delta}\right)$$

$$+ \int_{\lambda}^{x_+} e^{\theta_1(s)(\lambda - x)} \left(1 - e^{\theta(s)(x - x_+)}\right) f_1^o(x)\,dx \Big] \tag{4.43}$$

Similarly, in region b of Fig. 3-2, using (4.28, 4.40, 4.42) we have:

$$f_1^*(\lambda,s) = 2(\sigma^2\theta(s))^{-1} \left(1 - e^{\theta(s)(\lambda - x_+)}\right) \Big[g_o^*(s) e^{\theta_2(s)(\lambda - x_-)}$$

$$+ \int_{-\infty}^{\lambda} e^{\theta_2(s)(\lambda - x)} f_1^o(x)\,dx + \int_{\lambda}^{x_+} e^{\theta_1(s)(\lambda - x)} f_1^o(x)\,dx \Big] \tag{4.44}$$

Recalling (4.17) we have:

$$g_1^*(s) = -\frac{\sigma^2}{2} \frac{\partial f_{1b}^*}{\partial \lambda}(x_+,s) \tag{4.45}$$

Differentiation of (4.44) with respect to λ yields:

$$\frac{\partial f_1^*}{\partial \lambda}(\lambda,s) = 2(\sigma^2\theta(s))^{-1}\left(1 - e^{\theta(s)(\lambda-x_+)}\right)\frac{\partial}{\partial\lambda}\left[g_o^*(s)e^{\theta_2(s)(\lambda-x_-)}\right.$$

$$\left. + \int_{-\infty}^{\lambda} e^{\theta_2(s)(\lambda-x)} f_1^o(x)\,dx\right]$$

$$+ \frac{2}{\sigma^2} e^{\theta(s)(\lambda-x_+)}\left[g_o^*(s)e^{\theta_2(s)(\lambda-x_-)} + \int_{-\infty}^{\lambda} e^{\theta_2(s)(\lambda-x)} f_1^o(x)\,dx\right]$$

$$- 2(\sigma^2\theta(s))^{-1}\left[1 - e^{\theta(s)(\lambda-x_+)}\right]f_1^o(\lambda)$$

$$+ \int_{\lambda}^{x_+} \theta_1(s)e^{\theta_1(s)(\lambda-x)}\, 2(\sigma^2\theta(s))^{-1}\left(1 - e^{\theta(s)(x-x_+)}\right)f_1^o(x)\,dx \qquad (4.46)$$

At $\lambda = x_+$, (4,46), (4.45) and (4.20) yield:

$$g_1^*(s) = g_o^*(s)e^{\theta_2(s)\Delta} + \int_{-\infty}^{x_+} e^{\theta_2(s)(x_+-x)} f_1^o(x)\,dx \qquad (4.47)$$

Assuming $g_o^*(s)$ is known, equations (4.43)-(4.44) and (4.47) represent the solution of P_1 in the transform domain.

We now turn to the problem of deriving corresponding results for system P_2, i.e. for the "off" density. Lengthy computations can be avoided if it is recognized that by using a change of variable:

$$y = x_+ + x_- - \lambda$$

and replacing r by c and $g_o^*(s)$ by $g_1^*(s)$ in equations (4.19)-(4.22), system P_1 can be transformed into a system formally identical to P_2.

To verify this, note that:

$$f_1^*(\lambda,s) = f_1^*(-y + x_+ - x_-, s) = f_1^{*'}(y,s) \tag{4.48}$$

$$\frac{\partial}{\partial\lambda} f_1^*(\lambda,s) = -\frac{\partial f_1^*}{\partial y}(-y + x_+ + x_-, s) = -\frac{\partial f_1^{*'}}{\partial y}(y,s) \tag{4.49}$$

$$\frac{\partial^2}{\partial\lambda^2} f_1^*(\lambda,s) = \frac{\partial^2 f_1^*}{\partial y^2}(x_+ + x_- - y, s) = \frac{\partial^2 f_1^{*'}}{\partial y^2}(y,s) \tag{4.50}$$

Substituting (4.48)-(4.50) into (4.19), and replacing r by c yields:

$$sf_1^{*'}(y,s) - f_1^{0'}(y) = c\frac{\partial f_1^{*'}}{\partial y}(y,s) + \frac{\sigma^2}{2}\frac{\partial^2}{\partial y^2} f_1^{*'}(y,s) \tag{4.51}$$

Futhermore (4.20)-(4.21) yield:

$$f_1^{*'}(x_-,s) = 0 \tag{4.52}$$

$$\lim_{y\to+\infty} f_2^{*'}(y,s) = 0 \tag{4.53}$$

Finally, using (4.49) and replacing $g_o^*(s)$ by $g_1^*(s)$ in (4.22) yields:

$$\frac{\partial}{\partial y} f_{1c}^{*'}(x_+,s) - \frac{\partial}{\partial y} f_{1b}^{*'}(x_+,s) = \frac{-2}{\sigma^2} g_1^*(s) \tag{4.54}$$

Clearly (4.51)-(4.54) is a system of equations formally identical to (4.23)-(4.26). This means that in general:

$$f_o^*(\lambda,s) = f_1^{*'}(\lambda,s) = f_1^*(x_+ + x_- - \lambda,s) \tag{4.55}$$

i.e., the solution of system P_2 can be derived from the solution of system P_1 by replacing λ by $(x_+ + x_- - \lambda)$, r by c and $g_o^*(s)$ by $g_1^*(s)$.

Using the above remark, the following results are obtained: In region b of Fig 3-2,

$$f_o^*(\lambda,s) = 2(\sigma^2\gamma(s))^{-1}\Big[\big(g_1^*(s)e^{\gamma_2(s)(x_+-\lambda)} + \int_\lambda^{+\infty} e^{\gamma_2(s)(x-\lambda)} f_o^o(x)dx\big)$$

$$\big(1 - e^{\gamma(s)(x_--\lambda)}\big)$$

$$+ \int_\lambda^{x_-} e^{\gamma_1(s)(x-\lambda)}\big(1 - e^{\gamma_2(s)(x_--x)}\big)f_o^o(x)dx\Big] \qquad (4.56)$$

In region c of Fig. 3-2,

$$f_o^*(\lambda,s) = 2(\sigma^2\gamma(s))^{-1}\Big[\int_\lambda^{+\infty} e^{\gamma_2(s)(x-\lambda)} f_o^o(x)dx\big(1 - e^{\gamma(s)(x_--\lambda)}\big)$$

$$+ g_1^*(s)e^{\gamma_1(s)(x_+-\lambda)}\big(1 - e^{-\gamma(s)\Delta}\big)$$

$$+ \int_{x_-}^{\lambda} e^{\gamma_1(s)(x-x_-)}\big(1 - e^{-\gamma(s)(x_--x)}\big)f_o^o(x)dx \qquad (4.57)$$

Finally:

$$g_o^*(s) = g_1^*(s)e^{\gamma_2(s)\Delta} + \int_{x_-}^{+\infty} e^{\gamma_2(s)(x-x_-)} f_o^o(x)dx \qquad (4.58)$$

where in(4.56)-(4.58):

$$\gamma(s) = \frac{2}{\sigma^2}\,(c^2 + 2s\sigma^2)^{1/2},$$

$$\gamma_1(s) = \frac{c}{\sigma^2} + \frac{\gamma(s)}{2} , \tag{4.59}$$

$$\gamma_2(s) = \frac{c}{\sigma^2} - \frac{\gamma(s)}{2} . \tag{4.60}$$

Equation (4.47) and (4.58) yield:

$$g_1^*(s) = \int_{x_-}^{+\infty} \frac{e^{\theta_2(s)\Delta}\, e^{\gamma_2(s)(x-x_-)}}{F(s)} f_o^o(x)dx$$

$$+ \int_{-\infty}^{x_+} \frac{e^{\theta_2(s)(x_+-x)}}{F(s)} f_1^o(x)dx , \tag{4.61}$$

$$g_o^*(s) = \int_{-\infty}^{x_+} \frac{e^{\gamma_2(s)\Delta}\, e^{\theta_2(s)(x_+-x)}}{F(s)} f_1^o(x)dx$$

$$+ \int_{x_-}^{+\infty} \frac{e^{\gamma_2(s)(x-x_-)}}{F(s)} f_o^o(x)dx \tag{4.62}$$

where in (4.61)-(4.62)

$$F(s) = 1 - e^{(\theta_2(s) + \gamma_2(s))\Delta}$$

Recalling equations (3.31), (4.17)-(4.18) we have:

$$\frac{\overrightarrow{dm^*}}{dt}(s) = g_o^*(s) - g_1^*(s) \tag{4.63}$$

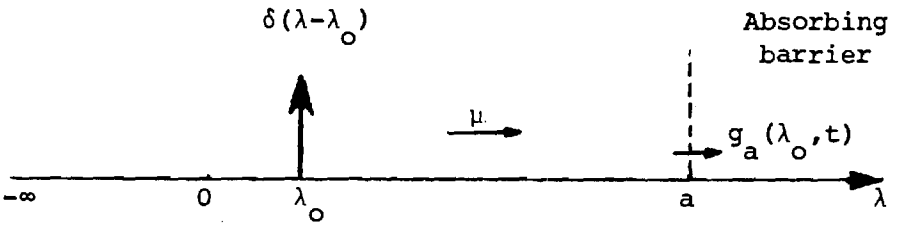

Fig. 4-2. Brownian Motion with Drift μ across an Absorbing Barrier. $g_a(\lambda_o,t)$ is the rate of probability absorption across the barrier.

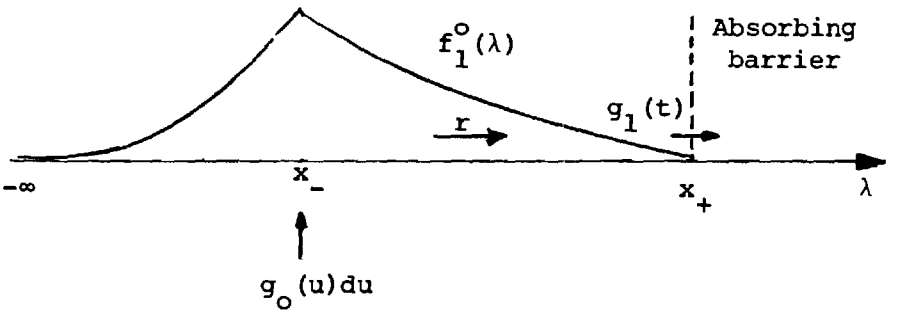

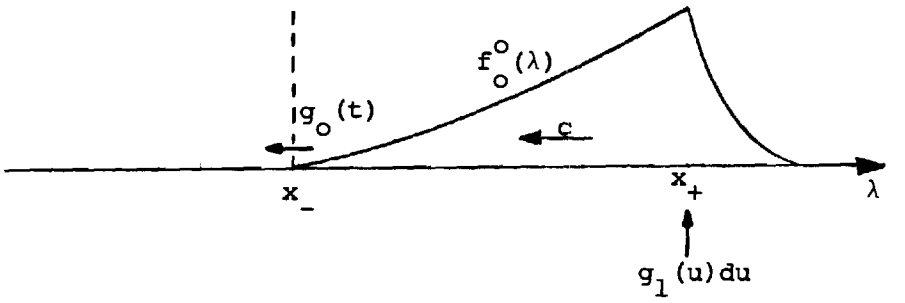

Fig. 4-3. Graphical Illustration of the Process of Probability Escape and Probability Injection in the CFPE Model.

(4.61)-(4.63) yield:

$$\frac{dm^*}{dt}(s) = \int_{x_-}^{+\infty} \frac{\left(1 - e^{\theta_2(s)\Delta}\right)}{F(s)} e^{\gamma_2(s)(x-x_-)} f_o^o(x)dx$$

$$- \int_{-\infty}^{x_+} \frac{\left(1 - e^{\gamma_2(s)\Delta}\right)}{F(s)} e^{\theta_2(s)(x_+-x)} f_1^o(x)dx \qquad (4.64)$$

Equation (4.64) gives an expression for the Laplace transform of $\frac{d\bar{m}}{dt}$ (t), i.e. the rate of change of the aggregate functional state $\bar{m}(t)$ for the homogeneous control group. Equations (4.43)-(4.44), (4.56)-(4.57), (4.61)-(4.62), (4.64) together represent the complete solution of the CFPE model in the transform domain. In section 4.3.1 the inversion problem of the Laplace transform in equation (4.64) will be considered.

A Superposition Approach. The results in the preceding section can be obtained in a natural way if superposition arguments are used. First however, some impulse response-like (or Green functions [58]) need to be determined.

In the following, a relationship is derived between the first-passage time density for a Brownian motion x(t) with positive drift μ and variance σ^2 across a barrier a, given $x(o) = \lambda_o$. The derivations are based on Cox [39].

On the interval $(-\infty,a)$ (see Fig. 4-2), the conditional probability density $P_a(\lambda,t,\lambda_o)$ of x(t) satisfies the Fokker-Planck equation [38]:

$$\frac{\partial P_a}{\partial t}(\lambda,t,\lambda_o) = -\mu \frac{\partial P_a}{\partial \lambda}(\lambda,t,\lambda_o) + \frac{\sigma^2}{2} \frac{\partial^2 P_a}{\partial \lambda^2}(\lambda,t,\lambda_o) \qquad (4.65)$$

with initial conditions:

$$\lim_{t\to 0} P_a(\lambda,t,\lambda_o) = \delta(\lambda - \lambda_o) \qquad (4.66)$$

and absorbing boundary condition:

$$P_a(a,t,\lambda_o) = 0 \qquad (4.67)$$

Let $g_a(\lambda_o,t)$ represent the corresponding first-passage time density across a, we have:

$$\Pr[-\infty < x(t) \leq a | x(o) = \lambda_o] = 1 - \int_o^t g_a(\lambda_o,\tau)d\tau$$

$$= \int_{-\infty}^{a} P_a(\lambda,t,\lambda_o)d\lambda \qquad (4.68)$$

Differentiating (4.68) with respect to t and assuming the orders of integration and differentiation in the right-hand side of (4.68) can be interchanged yields:

$$g_a(\lambda_o,t) = \int_{-\infty}^{a} -\frac{\partial P_a}{\partial t}(\lambda,t,\lambda_o)d\lambda \qquad (4.69)$$

(4.65), (4.67) and (4.69) yield:

$$g_a(\lambda_o,t) = -\frac{\sigma^2}{2} \frac{\partial P_a}{\partial \lambda}(a,t,\lambda_o) \qquad (4.70)$$

Equation (4.70) expresses the fact that at any time t, the first passage-time density is equal to the rate of probability absorption into barrier a.

The system (4.65)-(4.67), (4.69) is solved in [39] (see Appendix C for derivations). The results are as follows:

$$g_a(\lambda_o,t) = \frac{(a - \lambda_o)}{\sigma(2\pi t^3)^{1/2}} \exp\left[-\frac{(a - \lambda_o - \mu t)^2}{2\sigma^2 t}\right] \tag{4.71}$$

$$P_a(\lambda,t,\lambda_o) = \frac{1}{\sigma(2\pi t)^{1/2}}\left[\exp\left[-\frac{(a - \lambda_o - \mu t)^2}{2\sigma^2 t}\right]\right.$$

$$\left. - \exp\left[\frac{2\mu(a - \lambda_o)}{\sigma^2} - \frac{(\lambda - \lambda_o - 2(a - \lambda_o) - \mu t)^2}{2\sigma^2 t}\right]\right] \tag{4.72}$$

For our particular problem the following densities are needed:

$$g_1(\lambda,t) = \frac{(x_+ - \lambda)}{\sigma(2\pi t^3)^{1/2}} \exp\left[-\frac{(x_+ - \lambda - rt)^2}{2\sigma^2 t}\right] \tag{4.73}$$

$$g_o(\lambda,t) = \frac{(\lambda - x_-)}{\sigma(2\pi t^3)^{1/2}} \exp\left[-\frac{(\lambda - x_- - ct)^2}{2\sigma^2 t}\right] \tag{4.74}$$

$$P_1(\lambda,t,\lambda_o) = \frac{1}{\sigma(2\pi t)^{1/2}}\left[\exp\left[-\frac{(x_+ - \lambda_o - rt)^2}{2\sigma^2 t}\right]\right.$$

$$\left. - \exp\left[\frac{2r(x_+ - \lambda_o)}{\sigma^2} - \frac{(\lambda - \lambda_o - 2(x_+ - \lambda_o) - rt)^2}{2\sigma^2 t}\right]\right] \tag{4.75}$$

$$P_o(\lambda,t,\lambda_o) = \frac{1}{\sigma(2\pi t)^{1/2}}\left[\exp\left[-\frac{(\lambda_o - \lambda - ct)^2}{2\sigma^2 t}\right]\right.$$

$$\left. - \exp\left[\frac{2c(\lambda_o - x_-)}{\sigma^2} - \frac{(\lambda_o - \lambda - 2(\lambda_o - x_-) - ct)^2}{2\sigma^2 t}\right]\right] \tag{4.76}$$

Using superposition arguments, it can be shown that:

$$g_1(t) = \int_{-\infty}^{\lambda} f_1^o(\lambda) g_1(\lambda,t)dt + \int_o^t g_o(\tau) g_1(x_-,t-\tau)d\tau \qquad (4.77)$$

The above quantities are represented in Fig. 4-3. In the following, a heuristic proof of equation (4.77) is given. For this particular problem, and in view of the mathematical analogy with heat diffusion, we shall think of probability as a "substance" diffusing across various boundaries. Two rates of probability diffusion are of interest: $g_1(t)$ and $g_o(t)$. These rates were introduced in equations (4.71)-(4.18). $g_1(t)$ is the total rate of probability diffusion at time t from "on" to "off" across the boundary at x_+; $g_o(t)$ is the total rate of probability diffusion at time t from "off" to on" across x_-. Now (4.73) gives an expression for the probability diffusion rate at time t and across x_+, due to an impulsive initial density of magnitude 1 and at temperature λ. This means (using linearity) that an impulsive initial "on" density of magnitude $f_1^o(\lambda)d\lambda$ at λ contributes at time t an infinitesimal increment in the diffusion rate across x_+ of size $f_1^o(\lambda)g_1(\lambda,t)d\lambda$. The complete contribution of $f_1^o(\lambda)$ can be obtained by adding up all elementary contributions. This yields the first integral in the right-hand side of equation (4.77). Futhermore, if $g_o(t)$ is the total rate of probability diffusion from "off" to "on" across x_-, then by "probability conservation," this probability must be injected back into the "on" probability density of x_- (see Fig. 4-3). Let $g_o(\tau)d\tau$ be the amount

of probability injected during the time interval $[\tau,\tau + d\tau]$, then its effect on the rate of probability diffusion across x_+ at time t is identical to the effect of an impulse in the probability density at x_- and at time $t-\tau$, i.e. $g_o(\tau)g_1(x_-,t-\tau)d\tau$. On the time interval $[0,t]$, the total contribution of the "injections" to $g_1(t)$ is obtained by adding up the effects of all elementary contributions. This explains the second integral (convolution) on the right-hand side of equation (4.77). Clearly, throughout the above discussion, time invariance of (4.15)-(4.16) is assumed. This is equivalent to assuming a constant ambient temperature $x_a(t)$.

A similar analysis yields for $g_o(t)$:

$$g_o(t) = \int_{x_-}^{+\infty} f_o^o(\lambda)g_o(\lambda,t)d\lambda + \int_o^t g_1(\tau)g_o(x_+,t-\tau)d\tau \qquad (4.78)$$

Finally, $f_1(\lambda,t)$ and $f_o(\lambda,t)$ evolve according to:

$$f_1(\lambda,t) = \int_{-\infty}^{x_+} f_1^o(x)P_1(\lambda,t,x)dx + \int_o^t P_1(\lambda,t-\tau,x_-)g_o(\tau)d\tau \qquad (4.79)$$

$$f_o(\lambda,t) = \int_{x_-}^{+\infty} f_o^o(x)P_o(\lambda,t,x)dx + \int_o^t P_o(\lambda,t-\tau,x_+)g_1(\tau)d\tau \qquad (4.80)$$

Note that (4.77)-(4.80) represent an alternative integral equation representation of (3.36)-(3.43). It can be solved by first solving the coupled integral equations (4.77)-(4.78) for $g_1(t)$ and $g_o(t)$ and subsequently substituting these functions into (4.79)-(4.80).

In the following we show that (4.64) can be retrieved using (4.77)-(4.78). Recall from (3.31) that the Laplace transform of $\frac{d\bar{m}}{dt}$ is given by:

$$\frac{dm^*}{dt}(s) = g_o^*(s) - g_1^*(s) \tag{4.81}$$

Laplace transformation of (4.77)-(4.78) yields:

$$g_1^*(s) = \int_{-\infty}^{x_+} f_1^o(\lambda) g_1^*(\lambda,s)\,d\lambda + g_o^*(s) g_1^*(x_-,s) \tag{4.82}$$

$$g_o^*(s) = \int_{x_-}^{+\infty} f_o^o(\lambda) g_o^*(\lambda,s)\,d\lambda + g_1^*(s) g_o^*(x_+,s) \tag{4.83}$$

(4.81)-(4.83) yield:

$$\frac{dm^*}{dt}(s) = \int_{x_-}^{+\infty} \frac{g_o^*(\lambda,s)\,(1 - g_1^*(x_-,s))}{1 - g_o^*(x_+,s) g_1^*(x_-,s)} f_o^o(\lambda)\,d\lambda$$

$$- \int_{x_+}^{+\infty} \frac{g_1^*(\lambda,s)\,(1 - g_o^*(x_+,s))}{1 - g_o^*(x_+,s) g_1^*(x_-,s)} f_1^o(\lambda)\,d\lambda \tag{4.84}$$

The following are Laplace transform pairs [39]:

$$g_1(\lambda_o,t) \quad \bullet\!\!-\!\!-\!\!-\!\!-\!\!\bullet \quad \exp\left(-(x_+-\lambda_o)\left(\frac{-r + \sqrt{r^2 + 2s\sigma^2}}{\sigma^2}\right)\right) \tag{4.85}$$

$$g_o(\lambda_o,t) \quad \bullet\!\!-\!\!-\!\!-\!\!-\!\!\bullet \quad \exp\left(-(\lambda_o - x_-)\left(\frac{-c + \sqrt{c^2 + 2s\sigma^2}}{\sigma^2}\right)\right) \tag{4.86}$$

Using (4.85)-(4.86) and recalling the definitions (4.35)-(4.36), (4.59)-(4.60), we obtain:

$$g_o^*(\lambda,s) = e^{\gamma_2(s)(\lambda-x_-)}, \tag{4.87}$$

$$g_o^*(x_+,s) = e^{\gamma_2(s)\Delta}, \tag{4.88}$$

$$g_1^*(\lambda,s) = e^{\theta_2(s)(x_+-\lambda)}, \tag{4.89}$$

$$g_1^*(x_-,s) = e^{\theta_2(s)\Delta}. \tag{4.90}$$

Substituting (4.87)-(4.90) back into (4.84), equation (4.64) is retrieved.

In closing this section, it is verified that equation (4.64) and equation (4.11) both obtained using independent approaches are consistent equations. The following derivations are heuristic. A mathematically more rigorous discussion is included in the next section were the inversion problem of the transform in (4.64) is considered as well as the problem of determining the steady-state (if any) of $f_1(\lambda,t)$ and $f_o(\lambda,t)$.

Formal differentiation of (4.11) yields:

$$\frac{d}{dt}\left(E_w(m_i(t))\right) = \frac{d\bar{m}}{dt}(t)$$

$$= -f_\tau(t) + \sum_{i=1}^{\infty}\left[-\int_o^t f_\tau(t-v) f_t^{(i)}(v)\,dv + \int_o^{\infty} f_\tau(u) f_T^{(i)}(t)\,du\right] \tag{4.91}$$

However, if we note that:

$$\int_0^\infty f_\tau(u)\,du = 1 \tag{4.92}$$

Then (4.91) yields:

$$\frac{d\bar{m}}{dt}(t) = -f_\tau(t) + \sum_{i=1}^{\infty}\left[f_\tau * f_T^{(i)}(t) + f_T^{(i)}(t)\right] \tag{4.93}$$

Laplace transformation of (4.93) yields:

$$\frac{d\bar{m}^*}{dt}(s) = -f_\tau^*(s) + \left[1 - f_\tau^*(s)\right]\left[\sum_{i=1}^{\infty}\left(f_T^*(s)\right)^i\right] \tag{4.94}$$

(4.94) can be rewritten:

$$\frac{d\bar{m}^*}{dt}(s) = \frac{f_T^*(s) - f_\tau^*(s)}{1 - f_T^*(s)} \tag{4.95}$$

where use has been made of the series expansion:

$$\frac{1}{1 - f_T^*(s)} = 1 + f_T^*(s) + f_T^{*2}(s) + \ldots \tag{4.96}$$

for $|f_T^*(s)| < 1$. Finally, recalling that $f_\tau(t)$, $f_{\tau'}(t)$ are probability densities of "on" and "off" durations respectively, i.e. first passage time random variables, we have:

$$f_\tau(t) = g_1(\lambda,t)\Big|_{\lambda=x_-} \tag{4.97}$$

$$f_{\tau}(t) = g_o(\lambda,t)\Big|_{\lambda=x_+} \tag{4.98}$$

Equations (4.5), (4.97)-(4.98) yield:

$$f_{\tau}^*(s) = g_1^*(x_-,s) = e^{\theta_2(s)\Delta} \tag{4.99}$$

$$f_T^*(s) = g_1^*(x_-,s)g_o^*(x_+,s) = e^{(\theta_2(s) + \gamma_2(s))\Delta} \tag{4.100}$$

Then:

$$\frac{\overline{dm}^*}{dt}(s) = \frac{e^{\theta_2(s)\Delta}\left(e^{\gamma_2(s)\Delta} - 1\right)}{1 - e^{(\theta_2(s) + \gamma_2(s))\Delta}} \tag{4.101}$$

The above can be obtained from (4.64) by substituting the initial densities $f_1^o(\lambda)$ and $f_o^o(\lambda)$ for which (4.101) was obtained, i.e.:

$$f_1^o(\lambda) = \delta(\lambda - x_-) \tag{4.102}$$

$$f_o^o(\lambda) = 0 \tag{4.103}$$

This proves the mutual consistency of the two results.

4.3.2 Results in the Time Domain

Steady-State Densities. In this section, the steady-state (if it exists) for system (4.15)-(4.16) is determined by applying the final value theorem [45] to the Laplace transforms in equations (4.43), (4.44), (4.61), (4.62). The following results are obtained:

$$f_{1a}^{ss}(\lambda) = \lim_{s\to 0} s\, f_{1a}^{*}(\lambda,s)$$

$$= \frac{1}{r}\left(\lim_{s\to 0} s\, g_o^{*}(s)\right) e^{-\frac{2r}{\sigma^2}(x_- - \lambda)}\left[1 - e^{\frac{2r\Delta}{\sigma^2}}\right], \qquad (4.104)$$

$$f_{1b}^{ss}(\lambda) = \lim_{s\to 0} s\, f_{1b}^{*}(\lambda,s)$$

$$= \frac{1}{r}\lim_{s\to 0} s\, f_{ob}^{*}(\lambda,s), \qquad (4.105)$$

$$f_{ob}^{ss}(\lambda) = \lim_{s\to 0} s\, f_{ob}^{*}(\lambda,s)$$

$$= \frac{1}{c}\left(\lim_{s\to 0} s\, g_1^{*}(s)\right)\left[1 - e^{-\frac{2c}{\sigma^2}(\lambda - x_-)}\right], \qquad (4.106)$$

$$f_{oc}^{ss}(\lambda) = \frac{1}{c}\left(\lim_{s\to 0} s\, g_1^{*}(s)\right) e^{-\frac{2c}{\sigma^2}(\lambda - x_+)}\left(1 - e^{-\frac{2\Delta c}{\sigma^2}}\right). \qquad (4.107)$$

where in (4.104)-(4.107), a superscript ss stands for steady-state, and:

$$\lim_{s\to 0} s\, g_1^{*}(s) = \lim_{s\to 0} \frac{s}{1 - e^{-(\theta_2(s) + \gamma_2(s))\Delta}}\left[\int_{x_-}^{\infty} f_o^{o}(x)\,dx + \int_{-\infty}^{x_+} f_1^{o}(x)\,dx\right] \qquad (4.108)$$

However:

$$\int_{x_-}^{\infty} f_o^{o}(x)\,dx + \int_{-\infty}^{x_+} f_1^{o}(x)\,dx = 1 \qquad (4.109)$$

and using L'Hôpital's rule:

$$\lim_{s\to 0} \frac{s}{1 - e^{-(\theta_2(s) + \gamma_2(s))}}$$

$$= \lim_{s\to 0} \frac{1}{\Delta e^{-(\theta_2(s) + \gamma_2(s))\Delta} \frac{d}{ds}(\theta_2(s) + \gamma_2(s))} \qquad (4.110)$$

But, recalling (4.35) and (4.61), we have:

$$\frac{d}{ds}(\theta_2(s) + \gamma_2(s)) = \frac{1}{\sigma^2}\left[\frac{2\sigma^2}{\sqrt{r^2 + 2s\sigma^2}} + \frac{2\sigma^2}{\sqrt{c^2 + 2s\sigma^2}}\right] \qquad (4.111)$$

(4.108), (4.110)-(4.111) yield:

$$\lim_{s\to 0} s\, g_1^*(s) = \frac{1}{\frac{\Delta}{r} + \frac{\Delta}{c}} \qquad (4.112)$$

One can similarly show that:

$$\lim_{s\to 0} s\, g_o^*(s) = \frac{1}{\frac{\Delta}{r} + \frac{\Delta}{c}} \qquad (4.113)$$

Substituting (4.112)-(4.113) back into (4.104)-(4.107) yields:

$$f_{1a}^{ss}(\lambda) = \frac{c}{\Delta(r+c)}\left[e^{-\frac{2rx_-}{\sigma^2}} - e^{-\frac{2rx_+}{\sigma^2}}\right] e^{\frac{2r\lambda}{\sigma^2}} \qquad (4.114)$$

$$f_{1b}^{ss}(\lambda) = \frac{c}{\Delta(r+c)}\left[1 - e^{-\frac{2r}{\sigma^2}(x_+ - \lambda)}\right] \qquad (4.115)$$

$$f_{ob}^{ss}(\lambda) = \frac{r}{\Delta(r+c)} \left[1 - e^{-\frac{2c}{\sigma^2}(\lambda - x_-)}\right] \tag{4.116}$$

$$f_{oc}^{ss}(\lambda) = \frac{r}{\Delta(r+c)} \left[e^{\frac{2cx_+}{\sigma^2}} - e^{\frac{2cx_-}{\sigma^2}}\right] e^{-\frac{2c\lambda}{\sigma^2}} \tag{4.117}$$

Finally, $\bar{m}_{ss}$, the steady-state of $\bar{m}(t)$ is given by:

$$\bar{m}_{ss} = \int_{-\infty}^{x_-} f_{1a}^{ss}(\lambda)d\lambda + \int_{x_-}^{x_+} f_{1b}^{ss}(\lambda)d\lambda \tag{4.118}$$

Substituting (4.114)-(4.115) into (4.118) we obtain after simple computations:

$$\bar{m}_{ss} = \frac{c}{r+c} \tag{4.119}$$

Remark 1: The steady-state densities (4.114)-(4.117) are very important because they represent the natural state of the uncontrolled system.

Remark 2: At this point, it is possible to verify whether, at least in a steady-state, the constant rates approximation of section 4.3 is valid or not. One should remember that the approximation rests on the assumption that under normal conditions most of the temperature probability densities lie within the dead band. A quantitative measure of the validity of this assumption is the fraction of the probability density outside the dead band.

For the on density, the fraction is:

$$\frac{\int_{-\infty}^{x_-} f_{1a}^{ss}(\lambda)\,d\lambda}{\int_{-\infty}^{x_+} f_1^{ss}(\lambda)\,d\lambda} = \frac{\frac{\sigma^2 c}{2r(r+c)} \cdot \left[1 - e^{-\frac{2r\Delta}{\sigma^2}}\right]}{\frac{c}{r+c}} = \frac{\bar{\sigma}^2\bar{\tau}}{2}\left[1 - e^{-\frac{2}{\bar{\tau}\bar{\sigma}^2}}\right] \quad (4.120)$$

where $\bar{\sigma} = \frac{\sigma}{\Delta}$, and $\bar{\tau} = \frac{\Delta}{r}$ (average duration of "on" state). For the "off" density the corresponding measure is:

$$\frac{\int_{x_+}^{+\infty} f_{oc}^{ss}(\lambda)\,d\lambda}{\int_{x_-}^{+\infty} f_o^{ss}(\lambda)\,d\lambda} = \frac{\bar{\sigma}^2\bar{\tau}'}{2}\left[1 - e^{-\frac{2}{\bar{\sigma}^2\bar{\tau}'}}\right] \quad (4.121)$$

where $\bar{\tau}' = \frac{\Delta}{c}$ (average duration of "off" state). (4.120)-(4.121) will be used in chapter VI of the thesis where results of a numerical simulation of the CFPE model are reported. In both equations, it appears that "diffusion lengths" $\bar{\sigma}\sqrt{\bar{\tau}}$ and $\bar{\sigma}\sqrt{\bar{\tau}'}$ are the important quantities.

Remark 3: Note the surprising result in (4.119) which indicates that the steady state fraction of devices in the "on" state is independent of the noise variance. On the other hand, the result is intuitive because:

$$\bar{m}_{ss} = \frac{c}{r + c} = \frac{\Delta/\bar{\tau}'}{\Delta/\bar{\tau} + \Delta/\bar{\tau}'} = \frac{\bar{\tau}}{\bar{\tau}' + \bar{\tau}} \tag{4.122}$$

(4.122) essentially states that at steady-state, the fraction of devices in the "on" state is the ratio of average "on" time divided by average cycle duration.

Infinite Series Solution for the Equal Rates Case. Here, the inversion problem of the Laplace transform in (4.96) is considered. From (4.96):

$$\frac{\bar{dm}}{dt} = \int_{x_-}^{+\infty} f_o^o(\lambda) I_o(\lambda,t)\, d\lambda - \int_{-\infty}^{x_+} f_1^o(\lambda) I_1(\lambda,t)\, d\lambda \tag{4.123}$$

where:

$$I_o(\lambda,t) = L^{-1}\left\{\frac{e^{\gamma_2(s)(\lambda - x_-)}\left(1 - e^{\theta_2(s)\Delta}\right)}{(\gamma_2(s) + \theta_2(s))\Delta}\right\} \tag{4.124}$$

$$1 - e$$

$$I_1(\lambda,t) = L^{-1}\left\{\frac{e^{\theta_2(s)(x_+ - \lambda)}\left(1 - e^{\gamma_2(s)\Delta}\right)}{(\gamma_2(s) + \theta_2(s))\Delta}\right\} \tag{4.125}$$

$$1 - e$$

and in (4.124)-(4.125) $L^{-1}\{\cdot\}$ represents the inverse Laplace transform operator. The problem is to determine the functions $I_o(\lambda,t)$ and $I_1(\lambda,t)$, i.e. to find the inverses of the Laplace transforms in the right-hand sides of (4.124)-(4.125). The inversion is first carried out for the special case where the average heat gain rate r and the average heat loss rate c have a common value p. In this case, recalling (4.35) and (4.61):

$$\gamma_2(s) = \theta_2(s) = P(s) \tag{4.126}$$

where p(s) denots the common function of s. Some preliminary lemmas must be established before our main result can be developed.

LEMMA 1:

For Re[s] > 0, the principal determination of $(s+1)^{1/2}$ is such that $\mathrm{Re}[(s+1)^{1/2}] > 1$.

Proof:

Let $s+1 = Re^{j\theta}$ where in general: $0 \leq \theta \leq 2\pi$. In this case, since Re[s] > 0:

$$0 \leq \theta \leq \frac{\pi}{2} \quad \text{or} \quad \frac{3\pi}{2} \leq \theta < 2\pi \tag{4.127}$$

We now work with the function:

$$(s+1)^{1/2} = R^{1/2} e^{j\theta/2} \tag{4.128}$$

The above function is analytic over the range of θ. From (4.126):

$$0 \leq \frac{\theta}{2} < \frac{\pi}{4} \quad \text{or} \quad \frac{3\pi}{4} \leq \frac{\theta}{2} < \pi$$

So:

$$\mathrm{Re}[(s+1)^{1/2}] = R^{1/2} \cos\frac{\theta}{2} > 0 \tag{4.129}$$

Now since Re[s] > 0:

$$\mathrm{Re}[s+1] > 0 \tag{4.130}$$

So:

$$R \cos\theta > 1 \ , \tag{4.131}$$

and:

$$R > 1 \ . \tag{4.132}$$

(4.131)-(4.132) yield:

$$R(1 + \cos\theta) > 2 \ ,$$

or

$$R \cos^2 \frac{\theta}{2} > 1 \ . \tag{4.133}$$

(4.129) and (4.133) yield the required result.

LEMMA 2:

Let $I_o^*(\lambda,s)$ converge in a right-half plane such that $\mathrm{Re}\{s\} > \alpha_o$. Let α_1 be any positive (nonzero) real number. Finally let α be max (α_o,α_1). Then, for $\mathrm{Re}\{s\} > \alpha$ we have the series expansion

$$I_o^*(\lambda,s) = \sum_{i=0}^{\infty} \left[e^{P(s)(\lambda - x_-)} - e^{P(s)(\lambda+\Delta-x_-)}\right] e^{2i\Delta P(s)} \tag{4.134}$$

Proof:

Since $\mathrm{Re}\{s\} > \max(\alpha_o,\alpha_1)$, and α_1 is a strictly positive number, then $\mathrm{Re}\{s\} > 0$. Now:

$$p(s) = -\frac{p + \sqrt{p^2 + 2s\sigma^2}}{\sigma^2} = \frac{1}{\sigma^2}\left(-p + p\sqrt{1 + 2\sigma^2 s}\right) \tag{4.135}$$

(4.139), the fact that $\mathrm{Re}\{s\} > 0$ and Lemma 1 yield:

$$\mathrm{Re}\{P(s)\} < 0$$

This means:

$$|e^{2i\Delta P(s)}| < 0 \text{ for } i > 1 \; . \qquad (4.136)$$

(4.134) follows fromm (4.124) and (4.136) using the identity:

$$\frac{1}{1-x} = 1 + x + x^2 + \ldots \text{ for } |x| < 1 \qquad (4.137)$$

The following theorem on the term by term inversion of a Laplace transform in the form of an infinite series is quoted without proof.

THEOREM 2: [45]

A function $f^*(s)$ may be described as an infinite series of Laplace transforms in $\mathrm{Re}[s] > x_o$, i.e.:

$$f^*(s) = \sum_{i=0}^{\infty} f_i^*(s)$$

For this, all integrals

$$\int_o^{\infty} e^{-st} f_i(t)\,dt = f_i^*(s) \quad (i=0,1,\ldots)$$

must exist in a common half-plane $\mathrm{Re}[s] > x_o$. Two additional stipulations are also required:

(i) The integrals

$$\int_o^{\infty} e^{-st} |f_i(t)|\,dt = \phi_i(s) \quad (i=0,1,\ldots)$$

shall exist in the half plane $Re[s] > x_o$.

(ii) The series $\sum_{i=0}^{\infty} \phi_i(x_o)$ shall converge.

Then $\sum_{i=0}^{\infty} f_i(t)$ converged absolutely to a function $f(t)$ for almost all $t > 0$ and we have the transform pair:

$$\sum_{i=0}^{\infty} f_i(t) \bullet\!\!-\!\!-\!\!-\!\!-\!\!-\!\!\bullet \sum_{i=0}^{\infty} f_i^*(s)$$

CLAIM:

In the equal rates case, $I_o(\lambda,t)$ can be expanded as:

$$I_o(\lambda,t) = \sum_{i=0}^{\infty} g_o(\lambda + 2i\Delta,t) - g_o(\lambda + (2i+1)\Delta,t) \qquad (4.138)$$

where the function $g_o(\lambda,t)$ has already been defined in (4.80).

Proof: Using lemma 2, it is shown that theorem 2 can be applied for the term by term inversion of (4.138). In this case set:

$$f_i^*(s) = e^{P(s)(2i\Delta + \lambda - x_-)} - e^{P(s)(\lambda - x_- + \Delta(2i+1))} \qquad (4.139)$$

Also, recalling (4.80) and (4.90)-(4.92):

$$f_i(t) = g_o(\lambda + 2i\Delta,t) - g_o(\lambda + (2i+1)\Delta,t) \qquad (4.140)$$

Note that we have the transform pair:

$$f_i(t) \bullet\!\!-\!\!-\!\!-\!\!-\!\!-\!\!\bullet f_i^*(s) \quad \text{for } Re[s] > 0 \qquad (4.141)$$

This is because the terms of the right hand side of (4.144) can be interpreted as probability of first passage time random variables and therefore:

$$\int_0^\infty g_o(\lambda + 2i\Delta,t)dt = \int_0^\infty g_o(\lambda + (2i+1)\Delta,t)d\lambda$$

$$\leq 1 < \infty \qquad (4.142)$$

Now set $x_o = \alpha$ where α has been defined in lemma 2. Condition (i) of theorem 2 is satisfied because:

$$\int_0^{+\infty} |e^{-st} f_i(t)|dt \leq \int_0^\infty |f_i(t)|dt \text{ for } Re[s] > \alpha$$

$$\leq \int_0^\infty |g_o(\lambda + 2i\Delta,t)|dt + \int_0^\infty |g_o(\lambda + (2i+1)\Delta,t)|dt$$

$$\leq 2 \qquad (4.143)$$

Finally, condition (11) of theorem 2 is satisfied since:

$$\sum_{i=0}^{\infty} \phi_i(\alpha) = \sum_{n=0}^{\infty} \int_0^\infty e^{-\alpha t}|f_i(t)|dt$$

$$\leq \sum_{n=0}^{\infty} \int_0^\infty e^{-\alpha t}\left[|g_o(\lambda + 2i\Delta,t)| + |g_o(\lambda + (2i+1)\Delta,t)|\right]dt$$

$$< \sum_{i=0}^{\infty} e^{P(\alpha)(\lambda + 2i\Delta - x_-)} + \sum_{i=0}^{\infty} e^{P(\alpha)(\lambda + (2i+1)\Delta - x_-)} \tag{4.144}$$

But α is a positive number. Using lemma 1 and (4.136) we obtain:

$$\sum_{i=0}^{\infty} \phi_i(\alpha) < \frac{e^{P(\alpha)(\lambda - x_-)}\left(1 + e^{P(\alpha)\Delta}\right)}{1 - e^{2P(\alpha)\Delta}}$$

$$< \infty \tag{4.145}$$

Consequently, the term by term inversion of (4.138) can be carried out, and the claim is proved. One could similary show that:

$$I_1(\lambda,t) = \sum_{i=0}^{\infty} \left(g_1(\lambda + 2i\Delta,t) - g_1(\lambda + (2i+1)\Delta,t)\right) \tag{4.146}$$

Remark 1: There is a simple physical reason which makes the equal rates case particularly easy to deal with. Normally, if $r \neq c$, the switching pattern is as follows:

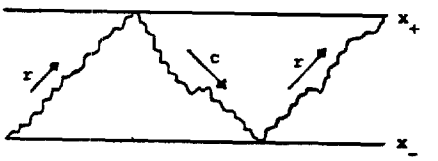

Fig. 4-4. Switching Pattern in the General Case.

If r=c, the process in Fig. 4-4 can be replaced by a continuously upwards process:

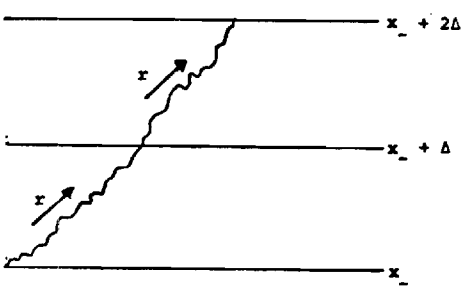

Fig. 4-5. Equivalent Dynamical Pattern for r=c.

The convolutions in (4.10) simplify because the probability density for a cycle duration becomes a first passage time problem with a barrier twice as remote as for the "on" cycle density. For two cycles, it is four times as remote, etc.

Remark 2: Although (4.137) and (4.145) represent a very particular case of the dynamics of (4.14)-(4.15), the traveling wave nature of the CFPE model is clearly exhibited. Once a probability impulse starts traveling, it gives rise to two types of contributions in the form of two infinite series: a positive "forward traveling" contribution and a negative "backward traveling" or "return" contribution.

Remark 3: (4.138) and (4.146) can be written in terms of normalized variables. We have:

$$g_o(\lambda + 2i\Delta, t) = \frac{\lambda + 2i\Delta - x_-}{\sigma(2\pi t^3)^{1/2}} \exp\left[-\frac{(\lambda + 2i\Delta - ct)^2}{2\sigma^2 t}\right]$$

$$= \frac{\bar{\lambda} + 2i - \bar{x}_-}{\bar{\sigma}(2\pi t^3)^{1/2}} \exp\left[-\frac{(\bar{\lambda} - \bar{x}_- - t/\bar{\tau}')^2}{2\bar{\sigma}^2 t}\right] \qquad (4.147)$$

where the $\bar{}$ indicates division by Δ and $\bar{\tau}'$ has been defined in (4.126). Similarly:

$$g_1(\lambda + 2i\Delta, t) = \frac{(\bar{x}_+ - \bar{\lambda})}{\bar{\sigma}(2\pi t^3)^{1/2}} \exp\left[-\frac{(\bar{x}_+ - \bar{\lambda} - t/\bar{\tau})^2}{2\bar{\sigma}^2 t}\right] \qquad (4.148)$$

Remark 4: Theorem 2 guarantees that the summations in (4.138) and (4.146) are absolutely convergent. In chapter six, results of a numerical evaluation of $\overline{m}(t)$ based on equation (4.146) are summarized in the form of a figure (Fig. 4-6). The question of determining the effect of noise variance parameter $\overline{\sigma}$ on the dynamics of $\overline{m}(t)$ is given particular consideration.

Further Approximations for the Distinct Rates Case. Here, some further approximations are proposed in an attempt to generalize the results in (4.138) and (4.146) to the distinct rates case.

Consider the inversion of the Laplace transform in (4.124). Using lemma 1, p. 87, and recalling (4.92)-(4.95) we have the infinite series expansion:

$$I_o^*(\lambda,s) = \sum_{i=0}^{\infty} g_o^*(\lambda + i\Delta,s)g_1^*(x_+ - i\Delta,s) - g_o^*(\lambda + i\Delta,s)g_1^*(x_+ - (i+1)\Delta,s) \qquad (4.149)$$

In the time domain the products in the right-hand side of (4.149) correspond to convolution operations of first-passage time densities. Now recalling remark 1, p. 92, we know that in the equal rates case, the products can be combined together to yield the transform of a new first passage time density. No such result seems to hold for the distinct rates case. However, if the products in (4.153) are approximated in some sense with the transform of some first passage time density, then term by term inversion can be carried out, thus

yielding results analogous to (4.148) and (4.150). This means in effect setting:

$$g_o^*(a,s)g_1^*(b,s) \simeq \frac{1}{\sigma_{ab}^2} \cdot \exp(\mu_{ab} - (\mu_{ab}^2 + 2s\sigma_{ab}^2)^{1/2}) \qquad (4.150)$$

for appropriate μ_{ab} and σ_{ab}. μ_{ab} and σ_{ab} can be obtained by imposing that the mean and variance of the approximating density be exactly equal to the mean and variance of the density resulting from the convolution in the left hand side of (4.150). The approximation becomes perfect in the equal rates case. In this case, elementary calculations (proof 3, Appendix A) show that:

$$I_o(\lambda,t) \simeq \frac{1}{(2\pi t^3)^{1/2}} \cdot \sum_{i=0}^{\infty} \left[\frac{1}{\sigma_o(i,i,\bar{\lambda})} \cdot \exp\left[-\frac{(1-\mu_o(i,i,\bar{\lambda})t)^2}{2\sigma_o^2(i,i,\bar{\lambda})}\right]\right.$$

$$\left. - \frac{1}{\sigma_o(i,i+1,\bar{\lambda})} \exp\left[-\frac{(1-\mu_o(i,i+1,\bar{\lambda})t)^2}{2\sigma_o^2(i,i+1,\bar{\lambda})}\right]\right] \qquad (4.151)$$

where in (4.151):

$$\sigma_o^2(i,j,\bar{\lambda}) = \bar{\sigma}^2 \cdot \frac{\beta^3(\bar{\lambda}+i) + j}{[\beta(\bar{\lambda}+i) + j]^3} \qquad (4.152)$$

for $i,j = 1,2,\ldots.$

$$\mu_o(i,j,\bar{\lambda}) = \frac{1}{\bar{\tau}} \cdot \frac{\beta^3(\bar{\lambda}+i) + j}{\beta(\bar{\lambda}+i) + j} \qquad (4.153)$$

with:

$$\beta = \frac{\bar{\tau}'}{\bar{\tau}}$$

A similar result can be derived for $I_1(\lambda,t)$ with:

$$\sigma_1^2(i,j,\bar{\lambda}) = \bar{\sigma}^2 \cdot \frac{(\bar{\lambda}+i) + \beta^3 j}{((\bar{\lambda}+i) + j\beta)^3} \qquad (4.154)$$

and:

$$\mu_1(i,j,\bar{\lambda}) = \frac{1}{\bar{\tau}} \cdot \frac{1}{(\bar{\lambda}+i) + j\beta} \qquad (4.155)$$

for $i,j = 1,2,\ldots$

Note: Intuitively we expect the approximation to get better and better as $\beta \to 1$. The approximation displays the travelling wave properties previously encountered in (4.138) and (4.146). Due to the absence of a theoretical bound on the error, the only means of evaluating the approximation is numerical. Finally, the expressions for $I_o(\lambda,t)$ and $I_1(\lambda,t)$ can be used to compute analytically the "sensitivity" coefficients in (3.82).

4.3.3 Estimation of Parameters in the Approximate Model

Recalling step c of the general load synthesis methodology (Fig. 2-1, p. 14), it is necessary to define and obtain the minimal amount of data for the estimation of the parameters of the group models in step b. A reasonable solution to this difficult problem is vital for the implementation of the methodology. Also step c can account for an important fraction of the cost of the approach proposed in this thesis. For this reason, one should strive to make the

required measurements as easy as possible, and keep their total number low.

In this section a simple approach is proposed for estimating the significant parameters in the approximate model, i.e. normalized heat gain rate $\bar{r}$, heat loss $\bar{c}$, and noise variance $\bar{\sigma}$ for an individual dwelling. The gathering of such data for a significant sample of houses eventually allows the division of the sector into homogeneous groups as defined in section 3.1. It is only then that the methods of chapter III can be applied. Here, we recall the definition of the parameters of interest:

$$\bar{r} = \frac{1}{\Delta} \cdot [\text{average value of } r_1(\lambda,t)] \tag{4.156}$$

$$\bar{c} = \frac{1}{\Delta} \cdot [\text{average value of } r_o(\lambda,t)] \tag{4.157}$$

$$\bar{\sigma} = \frac{\sigma}{\Delta} \tag{4.158}$$

where in (4.156)-(4.157):

$$r_1(\lambda,t) = R-a(\lambda - x_a(t)) \tag{4.159}$$

$$r_o(\lambda,t) = a(\lambda - x_a(t)) \tag{4.160}$$

Recall that Δ is the width of the thermostat dead band.

$$\bar{r}\Delta = \int_{-\infty}^{x_+} f_1(\lambda,t) r_1(\lambda,t) d\lambda = R-a(E_1(\lambda,t) - x_a(t)) \tag{4.161}$$

$$\bar{c}\Delta = \int_{x_-}^{+\infty} f_o(\lambda,t) r_o(\lambda,t) d\lambda = a(E_o(\lambda,t) - x_a(t)) \qquad (4.162)$$

where $E_1(\lambda,t)$ and $E_o(\lambda,t)$ are expected mean temperatures in the "on" and "off" states respectively at time t. Let $T = [t_1,t_2]$ be the time interval over which the load model is to be used. Throughout chapter IV, the quantities in (4.161)-(4.162) have been considered constant. This means in effect the following:

(i) The noise variance σ and the ambient temperature $x_a(t)$ cannot vary significantly over T.

(ii) The expectations in (4.161)-(4.162) can be considered constant over T.

In order to make (ii) possible, it will be assumed that the system starts in its steady-state and is not significantly removed from it during T. These assumptions are made in addition to the dead band confinement asssumption discussed in section 4.3. Clearly, the totality of the assumptions limits the applicability of the linearized model. However, if (i) and (ii) are verified, an algebraic estimation of $\bar{\sigma}$, $\bar{r}$, $\bar{c}$ is possible from a record of the "on"/"off" cycling of the thermostat during the time interval of interest. To show this, first define the following:

$\underline{\tau}$: sample mean of "on" durations

$\underline{\tau}'$: sample mean of "off" durations

$\underline{\sigma}_\tau^2$: sample variance of "on" durations

$\underline{\sigma}_{\tau'}^2$: sample variance of "off" durations.

As pointed out earlier, the probability densities of the "on" and

"off" durations are first passage time densities given by $g_1(x_-,t)$ and $g_o(x_+,t)$ respectively.

The theoretical means of these passage times are given by $\bar{r}^{-1}$ and $\bar{c}^{-1}$ respectively. The theoretical variances are given by $\frac{\bar{\sigma}^2}{\bar{r}^3}$ and $\frac{\bar{\sigma}^2}{\bar{c}^3}$ respectively.

Therefore, we have the estimates:

$$\hat{\bar{r}} = \frac{1}{\underline{\tau}} \tag{4.163}$$

$$\hat{\bar{c}} = \frac{1}{\underline{\tau}'} \tag{4.164}$$

$$\hat{\bar{\sigma}}^2 = \frac{1}{2}\left(\frac{\sigma_{\underline{\tau}}^2}{\underline{\tau}^3} + \frac{\sigma_{\underline{\tau}'}^2}{\underline{\tau}'^3}\right) \tag{4.165}$$

Clearly, the answers obtained will be a function of weather and time of the day. Thus table of coefficients as a function of weather and time would have to be set up for use under any conditions. Finally, it is believed that this same method can be extended for the estimation of the parameters in the more general (and in fact more widely applicable) space inhomogeneous model of equation 2.1.

4.3.4 Relationship to Previous Work

In [26], Ihara and Schweppe have developed on somewhat more heuristic grounds a very simple model which in essence however, closely resembles the approximate CFPE model in equations (4.14)-(4.15). The model is a traveling wave-type with a forward and backward wave traveling at different speeds (see Fig. 4-6). Although developed independently, the Ihara-Schweppe model can be shown to be

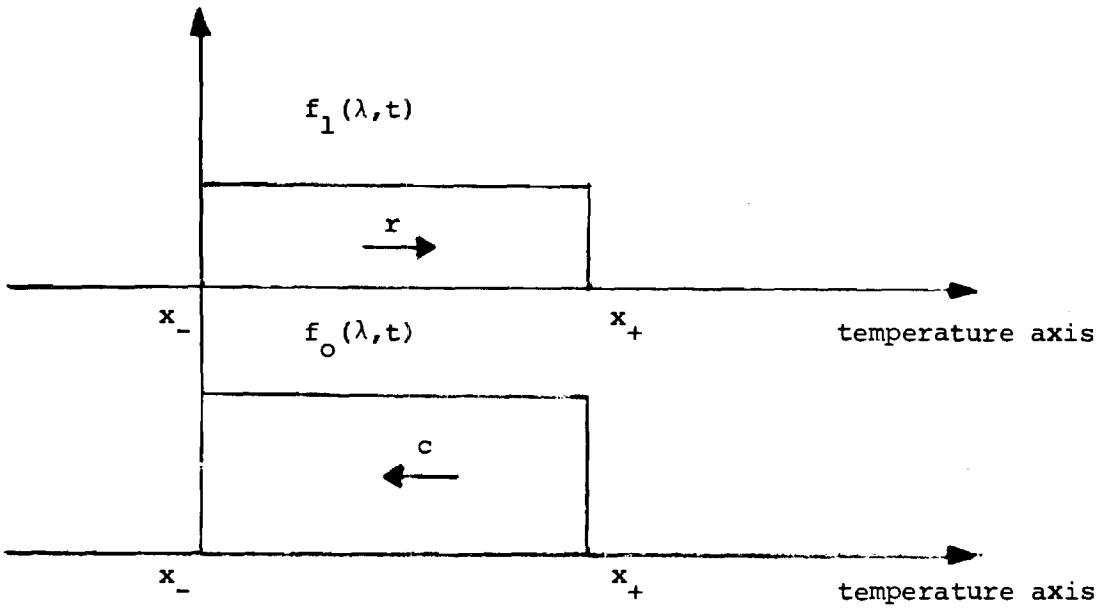

Fig. 4-6. Graphical Representation of the Ihara-Schweppe Model. Arrows indicate the direction of temperature drift.

related to our model. This is because it is a limiting case of the CFPE model under conditions that are now described. Consider equation (4.64) where the transform of $\frac{\overline{dm}}{dt}$ is expressed in terms of $\theta_2(s)$, $\lambda_2(s)$, i.e. r, c and σ. Under the conditions:

$$\sigma << r \ , \tag{4.166}$$

and:

$$\sigma << c \ , \tag{4.167}$$

i.e. when the effect of the noise in (2.1) is practically negligible. We have approximately:

$$\begin{aligned} \theta_2(s) &= \frac{r}{\sigma^2}\left(1 - (1 + \frac{2s\sigma^2}{r^2})^{1/2}\right) \\ &\approx \frac{r}{\sigma^2}\left(1 - (1 + \frac{1}{2} \cdot 2s\frac{\sigma^2}{r^2})\right) \\ &\approx -\frac{s}{r} \ . \end{aligned} \tag{4.168}$$

Similarly, using (4.167) it can be shown that:

$$\gamma_2(s) \approx -\frac{s}{c} \tag{4.169}$$

Equations (4.65), (4.168)-(4.169) yield approximately:

$$\frac{\overline{dm}}{dt}(s) = \int_{x_-}^{+\infty} \frac{1 - e^{-s\bar{\tau}}}{1 - e^{-s(\bar{\tau}+\bar{\tau}')}} \cdot e^{-\frac{s}{c}(x-x_-)} f_o^o(x)dx$$

$$- \int_{-\infty}^{x_+} \frac{1 - e^{-s\bar{\tau}'}}{1 - e^{-s(\bar{\tau}+\bar{\tau}')}} e^{-\frac{s}{r}(x_+ - x)} f_1^o(x)\,dx \qquad (4.170)$$

Now define:

$$T_o^*(x,s) = e^{-\frac{s}{c}(x - x_-)} - e^{-s\left(\frac{x-x_-}{c} + \bar{\tau}\right)}, \qquad (4.171)$$

$$T_1^*(x,s) = e^{-\frac{s}{r}(x_+ - x)} - e^{-s\left(\frac{x_+ - x}{r} + \bar{\tau}'\right)}, \qquad (4.172)$$

Then:

$$T_o(x,t) = \delta\left(t - \frac{(x-x_-)}{c}\right) - \delta\left(t - \bar{\tau} - \left(\frac{x-x_-}{c}\right)\right), \qquad (4.173)$$

$$T_1(x,t) = \delta\left(t - \frac{(x_+ - x)}{r}\right) - \delta\left(t - \bar{\tau}' - \frac{(x_+ - x)}{r}\right), \qquad (4.174)$$

where in (4.173)-(4.174) $\delta(\cdot)$ represents the Dirac delta function. Using theorem 2, it is possible to show that:

$$M_o(x,t) = L^{-1}\left[\frac{T_o^*(x,s)}{1 - e^{-s(\bar{\tau} + \bar{\tau}')}}\right] = \sum_{i=0}^{\infty} T_o[x, t - i(\bar{\tau} + \bar{\tau}')] \qquad (4.175)$$

and

$$M_1(x,t) = L^{-1}\left[\frac{T_1^*(x,s)}{1 - e^{-s(\bar{\tau} + \bar{\tau}')}}\right] = \sum_{i=0}^{\infty} T_1(x, t - i(\bar{\tau} + \bar{\tau}') \qquad (4.176)$$

Substituting (4.175)-(4.176) back into (4.170) yields:

$$\frac{dm^*}{dt}(s) = \int_{x_+}^{+\infty} M_o(x,t) f_o^o(x)\,dx - \int_{-\infty}^{x_+} M_1(x,t) f_1^o(x)\,dx \qquad (4.177)$$

This is essentially the result in [26].

CHAPTER V

NUMERICAL SIMULATION OF THE CFPE MODEL

In chapter IV, a number of analytical results have been developed for an approximate version of the CFPE model (4.14)-(4.15). These results provide great insight into the dynamics of the CFPE model and could allow the study of important questions such as the issue of stability. Unfortunately they do not apply to the more general time-varying case, or for large excursions of the system outside its normal steady state as in the case for a power outage of long duration. Therefore, in general, one has to resort to numerical simulation.

In this chapter, a numerical algorithm for the simulation of (3.36)-(3.43) is developed. The algorithm appears to be a reasonable compromise between ease of programming and computational efficiency for a given accuracy. The purpose of the numerical simulator is to allow a study of the dependence of the dynamics of a homogeneous or general control group on various parameters, as well as to test the "reasonableness" of the CFPE model as a description of aggregate load dynamics. In section 5.1, we describe results concerning some numerical difference methods for the approximation of a particular class of parabolic partial differential equations anayzed in [46]. The class is general enough however, to incorporate the equations of the CFPE model as a particular case. In section 5.2, a so-called "completely implicit difference scheme" for the simulation of the

dynamics of the CFPE model is developed. The computer implementation of this scheme is carried out in chapter VI, where numerical results are reported.

5.1 A Brief Description of Some Difference Methods for the Numerical Solution of a Class of Parabolic Partial Differential Equations

Let $u(x,t)$ be a function of two variables x and t, satisfying a general second order P.D.E. (Partial Differential Equation).

$$A(x,t)u_{xx} + 2B(x,t)u_{xt} + C(x,t)u_{tt} + D(x,t,u,u_x,u_t) = 0 \quad (5.1)$$

where $A(x,t)$, $B(x,t)$, $C(x,t)$ are arbitrary functions. Subscripts indicate partial differential with respect to the corresponding variables. Thus, for example:

$$u_{xt} = \frac{\partial^2 u(x,t)}{\partial x\, \partial t} \quad (5.2)$$

Let the discriminant of (5.1) be defined as:

$$\Delta(x,t) = B^2(x,t) - A(x,t)\, C(x,t) \quad (5.3)$$

Definition [59]: (5.1) is said to be a parabolic P.D.E. if:

$$\Delta(x,t) = 0 \quad (5.4)$$

In general, second order P.D.E.'s of the form (5.1) can also exhibit hyperbolic ($\Delta(x,t) > 0$) or elliptic ($\Delta(x,t) < 0$) behavior.

Clearly, equations (3.32) of the CFPE model are parabolic. In [46], difference methods for the solution of P.D.E.'s of the form:

$$u_t - a(x,t)u_{xx} - 2b(x,t)u_x + c(x,t)u - d(x,t) = 0 \qquad (5.5)$$

are considered. (5.5) incorporates (3.32) as a particular case.

Suppose it is desired to approximate the solution of (5.5) over a semi-infinite rectangular strip R of the form:

$$R:[0 \leq x \leq L;\ t > 0] \qquad (5.6)$$

Difference methods attempt to approximate u(x,t) over the points of a grid:

$$R_{h,k}:[x_j = jh\ ,\ \ j=0,1,\ldots,J+1\ ;\ t_n = nk,\ n=0,1,\ldots] \qquad (5.7)$$

where $h = L/(J+1)$. At each point (x_j,t_n) of the net, a quantity $v(x_j,t_n)$ is sought to approximate the solution $u(x_j,t_n)$ of (5.5). (5.5) is replaced by a difference equation which is obtained using a specific difference approximation formula for the derivatives involved.

The following notation is used [46]:

$$v(x_j,t_n) \equiv v_j^n \ , \quad u(x_j,t_n) \equiv u_j^n \tag{5.8}$$

for all quantities or functions defined at the points of $R_{h,k}$. In addition, the following interpolation formula is used to define the quantity at intermediate values of t:

$$v(x_j,t_n + \alpha_k) \equiv v_j^{n+\alpha} \equiv \alpha v_j^{n+1} + (1-\alpha)v_j^n \tag{5.9}$$

for some fixed α: $0 \leq \alpha \leq 1$. Finally, partial derivatives are approximated as follows:

$$\begin{aligned} u_x(x_j,t_n + \alpha_k) &\approx \frac{1}{2h}\left(v_{j+1}^{n+\alpha} - v_{j-1}^{n+\alpha}\right) , \\ u_{xx}(x_j,t_n + \alpha_k) &\approx \frac{1}{h^2}\left(v_{j+1}^{n+\alpha} - 2v_j^{n+\alpha} + v_{j-1}^{n+\alpha}\right) , \\ u_t(x_j,t_n + \alpha_k) &\approx \frac{1}{k}\left(v_j^{n+1} - v_j^n\right) . \end{aligned} \tag{5.10}$$

Setting $x=x_j$ and $t=t_n + \alpha_k$ in (5.1) and using (5.10) yields [46]:

$$\begin{aligned} &v_j^{n+1} - v_j^n - \rho a_j^{n+\alpha}\left(v_{j+1}^{n+\alpha} - 2v_j^{n+\alpha} + v_{j-1}^{n+\alpha}\right) \\ &\quad - \rho a_j^{n+\alpha}\left(v_{j+1}^{n+\alpha} - 2v_j^{n+\alpha} + v_{j-1}^{n+\alpha}\right) \\ &\quad - h\rho b_j^{n+\alpha}\left(v_{j+1}^{n+\alpha} - v_{j-1}^{n+\alpha}\right) + kc_j^{n+\alpha} v_j^{n+\alpha} = kd_j^{n+\alpha} \end{aligned} \tag{5.11}$$

Where in (5.11), the mesh ratio $\rho = k/h^2$, and $j=1,\ldots,J+1$. Substituting (5.9) into (5.11) together with initial condition and boundary values information yields a system of linear equations of the form:

$$\alpha_{ij} v_j^{n+1} + \alpha_{2j} v_j^{n+1} + \alpha_{3j} v_{n+1}^{n+1} = s_j^n \qquad (5.12)$$

for $j=1,\ldots,J+1$, which can be solved recursively. The solution requires no calculations if $\alpha=0$, thus yielding the so-called explicit scheme. For $\alpha \neq 0$, the scheme is called implicit and some labor is involved in solving the equations. Finally for $\alpha=1$, the scheme is called completely implicit.

Two performance criteria can be used to compare the various schemes:

Accuracy: i.e., what is the least upper bound to the error in terms of step sizes in the simulation?

Computational Complexity: i.e., what is the total number of operations involved in the algorithm?

However, no scheme is useful unless it is stable, i.e. the error should not build up from one computation to the next. The following results are proved in [46]:

- The explicit scheme is stable for:

$$k \leq \frac{h^2}{2a(x,t) + h^2(x,t)} \qquad (5.13)$$

Thus a fine spatial net requires a "finer" time net and the number of steps to reach at time t is of the order of

t/h^2. Finally the error at each step is of the order of h^2.

- The completely implicit difference scheme imposes no restriction on ρ but requires somewhat more labor to solve the equations. The total computations required to reach a time t can be made considerably less than in the explicit case by choosing k sufficiently large. The error bound, however, is now of the form

$$|\text{error}| \leq O(h^2) + O(k) \tag{5.14}$$

and thus, in the interest of accuracy k must not be too large.

- The Crank-Nicholson ($\alpha = \frac{1}{2}$) difference scheme is stable for:

$$k \leq \frac{2h^2}{2a(x,t) + h^2 c(x,t)} \tag{5.15}$$

The net spacings are related as in the explicit difference scheme but the time step can be twice as large. Since the solutions of the implicit equations do not require twice the amount of computations used to solve the explicit equations, a saving may be made in the total work required to reach a time t. In addition, the error bound is now of the order

$$|\text{error}| \leq O(h^2) + O(k^2) \tag{5.16}$$

which is an improvement over the completely implicit scheme. In the light of the above remarks, a completely implicit difference scheme was preferred.

5.2 An Implicit Difference Scheme for the Numerical Simulation of the CFPE Model

Reformulation of the CFPE Model in Terms of the Probability Distributions

The CFPE model is repeated here for convenience.

Dynamics

$$\frac{\partial f_1}{\partial t}(\lambda,t) = \frac{\partial}{\partial \lambda}\left[r_1(\lambda,t) f_1(\lambda,t)\right] + \frac{\sigma^2}{2}\left[\frac{\partial^2}{\partial \lambda^2} f_1(\lambda,t)\right] \tag{5.17}$$

$$\frac{\partial f_o}{\partial t}(\lambda,t) = \frac{\partial}{\partial \lambda}\left[r_o(\lambda,t) f_o(\lambda,t)\right] + \frac{\sigma^2}{2}\left[\frac{\partial^2}{\partial \lambda^2} f_o(\lambda,t)\right] \tag{5.18}$$

Boundary Conditions

$$f_1(x_+,t) = f_o(x_-,t) = 0 \tag{5.19}$$

$$f_1(-\infty,t) = f_o(+\infty,t) = 0 \tag{5.20}$$

$$f_{1a}(x_-,t) = f_{1b}(x_-,t) \tag{5.21}$$

$$f_{ob}(x_+,t) = f_{oc}(x_+,t) \tag{5.22}$$

$$\frac{\partial f_{1b}}{\partial \lambda}(x_-,t) - \frac{\partial f_{1a}}{\partial \lambda}(x_-,t) = -\frac{\partial f_o}{\partial \lambda}(x_-,t) \tag{5.23}$$

$$\frac{\partial f_{oc}}{\partial \lambda}(x_+,t) - \frac{\partial f_{ob}}{\partial \lambda}(x_+,t) = \frac{\partial f_1}{\partial \lambda}(x_+,t) \tag{5.24}$$

Since distribution functions are generally smoother than density functions, the above dynamics are rewritten in terms of the following functions:

$$F_1(x,t) = \int_{-\infty}^{x} f_1(\lambda,t)\,d\lambda \tag{5.25}$$

$$F_o(x,t) = \int_{+\infty}^{x} f_o(\lambda,t)\,d\lambda \tag{5.26}$$

For $x < x_-$, integration of (5.17) with respect to λ from $-\infty$ to x yields:

$$\frac{\partial F_1}{\partial t}(x,t) = r_1(x,t)f_1(x,t) - \lim_{\lambda \to -\infty} r_1(\lambda,t)f_1(\lambda,t)$$

$$+ \frac{\sigma^2}{2}\left(\frac{\partial f_1}{\partial x}(x,t) - \lim_{\lambda \to -\infty} \frac{\partial f_1}{\partial \lambda}(\lambda,t)\right) \tag{5.27}$$

Assuming the limits in (5.27) are zero, we have:

$$F_{1t}(x,t) = r_1(x,t)F_{1x}(x,t) + \frac{\sigma^2}{2} F_{1xx}(x,t) \tag{5.28}$$

For $x_- < x < x_+$, integration of (5.17) with respect to λ from x_- to x yields:

$$\frac{\partial F_1}{\partial t}(x,t) - \frac{\partial F_1}{\partial t}(x_-,t) = r_1(x,t)f_1(x,t) - r_1(x_-,t)f_1(x_-,t)$$

$$+ \frac{\sigma^2}{2}\left[\frac{\partial f_1}{\partial x}(x,t) - \frac{\partial f_{1b}}{\partial x}(x_-,t)\right] \qquad (5.29)$$

However at x_- (5.28) yields:

$$\frac{\partial F_1}{\partial t}(x_-,t) = r_1(x_-,t)f_1(x_-,t) + \frac{\sigma^2}{2}\frac{\partial f_{1a}}{\partial t}(x_-,t) \qquad (5.30)$$

Substituting (5.30) into (5.29) and recalling (5.23) yields:

$$F_{1t}(x,t) = r_1(x,t)F_{1x}(x,t) + \frac{\sigma^2}{2}F_{1xx}(x,t) + \frac{\sigma^2}{2}F_{oxx}(x_-,t) \qquad (5.31)$$

Equations (5.28) and (5.31) represent the "on" part of the dynamics of the CFPE model in regions a and b of Fig 3-2 respectively, in terms of $F_1(x,t)$.

Using a similar procedure, it can be shown that for $x > x_+$:

$$F_{ot}(x,t) = r_o(x,t)F_{ox}(x,t) + \frac{\sigma^2}{2}F_{oxx}(x,t) \qquad (5.32)$$

and for $x_- < x < x_+$.

$$F_{ot}(x,t) = r_o(x,t)F_{ox}(x,t) + \frac{\sigma^2}{2}F_{oxx}(x,t) + \frac{\sigma^2}{2}F_{1xx}(x_+,t) \qquad (5.33)$$

Approximating the CFPE Model

The following notation is used:

k: time step ,

h: temperature step ,

$$F^n_{1i} = F_1(x_1 + (i-1), nk) \ ,$$

$$F^n_{oi} = F_o(x_- + (i-1)h, nk) \ . \qquad (5.34)$$

Note, that in the above, since it is not possible to let x go to $+\infty$ or $-\infty$ in the simulation, artificial boundaries must be introduced to limit the size of x. These boundaries however, should be placed "far enough" so as not to introduce any significant error in the problem. We chose to use reflecting boundaries. It was assumed that x_1 and x_o are the minimum and maximum temperatures respectivly where a device can be found with any significant probability.

Dynamics

For an implicit scheme we have:

$$F^{n+1}_{jxi} = \frac{1}{2n}\left[F^{n+1}_{j(i+1)} - F^{n+1}_{j(i-1)}\right] \ , \qquad (5.35)$$

$$F^{n+1}_{jxxi} = \frac{1}{h^2}\left[F^{n+1}_{j(i+1)} - 2F^{n+1}_{ji} + F^{n+1}_{j(i-1)}\right] \ , \qquad (5.36)$$

$$F^{n+1}_{jti} = \frac{1}{k}\left[F^{n+1}_{ji} - F^{n}_{ji}\right] \ , \qquad (5.37)$$

for j=0,1. Using (5.35)-(5.37), (5.28) and (5.32) can be approximated by

$$F^{n+1}_{j(i-1)}\left[\frac{r^{n+1}_{jik}}{2h} - \mu\right] + F^{n+1}_{ji}[2\mu + 1]$$

$$+ F^{n+1}_{j(i+1)}\left[-\mu - \frac{r^{n+1}_{jik}}{2h}\right] = F^{n}_{ji} \qquad (5.38)$$

For j=0,1, i to be specified later, $n > 0$ and:

$$\mu = \frac{\sigma^2 k}{2h^2} \qquad (5.39)$$

Furthermore, $F_{1xx}(x_+,t)$ can be approximated using:

$$F_1(x_+-h,t) \approx F_1(x_+,t) + F_{1x}(x_+,t)h + \frac{1}{2} F_{1xx}(x_+,t)h^2 \qquad (5.40)$$

(5.40) and (5.19) yield:

$$F_{1xx}(x_+,t) = \frac{2}{h^2} S_1(t) \ , \qquad (5.41)$$

where

$$S_1(t) \equiv F_1(x_+-h,t) - F_1(x_+,t) \ . \qquad (5.42)$$

Similarly, one can write:

$$F_o(x_-+h,t) \approx F_o(x_-,t) + F_{ox}(x_-,t)h + \frac{1}{2} F_{oxx}(x_-,t)h^2 \qquad (5.43)$$

(5.43) and (5.19) yields:

$$F_{oxx}(x_-,t) = \frac{2}{h^2} S_o(t) \tag{5.44}$$

where:

$$S_o(t) \equiv F_o(x_-+h,t) - F_o(x_-,t) \tag{5.45}$$

Substituting (5.42) and (5.45) into equations (5.31) and (5.33) respectively yields:

$$F_{jt}(x,t) - \frac{\sigma^2}{h^2} S_j(t) = F_j(x,t)F_{jx}(x,t) + \frac{\sigma^2}{2} F_{jxx}(x,t) \tag{5.46}$$

for j=0,1. Using (5.35)-(5.37), (5.46) is approximated as

$$F^{n+1}_{j(i-1)}\left[-\mu + \frac{r^{n+1}_{ji}k}{2h}\right] + F^{n+1}_{ji}[1 + 2\mu] + F^{n+1}_{j(i+1)}\left[-\mu - \frac{r^{n+1}_{ji}k}{2h}\right]$$

$$= F^{n}_{ji} + 2\mu\, S^{n+1}_{j} \tag{5.47}$$

for j=0,1, i to be specified later and $n \geq 0$.

Boundary Conditions

It remains to approximate boundary conditions (5.19)-(5.22), as well as the artificial reflecting boundaries introduced at $x=x_1$ for the "on" density and at $x=x_o$ for the "off" density.

A. Reflecting Boundaries

a. $$F^{n}_{11} = 0 \quad \forall n \geq 0 \tag{5.48}$$

b. $$F^{n}_{oJ_o} = 0 \quad \forall n \geq 0 \tag{5.49}$$

B. Absorbing Boundaries

a. At x_+, we have from(5.31):

$$F_{1t}(x_+,t) = r_1(x_+,t)F_{1x}(x,t) + \frac{\sigma^2}{2} F_{1xx}(x_+,t) + \frac{\sigma^2}{2} F_{oxx}(x_-,t) \quad (5.50)$$

Using (5.19), (5.35)-(5.37) and recalling (5.44), we obtain:

$$(-2\mu)F^{n+1}_{1(J_1-1)} + (1 + 2\mu) F^{n+1}_{iJ_1} = F^{n}_{1J_1} + 2\mu S^{n+1}_{o} \quad (5.51)$$

where $x_+ = x_1 + (J_1 - 1)h$.

b. At x_-, we have from (5.33)

$$F_{ot}(x_-,t) = r_o(x_-,t)F_{ox}(x_-,t) + \frac{\sigma^2}{2} F_{oxx}(x_-,t) + \frac{\sigma^2}{2} F_{1xx}(x_-,t) \quad (5.52)$$

Using (5.19), (5.35)-(5.37) and recalling (5.41), we obtain:

$$(1 + 2\mu)F^{n+1}_{01} - 2\mu F^{n+1}_{02} = F^{n}_{01} + 2\mu S^{n+1}_{1} \quad (5.53)$$

C. Probability Conservation

a. At x_- we have:

$$F_1(x_- - h,t) = F_1(x_-,t) - F_{1x}(x_-,t)h + \frac{1}{2} F_{1xxa}(x_-,t)h^2 \quad (5.54)$$

and:

$$F_1(x_- + h,t) = F_1(x_-,t) + F_{1x}(x_-,t)h + \frac{1}{2} F_{1xxb}(x_-,t)h^2 \quad (5.55)$$

Adding (5.54) and (5.55) we obtain:

$$F_1(x_-h,t) + F_1(x_+h,t) = 2F_1(x_,t) + \frac{1}{2} F_{1xxa}(x_,t)h^2 + \frac{1}{2} F_{1xxb}(x_,t)h^2 \quad (5.56)$$

(5.23), (5.44) and (5.56) yield:

$$F_{1xxa}(x_,t) = \left[F_1(x_-h,t) - 2F_1(x_,t) + F_1(x_+h,t) + S_o(t)\right] \frac{1}{h^2} \quad (5.57)$$

Furthermore, subtracting (5.54) from (5.55) yields:

$$F_1(x_+h,t) - F_1(x_-h,t) = 2hF_{1x}(x_,t) + \frac{h^2}{2}\left[F_{1xxb}(x_,t) - F_{1xxa}(x_,t)\right] \quad (5.58)$$

(5.58) and (5.44) yield:

$$F_{1x}(x_,t) = \left[F_1(x_+h,t) - F_1(x_-h,t) + S_o(t)\right] \cdot \frac{1}{2h} \quad (5.59)$$

At $x=x_$, (5.28) yields:

$$F_{1t}(x_,t) = r_1(x_,t)F_{1x}(x_,t) + \frac{\sigma^2}{2} F_{1xxa}(x_,t) \quad (5.60)$$

From (5.57), (5.59) and (5.60) and recalling (5.35)-(5.37) we have:

$$F^{n+1}_{1(L_1-1)}\left[-\mu + \frac{r^{n+1}_{1L_1}k}{2h}\right] + F^{n+1}_{1L_1}\left[1 + 2\mu\right] + F^{n+1}_{1(L_1+1)}\left[-\mu - \frac{r^{n+1}_{1L_1}k}{2h}\right]$$

$$= F^{n}_{1L_1} + S^{n+1}_{o}\left[\mu + \frac{r^{n+1}_{1L_1}k}{2h}\right] \qquad (5.61)$$

where

$$x_- = x_1 + (L_1 - 1)h \ .$$

b. At x_+, a similar derivation yields:

$$F^{n+1}_{0(L_o-1)}\left[-\mu + \frac{r^{n+1}_{0L_o}k}{2h}\right] + F^{n+1}_{0L_o}\left[1 + 2\mu\right] + F^{n+1}_{0(L_o+1)}\left[-\mu - \frac{r^{n+1}_{0L_o}k}{2h}\right]$$

$$= F^{n}_{0L_o} - \left(\frac{r^{n+1}_{0L_o}k}{2h} - \lambda\right)S^{n+1}_{1} \qquad (5.62)$$

where:

$$x_+ = x_- + (L_o - 1)h \ .$$

D. Summary of the Equations

Combining (5.38), (5.47)-(5.49), (5.51), (5.53), (5.61)-(5.62) we obtain:

$$\underline{A}_1\underline{F}^{n+1}_1 = \underline{D}^{n+1}_1 \qquad \forall n \geq 0 \qquad (5.63)$$

and

$$\underline{A}_o\underline{F}^{n+1}_o = \underline{D}^{n+1}_o \qquad \forall n \geq 0 \qquad (5.64)$$

where in (5.63)-(5.64):

$$\underline{A}_1 = \begin{vmatrix} b_1(2) & c_1(2) & 0 & & \cdots & 0 \\ a_1(3) & b_1(c) & c_1(3) & 0 & \cdots & 0 \\ 0 & a_1(4) & b_1(4) & c_1(4) \; 0 & \cdots & 0 \\ \vdots & 0 & \ddots & \ddots & \ddots & \vdots \\ \vdots & \vdots & \ddots & \ddots & \ddots & \vdots \\ \vdots & 0 & \ddots & \ddots & \ddots & c_1(J_1-1) \\ 0 & 0 & 0 & 0 \; a_1(J_1) & & b_1(J_1) \end{vmatrix}$$

$$\underline{F}_1^{n+1} = \begin{vmatrix} F_{12}^{n+1} \\ F_{13}^{n+1} \\ \vdots \\ F_{1J_1}^{n+1} \end{vmatrix}$$

$$\underline{P}_1^{n} = \begin{vmatrix} d_1^n(2) \\ d_1^n(3) \\ \vdots \\ d_1^n(J_1) \end{vmatrix} \qquad (5.65)$$

$$\underline{A}_0 = \begin{vmatrix} b_o(1) & c_o(1) & 0 & & \cdots & 0 \\ a_o(2) & b_o(2) & c_o(2) & 0 & \cdots & 0 \\ 0 & a_o(3) & b_o(3) & c_o(3) \; 0 & \cdots & 0 \\ 0 & 0 & \ddots & \ddots & \ddots & \\ \vdots & \vdots & \ddots & \ddots & \ddots & \\ \vdots & \vdots & \ddots & \ddots & \ddots & 0 \\ 0 & 0 & \ddots & \ddots & \ddots & c_o(J_o-2) \\ 0 & 0 & 0 & 0 \; a_1(J_1) & & b_o(J_o-1) \end{vmatrix}$$

$$\underline{F}_o^{n+1} = \begin{vmatrix} F_{01}^{n+1} \\ F_{02}^{n+1} \\ \vdots \\ F_{o(J_o-1)}^{n+1} \end{vmatrix} \tag{5.66}$$

and

$$a_1(i) = -\mu + \frac{r_{1i}^{n+1}{}^k}{2h} \quad \text{for } i = 2,\ldots,J_1-1$$

$$a_1(J_1) = 2\mu$$

$$b_1(i) = -\mu + \frac{r_{1i}^{n+1}{}^k}{2h} \quad \text{for } i = 2,\ldots,J_1-1$$

$$b_1(J_1) = 1 + 2\mu$$

$$c_1(i) = -\mu - \frac{r_{1i}^{n+1}{}^k}{2h} \quad \text{for } i = 2,\ldots,J_1-1 \tag{5.67}$$

$$d_1^n(i) = F_{1i}^n \ , \quad \text{for } i = 2,\ldots,L_1-1$$

$$d_1^n(L_1) = F_{1L_1}^r + S_o^{n+1}\left(\mu + \frac{r_{1L_1}^{n+1}{}^k}{2h}\right)$$

$$d_1^n(i) = F_{1i}^n + 2\mu\, S_o^{n+1} \ , \quad \text{for } i = L_1+1,\ldots,J_1 \tag{5.68}$$

$$a_o(i) = -\mu + \frac{r_{oi}^{n+1}{}^k}{2h} \ , \quad \text{for } i = 2,\ldots,J_o-1$$

$$b_o(i) = 1 + 2\mu \ , \quad \text{for } i = 1,\ldots,J_o-1$$

$$c_o(1) = -2\mu$$

$$c_o(i) = -\mu - \frac{r_{oi}^{n+1}\,k}{2h}, \quad \text{for } i = 2,\ldots,J_o-1 \tag{5.69}$$

$$d_o^n(i) = F_{oi}^n + 2\mu\, S_1^{n+1}, \quad \text{for } i = 1,\ldots,L_o-1$$

$$d_o^n(L_o) = F_{oL_o}^n - \left(\frac{r_{oL_o}^{n+1}\,k}{2h} - \mu\right) S_1^{n+1}$$

$$d_o^n(i) = F_{oi}^n, \quad \text{for } i = L_o+1,\ldots,J_o-1 \tag{5.70}$$

Also:

$$S_1^{n+1} = F_{1(J_1-1)}^{n+1} - F_{1J_1}^{n+1}, \tag{5.71}$$

$$S_o^{n+1} = F_2^{n+1} - F_1^{n+1}. \tag{5.72}$$

Note that all the entries in $\underline{D}_1$ and $\underline{D}_o$ are known at time n except for S_1^{n+1} and S_o^{n+1}. We shall set:

$$S_1^{n+1} \approx S_1^n, \tag{5.73}$$

and

$$S_o^{n+1} \approx S_o^n. \tag{5.74}$$

This yields two decoupled tridiagonal systems (5.65)-(5.66) which can be solved separately at each time step. The algorithm (5.63)-(5.64),

(5.73)-(5.74) was implemented on the Georgia Tech Cyber. Numerical results are reported in chapter VI.

CHAPTER VI

SIMULATION RESULTS

In this chapter, results of a numerical study of the dynamic properties of homogeneous, nonhomogeneous and completely general control groups are reported. The results are summarized in a series of figures on pp. 128-133. These figures represent the expected dynamics of fractional (or per unit) power demand in a group of devices following a temporary interruption of power supply (cold load pickup). All simulations are based on the discretized version of the CFPE model in equations (5.63)-(5.64). In selecting the data for the runs, effort was made to retain possible "on"/"off" switching time constants ($\bar{\tau}$ and $\bar{\tau}'$). However, the data is entirely fictitious and was mainly designed for the purpose of illustrating the dynamics of the CFPE model. Three groups of figures can be distinguished corresponding to properties of homogeneous, nonhomogeneous and general control groups respectively. Data for each of the runs are given below. Finally, in Fig. 6-6, we report results of a numerical study of the properties of the infinite series in (4.146).

6.1 Simulation of Homogeneous Control Groups

The sensitivity of the post outage dynamics of an homogeneous control group to changes in noise variance, average heating rate, and outage duration was studied by starting from base case values and observing the effect of a change in one parameter at a time.

In the notation of equation (2.1), base case data was as follows:

$$\Delta = 1.1 \text{ deg C} ,$$

$$\frac{x_a(t)}{\Delta} = 15 ,$$

$$\frac{a}{\Delta} = .01774 \text{ (deg C mn)}^{-1} ,$$

$$\frac{R}{\Delta} = .4 \text{ (mn)}^{-1} ,$$

$$\bar{\sigma} = .3 \text{ (mn)}^{-1/2} . \qquad (6.1)$$

The data in (6.1) yields approximately:

$$\bar{\tau} \approx \bar{\tau}' \approx 5 \text{ mn} , \qquad (6.2)$$

i.e. the average duration of the "on" time is approximately equal to that of the "off" time and they are both in the neighborhood of five minutes.

Figures 6-1 and 6-2 demonstrate the effect of a change in noise variance for four different values of outage duration. Figures 6-3 and 6-4 demonstrate the effect of changes in the average heating rate and outage duration respectively.

6.2 Simulation of Nonhomogeneous Control Groups

Here, the effect of some parameter variance within the control group was assessed by simulating (5.63)-(5.64) for the mean data as well as two "neighboring" sets of data, and using this information to evaluate the sensitivity coefficients in (3.84) numerically. Subsequently (3.64) was used to generate post-outage dynamics in the nonhomogenenous control group for various levels of parameter variance. Only the effect of one parameter, namely thermostat set point x_-, was considered. The average data was identical to (6.1) except for $\bar{\sigma} = .2\ (\text{mn})^{-1/2}$. The results are summarized in Figure 6-5.

6.3 Simulation of General Control Groups

In this set of runs, the dynamics of a general control group were simulated by assuming that, at the outset, it has been broken up into its constitutive homogeneous control groups and, subsequently obtaining aggregate dynamics by superposition of the individual dynamics for each homogeneous subgroup.

The general control group that was studied was assumed to be made up of sixteen homogeneous groups. Data for the homogeneous groups was as follows:

$$\Delta = 1.1 \text{ deg C} ,$$

$$\frac{x_a(t)}{\Delta} = 15 , \quad \frac{x_-}{\Delta} = 35 ,$$

$$\frac{a}{\Delta} = .01774\ (\text{deg C mn})^{-1} ,$$

$$\bar{\sigma} = \sigma_j \, (mn)^{-1/2} \, . \tag{6.3}$$

for i = 1,...,4, and j = 1,...,4, where in (6.3):

$$\underline{R} \equiv [r_i] = \begin{vmatrix} .35 \\ .4 \\ .5 \\ .6 \end{vmatrix} \, , \quad \text{and} \quad \underline{V} \equiv [\sigma_j] = \begin{vmatrix} .1 \\ .3 \\ .5 \\ .8 \end{vmatrix} \tag{6.4}$$

The nominal size of the heating element was assumed to be identical for all devices. Several parameter distributions were studied. Each parameter distribution was characterized by a set of weights, w_{ij}, such that:

$$\Pr\left[\left(\frac{R}{\Delta} = r_i\right) \cap \left(\bar{\sigma} = \sigma_j\right)\right] = w_{ij} \tag{6.5}$$

for i = 1,...,4, and j = 1,...,4, where in (6.5):

$\underline{W} = [w_{ij}]$ is a given 4 x 4 matrix of weights.

The following values of $\underline{W}$ were used:

$$\underline{W}_1 = \frac{1}{16} \begin{vmatrix} 1 & 1 & 1 & 1 \\ 1 & 1 & 1 & 1 \\ 1 & 1 & 1 & 1 \\ 1 & 1 & 1 & 1 \end{vmatrix} \tag{6.6}$$

$$\underline{W}_2 = \frac{1}{64} \begin{vmatrix} 1 & 3 & 3 & 1 \\ 3 & 9 & 9 & 3 \\ 3 & 9 & 9 & 3 \\ 1 & 3 & 3 & 1 \end{vmatrix} \tag{6.7}$$

$$\underline{W}_3 = \frac{1}{64}\begin{vmatrix} 9 & 3 & 3 & 1 \\ 9 & 3 & 3 & 1 \\ 9 & 3 & 3 & 1 \\ 9 & 3 & 3 & 1 \end{vmatrix} \tag{6.8}$$

Finally, global dynamics were obtained using:

$$\bar{m}(t) = \sum_{i=1}^{4} \sum_{j=1}^{4} w_{ij}\, \bar{m}_{ij}(t) \tag{6.9}$$

where in (6.9) $\bar{m}_{ij}(t)$ denotes the aggregate functional state with parameters r_i and σ_j. The results are summarized in Figure 6-6.

6.4 Numerical Evaluation of Theoretical Impulse Response

Here the dynamics of the aggregate function state $\bar{m}(t)$ were evaluated for an initial distribution $f_1^o(\lambda) = \delta(\lambda - x_-)$, by numerical integration of the following theoretical expression:

$$\frac{d\bar{m}}{dt} = I_1(x_-,t) \approx \sum_{i=0}^{10} [g_1(x_- + 2i\Delta,t) - g_1(x_- + 2(i+1)\Delta,t)] \tag{6.10}$$

The above equation is based on (4.146).

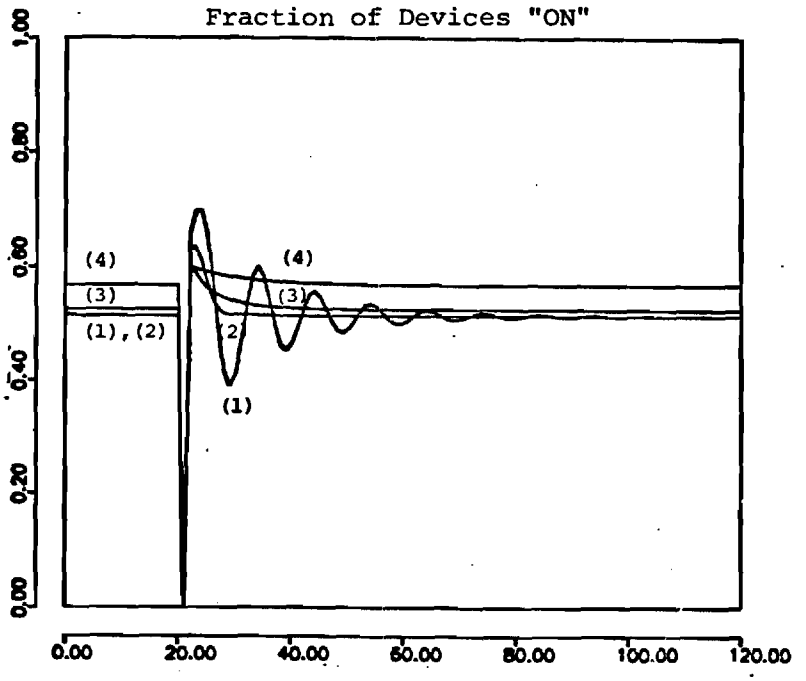

(a)

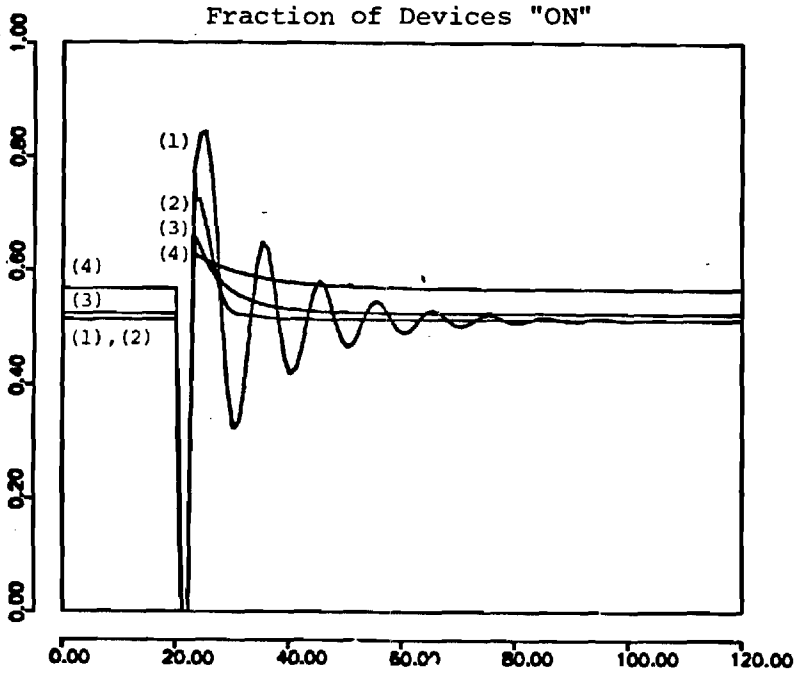

(b)

Fig. 6-1. Dependence of Cold Load Pickup Dynamics on Normalized Noise Variance Parameters $\bar{\sigma}$. Outage Durations: (a) 1 mn, (b) 2mns. Values of $\bar{\sigma}$ in $(mn)^{-1/2}$ are: (1) $\bar{\sigma}$ = .1, (2) $\bar{\sigma}$ = .3, (3) $\bar{\sigma}$ = .5, (4) $\bar{\sigma}$ = 1.0. All other parameters are as in base case. The horizontal axis corresponds to time in minutes.

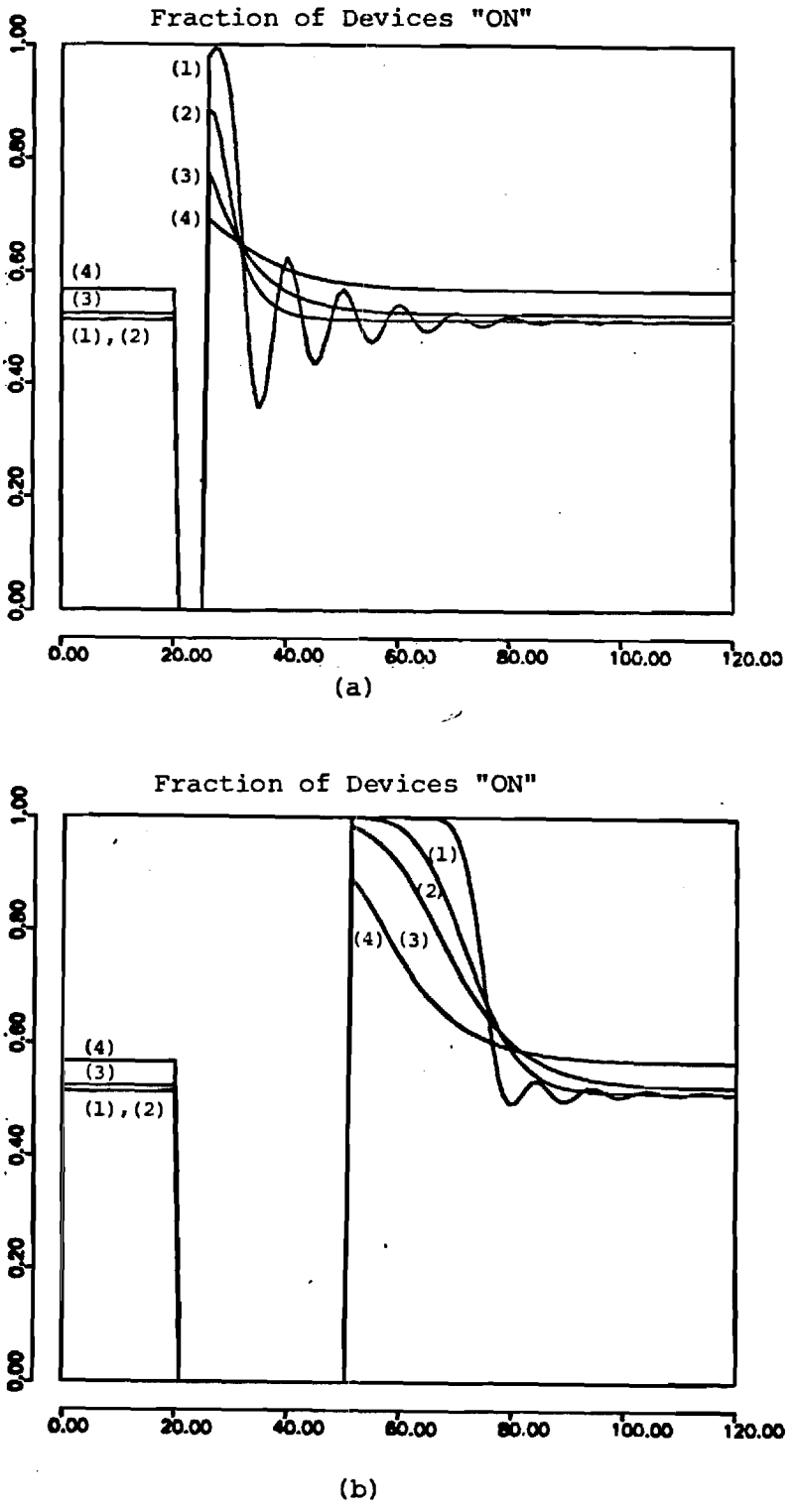

Fig. 6-2. Dependence of Cold Load Pickup Dynamics on Normalized Noise Variance Parameter $\bar{\sigma}$. Outage Durations are: (a) 5mns, (b) 30 mns. Values of $\bar{\sigma}$ in $(mn)^{-1/2}$ are: (1) $\bar{\sigma}$ = .1, (2) $\bar{\sigma}$ = .3, (3) $\bar{\sigma}$ = .5, (4) $\bar{\sigma}$ = 1.0. All other parameters are as in base case. The horizontal axis corresponds to time in minutes.

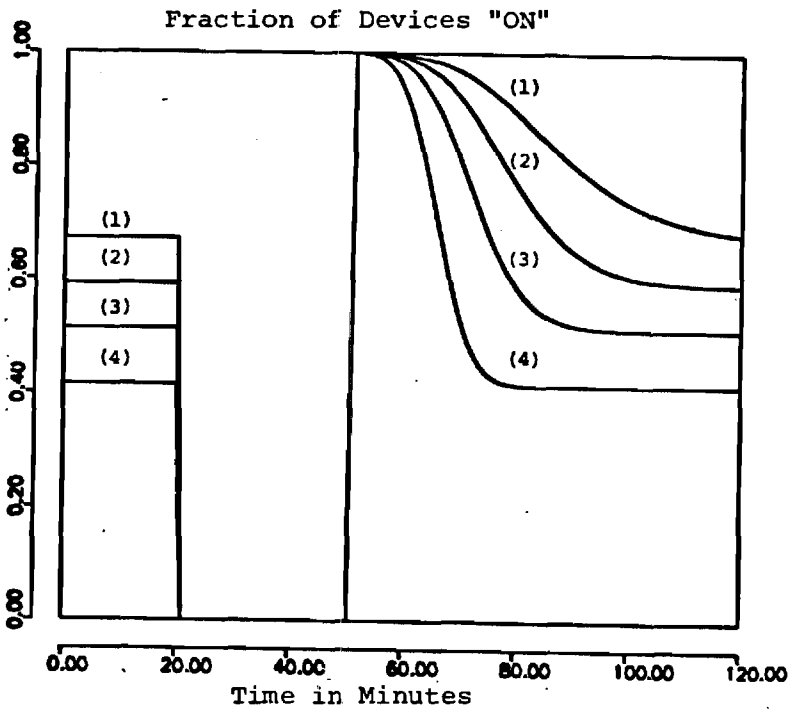

Fig. 6-3. Dependence of Cold Load Pickup Dynamics on the Heating Rate Parameter R for an Outage Duration of 30 mn. Values $R\Delta^{-1}$ in $(mn)^{-1}$ are .3, .344, .4 and .5 for responses (1), (2), (3), and (4) respectively. All other parameters are as in base case.

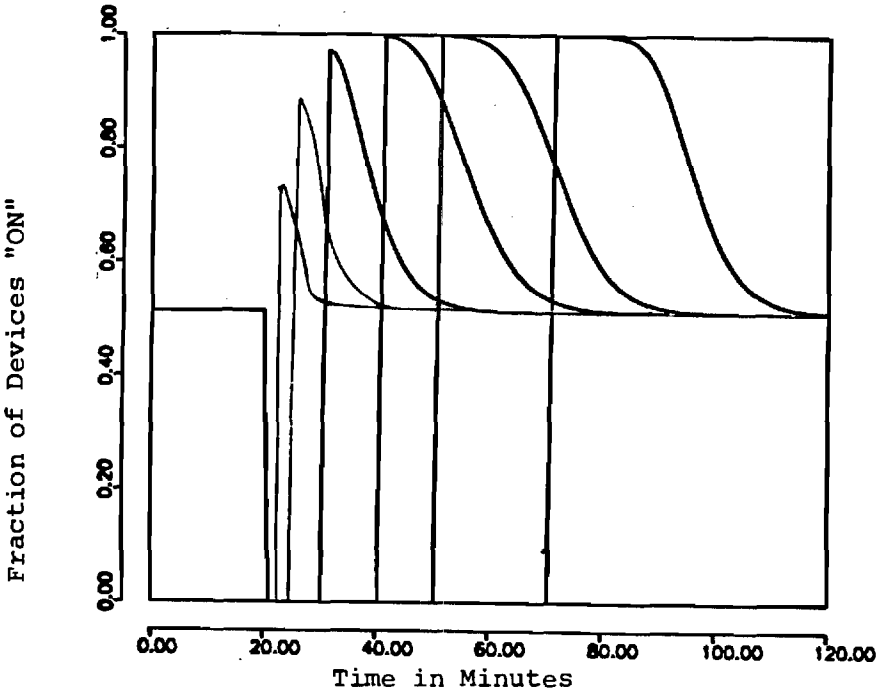

Fig. 6-4. Dependence of Cold Load Pickup Dynamics on Outage Duration. Outage durations are 2, 5, 10, 20, 30 and 50 mns respectively. All other parameters are as in base case.

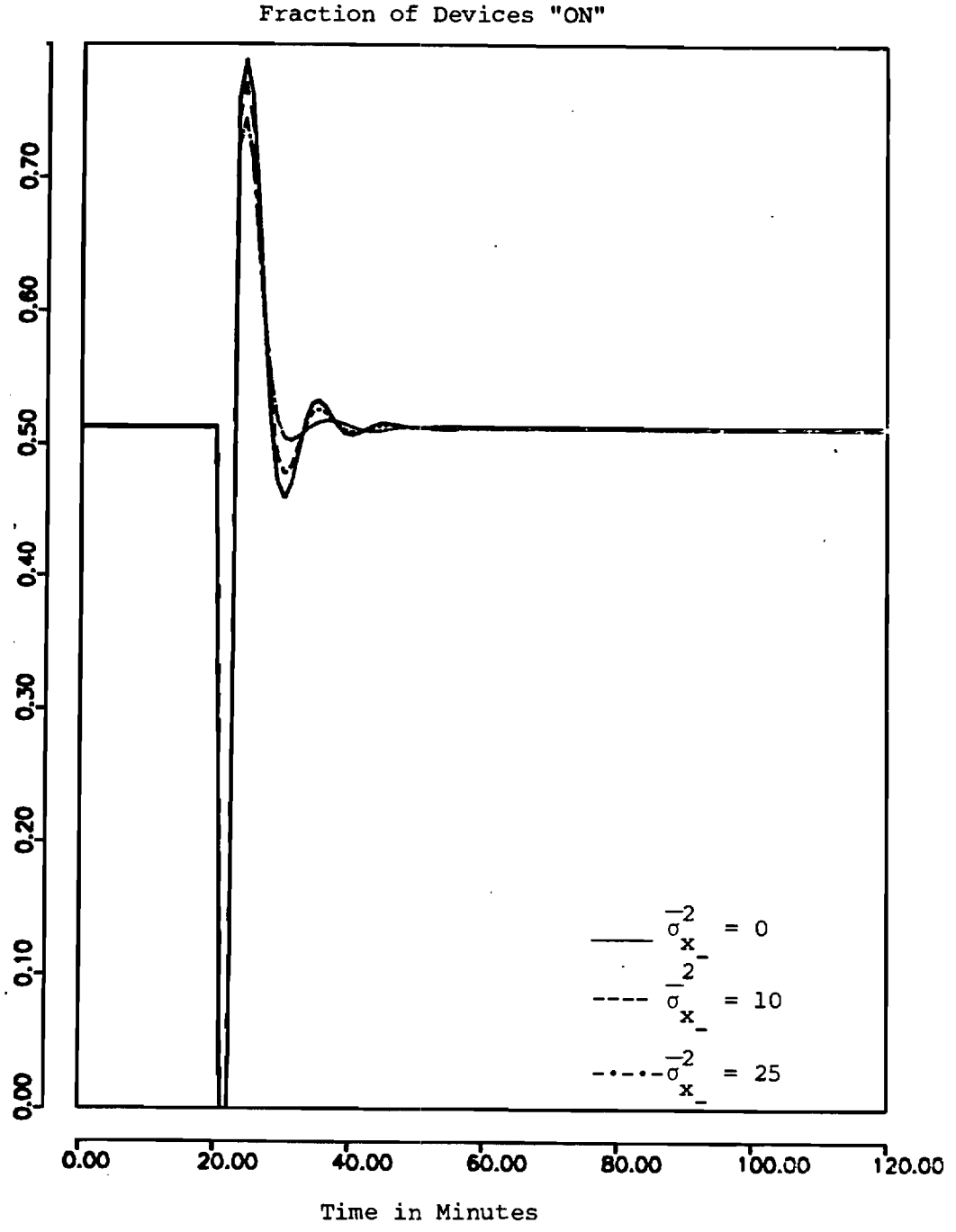

Fig. 6-5. Effect of Spread in Thermostat Set Points on Cold Load Pickup Dynamics for a Nonhomogeneous Control Group. Mean values are as in section 6.2. $\bar{\sigma}^2_{x_-}$ represents the normalized set point variance. The duration of the outage is 2 mn.

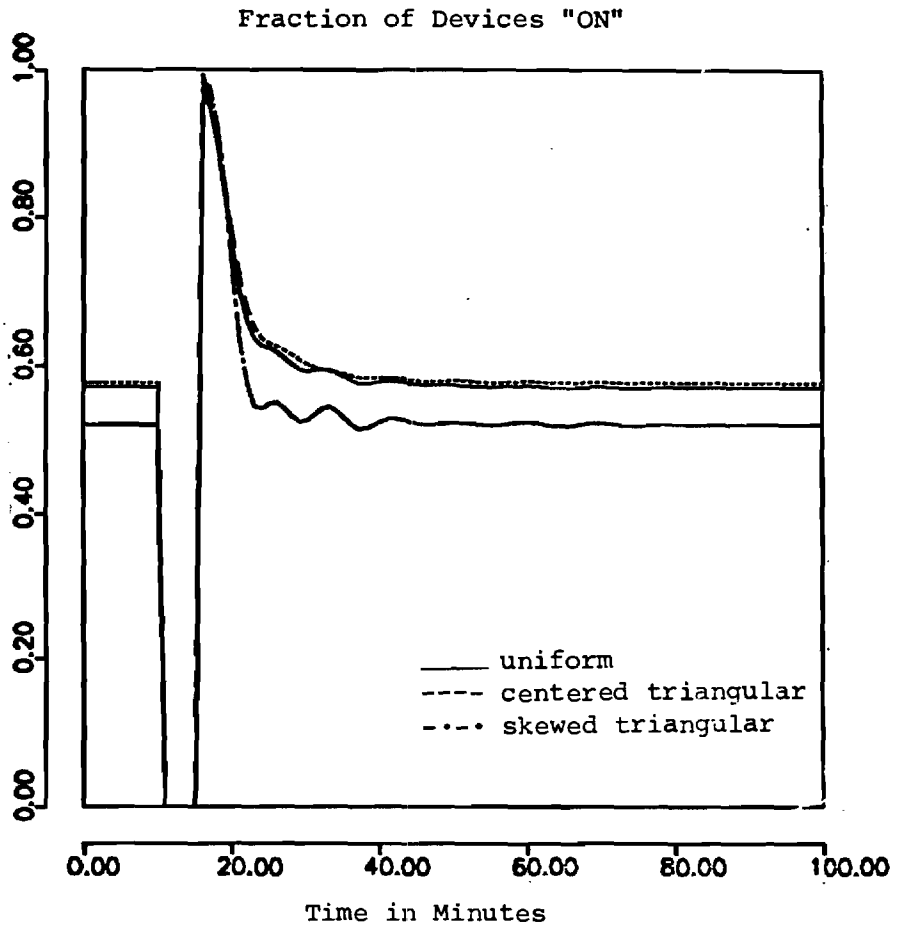

Fig. 6-6. Effect of Parameter Distribution on Cold Load Pickup Dynamics for a General Control Group. All values are as in section 6.3. The duration of the outage is 5 mn.

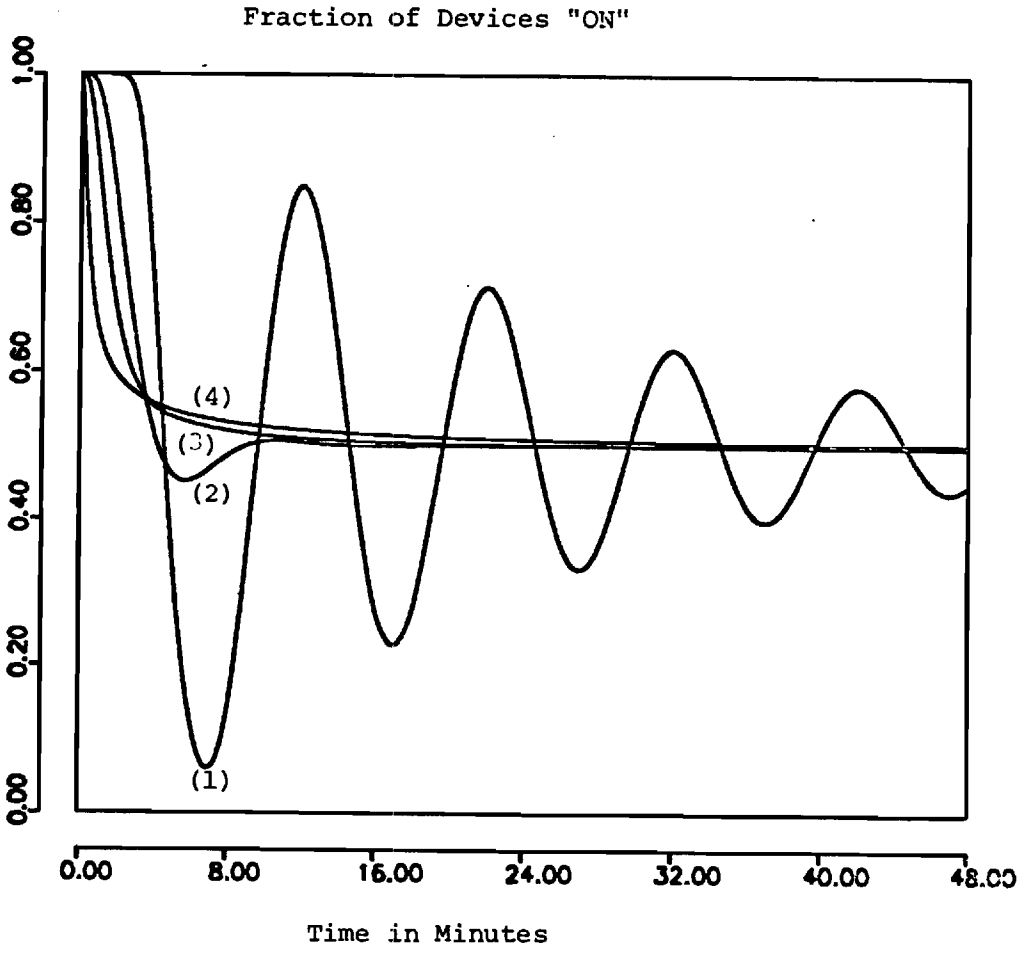

Fig. 6-7. Theoretical Impulse Responses for Four Values of Normalized Noise Variance Parameter. Values of $\bar{\sigma}$ in $(mn)^{-1/2}$ are: (1) $\bar{\sigma} = .1$, (2) $\bar{\sigma} = .3$, (3) $\bar{\sigma} = .5$, (4) $\bar{\sigma} = 1.0$. $\bar{\tau} = \bar{\tau}' = 5$ mn in all four cases.

6.5 A Few Observations on the Results

The following groups of remarks can be made:

(a) From Figures 6-1 and 6-2 it appears that:

- The noise variance parameter $\overline{\sigma}$ is crucial in shaping the dynamical response of homogeneous control groups. Therefore, ignoring this parameter completely, as is the case for the Ihara/Schweppe model, can result in serious error.
- As the noise variance parameter increases there is a simultaneous decrease in post-outage dynamical fluctuations. The system reaches its steady-state faster. $\overline{\sigma}$ acts like a damping factor. This is to be expected since an increase in system noise provokes an increase in the diversity of the system. This increase in diversity in turn tends to oppose the decrease in diversity caused by the power outage, thus yielding a more stable system.
- Unlike its approximate version (4.14)-(4.15) which predicts that the steady-state connected fraction of devices is independent of $\overline{\sigma}$, the CFPE model simulator indicates a dependence of the steady-state on noise variance. However, the dependence is apparent only for large values of $\overline{\sigma}$. This is consistent with the constant rate approximation validity criterion developed in equations (4.125)-(4.126) as we now show. In the simulations of figures 6-1 and 6-2, $\overline{\tau}$ = 5 mn.

Hence for $\bar{\sigma} = 1.0$, the performance criterion in (4.125) yields .82. This means that for $\bar{\sigma} = 1.0$, 82% of the steady state "on" density lies outside the thermostat dead band, thus invalidating the constant rates approximation.

(b) From figures 6-3 through 6-4, we have respectively the predictable results that as the average heating rate increases, the steady state fraction of devices in the "on" state decreases (mainly because a device spends on the average less time in the "on" state) and as the outage duration increases the fraction of devices in the "on" state after the recovery increases, as well as the duration of the restoration period.

(c) From Fig. 6-5, it appears that post-outage dynamic fluctuations for a nonhomogeneous control group decrease as the parameter variance within the group increases. As argued in (a), this effect can be understood by remarking that an increase in parameter variance results in an increase in the diversity of the system.

(d) From Fig. 6-6, it appears that the parameter distribution within a general control group can alter significantly the restoration dynamics following a power outage. Uniform and centered triangular parameter distributions yield smooth dynamics for our example.

(e) The theoretical results in Fig. 6-7 are consistent with the simulation results in Figures 6-1 and 6-2, namely:

- As the noise variance parameter $\bar{\sigma}$ increases, the dynamics become smoother.
- $\bar{\sigma}$ acts essentially like a damping factor.

This suggests that the constant rates approximate model (4.14)-(4.15) retains some of the essential dynamic features of the exact CFPE model (3.36)-(3.43). One important difference however, is that for the approximate model, there is no dependence of the steady-state connected fraction of devices on noise variance.

6.6 Future Work

One important final step remains to be taken before bringing the general load synthesis procedure of Figure 2-1 to completion: step e, or model validation. This implies a preliminary parameter estimation phase for a practical system, followed by the application of the results of this thesis to generate a model for the prediction of cold load pickup dynamics for the system. The predicted dynamics would then be compared to actual dynamics measured under the same conditions. Only after the completion of this task can the practical success or failure of our approach be unequivocally assessed.

It is likely that, in case of failure, the root of the problem be a possibly oversimplified group model (equation 2.1). In the light of the preceding remark, a first extension of this work would be to investigate how well the results obtained generalize to the case of a more complex (more states?) group model. It is not unexpected that for the more general case, one would have to deal with first passage times over hyperplane problems. Secondly, only the

case of what was refered to earlier as "weakly-driven" functional models was studied here. An obvious extension of this work would be the solution of the aggregation problem for the "strongly-driven" case, the practical benefit being the ability to model the loads due to groups of electric water heaters. Finally, on the theoretical level, the fundamental result of the thesis is expressed in equations (3.36)-(3.43). These equations characterize the evolution of "hybrid" probability densities $f_1(\lambda,t)$, $f_o(\lambda,t)$ associated with the hybrid-state vector Markov process $\binom{x(t)}{m(t)}$. Whereas continuous-state Markov processes have probability densities which satisfy the Fokker-Planck equation under fairly weak conditions, no formally correspondant result is known for the case of hybrid-state Markov processes. It is our conjecture that it is possible to write a system of equations similar to (3.36)-(3.43) i.e. a combination of Fokker-Planck equations associated with boundary conditions expressing a "conservation of probability" principle for a broad class of hybrid-state Markov processes still to be characterized. We feel this conjecture is well worth investigating.

6.7 Conclusion

It is our opinion, that the major contribution of this thesis, other than helping to bring about the solution of a very practical problem, has been to demonstrate that for modeling groups of loads for which assumptions of "elemental independence" (section 3.2) hold, methods inspired from the still very dynamic field of statistical mechanics can be applied with some success. At an earlier date, and in the area of neural networks, parallel conclusions were reached by

J. D. Cowan in his article "A Statistical Mechanics of Nervous Activity" [60]. It is hoped that the few results presented here will encourage further research in this direction which, although more perilous and expensive (in terms of data requirements) than the now classical time series parameter identification approaches to load modeling, could yield in the long run physically more meaningful and therefore more versatile analytical electric load models.

APPENDIX A.

MISCELLANEOUS PROOFS

In this appendix three proofs are presented. In proof 1, it is shown that the interchange of limits and integration order can be carried out in (3.59). In proof 2, the state transition matrix in (4.30) is calculated. Finally, in proof 3, equations (4.151) through (4.155) are established.

PROOF 1:

From (3.60) we have:

$$\lim_{h\to 0} \frac{1}{h} \int_{-\infty}^{\infty} f_{11}(\lambda,t,z,t+h)(z-\lambda)d\lambda = -a(\lambda-x_a(t)) + Rb(t) \qquad (A.1)$$

Let us set:

$$m(\lambda,t) = -a(\lambda-x_a(t)) + Rb(t) \qquad (A.2)$$

(A.1) implies that for some $\varepsilon > 0$, there exists $\delta(\varepsilon) > 0$ such that for $|h| < \delta(\varepsilon)$:

$$\left|\frac{1}{h} \int_{-\infty}^{\infty} f_{11}(\lambda,t,z,t+h)(z-\lambda)dz - m(\lambda,t)\right| < \varepsilon \qquad (A.3)$$

From (A.3) we have:

$$\left|\frac{1}{h} \int_{-\infty}^{\infty} f_{11}(\lambda,t)z,t+h)(z-\lambda)dz\right| < \varepsilon + m(\lambda,t) \qquad (A.4)$$

for all h such that $|h| < \delta(\varepsilon)$. Furthermore, since $R'(\lambda)$ is continuous on the compact interval $[x_- + \varepsilon, x_+]$ and zero elsewhere, it must be bounded for all λ. Let k be an upper bound. Similarly, the continuous function of λ, $|m(\lambda,t)|$ on the compact interval $[x_- + \varepsilon, x_+]$ must be bounded. Let M(t) be an upper bound. Using (A.4) and the preceding remarks:

$$|R'(\lambda) f_{11}(\lambda',t',\lambda,t) \frac{1}{h} \int_{-\infty}^{+\infty} f_{11}(\lambda,t,z,t+h)(z-\lambda)dz|$$

$$= 0 \text{ for } \lambda \in [x_- + \varepsilon, x_+]$$

$$\leq k(\varepsilon + M(t))\ f_{11}(\lambda',t',\lambda,t) \qquad \text{(A.5)}$$

for $\lambda \in [x_- + \varepsilon, x_+]$ and for $|h| < \delta(\varepsilon)$.

But:

$$\int_{x_-+\varepsilon}^{x_+} f_{11}(\lambda',t',\lambda,t)\ k(\varepsilon + M(t))d\lambda \leq k(\varepsilon + M(t))$$

$$< \infty \qquad \text{(A.6)}$$

(A.5) and (A.6) show that for $|h| < \delta(\varepsilon)$ the integrand of:

$$\lim_{h\to 0} \int_{-\infty}^{\infty} \left[f_{11}(\lambda',t',\lambda,t) \frac{1}{h} \int_{-\infty}^{\infty} f_{11}(\lambda,t,z,t+h)(z-\lambda)dz\ R'(\lambda) \right] d\lambda \qquad \text{(A.7)}$$

is dominated by the function defined by the right-hand side of (A.5), independent of h and that furthermore, this functionis absolutely integrable. By virtue of Lebesque's dominated convergence theorem, we can carry the limit operation past the integral sign. A similar proof holds for the remaining terms of (3.63). This completes proof 1. •

PROOF 2:

We use a transform technique to compute the state transition matrix in (4.30). If γ represents the complex variable in the transformation, we have:

$$\underline{\phi}(\lambda,s) = L^{-1}\left|\begin{matrix}\gamma & -1 \\ -\frac{2s}{\sigma^2} & \frac{\gamma-2r}{\sigma^2}\end{matrix}\right|^{-1} \tag{A.8}$$

where in (A.8), $L^{-1}\{\cdot\}$ represents the inverse Laplace transform operator. From (A.8):

$$\underline{\phi}(\lambda,s) = L^{-1}\left|\frac{\sigma^2}{\gamma^2\frac{2}{\sigma} - 2\gamma r - 2s}\left|\begin{matrix}\frac{\gamma-2r}{\sigma^2} & 1 \\ \frac{2s}{\sigma^2} & \lambda\end{matrix}\right|\right| \tag{A.9}$$

which yields:

$$\phi_{11}(\lambda,s) = L^{-1}\left[\frac{\lambda\sigma^2 - 2r}{\sigma^2(\gamma-\theta_1(s))(\gamma-\theta_2(s))}\right]$$

$$= \theta^{-1}(s)\left[\theta_1(s)e^{\theta_2(s)\gamma} - \theta_2(s)e^{\theta_1(s)\lambda}\right] \tag{A.10}$$

where in (A.10), $\theta(s)$, $\theta_1(s)$, $\theta_2(s)$ have already been defined in (4.35)-(4.36)

$$\phi_{12}(\lambda,s) = L^{-1}\left[\frac{\sigma^2}{\sigma^2(\gamma - \theta_1(s))(\gamma - \theta_2(s))}\right]$$

$$= \theta^{-1}(s)\left[e^{\theta_1(s)\gamma} - e^{\theta_2(s)\gamma}\right] \qquad \text{(A.11)}$$

$$\phi_{21}(\lambda,s) = L^{-1}\left[\frac{2s}{\sigma^2(\gamma - \theta_1(s))(\gamma - \theta_2(s))}\right]$$

$$= \frac{2s}{\sigma^2}\left[e^{\theta_1(s)\lambda} - e^{\theta_2(s)\lambda}\right] \qquad \text{(A.12)}$$

$$\phi_{22}(\lambda,s) = L^{-1}\left[\frac{\gamma\sigma^2}{\sigma^2(\gamma - \theta_1(s))(\gamma - \theta_2(s))}\right]$$

$$= \theta^{-1}(s)\left[\theta_1(s)e^{\theta_1(s)\lambda} - \theta_2(s)e^{\theta_2(s)\lambda}\right] \qquad \text{(A.13)}$$

This completes proof 2. •

PROOF 3:

Equation (4.153) is rewritten for convenience:

$$g_o^*(a,s)g_1^*(b,s) \approx \exp\left[-\frac{\left[-\mu_{ab} + \left(\mu_{ab}^2 + 2s\sigma_{ab}^2\right)^{1/2}\right]}{\sigma_{ab}^2}\right] \qquad \text{(A.14)}$$

In accordance with the developments in section (4.3.2), we impose the condition that the first and second moments (or equivalently the mean and variance) of the probability density function which transforms into the left-hand side of (A.14) be exactly retain-

ed by the approximating density function. This means in effect the following:

$$-\frac{\partial}{\partial s}\left[g_o^*(a,s)g_1^*(b,s)\right]\Big|_{s=0} = -\frac{\partial}{\partial s}\exp\left[-\frac{\left[-\mu_{ab} + \left(\mu_{ab}^2 + 2s\sigma_{ab}^2\right)^{1/2}\right]}{\sigma_{ab}^2}\right]\Bigg|_{s=0} \tag{A.15}$$

$$\frac{\partial^2}{\partial s^2}\left[g_o^*(a,s)g_1^*(b,s)\right]\Big|_{s=0} = \frac{\partial^2}{\partial s^2}\exp\left[-\frac{\left[-\mu_{ab} + \left(\mu_{ab}^2 + 2s\sigma_{ab}^2\right)^{1/2}\right]}{\sigma_{ab}^2}\right]\Bigg|_{s=0} \tag{A.16}$$

Now:

$$\frac{\partial}{\partial s}\exp\left[-\frac{\left(-\mu + \left(\mu^2 + 2s\sigma^2\right)^{1/2}\right)}{\sigma^2}\right]\Bigg|_{s=0}$$

$$= \exp\left[\frac{\left(-\mu + \left(\mu^2 + 2s\sigma^2\right)^{1/2}\right)}{\sigma^2}\right]\Bigg|_{s=0}\left[\left(-\frac{1}{2}\cdot\left(\mu^2 + 2s\sigma^2\right)^{1/2}\right]\Big|_{s=0}\right.$$

$$= -\frac{1}{\mu} \tag{A.17}$$

$$\frac{\partial^2}{\partial s^2}\exp\left[-\frac{\left(-\mu + \left(\mu^2 + 2s\sigma^2\right)^{1/2}\right)}{\sigma^2}\right]\Bigg|_{s=0}$$

$$= -\left(\mu^2 + 2s\sigma^2\right)^{-1/2}\frac{\partial}{\partial s}\left[\exp\left[-\frac{\left(-\mu + \left(\mu^2 + 2s\sigma^2\right)^{1/2}\right)}{\sigma^2}\right]\Bigg|_{s=0}\right.$$

$$-\frac{1}{2}\left(\mu^2 + 2s\sigma^2\right)^{-3/2}\,2\sigma^2\exp\left[-\frac{\left(\mu + \left(\mu^2 + 2s\sigma^2\right)^{1/2}\right)}{\sigma^2}\right]\Bigg|_{s=0} \tag{A.18}$$

(A.17) and (A.18) yield:

$$\frac{\partial^2}{\partial s^2} \exp\left[-\frac{\left(-\mu + (\mu^2 + 2s\sigma^2)^{1/2}\right)}{\sigma^2}\right] = \frac{1}{\mu^2} + \frac{\sigma^2}{\mu^3} \qquad \text{(A.19)}$$

Furthermore:

$$\frac{\partial}{\partial s}\left[g_o^*(a,s)g_1^*(b,s)\right]\Big|_{s=0} = g_o^*(a,s)\,\frac{\partial}{\partial s}\,g_1^*(b,s)\Big|_{s=0} + g_1^*(b,s)\,\frac{\partial}{\partial s}\,g_o^*(a,s)\Big|_{s=0} \qquad \text{(A.20)}$$

Recalling (4.85)-(4.86) and using (A.17) we obtain:

$$\frac{\partial}{\partial s}\left[g_o^*(a,s)g_1^*(b,s)\right]\Big|_{s=0} = -\frac{a}{r} - \frac{b}{c} \qquad \text{(A.21)}$$

Also:

$$\frac{\partial^2}{\partial s^2}\left[g_o^*(a,s)g_1^*(b,s)\right] = g_o^*(a,s)\,\frac{\partial^2}{\partial s^2}\,g_1^*(b,s)\Big|_{s=0} + 2\,\frac{\partial}{\partial s}\,g_o^*(a,s)\,\frac{\partial}{\partial s}\,g_1^*(b,s)\Big|_{s=0} + g_1^*(b,s)\,\frac{\partial^2}{\partial s^2}\,g_o^*(a,s)\Big|_{s=0} \qquad \text{(A.22)}$$

and using (4.85)-(4.86) and (A.17)-(A.21) we have:

$$\frac{\partial^2}{\partial s^2}\left[g_o^*(a,s)g_1^*(b,s)\right] = \frac{a^2}{r^2} + \frac{\sigma^2 a^2}{r^2} + \frac{2ab}{rc} + \frac{b^2}{c^2} + \frac{\sigma^2 b^2}{c^2} \qquad \text{(A.23)}$$

(A.15), (A.17) and (A.21) yield:

$$\frac{a}{r} + \frac{b}{c} = \frac{1}{\mu_{ab}} \tag{A.24}$$

or:

$$\mu_{ab} = \frac{rc}{ac + br} \tag{A.25}$$

(A.16), (A.19) and (A.23) yield:

$$\frac{a^2}{r^2} + \frac{\sigma^2 a^2}{r^2} + \frac{2ab}{rc} + \frac{b^2}{c^2} + \frac{b^2\sigma^2}{c^2}$$

$$= \left(\frac{a}{r} + \frac{b}{c}\right)^2 + \frac{\sigma^2_{ab}}{\mu^3_{ab}} \tag{A.26}$$

And:

$$\sigma^2_{ab} = \mu^3_{ab}\ \sigma^2\ \left(\frac{a^2}{r^2} + \frac{b^2}{c^2}\right) \tag{A.27}$$

(A.25) and (A.27) yield:

$$\sigma^2_{ab} = \sigma^2\ \frac{\left(\frac{a^2}{r^2} + \frac{b^2}{c^2}\right)}{\left(\frac{a}{r} + \frac{b}{c}\right)^3} \tag{A.28}$$

Equations (4.151) through (4.155) are easily obtained from (A.25) and (A.28) by substituting appropriate values for a and b. This completes the proof. ●

APPENDIX B

DERIVATION OF FIRST PASSAGE TIME DENSITY FOR BROWNIAN MOTION WITH DRIFT

This appendix is based on Cox [39]. Equation (4.65) is rewritten here for convenience:

$$\frac{\partial P_a}{\partial t}(\lambda,t,\lambda_o) = -\mu \frac{\partial P_a}{\partial \lambda}(\lambda,t,\lambda_o) + \frac{\sigma^2}{2} \frac{\partial^2 P_a}{\partial \lambda^2}(\lambda,t,\lambda_o) \qquad (B.1)$$

Subject to the conditions:

$$\lim_{t\to 0} P_a(\lambda,t,\lambda_o) = \delta(\lambda - \lambda_o) \qquad (B.2)$$

$$P_a(a,t,\lambda_o) = 0 \qquad (B.3)$$

If condition (B.3) is ignored for the moment, it can be easily verified that:

$$P(\lambda,t,\lambda_o) = \frac{1}{\sigma\sqrt{2\pi t}} \exp\left[-\frac{(\lambda - \lambda_o - \mu t)^2}{2\sigma^2 t}\right] \qquad (B.4)$$

satisfies (B.1) and (B.2).

Using the method of images, it is possible to simulate a zero boundary condition at a by placing an impulsive source at $(\lambda_o - 2a)$, i.e. symmetrically located with respect to the absorbing boundary at a, and of magnitude A to be determined. This is graphically represented in Fig. B-1.

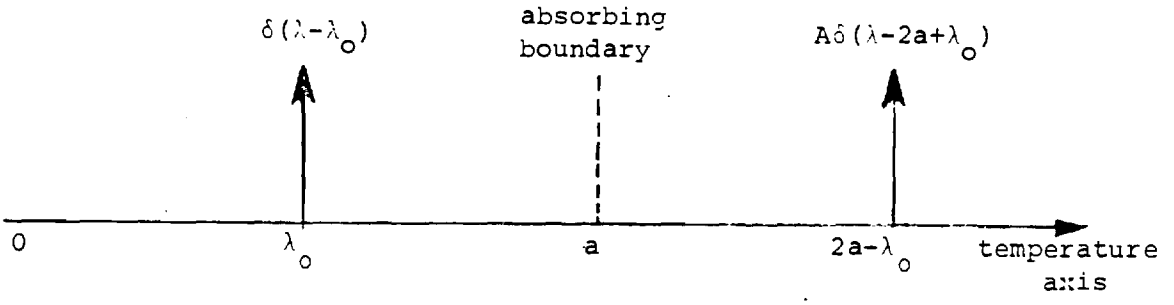

Fig. B-1. The absorbing boundary can be simulated by means of an additional source of appropriate magnitude and symmetrically located.

The resulting density would be the superposition of the densities due to each source separately, i.e.:

$$P_a(\lambda,t,\lambda_o) = \frac{1}{\sigma\sqrt{2\pi t}}\left[\exp\left[-\frac{(\lambda-\lambda_o-\mu t)^2}{2\sigma^2 t}\right] + A\exp\left[-\frac{(\lambda-2a+\lambda_o-\mu t)^2}{2\sigma^2 t}\right]\right] \tag{B.5}$$

Boundary condition (B.3) yields:

$$A = \exp\left[-\frac{(a-\lambda_o-\mu t)^2}{2\sigma^2 t}\right]\exp\left[\frac{(\lambda_o-a-\mu t)^2}{2\sigma^2 t}\right]$$

$$= e^{\frac{2\mu(a-\lambda_o)}{\sigma^2}} \tag{B.6}$$

(B.5) and (B.6) yield:

$$P_a(\lambda,t,\lambda_o) = \frac{1}{\sigma\sqrt{2\pi t}}\left[\exp\left[-\frac{(\lambda-\lambda_o-\mu t)^2}{2\sigma^2 t}\right] - \exp\left[\frac{2\mu(a-\lambda_o)}{\sigma^2} - \frac{(\lambda-2a+\lambda_o-\mu t)^2}{2\sigma^2 t}\right]\right] \qquad \text{(B.7)}$$

(4.71) follows from (4.70) and (B.7).

This completes the derivation. ●

BIBLIOGRAPHY

1. "System Load Dynamics - Simulation Effects and Determination of Load Characteristics," IEEE Trans. on Power Apparatus and Systems, vol. PAS-92, pp. 600-609, March-April 1973.

2. H. Kent, W. R. Schmus, F. A. McCrackin and L. M. Wheeler, "Dynamic Modeling of Loads in Stability Studies," IEEE Trans. on Power Apparatus and Systems, vol. PAS-88, pp. 138-146, May 1969.

3. F. P. DeMello, "Power System Dynamics Overview," Symposium on Adequacy and Philosophy of Modeling: Dynamic System Performance, IEEE pamphlet 75 CH0970-4-PWR, pp. 5-15.

4. G. T. Heinemann, D. A. Nordman, and E. C. Plant, "The Relationship between Summer Weather and Summer Loads - Regression Analysis," IEEE Trans. on Power Apparatus and Systems, vol. PAS-85, pp. 1144-1154, Nov. 1966.

5. P. C. Gupta and K. Yamada, "Adaptive Short Term Forecasting of Hourly Loads Using Weather Information," IEEE Trans. on Power Apparatus and Systems, vol. PAS-91, pp. 2085-2094, 1972.

6. J. Toyoda et. al., "An Application of State Estimation to Short Term Load Forecasting," IEEE Trans. on Power Apparatus and Systems, vol. PAS-89, pp. 1678-1682.

7. G. Singh et. al., "Load Modeling for Real Time Monitoring of Power Systems," IEEE Trans. on Power Apparatus and Systems, vol. PAS-96, pp. 1908-1914, Nov. 1977.

8. G. Singh et. al., "Power System Load Forecasting Using Smoothing Techniques," Int. J. Systems Science, vol. 9, no. 4, pp. 363-368, 1978.

9. J. F. De Queiroz, "A Load Demand Prediction Algorithm for Electric Power System Monitoring," presented at the 1979 Control of Power Systems Conference and Exposition Conference Record, College Station, pp. 161-166.

10. A. Gelb ed., Applied Optimal Estimation, M.I.T. Press, Cambridge, MA, 1974.

11. G. E. P. Box and G. M. Jenkins, Time Series Analysis - Forecasting and Control, Holden-Day, San Francisco, 1970.

12. R.L. Kashyap and A. R. Rao, Dynamic Stochastic Model from Operating Data, Academic Press, New York, 1976.

13. A. Keyhani and A. M. El-Abiad, "One-Step-Ahead Load Forecasting for On-Line Applications," paper C75 027-8, IEEE Winter Power Meeting, 1975.

14. F. D. Galiana et. al., "Identification of Stochastic Electric Load Models from Physical Data," IEEE Trans. on Automat. Control, vol. AC-19, pp. 887-893, Dec. 1974.

15. S. Vemuri et. al., "Load Forecasting Using Stochastic Models," in Proc. of 1973 PICA Conference.

16. A. R. Mahalanabis et. al., "Load Modeling of an Interconnected Power System for Short Term Prediction," Int. J. Systems Science, vol. 11, no. 4, pp. 445-453, 1980.

17. M. Hagan and R. Klein, "On-Line Maximum Likelihood Estimation for Load Forecasting," IEEE Trans. on Syst., Man and Cyber, vol. SMC-8, Sept. 1978.

18. Y. Gertler and Cs. Banyasz, "A Recursive (ON-line) Maximum Likelihood Identification Method," IEEE Trans. on Automat. Control, vol. AC-19, pp. 816-820, Dec. 1974.

19. IEEE Committee Report, "Bibliography on Load Management," IEEE Trans. on Power Apparatus and Systems, vol. PAS-100, no. 5, May 1981.

20. M. L. Chan, E. N. Marsh, J. Y. Yoon, G. B. Ackerman, and N. Stoughton, "Simulation-Based Load Synthesis Methodology for Evaluating Load Management Programs," IEEE Summer Power Meeting.

21. N. S. Rau and R. W. Graham, "Analysis and Simulation of the Effects of Controlled Water Heaters in a Winter Peaking System," IEEE Trans. on Power Apparatus and Systems, vol. PAS-98, no. 2, pp. 458-464, March/April 1979.

22. W. E. Mekolites, R. M. Murphy, and Y. L. Laine, "AEP Water Heater Load Management Test," American Power Conference, 1981.

23. "Pacific Gas and Electric Residential Air Conditioning Load Control Simulation Study," prepared by Honeywell Technology Strategy Center, 2600 Ridgeway Parkway, Minneapolis, MN, October 1980.

24. S. Ihara and F. C. Schweppe, "Physically Based Modeling of Cold Load Pickup," IEEE Winter Power Meeting, 1981.

25. W. W. Lang, M. D. Anderson, and D. R. Fannin, "An Analytical Method for Quantifying the Electrical Space Heating Component of a Cold Load Pickup," IEEE Summer Power Meeting, 1981.

26. S. Ihara, "An Algebraic Aggregation of Interconnected Power System Loads," CDC Proceedings, pp. 270-272, 1979.

27. M. M. Abdel-Hakim and Y. G. Berg, "Dynamic Single-Unit Representation of Induction Motor Groups," IEEE Trans. on Power Apparatus and Systems, vol. PAS-95, pp. 155-156, January/February 1976.

28. F. Illiceto and A. Capasso, "Dynamic Equivalents of Asynchronous Motor Loads in System Stability Studies," IEEE Trans. on Power Apparatus and Systems, vol. PAS-93, pp. 1650-1659, 1974.

29. C. Y. Chong and A. S. Debs, "Statistical Synthesis of Power System Functional Load Models," CDC Proceedings, pp. 264-269, 1979.

30. J. B. Woodard, Jr., "Electric Load Modeling," Ph.D. Thesis, Department of Electrical Engineering, M.I.T., September 1976, EPSEL Report No. 50.

31. M. F. Ruane, Y. Manichaikul, F. C. Schweppe, and J. B. Woodard, "Physically Based Load Modeling," IEEE Summer Power Meeting, 1979.

32. M. F. Ruane, F. C. Schweppe, and S. Ihara, "Physically Based Modeling of Aggregate Loads," IEEE Winter Power Meeting, 1981.

33. Y. Manichaikul, "Industrial Electric Load Modeling," Ph.D. Thesis, Department of Electrical Engineering, M.I.T., September 1974, EPSEL Report No. 54.

34. Y. Manichaikul and F. C. Schweppe, "Physically Based Industrial Electric Load," IEEE Trans. on Power Apparatus and Systems, vol. PAS-98, pp. 1439-1445, July 1979.

35. S. P. Reynolds and T. E. Creighton, Jr., "Time-of-Use Rates for Very Large Customers on the Pacific Gas and Electric Company System," IEEE Trans. on Power Apparatus and Systems, vol. PAS-99, pp. 147-157, Jan. 1980.

36. J. E. McDonald, A. M. Bruning, and W. R. Mahica, "Cold Load Pickup," IEEE Trans. on Power Apparatus and Systems, vol. PAS-98, pp. 1386-1387, July/August 1979.

37. K. L. Chung, A Course in Probability Theory, Academic Press, New York, 1968.

38. A. T. Bharucha-Reid, Elements of the Theory of Markov Processes and Their Applications, McGraw Hill, New York, 1960.

39. D. R. Cox and H. D. Miller, The Theory of Stochastic Processes, Wiley, New York, 1965.

40. D. A. Darling and A. J. Siegert, "The First Passage Time Problem for a Continuous Markov Process," Annals of Mathematical Statistics, vol. 24, pp. 624-639, 1953.

41. A. Holden, Models of the Stochastic Activity of Neurons, Springer Verlag, Berlin, 1976.

42. M. Fen Hoppen, "Probabilistic Firing of Neurons Considered as a First Passage Problem," Biophysical Journal, vol. 6, pp. 435-451, 1966.

43. H. Sugiyama, G. P. Moore, and D. H. Perkel, "Solutions for a Stochastic Model of Neuronal Spike Production," Mathematical Biosciences, vol. 8, pp. 323-341, 1970.

44. C. W. Helstrom, "Markov Processes and Their Applications," in Communication Theory, ed. A. V. Balakrishnan, McGraw Hill, New York, 1968.

45. G. Doetsch, Guide to the Applications of the Laplace and z Transforms, Van Nostrand Reinhold, London, 1971.

46. H. B. Keller, "The Numerical Solution of Parabolic Partial Differential Equations," in Mathematical Methods for Digital Computers, ed. A. Ralston and H. S. Wilj, New York.

47. J. L. Doob, Stochastic Processes, Wiley, New York, 1953.

48. A. N. Kolmogorov, "Uber Die Analytischen Methoden in Der Wahrscheinlichkeitsrechnung," Math. Ann., no. 104, pp. 415-458, 1931.

49. R. B. Bartle, The Elements of Integration, Wiley, New York, 1966.

50. N. Wiener, Differential Space, J. of Math. and Phys., no. 2, pp. 131-174, 1923.

51. P. Levy, Processus Stochastiques et Mouvement Brownien, Gauthiers, Paris, 1948.

52. K. Ito, H. P. McKean, Diffusion Processes and their Sample Path, Berlin, Heidelberg, New York.

53. E. B. Dynkin, Markov Processes, Moscow, 1963.

54. W. Feller, "The Parabolic Differential Equation and the Associated Semi-group," Ann. of Math., no. 55, pp. 468-519, 1952.

55. G. Gerstein and B. Mandelbrot, "Random Walk Models for the Spike Activity of a Single Neuron," Biophysical J., vol. 4, pp. 41-68, 1964.

56. P. I. M. Johanesma, "Diffusion Models for the Stochastic Activity of Neurons," in Neural Networks - Proceedings of the School on Neural Networks, June 1967 at Ravello. Ed. E. R. Caianiello, Springer-Verlag, New York, 1968.

57. P. Moran, The Theory of Storage, Wiley, New York, 1959.

58. S. Karlin and H. M. Taylor, A Second Course in Stochastic Processes, Academic Press, New York, 1981.

59. A. Friedman, Partial Differential Equations, Holt, Rinehart and Winston, New York, 1969.

60. J. D. Cowan, "A Statistical Mechanics of Nervous Activity," In Gerstenhaber, M. (ed.): Lecture on Mathematics in the Life Sciences, Providence, Rhode Island, Amer. Math. Soc.